# RESPONSE OF SENSORIMOTOR PATHWAYS OF THE SPINAL CORD TO INJURY AND EXPERIMENTAL TREATMENTS

Tao Meng

Bachelor of Medicine, Central South University, 2002

Master of Surgery, Lanzhou University, 2005

Thesis submitted for the degree of Doctor of Philosophy

Faculty of Biomedical and Life Sciences

University of Glasgow

September 2009

# Abstract

Many spinal cord injuries (SCI) are incomplete, variable numbers of spared fibres passing the lesion level and supporting some residual function below the injury. One approach to improving function following injury is to develop therapies that maximise the potential of these spared fibres. The aim of the work in this thesis was to investigate the spontaneous plasticity that occurs in spinal cord pathways following injury and then determine whether olfactory ensheathing cell (OEC) transplants or treatment with antibodies blocking the function of the myelin inhibitors Nogo and MAG could enhance this plasticity.

An electrophysiological approach was used to investigate these questions in rats which were subjected to a lesion of the dorsal columns at the C4/5 segmental level. This lesion interrupts the main component of the corticospinal tract which descends in the ventromedial dorsal column and also interrupts the ascending collaterals of sensory fibres from forelimb nerves. In this study, changes in the function of both of these pathways were assessed by recording cord dorsum potentials (CDPs) after stimulation in the pyramids (corticospinal activation) or of the radial nerve (sensory fibre activation). To enable plasticity in the corticospinal system to be investigated a method was developed for maximally activating the corticospinal projection on one side of the pyramids, whilst avoiding activation of the opposite pyramid and structures surrounding the pyramids. It was found that this could be achieved by careful positioning of bipolar stimulating electrodes.

Before investigating the effect of potential plasticity inducing agents, the degree to which plasticity occurs in the absence of treatments was first assessed in F344 rats. The function of corticospinal and sensory pathways was compared in normal animals, acutely lesioned animals, and at 1 week and 3 months after a dorsal column lesion. Corticospinally-evoked CDPs above the lesion were not altered following an acute lesion but were larger in 1 week and 3 month dorsal column lesioned animals than in normal animals. The increase in amplitude was similar in both lesioned animal groups. This suggests that plasticity occurs at the intact connections formed by corticospinal fibres axotomised more distally, that it occurs within a week of the lesion and persisits for at least 3 months.

Corticospinally-evoked CDPs were almost abolished below an acute dorsal column lesion and remained of minimal amplitude 1 week after lesioning. However, there was some recovery of CDPs between 1 week and 3 months. This suggests plasticity either at the connections formed by spared fibres of the minor non-dorsal column components of the corticospinal tract or in propriospinal pathways originating above the lesion. This plasticity has a longer time-course than that at the connections of axotomised fibres above the lesion. Plasticity of the connections formed by larger diameter sensory fibres in the radial nerve was also seen below the level of the dorsal column lesion. This had a similar time course to the plasticity of corticospinal connections above the lesion CDPs being larger both 1 week and 3 months after injury compared to normal animals. A modest enhancement of transmission in both corticospinal and sensory systems therefore occurred following a dorsal column lesion.

To investigate whether OEC transplants enhance plasticity after spinal cord injury, OECs were transplanted such that they became distributed within the spinal cord for several mm either above or below the lesion. Electrophysiological methods were then used, as above, to investigate whether transmission in the corticospinal and sensory fibre systems following a dorsal column lesion was improved in transplanted animals compared to 3 month survival animals. However, corticospinal actions rostral to the lesion were not enhanced by OEC transplants above the lesion and sensory transmission caudal to the lesion was not enhanced by cells below the lesion. OEC transplants are therefore unlikely to support recovery by promoting plasticity in the spinal cord after injury.

To investigate whether antibodies designed to block the function of the myelin inhibitors Nogo and MAG would enhance plasticity following spinal cord injury, antibodies were delivered intrathecally via implanted osmotic minipumps over a period of six weeks following a dorsal column lesion. Vehicle treated and normal animals were investigated for comparison. Placement of the cannula and/or delivery of vehicle alone was found to have a detrimental effect on corticospinal actions above the lesion when compared to normal animals. Treatment with an anti-Nogo antibody (GSK577548) raised against a human Nogo-A fragment and targeting the amino-Nogo terminal was found to enhance transmission of corticospinal actions both above and below the dorsal column lesion. Corticospinal actions above the lesion were significantly greater than in the

vehicle treated controls but did not exceed those in normal animals because of the detrimental effect of the intrathecal cannulae/vehicle treatment. Transmission at the terminals of sensory afferent fibres below the level of the lesion was also enhanced by anti-Nogo treatment. In this case the actions of sensory pathways were significantly greater than those in both vehicle treated and normal animals. The fact that enhanced transmission occurs on the 'wrong side' of the lesion to be explained by axonal regeneration and the sensory transmission is enhanced over normal, strongly suggests that anti-Nogo induces plasticity in spinal pathways. In contrast, treatment with the anti-MAG antibody (GSK249320A) had no effect on either corticospinal or sensory-evoked activity in the spinal cord above or below the lesion, CDPs evoked by these pathways being comparable to that in vehicle treated controls. Anti-MAG does not appear to induce plasticity but may have neuroprotective actions which cannot be adequately tested in this lesion model.

The results show that both corticospinal and sensory fibre systems show modest spontaneous plasticity following a dorsal column lesion. Plasticity at the terminations of axotomised fibres occurs relatively rapidly (within one week) while plasticity in spared systems occurs more slowly. This spontaneous plasticity does not appear to be enhanced by transplants of OECs, so that improvements in spinal cord function previously demonstrated in transplanted animals are probably due to a neuroprotective mechanism. The results obtained using function blocking antibodies targeting myelin inhibitors suggest that anti-Nogo but not anti-MAG treatment may enhance plasticity in the spinal cord after injury. This observation adds to the accumulating evidence that interfering with Nogo-A signalling may be a useful approach for improving function after spinal cord injury.

# Acknowledgements

First of all I would like to say thank you to my supervisor Dr. John Riddell for his encouragement, guidance and support from the very early stage of this research as well as giving me extraordinary experiences throughout the work and write up.

I would like to say thanks to a number of other people who have helped in this project. Thank you to Andrew Toft who has provided help and assistance in numerous ways. Thank you to Dugald Scott for teaching and helping me with the electrophysiology experiments. Thank you to Sue Barnett and Thomas Sardella for providing us with cells. Thank you also to Ryan and Colin for help in animal care. Thank you to my assessor Prof. Andrew Todd. A massive thank you to all people in spinal cord group for all your encouragement and help during my research and write up.

I want to express my gratitude to University of Glasgow and ORSAS for providing the finances necessary to carry out these projects and support me.

I dedicate my thesis to my dear mum, dad, and my family thank you so much for supporting me all these years. I would never have made it here without your faith and support.

**衷心感谢我的父母，焉得谖草，言树之背，养育之恩，无以回报，**

**你们永远健康快乐是我最大的心愿。**

**孝子之至，莫大乎尊亲。——孟子**

# Table of contents

Title page ..... 1
Abstract ..... 2
Acknowledgements ..... 5
Table of contents ..... 7
List of Tables ..... 10
List of Figures ..... 11
Author's declaration ..... 14
Abbreviations ..... 15
1 Introduction ..... 17
1.1 Spinal cord injury ..... 18
1.2 General anatomy of the spinal cord ..... 19
1.3 SCI type and level ..... 22
1.4 Experimental animal models ..... 25
1.4.1 Contusion 25
1.4.2 Compression 26
1.4.3 Transection 26
1.4.4 Chemical-mediated SCI 27
1.5 Pathological events following SCI ..... 27
1.5.1 Blood flow alterations 28
1.5.2 Oedema 29
1.5.3 Inflammatory response 30
1.5.4 Apoptosis and excitotoxicity 31
1.5.5 Axonal degeneration and demyelination 32
1.5.6 The glial scar 32
1.5.7 Cavity 33
1.6 Spontaneous recovery ..... 34
1.7 Repair Strategies ..... 40
1.8 Therapeutic approaches ..... 40
1.8.1 Neuroprotection 41
1.8.2 Neurotrophins 43
1.8.3 Myelin inhibitors 44
1.8.4 Scar inhibitors 53
1.8.5 Modulation of the immune system 55
1.8.6 Rho pathway antagonists 55
1.8.7 Cell transplantation 56
1.8.8 Conditioning stimulation 63
1.8.9 Impulse propagation 63
1.9 Anatomy of rat spinal cord ..... 63
1.9.1 Corticospinal tract 64
1.9.2 Ascending pathways in the dorsal columns of the spinal cord 67
2 Response of sensorimotor pathways to injury -spontaneous plasticity ..... 70
2.1 Introduction ..... 71
2.2 Methods ..... 73
2.2.1 Animals 73
2.2.2 Lesioning 73
2.2.3 Eelectrophysiological experiment 75
2.2.4 Histological processing 83
2.2.5 Microscopy 84
2.2.6 Off-line analysis of electrophysiology 85

2.2.7 Statistical analysis 85
2.3 Results ..... 86
2.3.1 Spinal cord function assessed by electrophysiology 86
2.3.2 Lesion 99
2.4 Discussion ..... 100
Methodological considerations 100
Maximal activation of afferent systems 100
Maximal activation of sensory afferents 100
Maximal activation of the corticospinal tract 102
Does axotomy affect the excitability of corticospinal fibres in the pyramids? 105
Validity of using CDPs as a measure of the strength of synaptic connections in spinal pathways 106
Evidence for spontaneous plasticity of the corticospinal tract after dorsal column lesions 107
Corticospinal tract plasticity above a dorsal column lesion 108
Corticospinal tract plasticity below a dorsal column lesion 109
Spontaneous plasticity in sensory circuits below the level of a dorsal column lesion 111
3 Effects of OEC transplants on sensorimotor pathways following injury ..... 157
3.1 Introduction ..... 158
3.2 Methods ..... 161
3.2.1 Animals 161
3.2.2 Cell culture 161
3.2.3 Lesioning 172
3.2.4 Acute cell transplantation 172
3.2.5 Electrophysiology 174
3.2.6 Histological processing 177
3.2.7 Microscopy 178
3.2.8 Off-line analysis of electrophysiology 179
3.2.9 Statistical analysis 180
3.3 Results ..... 181
3.3.1 Distribution of OECs in cervical spinal cord 181
3.3.2 Spinal cord function assessed by electrophysiology 181
3.3.3 Lesion size 186
3.4 Discussion ..... 187
Cell transplants 187
Lack of electrophysiological evidence for sprouting 188
Sensitivity of electrophysiological recording for detecting plasticity 188
Are the cells optimally located? 189
Comparison with previous evidence for sprouting 190
Does the injection process or presence of OECs have any detrimental effect? 191
Significance of findings in relation to previous electrophysiological observations on OEC transplanted animals 192
4 Effects of anti-Nogo and anti-MAG on sensorimotor pathways following injury ..... 214
4.1 Introduction ..... 215
4.2 Methods ..... 216
4.2.1 Animals 216
4.2.2 Antibody preparation 216
4.2.3 Lesioning, intrathecal cannulation and pump implantation 218
4.2.4 Electrophysiology 220

4.2.5 Histological processing 221
4.2.6 Microscopy 221
4.2.7 Off-line analysis of electrophysiology 221
4.2.8 Statistical analysis 221
4.3 Results ..... 222
4.3.1 Distribution of antibodies 222
4.3.2 Spinal cord function assessed by electrophysiology 223
4.4 Discussion ..... 228
Distibution of antibodies 228
Corticospinal and sensory CDPs in Sprague-Dawley compared to Fisher 344
animals 228
Effect of intrathecal cannulae and vehicle treatment 229
Effect of anti- Nogo treatment 229
Effect of anti-MAG treatment 230
Mechanisms of Nogo-induced plasticity - anatomical vs synaptic plasticity 231
Does plasticity occur in spared fibres or only axotomised fibres? 231
Does anti-Nogo treatment induce plasticity in contusion models of spinal cord injury? 232
Over what distance is plasticity induced following intrathecal delivery of anti-Nogo? 232
Is anti-Nogo treatment as effective after a delay? 233
Duration of anti-Nogo induced plasticity 234
Does Nogo-ab induced plasticity translate into improved sensorimotor function? 234
5 Final discussion and future directions..... 260
List of References ..... 266

# List of Tables

Table 2-1 Number of animals of each group for which histological verification of pyramidal electrode position was performed……112
Table 2-2 Threshold stimulus intensities for evoking CDPs on stimulation in the pyramids……113
Table 2-3 Amplitudes of maximal corticospinally-evoked CDPs following stimulation at different locations……114
Table 2-4 Summary of mean maximal amplitudes of CDPs evoked by pyramidal stimulation and recorded at +5mm……115
Table 2-5 Statistical analysis of the differences between pyramidal-evoked CDPs recorded in different animal groups at each recording location……116
Table 2-6 Contribution of spinal dorsal roots to CDPs……117
Table 2-7 Statistical analysis of the differences between radial nerve-evoked CDPs recorded in different animal groups at each recording location..118
Table 2-8 Quantification of lesion cavity size in the one week survival and three month survival groups……119
Table 3-1 Statistical analysis of the differences between pyramidal-evoked CDPs recorded in different animal groups at each recording location……193
Table 3-2 Statistical analysis of the differences between radial nerve-evoked CDPs recorded in different animal groups at each recording location..194
Table 3-3 Quantification of lesion cavity size in different groups……195
Table 4-1 Statistical analysis of the differences between pyramidal-evoked CDPs recorded in different animal groups at each recording location……..236
Table 4-2 Statistical analysis of the differences between radial nerve-evoked CDPs recorded in different animal groups at each recording location..237

# List of Figures

Figure 1-1 Structure of the spinal cord……20
Figure 1-2 The relationship of spinal cord segments and spinal nerves to vertebral column levels……...21
Figure 1-3 Functional deficits at different levels of SCI……..24
Figure 1-4 Pathological events following SCI……...28
Figure 1-5 Main pathological features of a SCI……34
Figure 1-6 Three Nogo isoforms……45
Figure 1-7 Inhibitors and intracellular signalling mechanisms……..…47
Figure 1-8 Schematic representation of the corticospinal reorganization……50
Figure 1-9 The olfactory nervous system……..57
Figure 1-10 Schematic representation of the organization of CST……...65
Figure 1-11 Schematic representation of the organization of ascending pathways……...68
Figure 2-1 Procedure for making dorsal column lesions using a wire knife……..120
Figure 2-2 Radial nerve dissection and stimulation……..121
Figure 2-3 Schematic diagram of preparation of electrophysiological experiments for assessing CDPs……122
Figure 2-4 Schematic diagram showing recording locations for CDPs and examples of CDPs…….....123
Figure 2-5 Conditioning of radial CDPs with pyramidal stimulation……124
Figure 2-6 Examples of CDPs evoked by pyramidal stimulation……..……125
Figure 2-7 Determination of CST conduction velocity in two normal animals…..126
Figure 2-8 Electrical stimulation of the pyramids……..127
Figure 2-9 Stimulus-recruitment curves for animals of the ‘Middle’ electrode placement group……128
Figure 2-10 Stimulus-recruitment curves for animals of the ‘Lateral’ electrode placement group……129
Figure 2-11 Stimulus-recruitment curves for animals of the ‘Medial’ electrode placement group……130
Figure 2-12 Stimulus-recruitment curves for animals of the ‘Midline’ electrode placement group……131
Figure 2-13 Stimulus intensities required to evoke CDPs 95% of maximal at different stimulus locations……132
Figure 2-14 Pyramidal-evoked CDPs recorded from the left and right sides of the spinal cord……...133
Figure 2-15 Stimulus-recruitment curves for CDPs recorded from the left and right sides of the spinal cord while stimulating the pyramids on one side….134
Figure 2-16 Examples of CDPs evoked by pyramidal stimulation in normal animals……135
Figure 2-17 Amplitudes of pyramidal-evoked CDPs recorded in normal animals……136
Figure 2-18 Plots showing the repeatability of CDP recordings……..137
Figure 2-19 Examples of CDPs evoked by pyramidal stimulation in acutely lesioned animals……138
Figure 2-20 Amplitudes of pyramidal-evoked CDPs recorded in acutely lesioned animals……139
Figure 2-21 Examples of CDPs evoked by pyramidal stimulation in one week survival DC lesioined animals……..……...140
Figure 2-22 Amplitude of pyramidal-evoked CDPs recorded in one week survival DC lesioned animals……..141

Figure 2-23 Examples of CDPs evoked by pyramidal stimulation in three months survival DC lesioned animals.....142
Figure 2-24 Amplitudes of pyramidal-evoked CDPs recorded in three month survival DC lesioned animals.....143
Figure 2-25 Examples of CDPs evoked by radial nerve stimulation.....144
Figure 2-26 Examples of CDPs evoked by radial nerve stimulation in normal animals.....145
Figure 2-27 Amplitudes of radial nerve-evoked CDPs recorded in normal animals.....146
Figure 2-28 Examples of CDPs evoked by radial nerve stimulation in acutely lesioned animals .....147
Figure 2-29 Amplitude of radial nerve-evoked CDPs recorded in acutely lesioned animals.....148
Figure 2-30 Examples of CDPs evoked by radial nerve stimulation in one week survival DC lesioned animals.....149
Figure 2-31 Amplitude of radial nerve-evoked CDPs recorded in one week survival DC lesioned animals.....150
Figure 2-32 Examples of CDPs evoked by radial nerve stimulation in three month survival animals.....151
Figure 2-33 Amplitudes of radial nerve-evoked CDPs recorded in three months survival DC lesioned animals.....152
Figure 2-34 Inhibitory control of sensory transmission by the corticospinal tract from a normal animal.....153
Figure 2-35 Inhibitory control of sensory transmission by the corticospinal tract in different groups.....154
Figure 2-36 Inhibitory control of sensory transmission by the corticospinal tract from a lesioned animal.....155
Figure 2-37 Lesion morphology.....156
Figure 3-1 18-day OECs in culture .....196
Figure 3-2 Experimental setup for field potential recording .....197
Figure 3-3 Distribution of OECs 3 months after injections into the dorsal column lesion site.....198
Figure 3-4 Distribution of OECs 3 months after injections above the lesion site.....199
Figure 3-5 Examples of CDPs evoked by pyramidal stimulation in the OEC below group.....200
Figure 3-6 Amplitudes of pyramidal-evoked CDPs recorded in the OEC below group.....201
Figure 3-7 Examples of CDPs evoked by pyramidal stimulation in the medium above group .....202
Figure 3-8 Amplitudes of pyramidal-evoked CDPs recorded in the medium above and OEC above groups.....203
Figure 3-9 Examples of CDPs evoked by pyramidal stimulation in the OEC above group .....204
Figure 3-10 Amplitudes of radial nerve-evoked CDPs recorded in the OEC below group.....205
Figure 3-11 Examples of CDPs evoked by radial nerve stimulation in the OEC below group.....206
Figure 3-12 Examples of CDPs evoked by radial nerve stimulation in the medium above group .....207
Figure 3-13 Amplitudes of radial nerve-evoked CDPs recorded in the medium above and OEC above groups .....208

Figure 3-14 Examples of CDPs evoked by radial nerve stimulation in the OEC above group .....209
Figure 3-15 Field potential recordings from a normal animal .....210
Figure 3-16 Field potential recordings from above the lesion in a 3 month dorsal column lesioned animal.....211
Figure 3-17 Field potential recordings from below the lesion in a 3 month dorsal column lesioned animal .....212
Figure 3-18 Lesion morphology of transplanted animals.....213
Figure 4-1 Schematic diagram of study design.....238
Figure 4-2 Localisation of intrathecal cannulae for antibody delivery.....239
Figure 4-3 Distribution of anti-Nogo within the spinal cord after intrathecal delivery at 5 weeks.....240
Figure 4-4 Distribution of anti-MAG within the spinal cord after intrathecal delivery at 5 weeks.....241
Figure 4-5 Distribution of antibodies within the spinal cord at 8 weeks.....242
Figure 4-6 Examples of pyramidal stimulus-recruitment curves and corresponding electrode positions for SD animals.....243
Figure 4-7 Examples of CDPs evoked by pyramidal stimulation in normal animals.....244
Figure 4-8 Amplitudes of pyramidal-evoked CDPs recorded in the normal group .....245
Figure 4-9 Examples of CDPs evoked by pyramidal stimulation in the vehicle treated group.....246
Figure 4-10 Amplitudes of pyramidal-evoked CDPs recorded in the vehicle treated group.....247
Figure 4-11 Examples of CDPs evoked by pyramidal stimulation in the anti-Nogo treated group.....248
Figure 4-12 Amplitudes of pyramidal-evoked CDPs recorded in the anti-Nogo treated group.....249
Figure 4-13 Examples of CDPs evoked by pyramidal stimulation in the anti-MAG treated group.....250
Figure 4-14 Amplitudes of pyramidal-evoked CDPs recorded in the anti-MAG treated group.....251
Figure 4-15 Examples of CDPs evoked by radial nerve stimulation in the normal animal group.....252
Figure 4-16 Amplitudes of radial nerve-evoked CDPs recorded in normal SD animals compared to F344's.....253
Figure 4-17 Examples of CDPs evoked by radial nerve stimulation in the vehicle treated group.....254
Figure 4-18 Amplitudes of radial nerve-evoked CDPs recorded in the vehicle treated group.....255
Figure 4-19 Examples of CDPs evoked by radial nerve stimulation in the anti-Nogo treated group.....256
Figure 4-20 Amplitudes of radial nerve-evoked CDPs recorded in the anti-Nogo treated group.....257
Figure 4-21 Examples of CDPs evoked by radial nerve stimulation in the anti-MAG treated group.....258
Figure 4-22 Amplitudes of radial nerve-evoked CDPs recorded in the anti-MAG treated group.....259

# Author's declaration

I declare that this thesis comprises my own original work, except where otherwise stated, and has not been accepted in any previous application for a degree. All sources of information have been referenced.

Tao Meng

September 2009

# Abbreviations

| | |
|---|---|
| °C | Degrees Celsius |
| µ | Micro ($10^{-6}$) |
| Ω | Ohm |
| A | Ampere |
| d | Day (s) |
| gm | Gram |
| h (r) | Hour (s) |
| i.m. | Intramuscular injection |
| i.t. | Intrathecal |
| i.v. | Intravenous injection |
| k | Kilo ($10^{3}$) |
| l | Litre |
| m | Milli ($10^{-3}$) |
| M | Molar |
| min | Minute (s) |
| mm | Millimeter |
| n | Number |
| s | Second (s) |
| V | Volt |
| ANOVA | Analysis of variance |
| APC | Astrocyte precursor cell |
| ASIA | American Spinal Cord Injury Association |
| ATP | Adenosine-5'-triphosphate |
| BBB | Open-field locomotor rating scale |
| BDA | Biotinylated Dextran Amine |
| BDNF | Brain-derived neurotrophic factor |
| cAMP | Cyclic adenosine monophosphate |
| CDP | Cord dorsum potential |
| ChABC | Chondroitinase ABC |
| CNS | Central nervous system |
| CSPGs | Chondroitin sulphate proteoglycans |
| CST | Corticospinal tract |
| DAPI | 4',6-diamidino-2-phenylindole |
| DMEM | Dulbecco's modified Eagle's medium |
| DMSO | Dimethyl sulfoxide |
| EGFR | Epidermal growth factor receptor |
| FACS | Fluorescence activated cell sorting |
| FBS | Fetal bovine serum |
| GAGs | Glycosaminoglycans |
| GDNF | Glia cell line derived neurotrophic factor |
| GFAP | Glial fibrillary acidic protein |
| GFP | Green fluorescent protein |
| GPI | Glycosyl-phosphatidylinositol |
| GSK | GlaxoSmithKline |
| LIF | Leukaemia inhibitory factor |
| LRR | Lleucine-rich repeat |
| MAG | Myelin-associated glycoprotein |
| NF | Neurofilament |
| NGF | Nerve growth factor |

| | |
|---|---|
| NgR | Nogo-66 receptor |
| NT-3 | Neurotrophin 3 |
| NT-4 | Neurotrophin 4 |
| OEC | Olfactory ensheathing cell |
| OMgp | Oligodendrocyte-myelin glycoprotein |
| PBS | Phosphate buffered saline |
| PKC | Protein kinase C |
| PNS | Peripheral nervous system |
| RHD | Reticulon-homology domain |
| SCI | Spinal cord injury |
| SEMA3 | Semaphorin 3 |
| ROCK | Rho-associated kinase |

# Introduction

## 1.1 Spinal cord injury

The spinal cord is a caudal extension of the brain and its function is the transmission and integration of sensory, motor and autonomic signals. It receives sensory information from skin, muscles, joints and visceral organs, and distributes motor signals to the muscles of the body. Spinal Cord Injury (SCI) interrupts ascending and descending pathways in the white matter of the spinal cord that carry sensory and motor signals to and from the brain. It also damages grey matter in the central part of the spinal cord which causes segmental loss of interneurons and motoneurons. As a consequence, severe SCI can lead to deficits of sensory, motor and autonomic functions, which are usually permanent because the injured spinal cord has a very limited capacity for repair.

It is estimated that the annual incidence of SCI, not including those who die at the scene of the accident, is approximately 1,000 new cases each year, and there are thought to be 40,000 people living with SCI in the UK alone (Spinal Injuries Association, http://www.spinal.co.uk). In the United States, the incidence of SCI has been estimated to be about 40 cases per million of population per year, or approximately 12,000 new spinal cord injuries per year, not including those who die at the scene of the accident. The number of people living with SCI has been estimated to be approximately 259,000 persons in 2008 in the United States, with a range of 229,000 to 306,000 persons (Spinal Cord Injury Information Network, http://www.spinalcord.uab.edu). In China, the incidence of SCI was recently estimated to be as high as 65 cases per million of population per year in urban areas. If so, assuming a population of 1.3 billion, this would suggest an incidence of 84,500 per year. The annual global incidence of SCI in developed countries varies from 11.5 to 57.8 per million when only patients that survived before hospital admission were included (Reviewed by Ackery et al. 2004), and since the long-term survival is improved in developed countries, there are a large number of people who are chronically disabled by SCI.

A SCI can be caused by a number of factors, from traffic accidents through to sporting activities and diseases. However, traffic accidents including motor vehicle, bicycle, and pedestrian, account for approximately half of reported SCI

cases (Lenehan et al. 2009). The majority of patients are 20–40 years old at the time of the injury. Recently, it appears that developed countries have higher mean ages at the time of SCI because of higher life expectancies and advance medical care, compared to less developed countries. It has been well documented that SCI in males is more prevalent than in females (Reviewed by Ackery et al. 2004; Lenehan et al. 2009).

The majority of injuries lead to paralysis, and the effects of such an injury can be a disaster to individuals living with SCI and their families who are faced with not only the challenge of coming to terms with the injury, but also rebuilding their lives with a disability. Apart from the physical, emotional and social costs of SCI, the actual monetary costs are relatively high. The average yearly health care and living expenses and the estimated lifetime costs that are directly attributable to SCI vary greatly according to severity of the injury (Harvey et al. 1992). Moreover, indirect costs have to be considered, such as losses in wages, fringe benefits and productivity.

Mortality rates are significantly higher during the early stage after injury than during subsequent years (Reviewed by Strauss et al. 2006). Age, level of injury, and neurological grade are the most important premorbid factors for survival after SCI. Before World War II , most people with SCI died within a few weeks after injury because of respiratory infection, urinary dysfunction or bedsores, and other complications (DeVivo et al. 1999). With the advent of modern medicine and better procedures for dealing with SCI, life expectancy for people with SCI continues to increase, and is now approaching that for the general population. Recent studies show that the leading cause of death after SCI is now respiratory complications (Strauss et al. 2006; DeVivo et al. 1999).

## 1.2 General anatomy of the spinal cord

The spinal cord is contained within the vertebral column which supports and protects the vulnerable cord. In addition, the spinal cord is covered by three meninges (the outer dura mater, the arachnoid mater, and the innermost pia mater) and surrounded by cerebral spinal fluid which acts as a cushion to protect the delicate cord (Figure 1-1).

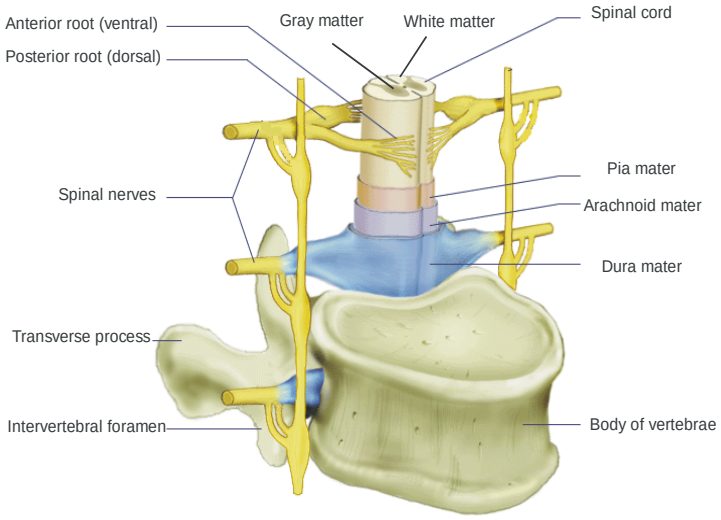


**Figure 1-1 Structure of the spinal cord**
The spinal cord is protected by the vertebral column and three meninges: the dura mater, the arachnoid mater, and the pia mater. The anterior roots (motor nerve roots) exit from ventral aspect of the spinal cord while the posterior roots (sensory nerve roots) enter the dorsal aspect. These two roots join to form paired spinal nerves. In cross section, the spinal cord is composed of a centrally placed butterfly- or H-shaped area of grey matter surrounded by white matter. The grey matter of the cord contains primarily the cell bodies of neurons and glia. The white matter of the cord contains primarily fibre tracts (adapted from online information www.mmi.mcgill.ca).

The human spinal cord is divided into 31 segments: 8 cervical segments, 12 thoracic segments, 5 lumbar segments, 5 sacral segments and 1 coccygeal segment (Afifi and Bergman 2005). The segmental levels of the spinal cord do not relate exactly to that of the corresponding vertebral bones at all levels of the cord. For example, the sixth cervical spine corresponds to the level of the seventh spinal cord segment in the cervical region, the fourth thoracic spine corresponds to the sixth cord segment in the thoracic region, and the tenth thoracic spine corresponds to the first lumbar cord segment in the lower thoracic and lumbar regions (Afifi and Bergman 2005) (Figure 1-2).

There are two enlargements along the spinal cord: the cervical enlargement (third cervical to second thoracic segments) and the lumbosacral enlargement (first lumbar to third sacral segments). These two enlargements are sites of

neurons that innervate the upper and lower limbs respectively (Afifi and Bergman 2005).

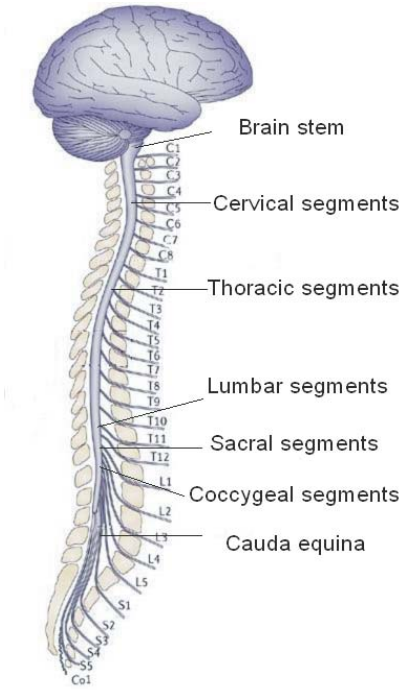


**Figure 1-2 The relationships of spinal cord segments and spinal nerves to vertebral column levels**

The spinal cord is segmentally arranged: 8 cervical segments, 12 thoracic segments, 5 lumbar segments, 5 sacral segments and 1 coccygeal segment. It is encased in vertebral bone. In the 3-month foetus, the spinal cord and vertebral canal are the same length but the vertebral canal grows more rapidly so that in the adult the cord extends from the foramen magnum to the level of the first or second lumbar vertebra. Thus, the adult spinal cord occupies only the upper two-thirds of the vertebral canal. 31 pairs of spinal nerves emerge from the cord and, since the adult spinal cord is shorter than the vertebral canal, these nerve roots descend in the canal, with increasing obliquity and length, to reach their appropriate intervertebral foramina, through which they exit the canal. The lumbar and coccygeal nerves are the longest and descend beyond the end of the spinal cord as the cauda (adapted from Bradbury and McMahon 2006).

The spinal cord, which consists of millions of nerve fibres, is the major pathway for transmitting information to and from the limbs, trunk and organs of the body. The motor nerve roots exit from the ventral aspect of the spinal cord while the sensory nerve roots enter the dorsal aspect. These two roots join to form paired spinal nerves (Figure 1-1). A pair of spinal nerves exits from each

segment of the spinal cord and they are numbered according to the corresponding spinal segment. Spinal nerves carry information from the spinal cord to the rest of the body. Cervical nerves are responsible for movement of, and feeling in, the arms, neck and upper trunk. Thoracic nerves transmit signals to and from the trunk and abdomen, while lumbar and sacral nerves carry information to and from the legs, the bladder, bowel and sexual organs (Afifi and Bergman 2005) (Figure 1-2).

## 1.3 SCI type and level

The exact effects of a SCI depend on the type and level of the injury. SCIs can be divided into two types depending on neurological evidence of sparing of sensory and/or motor functions: complete and incomplete injuries. In a complete injury, there is no sensation or voluntary movement below the level of the injury which is defined as the lowest level that has normal neurological function. An incomplete injury means that there is some sort of functionality below the level of the injury, which could be sensory or motor or both.

According to the American Spinal Cord Injury Association's (ASIA) International Standards for Neurological Functional Classification of Spinal Cord Injury (revised 2002) (http://www.asia-spinalinjury.org), SCIs can be classified into five different degrees from A to E based on neurological levels, touch and pinprick tests of sensory function and strength of key muscles on both sides of the body after injury. A=complete: no motor or sensory function is preserved in the sacral segment S4-S5. B=incomplete: sensory but not motor function is preserved below the neurological level and includes the sacral segments S4-S5. This is usually a transient phase and if there is any motor function recovered below the neurological level, it becomes a motor incomplete, i.e. ASIA C or D. C=incomplete: motor function is preserved below the neurological level, and more than half the key muscles below the neurological level have a muscle grade less than 3. D=incomplete: motor function is preserved below the neurological level, and at least half the key muscles below the neurological level have a muscle grade of 3 or more. E=normal: motor and sensory functions are normal.

Based on the ASIA scale, approximately two thirds of SCIs were complete forty years ago. Nowadays, incomplete SCIs are becoming more common with approximately 55% of injuries being of this type because of the improved initial care and retrieval systems, greater awareness of the importance of immobilization after injury, use of air bags in vehicles, and hospital treatments to limit secondary injury such as administration of steroid drugs to reduce inflammation (Strauss et al. 2006).

The part of the body from which function may be lost can determine the level of a SCI. SCIs occurring in the cervical region account for a relatively high percentage of approximately 51%; while SCIs in every other region, i.e. thoracic region, thoracolumbar region and lumbosacral region, contribute approximately equally (Lenehan et al. 2009). Cervical SCIs usually result in quadriplegia while thoracic level injuries or below result in paraplegia (Figure 1-3). Quadriplegia, also known as tetraplegia, is a symptom in which a person suffers paralysis affecting all four limbs after SCIs, although not necessarily complete paralysis or loss of function. In addition to the arms and legs being paralyzed, the abdominal and chest muscles will also be affected resulting in breathing deficits and inability to cough properly. Paraplegia is when the injury occurs below the level of the first thoracic spinal nerve. The degree of paralysis can vary from the impairment of leg movement to complete loss function of the legs and abdomen up to the nipple line. However, paraplegics have full function of their arms and hands (Figure 1-3).

Lumbar and sacral injuries (L1-S5) result in a decreased control of the legs and hips, urinary system, and anus. Partial paralysis of lower body and legs can be seen in lower thoracic injuries (T9-T12). However, unlike lower thoracic injuries, upper thoracic (T1-T8) injuries result in poor trunk control as the result of lack of abdominal muscle control. In addition, the function of sympathetic nervous system may be compromised. People with injuries at the thoracic level or below usually have full control of the hands. Individuals with C7-T1 injuries may have arm control but not complete control of hands and fingers. C7 is generally the highest injury level where the patients are able to live relatively independently. C6 injuries allow wrist control but no hand and finger function. A passive key grip may be present by flexing the wrist backwards, but will be weak. C5 injuries usually result in only shoulder and biceps control, no control at the wrist or

hand. Individuals with C4 injuries may have some use of biceps and shoulders, but weaker. In higher cervical injuries, above the C3 level, patients typically lose diaphragm function and require a ventilator to breathe. The head and neck movements usually are affected depending on residual muscle strength (International Standards for Neurological and Functional Classification of Spinal Cord Injury 2002) (Figure 1-3). In addition to these symptoms, people with SCI will often suffer other complications such as spasticity and neuropathic pain (Burchiel and Hsu 2001).

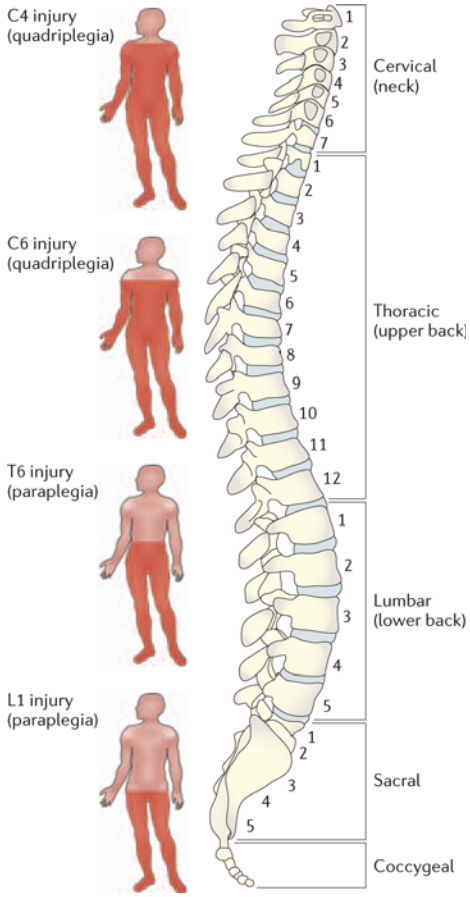


**Figure 1-3 Functional deficits at different levels of SCI**
The symptoms of SCI depend on two factors: where the damage occurs and how serious it is. Cervical spinal cord injuries usually result in quadriplegia while thoracic level injuries or below result in paraplegia. Quadriplegia is a symptom in which a person suffers paralysis affecting all four limbs after SCI, although not necessarily complete paralysis or loss of function. Paraplegia is when the injury occurs below the level of the first thoracic spinal nerve, which leads paralysis of the lower half of the body. Paraplegics have full function of their arms and hands. The area of paralysis is indicated in red (taken from Thuret et al. 2006).

Depending on the mechanical mechanisms of the injury, several physically distinct types of injuries are recognized. When sudden and violent jolts injure the nearby tissues of the spinal cord, a temporary spinal concussion occurs. This type of injury stays only for a few hours. If the violent force injures the spinal cord directly, a contusion or bruise may happen. It causes bleeding in the spinal canal and a range of further secondary damage, details which are described below. A spinal compression occurs when an object, such as a tumour, occupies some space in the bony vertebral column and gives pressure to the spinal cord. The spinal cord can be cut such as following a knife injury. Spinal transection describes the complete severing of the cord (Bohlman et al. 1992).

## 1.4 Experimental animal models

The need to be able to investigate the mechanisms and possible treatments for SCI has led to the development of different types of animal models. Since there is no particular model that completely addresses all aspects of traumatic SCI, a number of models ranging from sharp transections to blunt contusions have been developed in a variety of animal species.

Among animal species used for SCI models, the rat and mouse are the most common animals because of cost, accessibility, ease of care, low susceptibility to infections and well-established techniques for functional analysis (Onifer et al. 2007; Rice et al. 2007; Toft et al. 2007). The mouse is becoming more popular because of its transgenic potential (Carter et al. 2008; Simonen et al. 2003; Kim et al. 2003; Zheng et al. 2003). Larger mammals such as dogs, pigs, and cats, (Blight and Young 1989; Blight 1991) have also been used occasionally and primate experiment may be necessary to prove safety and efficacy before clinical trials (Freund et al. 2006; 2007).

### *1.4.1 Contusion*

After the first well-documented weight drop model by Allen in 1911, a range of animal models in different species have been developed to produce a blunt contusive force to the spinal cord, which simulates the evolution of neuropathology after SCIs in humans (Wrathall et al. 1985; Soblosky et al. 2001).

The contusion model provides a good setting for evaluating neuroprotective strategies, plasticity and demyelination. However, it is not an ideal model for investigation of regeneration due to the incomplete nature of the injury and the complexity of the tracts. With continuous refinements, current contusion models, including New York University Impactor (NYU device) (Gruner 1992), Ohio State University Impactor (OSU device) (Noyes 1987) and Infinite Horizon Impactor (IH) (Scheff et al. 2003), can optimize the consistency and precision of the mechanical forces applied during the injury, generate different degrees of injury severity and functional outcomes by monitoring injury parameters such as impact velocity and tissue displacement, and also are relatively easy to perform because of highly refined devices. The contusion model has become one of the most commonly used and well developed injury models.

### *1.4.2 Compression*

Because most contusion devices deliver a rapid impact to the spinal cord, they do not simulate ongoing cord compression secondary to residual spinal column displacement. A clip compression model was developed to produce static compression injuries, in which a relation between the severity of neurological injury and the duration of compression was illustrated (Rivlin and Tator 1978). Blight (1991) developed a moderate-severity injury technique in the guinea pig using modified forceps which produces a relatively larger volume of tissue compression and displacement than the clips. As in the contusion model, the compression model can also produces different severities of SCI by adjusting the closing force of the clips or forceps and/or duration. The compression model is valuable for investigation of the acute pathophysiology after cord injury, the timing of decompression, and potential therapies such as neuroprotective agents.

### *1.4.3 Transection*

Partial or complete transections of the spinal cord have also been frequently used to model SCI. Because these models can effectively disconnect designated axonal pathways at required levels of the cord, they mainly are applied for testing axonal regeneration that is impossible to assess from contusion or

compression models, in which many axons are invariably spared (Liu et al. 1999; Gauthier et al. 2002; Polentes et al. 2004). Transection models produce relatively consistent injuries compared to contusion and/or compression models. In a complete transection model, the completeness of the injury provides an easy way to determine the degree of the axonal regeneration and functional recovery (López-Vales et al. 2006; Steward et al. 2006; Coumans et al. 2001). In a partial transection model produced by a variety of techniques, a selected tract is cut in order to collect information about this specific tract (Toft et al. 2007; Lu et al. 2006). Compared to a complete transection, a partial transection is milder and therefore the postoperative animal care is easier, especially regarding bladder care. A unilateral partial transection model also allows comparison of the responses in a particular tract with its uninjured counterpoint on the contralateral side (Xu et al. 1999).

### *1.4.4 Chemical-mediated SCI*

Chemically-mediated SCI models also exist. They are not so widely used but can be employed to model specific aspects of the secondary injury cascade, demyelination, or to induce ischemia (Cameron et al.1990; von Euler et al 2002).

## 1.5 Pathological events following SCI

Information from clinical injuries on the pathological events following SCI is relatively limited so that most of our understanding of this area comes from experiments on animals. Injury to the spinal cord triggers a complex series of biological events which are summarized in Figure 1-4.

SCI includes two stages: primary and secondary injury processes. The primary injury process, initial mechanical injury due to local deformation and energy transformation, is quickly followed by a series of time-dependent pathophysiological changes, i.e. the secondary injury process, including blood flow changes, excitotoxicity, oedema, inflammation, demyelination, axotomy, axonal degeneration and dieback, and apoptotic cell death (Dumont et al. 2001a) (Figure 1-4). Most participating cells reside in the spinal cord while others

are recruited from the circulatory system to the injury site (Schwab and Bartholdi 1996).

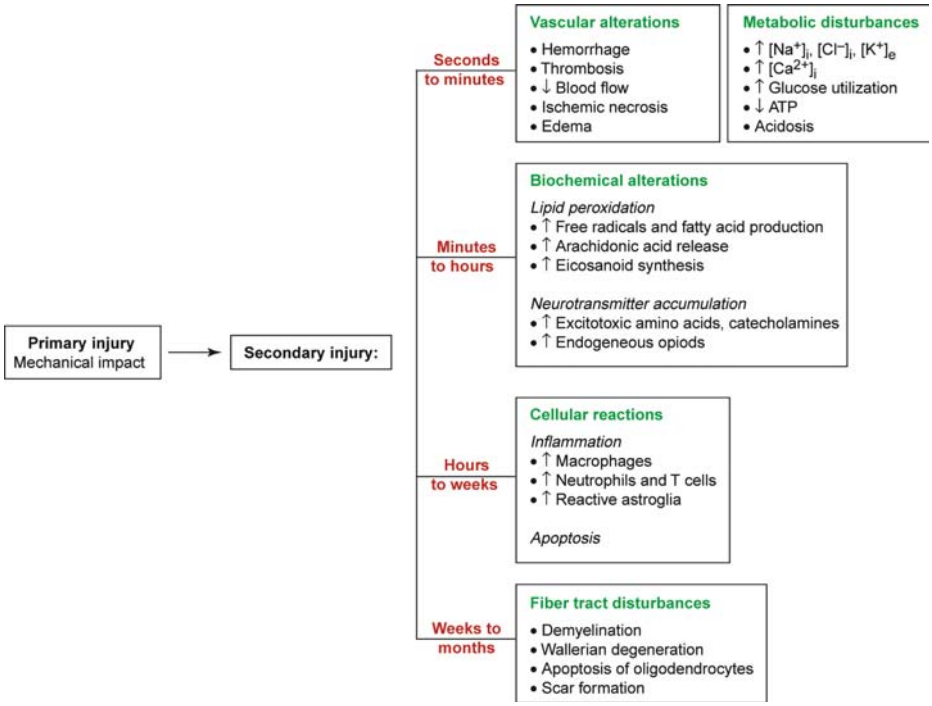


**Figure 1-4 Pathological events following SCI**
SCI includes two stages: primary and secondary injury processes. The primary injury process, initial mechanical injury due to local deformation and energy transformation, is quickly followed by a series of time-dependent pathophysiological changes, i.e. the secondary injury process, including blood flow changes, excitotoxicity, oedema, inflammation, demyelination, axotomy, axonal degeneration and dieback, and apoptotic cell death (taken from Bareyre and Schwab 2003).

### *1.5.1 Blood flow alterations*

SCI disrupts the blood flow at the actual injury site and also changes blood flow in the vicinity of the injury site. The damage of the regional blood vessels is vital for the evolution of destructive events during the secondary injury process (Mautes et al. 2000). Breakdown of the blood brain barrier that normally helps protect the central nervous system (CNS) at the site of SCI results in the influx of inflammatory cells (see below; Bareyre and Schwab 2003).

Haemorrhage occurs when injury disrupts blood vessels, which is a common feature in both experimental models and in human SCIs (Mautes et al. 2000; Tator and Koyanagi 1997). Haemorrhage is usually found in the central region of the injured cord, especially the grey matter (Mautes et al. 2000). The majority of these haemorrhages are relatively small. Occasionally, major bleeding termed as haematoma can be seen in the cord following contusion or laceration injuries.

Vasospasm, which is a narrowing of the blood vessels that can often decrease blood flow by up to 80 percent (Anthes et al. 1996) and small vessel thrombosis, can lead to ischemia, which deprives neurons and other cells of the oxygen and other nutrients they need to survive (Tanaka et al. 2005). Most cell types produce reactive oxygen species and other free radicals during the ischemic period, which have been shown to be crucial in the progressive death of cells after SCIs (Cayli et al. 2004; Usul et al. 2004). Inadequate flow of oxygen and nutrients into the spinal tissue can contribute to spinal shock, which is a stage of failure of the spinal cord to function within the first few weeks after injury (Krassioukov and Claydon 2006).

Complete cervical injuries can cause systemic changes to the cardiovascular system including bradycardia and hypotension that can lead to further damage to the cord (Krassioukov and Claydon 2006; Guízar-Sahagún et al. 2004).

### *1.5.2 Oedema*

Rapid bleeding into the normal fluid-filled spaces of the spinal cord contributes to local oedema, which can be easily observed at the injury site very soon after SCI (Griffiths and Miller 1974) and reaches maximum in the first days after injury. Oedema starts from the central portion of the cord and then spreads into white matter of the cord (Noble and Wrathall 1989). It can also spread for a considerable distance rostrally and caudally from the injury site in both experimental models and clinical patients (Wang et al. 1993). The most important of the various factors contributing to oedema is the increased permeability of blood vessels around the injury site. It is suggested that oedema exerts deleterious effects probably by providing an abnormal environment and compressing the local tissue (Balentine 1985).

### *1.5.3 Inflammatory response*

The inflammatory response, which involves four major categories of immune cells: neutrophils, monocytes, microglia, and T-lymphocytes, begins within hours after SCI and reaches its peak within the first few days (Schnell et al. 1999; Bareyre and Schwab 2003). This complex process includes the release of chemical mediators, epithelial damage, changes of vascular permeability, oedema, activation of microglia, and recruitment of peripheral inflammatory cells. The inflammatory cells recruited in the CNS after SCI are much higher and have been infiltrated into wider areas (i.e. not restricted to the lesion site) compared to those following brain injury (Schnell et al. 1999; Donnelly and Popovich 2008).

It is commonly believed that inflammation has both destructive and constructive effects to the cord (Bethea 2000). On the one hand, improved functional recovery can be observed by reducing inflammatory response (Stirling et al. 2004). On the other hand, cellular debris and breakdown products can be eliminated through inflammation events (Rice et al. 2007; Fleming et al. 2006).

Macrophages are one of the most active cellular factors in the inflammation and have both detrimental and beneficial roles in the progression of SCI and following repair (Bethea 2000). A large number of macrophages produce and secrete cytokines that contribute to further cell death and maintain the inflammatory process. They also produce reactive oxygen species that eventually lead to severe membrane damage. However, the macrophages are also active in constructive events by secreting factors that could promote axonal growth, stimulate Schwann cells proliferation and remove cellular debris after injury, which might improve functional recovery later (Schwartz and Yoles 2005).

Local microglia are also activated in the vicinity of lesion and within tracts that undergo Wallerian degeneration, which represents the anterograde disintegration of axons and their myelin sheaths that have been damaged following injury. These activated microglia secrete various cytokines, nitric oxide, superoxide anions, glutamate, and proteases (Banati et al. 1993), which indirectly induce apoptosis. Moreover, microglia can cause oligodendrocyte death (Li et al. 2005). However, many of the cytokines released by microglia

may have beneficial actions, including inducing neurite sprouting, stimulating the production of nerve growth factor, facilitating CNS regeneration, and neuroprotective actions (DeKosky et al. 1996; Banati et al. 1993; Li et al. 2005). Activation of macrophages and microglia is sustained over the course of weeks.

### *1.5.4 Apoptosis and excitotoxicity*

The mechanical injury to the cord causes some cells to die instantaneously by necrosis, which is a process of cell swelling and then cell membrane rupture. Later on, apoptosis (programmed cell death), another type of cell death in which cells condense and break apart into small fragments in a very orderly process, afflicts many cell types including neurons, oligodendrocytes, astrocytes, and other cells of the spinal cord (Reviewed by Beattie et al. 2000). Injury-induced rush of calcium into cells is the major trigger for apoptosis after injury. Apoptosis has been reported to last for about one month in experimental animals (Crowe et al. 1997), and has also been detected in humans (Emery et al. 1998).

Oligodendrocyte death may occur at the injury site and distant from the impact site after SCI in both humans (Emery et al. 1998) and in experimental animals (Li et al. 1999). As mentioned above, microglia are one important cause of oligodendrocyte death. Along with microglia, loss of trophic supports due to degeneration of axons and an increase in nerve growth factor after injury are causes of oligodendrocyte apoptosis (Beattie et al. 2002; Krenz and Weaver, 2000).

Injury induces the accumulation of the excitatory amino acids glutamate and aspartate with peak levels within the very first minutes (Farooque et al. 1997). All sorts of neural cells in the injured cord are susceptible to excitotoxic cell death. Over-excitation of α-amino-3-hydroxy-5-methylisoxazole-4-propionic acid receptors and N-methyl-D-aspartate receptors may cause the death of neurons (Das et al. 2005). Oligodendrocytes are the most vulnerable cell type, while other glial cells are also susceptible to excitotoxic cell death via α-amino-3-hydroxy-5-methylisoxazole-4-propionic acid and kainite receptors (Rosin et al. 2004).

### *1.5.5 Axonal degeneration and demyelination*

Following injury, the axons may have simply been disrupted, or may be still intact anatomically in the early stage and then degenerate afterwards. Those spared axons are commonly dysfunctional. Lack of vascular and glial support after injury, an ionic imbalance with an influx of calcium, and the inherent reaction of neurons to injury all contribute to the progress of axonal degeneration (Iwata et al. 2004; Araki et al. 2004). The dieback of the severed axons may lead to loss of collateral connections, and therefore minimise residual functions and reduce the degree of ensuing plasticity (see 1.6 spontaneous recovery).

Demyelination is a process whereby myelin has been damaged while the axons are still relatively intact following SCI (Waxman 1989) (Figure 1-5). Literature suggests that primary demyelination occurs early following SCI in experimental animals (Salgado-Ceballos et al. 1998). However, it seems only isolated axons have been affected in human SCIs (Norenberg et al. 2004). The ensuing demyelination has strong negative effects on the normal function of surviving axons, which contributes to the functional deficits of SCI.

### *1.5.6 The glial scar*

The formation of the glial scar after injury is a complex event in which various cell types may be involved such as activated astrocytes, microglial cells, oligodendrocytes, inflammatory cells and connective tissue (Reviewed by Fawcett and Asher 1999) (Figure 1-5). Astrocytes are the most commonly found and important cell type in the evolution of CNS scars. Following injury, astrocytes become activated and proliferate to form a solid network surrounding the lesion site (Faulkner et al. 2004).

The glial scar is not only a physical barrier for regeneration, but also can release inhibitory factors which inhibit axon outgrowth. The extracellular matrix molecules associated with the glial scar have potent growth inhibitory properties in vitro and therefore may contribute to the non-permissive environment of the glial scar (Fawcett and Asher 1999; Davies et al. 1999). It has been shown that the impairment of axonal regeneration by the glial scar also occurs in immature

CNS. However, scar formation is much less severe than in the adult system (Firkins et al. 1993).

In addition to the non-permissive effects on axonal regeneration, the glial scar might have some beneficial effects such as repair of the blood-brain barrier, limiting cellular degeneration and inflammation (Faulkner et al. 2004; Rolls et al. 2009). Moreover, the glial scar isolates the injury site from surrounding healthy tissue (Figure 1-5).

### *1.5.7 Cavity*

Over time, the lesion site begins to form a fluid-filled cavity in the centre. In animal models, it may extend several segments above and below the site of injury within a few weeks (Figure 1-5). The injury may develop a single, multiloculated or multiple cavities in humans. These cavities are filled with extracellular fluids which contain residual macrophages, small pieces of connective tissue and blood vessels (Norenberg et al. 2004).The cavity represents the final healing phase of the necrotic process and provides a physical gap that impedes axon regeneration. About 4% of individuals with SCI develop syringomyelia, which results from the extension of a cavity or coalescence of a few small cavities in the centre of the spinal cord over time from as early as 2 months to as late as 30 years after injury (Schurch et al. 1996).

SCIs are usually relatively stable after a period of weeks to months. The injury site following SCI develops typically characterized by axotomized nerve fibres, a fluid-filled cavity surrounded by a glial scar which engulfs inhibitory molecules, and variable amounts of intact tissue surrounding the lesion. In this peripheral rim of intact tissue harbours spared fibres that are either uninjured or demyelinated (Figure 1-5).

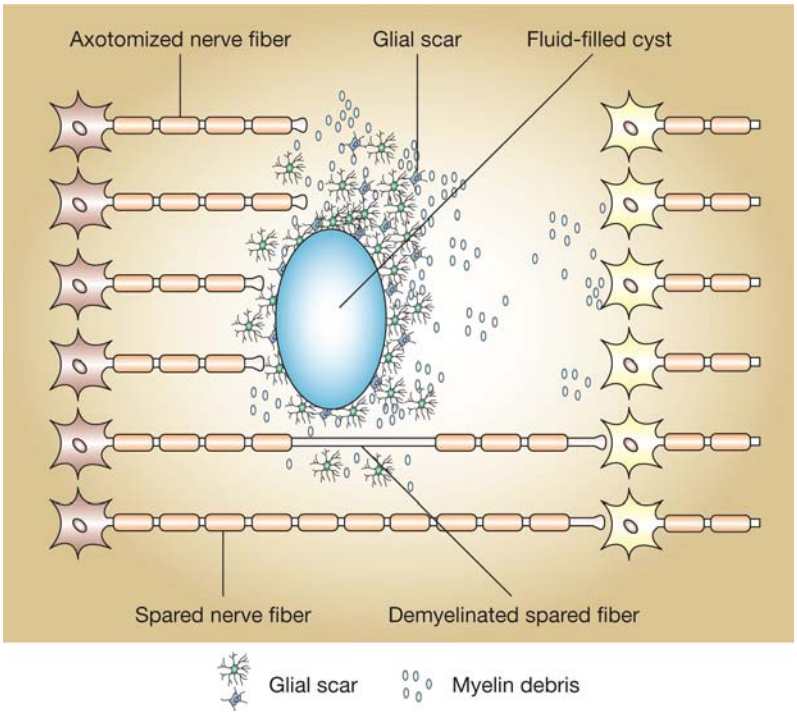


**Figure 1-5 Main pathological features of a SCI**
Following SCI, large numbers of nerve fibres become axotomized, interrupting communication in the long ascending and descending pathways responsible for normal motor, sensory and autonomic functions. Axotomized fibres are prevented from regenerating by inhibitory molecules associated with myelin debris and the glial scar, which is composed of reactive astrocytes and a variety of other cell types. Over time, a fluid-filled cyst can develop at the site of injury, forming a physical barrier to regeneration. If the injury is incomplete, spared fibres can provide some residual function. Impulse conduction along some of these fibres might, however, be compromised by demyelination (taken from Barnett and Riddell 2007).

## 1.6 Spontaneous recovery

SCI causes obvious functional deficits in the early stage of the course of lesion evolution in clinical patients. Although spontaneous regeneration of lesioned fibres is very limited in the adult CNS, some functional recovery below the initial spinal injury level can be observed in almost all SCIs during a period of days, weeks or even years after the injury (Reviewed by Fawcett et al. 2007; Burns et al. 1997).

The spontaneous recovery of motor function in people with complete SCIs is limited and predictable (Fisher et al. 2005; Brown et al. 1991). However, it is relatively substantial and highly variable in incomplete SCI patients (i.e. ASIA C and ASIA D) (Ditunno et al. 2000; Burns et al. 1997). The extent of this motor functional recovery is nearly complete in some but very limited in others. The rate of spontaneous motor recovery is rapid during the first few months, and almost reaches the peak by 9 months. However, a small amount of ongoing recovery can persist for up to 18 months or occasionally longer. Some sensory recovery can also be seen after the initial injury over the same time course as motor recovery. Once there is no further improvement in functional capacity, the injury is considered to be stable (Fawcett et al. 2007).

The severity of the initial injury has a strong impact on the following spontaneous recovery. Data from US Model systems Sygen and EMSCI databases show that the majority of ASIA A patients remain as ASIA A, with about 10% regaining some sensory function (ASIA B) and about 10% converting to ASIA C (some motor function) over the first year after SCI. However, patients initially classed ASIA B or C showed greater spontaneous recovery compared to ASIA A patients; about 15-40% of ASIA B patients showed a conversion to ASIA C, and 40% to ASIA D. ASIA C conversion to D was between 60-80% of all the patients examined. Very few ASIA D patients converted to ASIA E (reviewed by Fawcett et al. 2007).

Spontaneous functional recovery can also be seen in experimental animal models of incomplete SCI (McKenna and Whishaw 1999; Weidner et al. 2001; Bareyre et al. 2004; Courtine et al. 2005; Ballermann and Fouad 2006; Gulino et al. 2007). However, the degree and time course of spontaneous functional recovery vary from species to species. It also depends on the level and severity of the lesion (Noble and Wrathall 1989).

In rats, a number of behavioural tests and electrophysiological techniques are available to evaluate function outcomes. Different tests are applied for assessing different functions in different models of SCI. A pellet retrieval test may be chosen to assess reaching and grasping functions in cervical SCI models (McKenna and Whishaw 1999; Weidner et al. 2001). The cylinder test is used to examine forelimb and forepaw usage for support during spontaneous vertical exploration

after cervical SCIs (Liu et al. 1999). Gait analysis tests such as catwalk may be chosen for obtaining quantitative information on a range of parameters relating to gait (Hamers et al. 2001). There are also studies for evaluating limb placing and footfalls while the rat walks on a grid, ladder, and beam or rope (Onifer et al. 2007).

The Basso, Beattie, and Bresnahan open-field locomotor rating scale (BBB scale) (Basso et al. 1995) is one of the most commonly used tests to assess locomotion in rats. The BBB scale has a range from zero (no hindlimb movements) to 21 (normal coordinated gait) by analysing paw placement, joint movement, and trunk stability. Scores from zero to 7 focus on joint movement in the hindlimbs, scores from 8 to 13 relate to paw placement and coordination, and scores from 14 to 21 are determined by trunk stability, tail position, and paw placement.

As mentioned above, spontaneous functional recovery also depends on the severity of the original injury. One study suggests that even though spontaneous recovery can be observed in both mild and moderate contusion groups in rats, the differences of average BBB scores between them can be as high as 5 (Collazos-Castro et al. 2006). Another study reported that the BBB score is 0 on post-operative day 1 after spinal hemisection, and then rapidly reaches 11 on post-operative day 7 (Gwak et al. 2004). The prognosis for functional return may be better in experimental animals than in humans because quadruped animals adapt trunk, forelimb and hindlimb movements to compensate for deficits. Therefore, they can walk satisfactorily although probably with poor balance or coordination (Rossignol et al. 2004; Ballermann and Fouad 2006).

The mechanisms behind this spontaneous functional recovery are not fully understood. It has been proved that CNS axons have the intrinsic capacity for regrowth over long distances (David and Aguayo 1981). However, they are inhibited by the unfriendly environment after injury (Davies et al. 1999). The local expression of neurotrophic factors are increased after SCI, but apparently not sufficiently to overcome inhibitory factors and maintain regenerative axonal response (Brown et al. 2004; Oyesiku et al. 1997; Satake et al. 2000). Therefore, axonal regeneration can be excluded from the mechanisms of spontaneous

recovery. Remyelination and plasticity may contribute to this spontaneous functional recovery.

A degree of spontaneous remyelination within the spinal cord probably contributes to functional recovery in experimental animals. Remyelination can occur in two different ways, i.e. by Schwann cells and oligodendrocyte precursors. Schwann cells normally myelinate fibres of the peripheral nervous system (PNS), but migrate into the spinal cord after injury, and then myelinate demyelinated axons (Takami et al. 2002; Imaizumi et al. 2000). Blight and Young (1989) have reported that remyelination by Schwann cells is prevalent in a cat contusion model. Their electrophysiological assessment also showed that the remyelination by Schwann cells is capable of restoring effective action potential conduction in mammalian spinal cord sensory tracts. Oligodendrocyte precursors in the spinal cord also migrate to the site of injury, and differentiate into mature oligodendrocytes and produce myelin (Gensert and Goldman 1997; Yang et al. 2006). The remyelination of spared projections by newly generated oligodendrocytes could contribute to functional recovery.

Plasticity is a generic term that denotes the capacity of the nervous system to change. Neuronal plasticity has been traditionally associated with learning and memory processes in the hippocampal regions of the brain (DeFelipe 2006). It is now generally accepted that plasticity is also associated with cellular changes and modifications occurring in all areas of the CNS after injury including SCI. This reorganization might happen with two different main mechanisms: synaptic plasticity which occurs in pre-existing circuits by modifications of synaptic strength (Gulino et al. 2007) and anatomical plasticity in which new connections arise through sprouting and anatomical reorganization (Bareyre et al. 2004). A number of experiments have been done to investigate plasticity after SCI (reviewed by Raineteau and Schwab 2001; Edgerton and Roy 2002). These experiments show that plasticity has been seen in different types of injuries and different animal models during hours to months after injury. They also show that the CNS is capable of reorganising the circuitry in different levels under certain conditions, i.e. cortical level (Jain et al. 1997), subcortical level and local spinal cord, based on unlesioned fibres in incomplete SCI. Furthermore, it has been proved that this plasticity can contribute to functional recovery in both animal

models and humans (reviewed by Raineteau and Schwab 2001; Edgerton and Roy 2002).

At the cortical level, it is observed that cortical territories controlling intact body parts tend to enlarge and invade cortical regions that have lost their peripheral target regardless of different species, i.e. in experimental and clinical SCI. The structure of the dense network that interconnects the different subregions of the primary motor cortex provides the basis of rapid cortical reorganization. This cortical reorganization includes physiological change and anatomical change. Jain et al (1997) reported that massive cortical reorganization was observed in monkeys with a dorsal column SCI. Some studies (Bareyre et al. 2004; Fouad et al. 2001) also proved that rearrangement of the motor cortical area can be seen following SCI in rats. A reorganization of axonal connections has also been described at the subcortical level (Kaas et al. 1999; McKenna and Whishaw 1999). Bruehlmeier et al (1998) showed that patients with SCI exhibit extensive changes in the activation of cortical and subcortical brain areas during hand movements, irrespective of normal or impaired hand function. The strong activation changes suggest that a reorganization of neuronal activity occurs in patients with SCI. The cortical plasticity was also investigated by using functional magnetic resonance imaging in SCI patients (Jurkiewicz et al. 2007).

Injury induced reorganization has also been seen at the level of spinal cord. Aoki et al (1986) reported that newly formed synapses have been observed on the side of spinal cord hemisection in monkeys. Brus-Ramer et al. (2007) suggested that there is a significant increase in the length of spared ipsilateral corticospinal tract (CST) axons after injury in rats. They also reported that electrical stimulation of spared corticospinal axons augments connections with ipsilateral spinal motor circuits. Weidner et al (2001) reported that spontaneous sprouting of the minor unlesioned ventral CST can be observed after the transection of the main dorsal CST component in rats, and this sprouting correlates with functional recovery. Bareyre et al (2004) reported that a new intraspinal circuit spontaneously formed in rats with incomplete mid-thoracic dorsal hemisection, and confirmed the functionality of this new circuit by electrophysiological and behavioural testing. They also demonstrated that transection of the main dorsal CST component resulted in spontaneous sprouting

of the unlesioned dorsolateral and ventral CST components in a transgenic mouse (Bareyre et al. 2005).

Like the CST, Ballermann and Fouad (2006) showed that spared reticulospinal fibres sprouted caudal to the lesion in rats with lateral thoracic hemisection, and this change correlated to improved locomotor function. However, they did not find changes in the projection of injured fibres rostral to the lesion. Lawrence DG and Kuypers (1968) demonstrated that the unlesioned rubrospinal tract could take over some of the functions of the lesioned CST which is one of the main descending motor tracts in monkeys. Furthermore, indirect propriospinal connections can mediate the functional recovery after severe SCI (Courtine et al. 2008). In addition, spontaneous sprouting of the lesioned axons has been observed in other partial transection models (Fouad et al. 2001), contusion model (Hill et al. 2001), and ischemic injury model (von Euler et al. 2002).

However, it should be kept in mind that plasticity in the injured spinal cord does not always result in a positive outcome. For instance, sprouting of uninjured sensory afferents is thought to contribute to two serious and debilitating consequences of SCI in humans, i.e. autonomic dysreflexia (Weaver et al. 2006) and pain (Finnerup and Jensen 2004).

The central pattern generator is a network of locomotor neurons in the spinal cord, which can produce the basic pattern of neural activities required for walking. It can do so even in the absence of inputs from the brain and the peripheral sensory system. Experiments performed by Grillner and Zangger (1979) proved the existence of a central pattern generator in mammalian species. Gulino and co-worker (2007) believed that the rhythmic activity of a central pattern generator could be the early component of functional recovery (Gulino et al. 2007). Although a clear demonstration of a central pattern generator existence in humans has remained difficult because only data from an entirely deafferented and complete SCI patient would satisfy all criteria, some data strongly suggested that humans possess a central pattern generator within the spinal cord that is capable of generating stepping (Dimitrijevic et al. 1998; Gurfinkel et al. 1998; Calancie et al. 1994).

However, there are limitations to the extent of this spontaneous functional recovery. Understanding these limitations and investigating the mechanisms behind them may aid understanding of SCI, and therefore the development of new therapeutic strategies that facilitate these mechanisms of recovery.

## 1.7 Repair Strategies

As mentioned above, many patients show some spontaneous recovery following injury. However, the degree of this kind of recovery is normally too limited to retrieve the lost functions completely. Therefore, the functional deficits are usually permanent after SCI. Currently, damage to the spinal cord can not be repaired by any therapy.

SCI leads to a series of biological events as listed before. Most of them have detrimental effects on the injured cord and therefore hamper the repair process of the cord. Repair of the injured spinal cord in the adult is more than a simple matter of damaged tissue rebuilding itself but, rather, it is a highly complex multi-step process. First of all, the injured neuron must survive, and then the damaged axon must extend its cut processes to its original neuronal targets. Once contact is made, the axon needs to be remyelinated and functional synapses need to form on the surface of the targeted neurons. Consequently, treatments strategies are designed to tackle those problems following injury. The targets of curing SCI, therefore, are to minimize secondary damage progression and preserve residual functions (i.e. neuroprotection strategy), supply a permissive environment to axonal regeneration (i.e. regeneration strategy), and promote axonal sprouting (i.e. plasticity strategy) and repair demyelination and conduction deficits (i.e. remyelination strategy).

## 1.8 Therapeutic approaches

Ongoing research to test possible new treatments for SCI is progressing rapidly, and a number of therapeutic strategies are being examined in clinical trials (Hawryluk et al. 2008). However, there is no cure for SCI in clinic so far. Current medical interventions focus on two conservative aims. The first is to administer high dose steroids and/or surgical procedures if necessary to prevent further

damage shortly after injury. The other one is to help patients and family with rehabilitative training in order to optimize residual function and minimise problems like poor ventilation, bladder infections, joint fixation, and muscle wastage.

Although individual therapy developed to solve one specific aspect of SCI might restore important functions, a multidisciplinary approach probably will be the solution for SCI treatment. The interventional therapies may involve treatments to prevent secondary damage and protect residual neurons, overcome myelin inhibition and combine with neurotrophic factors to prevent neuronal atrophy and promote axonal regeneration, reduce non-permissive effects of the glial scar, enhance plasticity to maximize the spontaneous recovery, and form remyelination. At the late stage, intensive rehabilitative training programmes will help the patient to regain independence.

### *1.8.1 Neuroprotection*

Neuroprotection counts all the therapeutic strategies aiming at counteracting secondary injury mechanisms and/or minimising the extent of damage caused by destructive cellular and tissue events and preserving residual functions. On the basis of co-existence of several different injury mechanisms, a large number of potentially neuroprotective substances are being investigated in animal studies.

Methylprednisolone sodium succinate is the most extensively studied agent and it has been reported that a high dose of methylprednisolone sodium succinate administration during early acute stage (<8h) can help to improve energy metabolism, anti-inflammation (Fu ES and Saporta S 2005), reduce the formation of cytotoxic oedema, and the release of glutamate and free radicals (Farooque et al. 1996; Cayli et al. 2004). It is commonly applied clinically in the United States (Bracken and Holford 1993; Bracken et al. 1998; Aito et al. 2005) (National Acute Spinal Cord Injury Study, NASCIS 2 and 3). However, this therapy is still controversial because of inadequate evidence of efficacy and a higher rate of complications in clinic (Sayer et al. 2006; Suberviola et al. 2008).

Erythropoietin, a potent neuroprotective cytokine, has recently been discovered as a potential treatment for SCIs (Reviewed by Brines and Cerami 2008).

Erythropoietin functions not only as an anti-inflammatory and anti-apoptotic role, but also as a mediator of neuroprotective hypoxic preconditioning. Erythropoietin plays its beneficial role by apoptosis blockage (Arishima et al. 2006), reduction of inflammation, restoration of vascular integrity, and neuronal regeneration (Reviewed by Brines and Cerami 2008). However, Erythropoietin has a rheological disadvantage of causing an increased aggregation of thrombocytes and augmented hematocrite (Reviewed by Brines and Cerami 2008). Erythropoietin analogues such as asialoerythropoietin (Erbayraktar et al. 2003) and carbamylated erythropoietin (Kirkeby et al. 2008) have been generated as mutants of erythropoietin. They still have the same neuroprotective properties but without the rheological problems.

CD95 is a member of the tumour necrosis factor receptor family, and CD95 ligand can initiate cell death. Inhibition of the CD95 pathway has been proved to limit neuronal and glial apoptosis after SCI in mice (Demjen et al. 2004; Casha et al. 2005). Systemic application of minocycline, a synthetic tetracycline, has been shown to reduce apoptotic cell death of oligodendrocytes and the gliotic response with concomitant improvement in neurological function (Stirling et al. 2004; Beattie 2004). However, it is still not clear whether the altered cell, which is forced to survive, is still functional, and how long it can survive.

Furthermore, a remaining problem for all possible pharmacological treatments in the acute stage is still unclear: therapeutic windows. Even though the pre-clinical results are very promising, almost all phase II/III clinical neuroprotection trials have failed to achieve a consistently improved outcome for SCI patients (Dumont et al. 2001b; Hawryluk et al. 2008).

Besides these pharmacological interventions, early decompression also has been claimed to contribute to neuroprotection (Mirza et al. 1999). This non-pharmacological surgical intervention can reduce neurological deficits after SCI by decompressing the swollen, oedematous lesioned spinal cord (Papadopoulos et al. 2002).

### *1.8.2 Neurotrophins*

After David and Aguayo (1981) proved that injured axons can regenerate in a permissive environment such as peripheral nerve tissues, several regeneration obstacles have been identified including inhibitory substances, cavity, scar, and lack of neurotrophins. Following SCI, the injured neurons are eventually atrophic and may even die in such a non-permissive environment harbouring inhibitors such as Nogo-A protein and myelin-assoiated glycoprotein (MAG) produced by oligodendroglial cells (described below). Consequently, they are unable to give sufficient growth response which is necessary to axonal regeneration. Also the scar and cavity provide a mechanical and chemical barrier. Various strategies have been investigated to tackle these obstacles in order to enhance axonal regeneration.

The neurotrophin family of growth factors are small molecules including nerve growth factor (NGF), brain-derived neurotrophic factor (BDNF), neurotrophins 3 and 4 (NT-3/NT-4), fibroblast growth factor (FGF), glia cell line derived neurotrophic factor (GDNF) and the leukaemia inhibitory factor (LIF). Neurotrophins can stimulate the injured axons to activate the regeneration-associated genes in order to promote the intrinsic growth capacity of neurons for regeneration after SCI (Ramer et al. 2000; Blesch and Tuszynski 2003; Bradbury et al. 1999). Moreover, neurotrophins can promote neuron survival and regulate neuron-target interactions (Kobayashi et al. 1997; Kwon et al. 2002; Novikova et al. 2002). The different density of the corresponding receptors in the injured spinal cord may explain the different performance among those neurotrophins.

However, a few crucial questions still need to be investigated. Firstly, some growth factors promote axons that conduct nociceptive information and cause increased pain (Pezet and McMahon 2006). Secondly, different neurotrophins work at different time points during the repair (Novikova et al. 2002). Thirdly, they can not cross the blood-brain barrier. Although a number of growth factors show positive effects on axon growth, it still needs to be determined which growth factors are suitable, when and by what methods they should be administered.

### *1.8.3 Myelin inhibitors*

The normal uninjured spinal cord contains inhibitory substances that regulate neurite growth. It is thought that they may play an important role in restricting axonal growth once development has occurred. However, this vital function becomes a major obstacle to the regeneration of injured axons after SCI. A variety of neurite growth inhibitors present in CNS myelin has been well defined such as Nogo-A protein (GrandPré et al. 2000; Chen et al. 2000), myelin-associated glycoprotein (MAG) (McKerracher et al. 1994; Schachner and Bartsch 2000) and oligodendrocyte-myelin glycoprotein (OMgp) (Wang et al. 2002a).

#### 1.8.3.1 Nogo

Nogo-A is possibly the best characterized and has been investigated in closest detail among inhibitors in myelin (Schweigreiter and Bandtlow 2006). The Nogo gene gives rise to three protein isoforms (Nogo-A, Nogo-B, and Nogo-C) via both alternative splicing and promoter usage (Figure 1-6). All three Nogo isoforms share a C-terminus of 188 amino acids which contains a short loop of 66 amino acids called Nogo-66 and two long hydrophobic domains. This common C-terminus is called the reticulon-homology domain (RHD). This sequence characterizes the Nogo gene as a member of the reticulon protein family (GrandPré et al. 2000).

Nogo-A is a glycosylated transmembrane myelin protein with a high molecular weight highly expressed by oligodendrocytes (Schwab 2004). During development, Nogo-A is also expressed in subpopulations of neurons and down-regulated in most of these regions in the adult CNS (Richard et al. 2005). There are at least three active sites of Nogo-A that are exposed to the extracellular space (Oertle et al. 2003). First, the Nogo-66 domain, which is positioned between two hydrophobic stretches (Schweigreiter and Bandtlow 2006). Second, a central inhibitory domain termed as NiG which is a large stretch specific to Nogo-A. Both of these two sites inhibit neurite growth and induce growth cone collapse (GrandPré et al. 2000; Oertle et al. 2003). The third site is found in the Nogo-A/B-specific N-terminus. This site inhibits the spreading of cultured fibroblast, enhances adhesion of vascular cells and stimulates endothelial cell migration (Acevedo et al. 2004; Miao et al. 2006) (Figure 1-6).

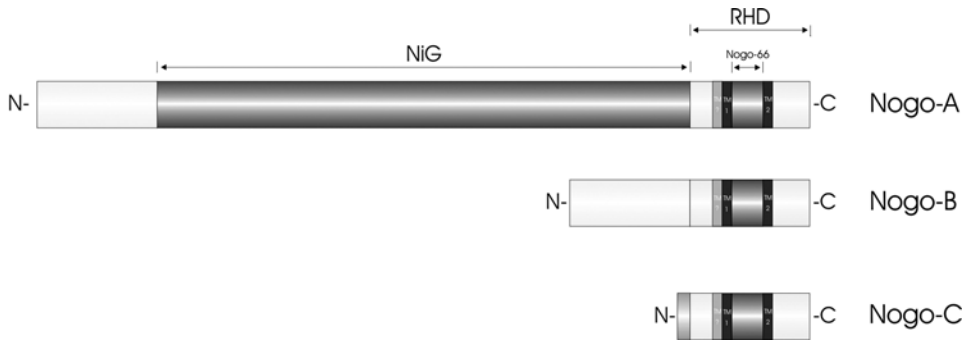


**Figure 1-6 Three Nogo isoforms**
The Nogo gene gives rise to three protein isoforms—Nogo-A, Nogo-B, and Nogo-C—via alternative splicing and promoter usage. Nogo-A harbors two inhibitory domains: Nogo-66 (which is common to all Nogo isoforms) and NiG (which is unique to Nogo-A). Nogo-66 is defined by two hydrophobic regions; however, it is believed that the first hydrophobic stretch traverses the membrane twice. Therefore, both inhibitory domains face the extracellular space when the protein is localized to the plasma membrane (taken from Schweigreiter and Bandtlow 2006).

Various lines of Nogo knockout mice lacking one or more Nogo molecules have been reported by three different independent laboratories (Simonen et al. 2003; Kim et al. 2003; Zheng et al. 2003). Two laboratories (Simonen and Kim) claim modest improvement in axonal regeneration and functional recovery. However, Zheng reports that no regeneration or sprouting has been observed in both Nogo-A/B and Nogo-A/B/C mutant mice. The genetic background of different mouse lines (Dimou et al. 2006), compensatory up-regulation of other Nogo proteins (Simonen et al. 2003) and the lesion paradigms (Cafferty and Strittmatter 2006) used may account for this discrepancy.

A glycosyl-phosphatidylinositol (GPI)-linked cell surface protein is widely expressed in many neurons. It has been characterized as a neuronal receptor that binds to the Nogo-66 site and termed as NgR (Fournier et al. 2001). Since NgR is a cell surface protein which lacks a cytoplasmic domain, co-receptors are required to mediate signal transduction across the cell membrane such as p75 (Wang et al 2002b; Wong et al. 2002), TROY (Park et al. 2005; Shao et al. 2005), and LINGO-1 (Mi et al. 2004) (Figure 1-7). A number of groups have also reported that another receptor or an additional receptor subunit may mediate Nogo-A-

specific signalling (Oertle et al. 2003; Song et al. 2004; Zheng et al. 2005). Recently, a new functional receptor for myelin inhibitors of axonal regeneration, PirB, has been identified (Atwal et al. 2008).

The binding of Nogo-A to these Nogo-A receptors on the surface of the injured neurons leads to inhibition of axon elongation and growth cone collapse (Fournier et al. 2001; Yamashita et al. 2005; Atwal et al. 2008). The intracellular signalling pathways of Nogo-A involve RhoA and Ca2+. RhoA is a GTPase of the Rho family and plays a central role in the signal transduction of axonal guidance molecules during development (Figure 1-7). Activation of RhoA may be the major intracellular signalling mechanism of Nogo-A (Alabed et al. 2006; Fournier et al. 2003). Nogo-A also can increase intracellular calcium, and therefore induces growth cone collapse (Wong et al. 2002; Bandtlow et al. 1993). This pathway may act in parallel or in sequence with RhoA. Targeting these downstream effectors of Nogo-A with specific blocking compounds therefore prevents the signalling of myelin inhibitors (Figure 1-7). However, the picture of myelin inhibitors and their signalling machinery is still far from complete.

Studies revealed that the failure of axonal regeneration is the main contributor to the lack of substantial functional recovery after SCI, and the regeneration is limited by neurite growth inhibitors such as Nogo-A (Schwab 2004). Information from different experimental animals has shown that inactivation of Nogo-A either by function-blocking antibodies or by interfering with Nogo-A receptors or signalling pathways results in an increased axonal regeneration below the site of injury(Li et al. 2004; Schnell and Schwab 1990; Fouad et al. 2004; Liebscher et al. 2005; Freund et al. 2006; 2007).

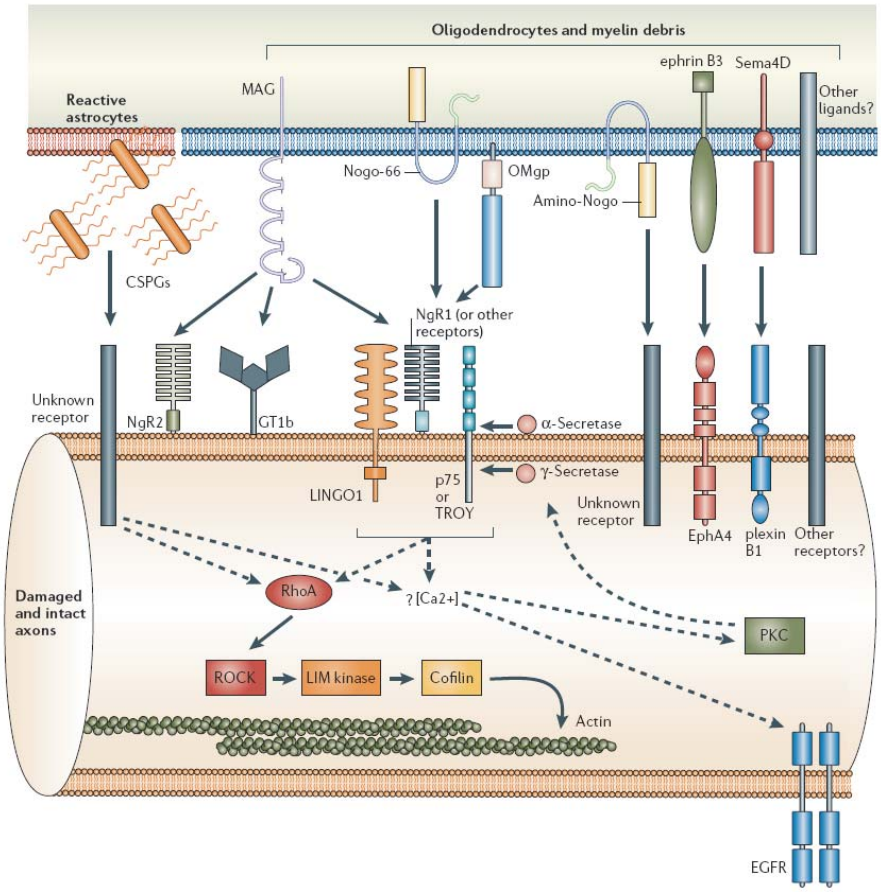


**Figure 1-7 Inhibitors and intracellular signalling mechanisms**
The molecular inhibitors of the adult CNS glial environment include chondroitin sulphate proteoglycans (CSPGs) associated with reactive astrocytes from the glial scar, and myelin-associated inhibitors from intact oligodendrocytes and myelin debris, including myelin-associated glycoprotein (MAG), Nogo-A, oligodendrocyte myelin glycoprotein (OMgp), ephrin B3 and the transmembrane semaphorin 4D. Although the topology of Nogo-A remains unclear, both the 66 amino acid loop (Nogo-66) and the amino-terminal domain (amino-Nogo) are known to be inhibitory to axon outgrowth. The neuronal receptors and downstream signalling pathways known to be involved in transducing these inhibitory signals are shown. Among the signalling components that are common to both CSPG and myelin inhibition are the activation of RhoA and the rise in intracellular calcium. Whereas the signals downstream of RhoA that lead to the actin cytoskeleton are well characterized (solid arrows), the relationship between components upstream of RhoA and the role of calcium influx are still ambiguous (dashed arrows). For example, calcium transients might activate protein kinase C (PKC), which is required for p75 cleavage by ϒ-secretase, or trigger the transactivation of epidermal growth factor receptor (EGFR) (taken from Yiu and He 2006).

Schnell and Schwab reported that up to 11mm CST regeneration beyond the injury site has been observed in anti-Nogo-A antibody group compared to very limited regeneration in control animals (Schnell and Schwab 1990). Liebscher and colleagues used an intrathecal catheter to deliver highly purified anti-Nogo-A antibody from an osmotic minipump. Their results also demonstrated that neutralization of the Nogo-A leads to enhanced regeneration and reorganization of the injured CNS (Liebscher et al. 2005). It is believed that the axons in the anti-Nogo-A antibody treated group grow through the denervated spinal cord for long distances (more than 1-2mm) and could form extensive terminal arbours in the caudal spinal cord. Sprouting collaterals of spared axons above and below the lesion site have been also observed. These short (less than 1mm) fibres can innervate targets around the lesion (Wang et al. 2006; Li et al. 2005; Simonen et al. 2003). Recently, a study shows that Nogo signalling can also be suppressed by phosphorylation of the NgR in vitro (Takei 2009). Inactivation of Nogo functions by blocking NgR with a blocking peptide or by targeting effectors in signalling pathways with blocking compounds also leads to similar CST regeneration (Fournier et al. 2003; GrandPré et al. 2002). However, only a modest disinhibitory effect has been seen after blocking the NgR or PirB receptor alone. A recent study shows that blocking both PirB and NgR activities leads to near-complete release from myelin inhibition (Atwal et al. 2008).

The CST has been chosen for the assessment of regeneration in most studies because of the relative ease with which it can be anatomically traced. However, other spinal tracts such as raphespinal (serotonergic) axons (GrandPré et al. 2002), coeruleospinal (noradrenergic) axons (Bregman et al. 1995), and cholinergic septohippocampal axons (Cadelli and Schwab 1991) have also been reported to show substantial regeneration after inactivation of Nogo function.

This enhanced regenerative and compensatory fibre growth is commonly accompanied by a substantial improvement in the functional recovery after injury. Animals treated with anti Nogo-A antibodies scored significantly better than control animals in various behavioural tests, in particular in precision tests, e.g. crossing a unevenly spaced ladder or climbing a rope (Bregman et al. 1995; Liebscher et al. 2005). Similar functional recovery was observed when Nogo-A receptors were blocked, or following interference with signalling pathways (GrandPré et al. 2002; Li et al. 2004; 2005). Neutralizing Nogo-A in the lesioned

spinal cord enhances sprouting and functional recovery not only in rodents but also in primates (Freund et al. 2006; 2007). Interestingly, common malfunctions such as pain or spasticity have not been seen in animals treated with reagents that block the Nogo-A receptor pathway (Liebscher et al. 2005; Freund et al. 2006).

Because functional recovery and axonal regeneration have been seen in the same animal, it has been suggested that regenerated axons contribute significantly to functional recovery after neutralizing myelin inhibitors. However, close anatomical observations reveal that only a small proportion of interrupted fibres regenerate beyond the lesion site. It therefore suggests that other mechanisms such as collateral sprouting of spared axons may also play an important role in the functional recovery (Liebscher et al. 2005; Freund et al. 2007). In vivo, both axonal regeneration and axon collateral sprouting can be enhanced by anti-Nogo-A antibody treatment. A study showed that sprouting of damaged axons resulted in new synapse formation between the damaged axons and propriospinal neurons, and that these new intrinsic spinal circuits enhanced functional recovery after experimental SCI (Bareyre et al. 2004). Another study reported that almost complete functional recovery was paralleled by a surprising capability of the CST to reorganize anatomically after unilateral pyramidotomy and treatment of the animals with the IN-1 antibody (Z'Graggen et al. 1998) (Figure 1-8). Reorganization in the spinal cord and restitution of fine motor skill were also observed in rats treated with IN-1 (Raineteau et al. 2002). Therefore, axonal regeneration, sprouting and plasticity may all contribute to restoring function after SCI, rather than each mechanism alone.

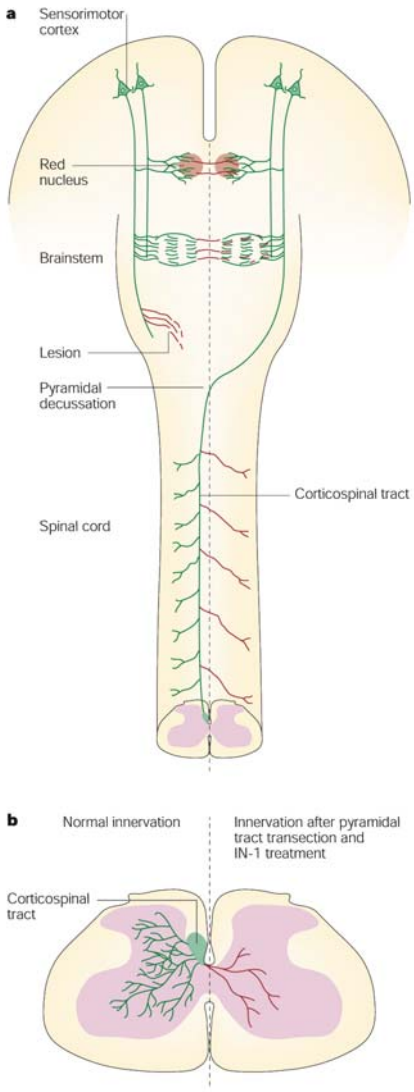


**Figure 1-8 Schematic representation of the corticospinal reorganization occurring after pyramidotomy and mAb IN-1 treatment**

Schematic diagram shows the corticospinal reorganization after pyramidotomy and mAb IN-1 treatment. a: Unilateral transection of the CST in the brainstem above the decussation interrupts axons from the sensorimotor cortex of one hemisphere to the spinal cord grey matter on the contralateral side. CST projections to mid- and hindbrain nuclei are spared. Hybridoma cells were implanted over the contralateral cortex to secrete IN-1 antibody. In response to IN-1, CST fibres from the injured side were induced to sprout (red) within nuclei of the contralateral side, including the red nucleus. b: In the spinal cord, CST fibres from the intact side (green) were induced to sprout collaterals (red), which cross the midline to innervate the denervated side (taken from Raineteau and Schwab 2001).

While the results of animal experiments aimed at neutralizing Nogo-A are quite promising, full functional recovery will require a combination of several therapeutic strategies. Maier and colleagues (Maier et al. 2009) compared the effects of anti-Nogo-A antibody treatment and treadmill training in rats with incomplete SCI. Even though functional recovery was observed in both groups, axonal regeneration and sprouting of descending systems was seen only in rats with antibody treatment. Surprisingly, combinatorial treatment of both produced a poorer locomotor performance, compared to individual treatments. It is suggested that the mechanisms underlying these changes with each treatment are not only different but possibly competitive. Therefore, the understanding of the mechanism underlying each individual treatment as well as their potential interactions will be crucial to finding the most effective combination for future therapies.

#### 1.8.3.2 MAG and OMgp

MAG is a type I trans-membrane glycoprotein and was the first identified myelin inhibitor of axonal regeneration (McKerracher et al. 1994; Mukhopadhyay et al. 1994). As a member of the immunoglobulin superfamily, MAG contains five extracellular immunoglobulin Ig-like domains. The alternative splicing of MAG mRNA in rodents generates two MAG isoforms: large (L) and small (S). These two isoforms differ only in their cytoplasmic sequences that may activate different signal transduction pathways in myelin-forming cells (Lai et al. 1987; Salzer et al. 1987). MAG is also known to be a sialic acid-binding protein and a member of the Siglec family of proteins (sialic acid-binding, Ig-like lectins) (Schachner and Bartsch 2000).

MAG is selectively localized in the periaxonal Schwann cell and oligodendroglial membranes of myelin sheaths where it functions in glia-axon interactions in both the PNS and CNS (Sternberger et al. 1979; Schachner and Bartsch 2000). MAG is important for the normal formation and maintenance of myelinated axons. Furthermore, it may play a role in signalling in both directions between axons and glia, although some of these roles may be different in the CNS and PNS (Quarles 2007; Schachner and Bartsch 2000). The higher concentration of MAG in the CNS, compared to in the PNS, may reflect the higher need for signalling at the oligodendroglial-axon junction than at the Schwann cell-axon junction

(Trapp BD 1990). A recent study reports that MAG also promotes axonal stability and prevents axonal degeneration both in cell culture and in vivo (Nguyen et al. 2009). In addition to the protective role, MAG also has the capacity to inhibit neurite outgrowth as one of the myelin inhibitors of axonal regeneration (McKerracher et al. 1994; Mukhopadhyay et al. 1994). Inactivation of MAG function by using anti-MAG antibody has shown neuroprotective effects in brain injury models such as stroke (Irving et al. 2005). Improved functional recovery was associated with smaller lesion volume and better tissue sparing observed in animals receiving anti-MAG antibody (Irving et al. 2005; Thompson et al. 2006). Immunization with myelin or recombinant Nogo-66/MAG promotes long distance axon regeneration and sprouting in a spinal cord hemisection model (Sicotte et al. 2003).

Oligodendrocyte myelin glycoprotein (OMgp) was first described many years before it was identified as the third myelin-associated molecule possessing potent growth cone collapsing and neurite growth inhibitory activity (Mikol Stefansson 1988; Wang et al. 2002a). OMgp is a glycosyl phosphatidylinositol (GPI)-linked protein that contains a leucine-rich repeat (LRR) domain and a C terminal domain containing serine/threonine repeats. It is relatively minor component in both CNS and PNS myelin, and may be expressed in more abundance by other non-myelinating cells (Huang et al. 2005).

Interestingly, MAG and OMgp also exert their inhibitory effects through binding of Nogo-66-receptor (NgR), despite the fact that they have little sequence similarity or even domain similarity. Shortly after the NgR was discovered by the Strittmatter group, they and Domeniconi's laboratory simultaneously found that MAG was also a ligand for this receptor (Domeniconi et al. 2002; Liu et al. 2002). Their studies provide strong evidence that the NgR is necessary for MAG to inhibit axonal regeneration. In addition, it was discovered that binding of MAG to the NgR is sialic acid-independent. This evidence suggests that the sialic acid-binding site is distinct and independent of the inhibitory domain. At approximately the same time that these experiments were carried out, it was independently discovered that the NgR is also a receptor for OMgp and mediates its inhibitory actions (Oertle et al. 2003). A transmembrane protein termed as p75 is required for NgR-mediated signalling. Therefore, interfering with p75 and

its downstream signalling pathways may reduce the inhibitory activities of myelin inhibitors, and promote neurite growth in vitro (Wang et al. 2002a) (Figure 1-7).

Interfering with PirB function, a newly discovered functional receptor for myelin inhibitors, can partially rescue neurite inhibition and myelin in cultured neurons. Blocking both PirB and NgR activities leads to significant release from myelin inhibition (Atwal et al. 2008). Since all three myelin inhibitors i.e. Nogo, MAG, OMgp, can bind to the same receptors, it seems feasible to antagonize the effects of all three myelin inhibitors at once.

In addition to these three relatively well defined myelin inhibitors, some repulsive axon guidance cues with roles in axon pathfinding during development, such as ephrin B3 and Semaphorin 4D, continue to be expressed in adult CNS myelin. They have been implicated as inhibitors of axonal regeneration. Ephrin B3 functions as a midline repellent for growing CST fibres during development, but continues to be expressed in myelinating oligodendrocytes during postnatal stages and strongly inhibits axonal growth in vivo (Benson et al. 2005). Semaphorin 4D, also called CD100, is also present in mature oligodendrocytes, inhibits neurite growth and triggers growth cone collapse (Moreau-Fauvarque et al. 2003) (Figure 1-7).

### *1.8.4 Scar inhibitors*

Scar formation is a natural response to injury but leads to an environment hostile for regeneration of injured axons. The glial reaction may have some beneficial effects such as isolating the injury site and minimizing the area of inflammation and cellular degeneration but inhibitory extracellular matrix molecules occur in the glial scar, and it is also a physical barrier for axonal regeneration.

Astrocytes and oligodendrocyte precursor cells, together with invading meningeal cells produce chondroitin sulphate proteoglycans (CSPGs) which are the major inhibitory species associated with the glial scar, and release them into the extracellular space (Morgenstern et al. 2002) (Figure 1-7). CSPGs are a relatively big family including NG2, neurocan, aggrecan, versican, phosphacan

and brevican (Silver and Miller 2004; Tang et al. 2003). These molecules consist of a protein core to which large, highly sulphated glycosaminoglycan (GAG) chains are attached (Morgenstern et al. 2002). Following injury, CSPGs are secreted rapidly (within 24 hours) at and around the lesion site which forms a physical and chemical barrier to axonal growth. CSPG expression quickly reaches its peak in the first two weeks, and may persist for many months (Tang et al. 2003).

CSPGs have been proved to be strong inhibitors of neurite growth which impede sprouting and regenerating axons from crossing the lesion site (Silver J and Miller JH 2004). CSPGs inhibit axon growth *in vitro* and stop axonal regeneration *in vivo* (Davies et al. 1999). The inhibitory effects produced by CSPGs can be enzymatically degraded by bacterial chondroitinase ABC (ChABC), an enzyme that removes GAG chains from the protein core (Bradbury et al. 2002). Therefore, it suggests that the GAG components play a key role for the inhibitory activity of CSPGs. Bradbury and colleagues delivered ChABC to rats with dorsal column lesions. Their results showed that intrathecal infusion of ChABC degraded CSPGs at the injury site, up-regulated a regeneration-associated protein in injured neurons, and promoted regeneration of both ascending and descending tracts caudal to the lesion site. They also claimed that enhanced functional recovery has been observed after this treatment (Bradbury et al. 2002). However, the functional recovery is probably due to the stimulation of plasticity because it is seen as soon as 1 week after injury – too fast to be due to axonal regeneration and formation of functional connections. In other studies, ChABC has also been proved to stimulate the growth of uninjured systems within the CNS, for instance when one corticospinal tract is lesioned the contralateral tract can sprout across to the denervated side of the cord, which demonstrate the potency with which ChABC can enhance plasticity (Barritt et al. 2006). Recently, electrophysiological recordings also confirmed that behavioural recovery observed in ChABC treated animals was consequent to reorganization of intact primary afferent terminals after SCI (Cafferty et al. 2008). Carter LM recently demonstrated that ChABC treatment regulates multiple signalling cascades at the injury site and exerts protective effects on injured neurons (Carter et al. 2008). A study of the therapeutic time window for the application

of ChABC shows that ChABC treatment can be successfully applied starting seven days after SCI (García-Alías et al. 2008).

In addition to CSPGs, several other inhibitory molecules in the glial scar have been identified. Semaphorin 3 (SEMA3) is one of these molecules, and has been showed to prevent the penetration of regenerating axons past the lesion (De Winter et al. 2002). Together with the other inhibitory molecules, such as ephrin-B2 and Slit proteins, these additional inhibitors in the glial scar add additional levels of complexity to the source of regeneration failure in SCI (Bundeson et al. 2003; Brose and Tessier-Lavigne 2000).

### *1.8.5 Modulation of the immune system*

Inflammation contributes to the non-permissive environment for neuron survival and regeneration after SCI. It has been suggested that immune system activation following SCI is both destructive and protective. Consequently, modulating the immune system is a potential treatment for SCI (Schwartz and Yoles 2005; 2006; Popovich et al. 2002).

Macrophages play a key role in the inflammatory process (Chang 2007). Inadequate macrophage response following injury may be the other contributory factor to failure of axon regeneration. Therefore, the successful activation of macrophages is the key to efficient phagocytic removal of myelin debris from the injured cord (Popovich et al. 2002; Vallieres et al. 2006; Schwartz and Yoles 2005). By modulating some molecules such as intercellular cell adhesion molecule and interleukin, which play key roles in inflammation, it might thereby be possible to regulate the inflammatory response in SCI (Mabon et al. 2000; Brewer et al. 1999).

### *1.8.6 Rho pathway antagonists*

Rho, a small GTPase, plays a key role in many signalling pathways to block axonal regeneration and exacerbate posttraumatic neural cell death (McKerracher and Higuchi 2006). A few studies reported that inhibition of either Rho or Rho-associated kinase (ROCK) can enhance axonal regeneration and function recovery in mice (Dergham et al. 2002; Fournier et al. 2003). Based on

these persuasive preclinical animal data, a phase I /II a non-placebo-controlled dose-escalation study with Cethrin (a novel Rho inhibitor recombinant protein) administered in patients with acute complete SCI is underway in North America (Baptiste et al. 2009).

### *1.8.7 Cell transplantation*

Typically, a fluid-filled cavity surrounded by a glial scar will develop in the late stage of SCI (Figure 1-5). A scaffold thereby will be needed for injured axons to regenerate through this gap. Cell transplantation can be the supportive structure to fill the gap. It can also theoretically contribute to repair of SCI in the following ways. Transplanted cells can reduce further death of neurons and supporting glia, replace damaged neural tissue, promote axonal regeneration, enhance plasticity, induce remyelination, and limit progressive myelin loss from secondary injury. Several different cells have been investigated for cell transplantation in the repair of SCI, for example, embryonic stem cells (McDonald et al. 1999), adult neural stem cells (Akiyama et al. 2001), foetal tissue (Coumans et al. 2001), mesenchymal stem cells (Akiyama et al. 2002), and glial cells such as olfactory ensheathing cells (OECs) (Franklin et al. 1996; Li et al. 1997; Ramón-Cueto et al. 1998; Riddell et al. 2004; Toft et al. 2007), Schwann cells (Duncan et al. 1981; Tuszynski et al. 1998) and oligodendrocyte precursor cells (Groves et al. 1993; Bambakidis and Miller 2004).

#### 1.8.7.1 OEC

In the past two decades, they have attracted increasing attention from neuroscientists as potential therapeutic agents for use in the repair of SCI. The olfactory nervous system has ability for regrowth that is uncharacteristic of other CNS regions (Figure 1-9). The olfactory system consists of the olfactory epithelium, which is the peripheral component, and the olfactory bulb, which belongs to the CNS. Olfactory receptor neurons, whose cell bodies are found in the olfactory epithelium, send their axons to the olfactory bulb and their axons are ensheathed along their length by OECs (Figure 1-9). Throughout life, olfactory neurons constantly die and are replaced by neurons from the basal stem cell layer of the olfactory epithelium. During normal cell turnover or after

injury, axons from new olfactory receptor neurons supported by OECs grow into the olfactory bulb and make functional synaptic connections (Doucette 1984; 1991). Like other glial cells, OECs provide structural, functional and metabolic support to neurons.

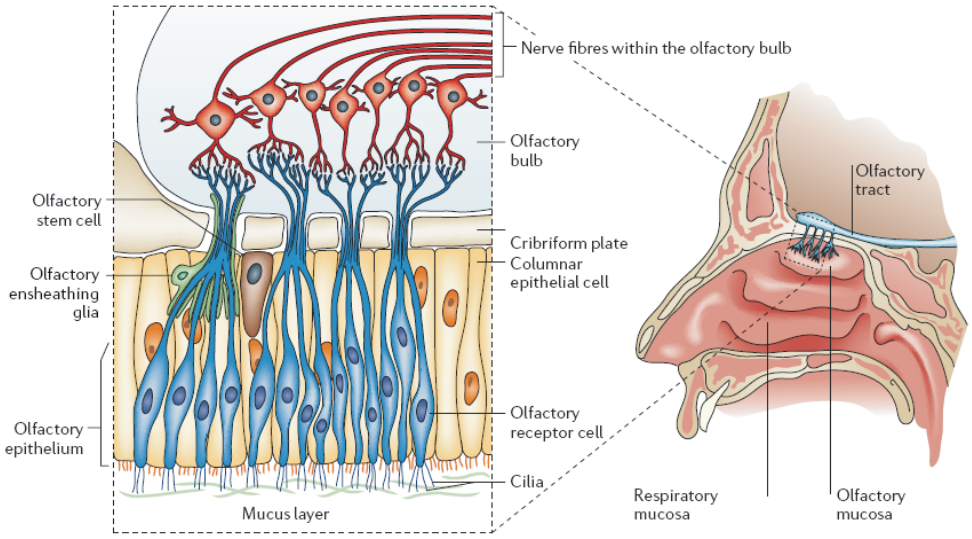


**Figure 1-9 The olfactory nervous system**
Schematic of a sagittal section through the human head, showing the olfactory nervous system (right), with a section of the olfactory nervous system depicted in greater detail (inset). The olfactory system has PNS and CNS components. The olfactory mucosa comprises the olfactory epithelium and lamina propria. The olfactory epithelium contains olfactory receptor neurons (which project cilia into the nasal cavity), sustentacular cells (non-neuronal supporting cells), globose basal cells (putative stem cells for the epithelium), horizontal basal cells and Bowman's gland and ducts. The lamina propria consists of loose connective tissue and OECs, which ensheath bundles of olfactory receptor axons extending from the olfactory epithelium into the CNS via the cribriform plate. Many cell types make up connective tissue, including fibroblasts, macrophages, pericytes, endothelial cells and smooth muscle cells from the lining of blood vessels, in addition to Schwann cells that ensheath the nerves that innervate the blood vessels (taken from Thuret et al. 2006).

OECs operate in both PNS and CNS environments to support the ongoing axonal growth, ensheathment, and targeting of olfactory neurons (Farbman and Squinto 1985; Chuah and Au 1994). OECs can assist axon growth, like Schwann cells, and

are able to live within the CNS, like astrocytes (Smale et al. 1996; Li et al. 1997; Franklin et al. 1996) throughout adult life, including in humans. This property makes OECs a unique glial cell and a promising candidate for SCI repair (Figure 1-9).

A number of studies have been undertaken to investigate the ability of OEC transplants to repair injured spinal cord in various types of experimental animal models including partial transection models, complete transection models, and contusion models that typify clinical injuries (see below). Functional recovery, axonal regeneration and remyelination have been the main focus of investigation.

Functional recovery after OEC transplantation has commonly been evaluated by applying behavioural tests of sensorimotor control in animal models of SCI. The evidence for improved functional recovery is mixed. Raisman and colleagues (1997) transplanted OECs into rats with a unilateral electrolytic lesion of the corticospinal tract at C1. These lesions abolished the ability to reach for food pellets using the paw on the affected side. They found that rats partially regain this ability after OEC transplantation (Li et al. 1997). They also reported that OEC transplantation improves climbing ability and activity in pathways controlling breathing in animals with more extensive cervical hemisection injuries (Li et al. 2003). Electrophysiological study also showed that substantial recovery of the respiratory function can be obtained following OEC transplantation (Polentes et al. 2004).

Promising results have also been reported following transplantation of OECs after complete transection injuries of the thoracic spinal cord. Ramón-Cueto and colleagues (2000) reported that animals with transplantation recovered locomotor functions and sensorimotor reflexes better than animals without. They also described dramatic improvements in hindlimb use in an inclined grid climbing task, body weight support and recovery of proprioception and tactile sensation (Ramón-Cueto et al. 2000). Modest functional recovery has also been reported after complete transection injuries (López-Vales et al. 2006) and contusion injuries (Plant et al. 2003).

However, Ruitenberg and colleagues reported no significant differences in functional recovery between experimental groups after unilateral lesions of C4 dorsal columns interrupting both corticospinal tract and ascending sensory pathways (Ruitenberg et al. 2005). Riddell and colleagues (2004) also showed that OECs grafts are of little or no advantage in promoting regeneration following rhizotomy. Other studies also showed no observable functional recovery in both complete transection (Steward et al. 2006) and contusion injury models (Takami et al. 2002).

Reports on the extent of axonal regeneration are also mixed. Axonal regeneration was reported to occur not only within a transplant but also beyond the transplant in early studies (Ramón-Cueto et al. 2000; Li et al. 1998; Nash et al. 2002; Imaizumi et al. 2000). It was therefore suggested that OEC transplantation promotes long distance axonal regeneration, and that this might be the explanation for the improved functional recovery sometimes observed. However, a number of later studies have failed to observe long distance axon regeneration across and beyond a lesion (Ruitenberg 2003; 2005; Lu et al. 2006; Ramer et al. 2004a, b; Andrews and Stelzner 2004). The discrepancies in results do not seem to be related in any consistent way to experimental design.

Toft and colleagues (2007) used anatomical and electrophysiological techniques to investigate the repair promoted by OEC transplants following a dorsal column lesion. Although their anatomical results suggest that OEC transplantation did not support axon regeneration across the lesion site, electrophysiological results showed that the function of circuitry in the region of the lesion site and of ascending pathways originating near the injury was improved. Therefore, other mechanisms, such as plasticity or a neuroprotective action, were suggested to be responsible for the improved functional recovery, rather than axonal regeneration.

Chuah (Chuah et al. 2004) reported that more collateral branches in the minor component of the corticospinal tract projecting through ventral white matter were seen near OEC transplant in lesioned animals than those without transplants. They suggested that this may reflect corticospinal axon sprouting induced by OECs. Furthermore, a number of studies suggest that OECs have a neuroprotective effect after transplantation by reducing cavity formation at

contusion and transection injury sites (Takami et al. 2002; Ramer et al. 2004a), by protecting neurons with fibres projecting to an OEC transplanted lesion (Sasaki et al. 2006) and preventing loss of cord parenchyma by means of neoangiogenesis at transection and photo-chemical lesions (López-Vales 2004). Consequently, neuroprotective effects of OEC transplantation might also explain some of the improved functional recovery.

Regenerating axons in SCI must also acquire a myelin sheath to enable efficient propagation of action potentials, apart from achieving long regeneration and forming functional synaptic connections. Although OECs do not normally form myelin in the olfactory system, peripheral-type myelination has been seen when OECs encounter axons of an appropriate diameter (Franklin et al. 1996). These axons include those regenerating within an OEC transplant (Sasaki et al. 2004). However, it is difficult to prove that OECs, rather than Schwann cells, are responsible for the peripheral-type myelination. There is no a specific marker that reliably discriminates between OECs and Schwann cells which might contaminate OEC preparations (Rizek and Kawaja 2006), or Schwann cells from the host that might infiltrate the injury site (Takami et al. 2002; Blight and Young 1989; Sasaki et al. 2004).

Some scientists have successfully cultured and harvested human OECs from human olfactory tissue (Barnett et al. 2000; Bianco et al. 2004; Féron et al. 2005; Mackay-Sim et al. 2008). However, it is still difficult to grow pure populations of human OECs in the numbers required to fill a typical human SCI (Choi et al. 2008). Some studies have proved that two or three biopsies of olfactory mucosa can be safely obtained from patients without any detriment to their sense of smell (Lanza et al. 1994; Féron et al. 1998). Based on the feasibility of isolating OECs from the human olfactory system and the promising results observed in experimental animals, several clinical programs of OEC transplantation are in progress in China (Guest et al. 2006), Portugal (Lima et al. 2006) and Australia (Féron et al. 2005; Mackay-Sim et al. 2008) and planned for the UK (Ibrahim et al. 2006). These clinical programs hopefully can provide important information which can not be obtained from animal experiments due to the intrinsic differences between human and animals.

### 1.8.7.2 Stem cells

Stem cells are not-transformed cells that are self-regenerative, multipotent for a tissue type, and highly proliferative. Stem cell therapy is widely accepted to treat diseases of modular organs such as the heart and the endocrine pancreas nowadays. Stem cells also show great potential for cell transplantation for SCI (Tewarie et al. 2009). They can expand to sufficient quantities for use in human therapy which is relatively difficult to achieve in many other popular candidates for cell transplantation.

Stem cells may be used to replace the lost neurons after injury, generate new supporting cells to stimulate regrowth of damaged nerves and myelinate them, and protect the cells at the injury site from further damage by producing protective factors. A variety of stem cells or stem cell-derived cells have been evaluated for their effects on different animal models of SCI (McDonald et al. 1999). Many of them indicated that stem cell transplantation plays a beneficial role in SCI (Nayak et al. 2006; Barnabé-Heider and Frisén 2008). However, it is often difficult to establish the mechanism by which transplanted stem cells may promote recovery. Functional benefits can be achieved by creating a permissive substrate for axonal growth, supplying trophic support reducing the damage and rescuing neurons and oligodendrocytes, providing cells that remyelinate spared but demyelinated axons (Parr et al. 2007). A clinical trial of a human embryonic stem cell-based therapy is ongoing in an American company Geron (Vogel 2005).

### 1.8.7.3 Schwann cells

Since Santiago Ramon Y Cajal (1928) documented the axonal growth promoting abilities of peripheral nerve grafts in the injured CNS, Schwann cells became one of most widely studied cell types for repair of the injured spinal cord. These cells play a crucial role in endogenous repair of peripheral nerves due to their ability to dedifferentiate, migrate, proliferate, express growth promoting factors, and promote axonal regeneration (Xu et al. 1997; Tuszynski et al. 1998; Weidner et al. 1999) and myelinate regenerating axons (Baron-Van Evercooren et al. 1992; Franklin et al. 1997). Schwann cells have many properties that are desirable for axonal regeneration in the PNS, such as neurotrophic and cell adhesion (Bray et al. 1981). One of the advantages of Schwann cells is that they

can be readily harvested from the peripheral nerves and easily purified and grown in culture in large numbers from both rat and human tissue. Some studies revealed Schwann cells can help remyelinate demyelinated axons and promote regeneration (Li and Raisman 1994; Kohama et al. 2001; Tuszynski et al. 1998). However, the inhibitory interaction between Schwann cells and astrocytes limits their usefulness in CNS repair (Baron-Van Evercooren et al. 1992; Lakatos et al. 2000; Shields et al. 2000). Clearly, Schwann cells have great potential for repair of the injured spinal cord, but they need to be combined with other interventions to maximize axonal regeneration and functional recovery.

#### 1.8.7.4 Foetal Cell

Foetal cell transplants have been the focus of much interest in animal models of human neurodegenerative disorders. The successful use of foetal transplants is most evident in Parkinson's disease (Freed et al. 1992; Spencer et al. 1992).

Trophic agents released by the transplants appear to facilitate the survival of host neurons. Of further importance, regenerating axons appear to readily traverse the boundary between the transplants and host tissue, suggesting that the continuity of axonal tracts can potentially be re-established (Reier et al. 1992). Possibly because of the more general plasticity found in the immature nervous system, foetal cell transplants appear more effective in neonatal recipients than in adults.

One of the limiting factors in using foetal cell transplants has been the availability of foetal tissue as well as the ethical issues surrounding its use in clinical settings. However, this may be a general problem in most strategies.

#### 1.8.7.5 Oligodendrocytes

Oligodendrocytes were used as a source for remyelination in different animal models in some reports (Crang and Blakemore 1991; Tontsch et al. 1994). Although the use of oligodendrocytes as remyelinating substrates has been shown to be successful in demyelinating animal models, their use in SCI has not been extensive. There are some therapeutic limitations to their use, particularly in light of recent evidence linking the oligodendrocyte's potential role in inhibiting

axonal regeneration by producing an inhibitory substrate during the acute phase of injury (Cadelli et al. 1992).

### *1.8.8 Conditioning stimulation*

Conditioning lesions of the peripheral processes of dorsal root ganglia neurones has been shown to induce a stronger regenerative response when the central processes of these neurones are lesioned in the dorsal columns (Richardson and Issa 1984; Neumann et al. 2005). The conditioning stimulation is thought to enhance the intrinsic growth capacity and modify the response of axons to inhibitory molecules by increasing intracellular levels of cAMP (Qiu et al. 2002). A combination of conditioning lesion with OEC transplantation can enhance the regeneration (Andrews and Stelzner 2004).

### *1.8.9 Impulse propagation*

In all fast conducting nerves, the nerve fibres are surrounded by a myelin sheath. Following injury, spared axons probably lose their myelin partially or completely (Waxman 1989). The impulse propagation thereby is insecure or even totally stopped. Moreover, the electrical impulse propagation could be spread between demyelinated axons. Conduction failure happens as a result of potassium appearance in the extracellular space released by exposed potassium channels on demyelinated axons following SCI.

Fampridine-SR allows demyelinated axons in injured spinal cord to send signals. Fampridine-SR can block the potassium channels and thereby to restore the impulse propagation for demyelinated axons (Hayes 2004; Cardenas et al. 2007). Fampridine-SR's effects can range from increases in strength and reduced spasticity and pain. Somel clinical trails have reported beneficial effects in SCI (Hansebout et al. 1993).

## 1.9 Anatomy of rat spinal cord

The spinal cord in rats is divided into 8 cervical segments, 13 thoracic segments and 6 lumbar segments. The grey matter in the centre contains cell bodies of neurons and is divided into the dorsal horn, the intermediate grey, the central

grey, and the ventral horn. The white matter embraces ascending and descending pathways and is divided into dorsal, dorsolateral, ventrolateral, and ventral funiculi. Based on cytoarchitectonic characteristics, the grey matter is subdivided into 10 laminae from dorsal to ventral (Molander and Grant 1995).

## *1.9.1 Corticospinal tract*

The corticospinal tract (CST) is one of the main descending pathways and is found only in the mammalian CNS. It is an important descending pathway best developed in primates and particularly associated with fine control of the hand in human beings (Afifi and Bergman 2005).

### 1.9.1.1 The origin and course of the CST in the rat

Corticospinal neurons are found in the sensorimotor cortex. Their distribution in rats is similar with the organization of corticospinal system in higher animals. Considerable overlap between somatosensory and motor cortex exists in the rat cerebral cortex (Miller 1987; Dum and Strick 1991). Corticospinal fibres have been shown to send collaterals to various brain stem nuclei including the red nucleus, pontine nuclei, inferior olivary nuclei and dorsal column nuclei (O'Leary and Terashima 1988).

The CST can be divided into a crossed and uncrossed component (Figure 1-10). The majority of the axons cross to the contralateral side in the medulla oblongata level (pyramidal decussation) to descend through the dorsal column of the spinal cord. The main (90% of fibres) crossed component is located in the ventromedial aspect of the dorsal funiculus (Rouiller et al. 1991; Hicks and D'Amato 1975; Miller 1987). However, minor components have been described to exist in the ipsilateral dorsal, contralateral lateral and ipsilateral ventral funiculi (Casale et al. 1988; Rouiller et al. 1991; Brosamle and Schwab 1997; Liang et al. 1991). Earlier studies did not reveal ventral, uncrossed fibres below thoracic levels (Vahlsing and Feringa 1980; Joosten et al. 1992). But tracing with BDA, Brosamle and Schwab (1997) showed that the ipsilateral, ventral CST projections extend to low spinal levels (Figure 1-10).

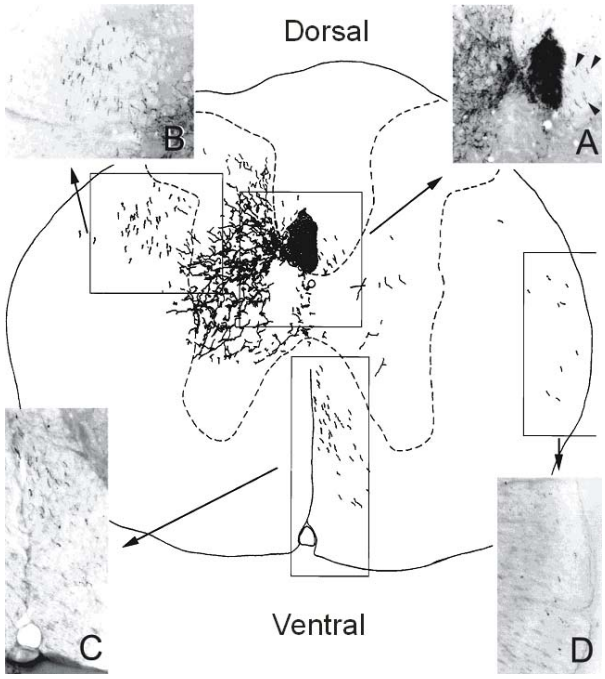


**Figure 1-10 Schematic representation of the organization of CST.**
Schematic diagram shows cross section at midthoracic level. Biotin Dextran-amine (BDA) tracing of the adult rat corticospinal tract from the right hemicortex reveals several components of the corticospinal tract (CST). Camera lucida drawing with the areas of the different components photographed (A-D) and marked in the drawing as boxes. A: The main CST component and the ipsilateral dorsomedial funiculus (arrowheads) B: The contralateral component. C: Ipsilateral ventromedial funiculus. D: Ipsilateral lateral white matter. The dashed line delineates the border between grey matter and white matter. Scale bar 5 250 um (taken from Brosamle and Schwab 1997).

The dorsal column component of the rat CST descends to reach the cervical, thoracic, lumbar and even sacral levels (Hicks and D'Amato 1977; Casale et al. 1988; Raineteau et al. 2002), although the number of fibres reaching more caudal levels probably progressively decreases. A number of electron microscope studies have revealed that unmyelinated fibres outnumber myelinated fibres at the medullary level (Leenen et al. 1982; Harding and Towe 1985). Although there are some unmyelinated fibres at the spinal cord level, the number decreases substantially (Leenen et al.1985).

Studies of the terminal pattern of CST fibres showed that the CST terminates mainly within a region corresponding approximately to laminae III-V in the

contralateral grey matter of the spinal cord at cervical and lumbar levels, and within lamina VI in the enlargements. However, terminations have also been found within other laminae including ipsilateral laminae III-X, with an emphasis in laminae VII, VIII and X, contralateral laminae VI-X, and sparse projections to the more superficial laminae I and II (Casale et al. 1988).

The existence of monosynaptic corticomotoneuronal connections is believed to be responsible for the ability to conduct independent digit movements in primates and man. In the rat, however, evidence of direct CST connections onto motoneurones is controversial (Liang et al. 1991; Alstermark et al. 2004; Yang and Lemon 2003). Previous electrophysiological studies suggested the existence of a monosynaptic corticomotoneuronal projection (Babalian et al. 1993; Liang et al. 1991). However, a recent electrophysiological study suggested that these were probably reversed corticospinal field potentials which has been mistaken as excitatory postsynaptic potentials, and therefore claimed that no monosynaptic corticomotoneuronal excitatory postsynaptic potentials can be evoked in the rat (Alstermark et al. 2004). One study showed anatomical evidence for close appositions between corticospinal boutons and motoneurons by using light microscopic technique (Liang et al. 1991). Yang and Lemon also observed close appositions at light microscopic level. However, they did not find any positive ultrastructural evidence for corticomotoneuronal monosynaptic connections at electron microscopic level (Yang and Lemon 2003).

#### 1.9.1.2 Functions of the CST

The CST is one of the most important descending motor tracts and plays an important role in motor function. For example, the forelimb reaching task especially involves the type of fine, voluntary movement that is thought to be controlled by the CST (Anderson et al. 2005). Some studies proved that a dorsal CST injury or damage to the motor cortex resulted in deficits in fine digital control in the rat (McKenna and Whishaw 1999; Schrimsher and Reier 1993). Furthermore, Kennedy (1990) proposed that the CST can compensate for damage to the rubrospinal tract via activation of the rubro-olivary projection.

### *1.9.2 Ascending pathways in the dorsal columns of the spinal cord*

Ascending pathways in the spinal cord conduct information from sensory receptors in the trunk and limbs to the brain. There are two main groups of ascending fibres in the dorsal columns of the spinal cord, a direct dorsal column pathway and a postsynaptic dorsal column pathway (Tracey and Waite 1995). In addition, approximately 25% of the fibres in the dorsal funiculus are propriospinal (Chung et al. 1987).

The direct dorsal column pathway is made up of the ascending branches of primary afferents of sensory neurons. The cell bodies of sensory neurons within the dorsal root ganglia give rise to axons which bifurcate (Figure 1-11). One branch innervates receptors in the skin, muscle and viscera. The other branch enters the spinal cord through the dorsal roots. These central branches then bifurcate into descending (caudally) and ascending (rostrally) projecting fibres (Willis and Coggeshall 2004). In general, the descending fibres maintained a less organised topographic distribution, and typically only a small amount of fibres descend two segments from their site of entry (Smith and Bennett 1987). Only a fraction of the ascending branches of primary afferents actually reach the dorsal column nuclei. Other fibres end in the grey matter at some level of the spinal cord. A much larger proportion of dorsal root ganglion cells in the cervical enlargement projected to the dorsal column nuclei, compared to lumbar dorsal root ganglion cells (Smith and Bennett 1987; Giuffrida and Rustioni 1992). Axons travelling within the dorsal column may give rise to collateral branches which terminate in various regions of the grey matter, including the dorsal horn, intermediate region, and ventral horn (Willis and Coggeshall 2004) (Figure 1-11).

The ascending branches of primary afferents have a somatotopic organization in the dorsal column, i.e. fibres from the tail project close to the midline, whereas fibres from the hind limb, trunk, and forelimb are added to the lateral border of the column at progressively more rostral levels (Willis and Coggeshall 2004; Smith and Bennett 1987).

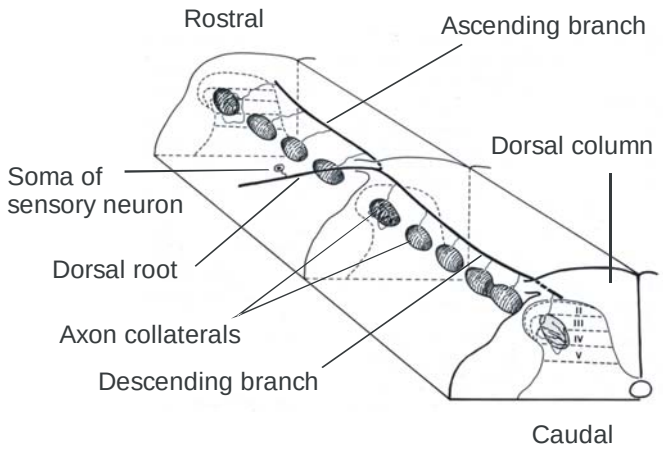


**Figure 1-11 Schematic representation of the organization of ascending pathways.**
Schematic diagram show the organization of ascending pathways. The soma of sensory neurons within the dorsal root ganglia give rise to axons which bifurcate. One branch innervates receptors in the peripheral system. The other branch enters the spinal cord through dorsal root. These central branches then bifurcate into ascending and descending branches. Axons travelling within the dorsal column may give rise to collateral branches which terminate in various regions of the grey matter (adapted from Brown et al. 1981).

A study shows that about 25% of primary afferents in the dorsal columns are unmyelinated in the rat (Chung et al. 1987). Many of these unmyelinated fibres contain calcitonin gene-related peptide. It is suggested that unmyelinated afferents in the dorsal columns might carry information from nociceptors or visceral receptors to the dorsal column nuclei (McNeill et al. 1988; Tamatani et al. 1989; Patterson et al. 1990).

The postsynaptic dorsal column pathway is formed by the axons of the spinal neurons originating in the spinal cord and projecting to the dorsal column nuclei (Giesler et al. 1984). The cells are in the nucleus proprius just ventral to the substantia gelatinosa. The axons of postsynaptic dorsal column neurons terminate at all rostrocaudal levels of the gracile and cuneate nuclei and also terminate in the external cuneate nucleus (de Pommery et al. 1984); they make apparent synaptic contacts with lemniscal neurons projecting to the ventrobasal thalamus (Cliffer and Giesler 1989). The postsynaptic dorsal column pathway projects in a somatotopic fashion to the dorsal column nuclei, since the nucleus cuneatus receives an input from cells in the cervical enlargement and the

nucleus gracilis from the lumbar enlargement (Giesler et al. 1984; de Pommery et al. 1984).

# Response of sensorimotor pathways to injury -spontaneous plasticity

## 2.1 Introduction

Following SCI, the disruption of both descending and ascending axonal pathways leads to loss of motor, sensory and autonomic function. Significant spontaneous functional recovery, that is recovery without any intervention or treatment, has been observed in both experimental animals and humans over a period of days, weeks or months following injury (Weidner et al. 2001; Gulino et al. 2007; Ballermann and Fouad 2006; Burns et al. 1997). The mechanisms behind this spontaneous functional recovery have been investigated mainly using anatomical and behavioural approaches but remain unclear.

Although adult CNS neurons have the intrinsic capacity for regrowth over long distances (David and Aguayo 1981), anatomical studies described earlier show that regrowth is inhibited by an inhospitable environment after SCI and axonal regeneration is unlikely to contribute importantly to spontaneous recovery. For this reason, interest has focused on other mechanisms including remyelination and plasticity.

It is believed that several types of so-called 'injury-induced plasticity' or rearrangements of the nervous system may occur in response to SCI, and could play a role in generating functional recovery. The existence of synaptic and anatomical (sprouting) plasticity in the injured and remaining uninjured axons has been observed by molecular and anatomical approaches in animals in which spontaneous functional recovery has been seen. Shortly after an injury, inactive synapses or pathways may be transformed to be functional (Merzenich et al. 1984). Later on, the target of a partially lesioned projection may produce a greater number of receptors to bind a reduced number of available neurotransmitter molecules (Gulino et al. 2007). The spared axons may also sprout to form new functional synapses (Brus-Ramer et al. 2007; Bareyre et al. 2004; Weidner et al. 2001).

So far, evidence for plasticity following injury has been based mainly on anatomical observation and evidence for improved function on behavioural observation. However, direct functional investigations of injured and uninjured

pathways following SCI which are needed to prove changes in these systems are relatively rare.

The main aims of the experiment described in this chapter were therefore: 1) to determine whether an electrophysiological approach can be used to detect changes in spinal cord function in response to injury; 2) if so, to determine in which locations of the cord the plasticity happens; 3) to determine the degree of the plasticity that occurs; 4) to determine the time course over which the plasticity develops.

To assess functional changes in ascending and descending pathways of the spinal cord, cord dorsum potentials (CDP) evoked by pyramidal or radial nerve stimulation were recorded rostral and caudal of a dorsal column lesion. These potentials were compared in normal animals, acutely lesioned animals, and in dorsal column lesioned animals at 1 week and 3 months after lesioning.

Electrophysiological assessment is a potentially powerful means to directly evaluate changes of pathways of interest in response to spinal cord injury and experimental treatments designed to improve function. However, it is crucial that the stimulation and recording conditions are properly understood and appropriately controlled so that valid quantifiable results are obtained in order to compare among different groups. Ideally, the electrical stimulation used to activate the pathway of interest should be applied at a location and at an intensity which will fully activate the whole of that pathway but do so selectively. It is relatively easy to achieve this when stimulating peripheral nerve to activate sensory pathways because peripheral nerves can be isolated from surrounding tissues. However, the problem is much greater when activating the descending corticospinal tract because the target pyramid is surrounded by the reticular formation and close to the contralateral pyramid. The first aim of this part of the study was therefore to establish a reliable approach to fully activate the CST by stimulating within the pyramid on one side without activating fibres in the contralateral pyramid or reticular formation.

# 2.2 Methods

## *2.2.1 Animals*

All experiments were approved by the Ethical Review Process Applications Panel of the University of Glasgow and performed in accordance with the UK Animals (Scientific Procedures) Act 1986.

The observations reported in this chapter are based on investigation of 61 male Fischer 344 rats (Harlan, Loughborough, UK). Twenty-four rats were naïve non-lesioned animals from which normal data was obtained in an acute electrophysiological experiment. Subsequently, 7 of them were subjected to acute bilateral dorsal column lesions and further electrophysiological assessment. The remaining 37 rats were subjected to dorsal column lesions and were allowed to recover. Of these, 19 animals were investigated electrophysiologically after 1 week survival and 18 were investigated after 3 months survival. Rats used for the naïve group weighed 310 –385g at the time of electrophysiology to approximately match the weight of animals which had been lesioned and allowed to survive for 3 months. At the time of surgery, rats used for the lesioned group weighed 246-290g (1 week survival) and 203 - 255g (3 months survival).

## *2.2.2 Lesioning*

All the dorsal column lesions in this study were carried out by Dr. John Riddell.

### 2.2.2.1 Drugs

Lesioned animals routinely received the following peri-operative medication as required:

Buprenorphine (Vetergesic): 0.05mg/kg subcutaneous route, one dose at the time of induction and a further dose the following morning.

Carprofen (Rimadyl): 5mg/kg subcutaneous route, one dose at the time of induction and as required.

Saline: 0.2-0.4ml/100gm body weight (subcutaneous route), two or three times daily for up to three days and as required.

Enrofloxacin (Baytril): 5mg/kg subcutaneous route, twice daily from day of surgery for 7 days.

Amfipen (antibiotic): 22.5mg/kg, pre-op subcutaneously.

An ophthalmic ointment was applied to the eyes to prevent drying.

#### 2.2.2.2 Dorsal column lesion procedure

The dorsal columns were lesioned bilaterally at the C4/C5 junction. This location was chosen because it is accessible surgically and allows electrophysiological assessment of corticospinal and sensory input originating from the forelimb. The lesion of the dorsal columns interrupts the main component of the corticospinal tract which runs in the ventral aspect of the dorsal columns and the ascending dorsal column pathway more dorsally. Surgical materials and instruments were sterilised and precautions were taken to minimise the risk of infection.

Animals were anaesthetised with 5% halothane and oxygen at the time of induction, 1.5% halothane and oxygen during the surgery. The cervical spinal cord was exposed by laminectomy between C3 and C5. The dorsal columns were lesioned close to the C4/5 segmental border using a wire knife (David Kopf Instruments, Tujunga, USA; Figure 2-1). The wire knife, made of a 100μm diameter tungsten wire ensheathed within a Teflon cannula, is such that when the wire is protruded from the cannula, it coils to form an arc. The knife was mounted on a stereotactic device fitted with a stepper motor. The C4/5 segmental border was identified by locating the C2 Processus spinosus and dorsal roots. The sheathed knife was inserted through a slit in the dura over the left dorsal root entry zone, approximately 700 μm left from the midline of the spinal cord lowered to a depth of 950 μm and then protruded to form an arc (approximately 1.8 mm diameter) encompassing the dorsal columns. This was then raised against a glass rod placed on the surface of the cord, cleanly transecting the dorsal columns without damage to the surface vessels. To ensure transection of the most superficial fibres while preserving the integrity of the

dorsal vein, a pointed cotton bud was pressed into the arc created by the wire knife for approximately 20 seconds. The advantage of this method is that it is accurate and reproducible and this provides greater consistency across and within groups of animals.

A suture was placed in the dura over the lesion so that the location could be identified at the later electrophysiological experiment and the segmental level confirmed at the end of the experiment. The wound was closed and analgesia, antibiotics and s.c. saline routinely administered as mentioned before. Animals were recuperated in a warm environment in which easy access to food and water was provided. Animals were allowed to survive up to 3 months.

### *2.2.3 Eelectrophysiological experiment*

#### 2.2.3.1 Anaesthesia

Anaesthesia was induced with 5% halothane in oxygen, maintained with 1.5-2% halothane in oxygen during the initial surgical procedures, and subsequently with frequent doses of sodium pentobarbital (10 mg/kg i.v.), given as required. The depth of anaesthesia was assessed during the dissection by monitoring withdrawal reflexes, the corneal reflex, arterial blood pressure and an electrocardiogram. Additional doses of anaesthetic were given if a withdrawal reflex was seen on pinching or if blood pressure increased on pinching or was abnormally high. During the recording phase of the experiment, when the animal was paralysed and artificially ventilated (see below), administration of anaesthetics was continued at a rate commensurate with that required before paralysis. The adequacy of this regime was checked by continuously monitoring the arterial blood pressure and its response to noxious stimuli.

#### 2.2.3.2 Preparatory surgery

The animal was placed in the supine position on an operating table and secured with adhesive tapes attached to each of the limbs. The animal's core temperature was continuously measured by a rectal probe and maintained by a heating blanket and radiant heat close to 38$^{o}$C. The electrocardiogram was monitored during dissection through needle electrodes which were inserted

through skin of the left and right forelimb and the right hind-limb (when a surgical level of anaesthesia had been obtained heart rate was typically between 360-400 beats/minute). Before starting the surgery, dexamethasone sodium phosphate (2-3 mg/kg i.m., Faulding Pharmaceutics Plc, UK) was injected to prevent the swelling of the brain and spinal cord. Atropine sulphate (Martindale Pharmaceuticals, UK) at a dose of 0.05 mg/kg was also injected intraperitoneally to reduce bronchial constriction and salivary secretions. Before making skin incisions, fur was removed from the relevant areas using an animal fur clipper. Fine surgery including cannulation, nerve dissection and laminectomy were performed with the aid of a dissecting microscope (Zeiss S5, Germany). A cautery (Eschmann equipment, TDB 50, UK) or soldering iron was used to prevent bleeding from blood vessels.

#### 2.2.3.3 Cannulation

A carotid artery, jugular vein and the trachea were cannulated. A midline incision was made through the skin overlying the trachea, the skin was retracted and the superficial muscles covering the trachea were separated. A carotid artery (usually right side) was carefully exposed by blunt dissection and about 2 cm of the artery freed from surrounding connective tissue, avoiding damage to the vagus nerve. The artery was ligated distally and a cannula inserted proximally (i.e. towards the heart) to permit continual monitoring of arterial blood pressure which was maintained above 80mm Hg (usually at 100-120mm Hg) during the experiment. The arterial cannula was filled with heparinised saline (1% heparin in sterile saline) to help prevent blood clot formation and maintain patency for chronic blood pressure measurement. A jugular vein was cannulated to allow intravenous administration of anaesthetics and other drugs. The skin and muscles overlying the trachea were retracted and a small length of the trachea was separated from the surrounding tissues. The trachea was opened and a cannula with appropriate diameter inserted and tied in position. From time to time excessive secretions in the trachea were removed by suction. All cannulae were secured to the skin by threads in order to prevent them being accidentally dislodged and skin incisions were closed with Michel clips.

#### 2.2.3.4 Radial nerve dissection

To dissect superficial branches of the left radial nerve, the animal was placed in the pronate position and an incision was made on the dorsal aspect of the left forelimb from the shoulder proximally to about the elbow distally. The tensor of triceps brachii muscle was cut to expose the superficial branches of the radial nerve. The branches were dissected free (approximately 2 cm) and sectioned distally. A suture loop was tied to the end of the radial nerve in order to lift it without damage. The exposed nerve was covered with cotton soaked with saline to prevent the nerve from drying (Figure 2-2).

#### 2.2.3.5 Laminectomy

A laminectomy was performed to expose the cervical (C1-T1) segments of the spinal cord. A mid-line skin incision was made from skull to upper thoracic region. The skin was retracted and the cervicoauricular muscles and trapezius muscles were separated (partially removed if necessary) from the vertebral column. Afterwards, the posterior arch was cautiously removed by using small bone rongeurs and bone cutting instruments to expose the cervical spinal cord. In lesioned animals, the lesion location was identified from a 10/0 marking suture left in the dura at the end of the lesion operation and by its darker appearance compared to the surrounding cord. Bone wax and plasticine were used to prevent the seeping of blood from the cut edge of vertebrae and gel foam was also used to prevent bleeding. Care was taken to avoid damage to the cord which is vital.

#### 2.2.3.6 Transferring to recording frame

After completing the surgery, the animal was transferred to the recording frame. The animal’s head was secured by an incisor bar and ear bars. The vertebral column was fixed rigidly by the incisor bar, ear bars and a clamp which gripped the spinal processes of lower-thoracic vertebrae.

### 2.2.3.7 Paraffin pools

Paraffin pools were formed around the posterior side of the left forelimb and the laminectomy region by attaching threads passed through the edge of the skin incision to part of the frame. The pools were filled with liquid paraffin at about 37$^{o}$C so as to cover all exposed tissues. This insulation prevented current spread to other tissue on electrical stimulation of peripheral nerves. In addition, heat loss and drying of tissue were also avoided. The lesion site and/or the C4/5 border were identified and a strip of paper with mm markings placed along side the cord to provide a reference for the positioning of recording electrodes. The dura was carefully opened. The C2, C3 and C4 left dorsal roots were cut to avoid any input to the spinal cord above the lesion from afferents travelling in these roots. Care was taken to avoid damage to the cord.

### 2.2.3.8 Artificial ventilation

Before beginning recording, it was necessary to paralyse and artificially ventilate the animal in order to prevent movements while stimulating in the pyramids. The trachea was cleared of excessive secretions by suction and the animal was paralysed with Pancuronium Bromide (Sigma, induce with 0.3 mg/kg i.v. and top-up with doses of 0.04mg every 30 minutes or as required). The animal was artificially ventilated with air by connecting the tracheal cannula to a respiratory pump (6025 ventilator, UGO basile, Italy). The level of carbon dioxide was monitored (Micro-Capnometer, Columbus Instrument, USA) and was kept about 4% throughout the experiment by adjusting the ventilation rate.

### 2.2.3.9 Craniotomy

A small craniotomy was performed on the interparietal bone by using a fine dental drill. Care was taken to prevent continuous bleeding. The appropriate location (between lambda and the ridge on the back of the skull) was chosen to allow access for the stimulating electrode to be sited in the pyramids (see below).

### 2.2.3.10 Stimulation of the corticospinal tract

The corticospinal tract was activated by stimulation within the pyramids by a dorsal approach (Stone 1972) (Figure 2-3B). A bipolar electrode was used in order to maximise the current density close to the tip and reduce stimulus spread (SNE-100X, shaft diameter 0.25mm, shaft length 50mm, Kopf instruments, Tujunga, CA, USA). The electrode was checked before each experiment for impedance and for the integrity of the insulation. The electrode was mounted in a Kopf electrode holder at an angle of 20 degrees with the tip pointing rostrally. The electrode holder was mounted on the Kopf U-frame (head holder), the tip was then calibrated to ear bar zero by alignment with an ear bar set in the frame. The electrode and its carrier were then removed and replaced once the animal was in the frame and the craniotomy was completed. After examining a stereotaxic atlas of the rat brain (Paxinos and Watson 1998), the following stereotaxic co-ordinates were chosen with the aim of targeting the middle of the right pyramidal tract at a point in the brainstem where it is discrete and compact (Medio-lateral: 0.7mm to the right; Anterior-posterior: slightly rostral to the intra-aural line, depth: approximately 1mm below intra-aural line).

After adjusting the medio-lateral positioning of the electrode carriage appropriately for the above co-ordinates, the electrode was lowered through the dura and into the brain. Once in the brain it was lowered to a position approximately 1mm above the intra-aural line.

Electrical stimuli (0.2ms duration square waves, up to 5mA in amplitude) were then applied and the final positioning of the electrode was completed while monitoring the cord-dorsum potential evoked on the surface of the cervical spinal cord (for details of recordings, see below). Recordings were routinely made at a position 5 mm rostral to the C4/5 border which was used as a reference point in non-lesioned animals and is above the dorsal column lesion in the lesioned groups of animals. The electrode was advanced in 0.1 or 0.2mm steps while observing the size of the CDP and determining the threshold intensity for its appearance.

Sometimes the base of the skull was reached without the optimum conditions for eliciting pyramidal-evoked CDPs from being found. In this case, the electrode was raised to the surface again and, after moving medially or laterally by 0.5mm, lowered once more to find the optimum location. Sometimes stimuli were also applied within the left pyramids to activate the contralateral tracts. Once the optimum position was located, a stimulus-recruitment curve for the pyramidal-evoked CDP at this location was collected. Recordings of the CDP (averages of 25 or 50 sweeps) were made at the same location while increasing the intensity of the stimuli applied within the pyramids in graduated steps from threshold to values that were supramaximal. The stimulus intensity producing a maximal CDP response was determined from this procedure and a supramaximal value for use in the experiment was then chosen (see Results).

#### 2.2.3.11 Stimulation of the radial nerve

The radial nerve was mounted on bipolar silver wire electrodes immersed in the paraffin pool made from the skin flaps of the forelimb surgical site (Figure 2-2C). Care was taken to avoid any contact of the nerve with surrounding tissues and the electrode was firmly secured in position once adjusted. The nerve was stimulated electrically using single square wave stimulus pulses of 0.2ms duration and up to 500μA. The maximal intensity for evoking activity in the myelinated group I and group II fibres in the nerve was determined by recording at a position 5 mm below the C4/5 border which is where a large radial-evoked CDP is normally produced and is below the level of the dorsal column lesion in the lesioned group of animals (Figure 2-3A). The stimulus intensity was then set at a value that was supramaximal for the radial-evoked CDP (typically 100-200μA).

#### 2.2.3.12 Recordings of cord dorsum potentials

To assess spinal cord function in the region of the lesion, CDPs evoked by electrical stimulation of the radial nerve and/or corticospinal tract were recorded. Recordings were made using a silver ball electrode placed on the dorsal surface of the cord, with the indifferent electrode placed on nearby back muscles. Recordings were made at 1mm intervals for 8 mm above and below the C4/5 reference level (position of the dorsal column lesions in the lesioned

animal group; see Figure 2-4A). The positioning of the electrode was guided with reference to mm graduated paper placed alongside the exposed spinal cord. At each rostro-caudal position the electrode was placed over the dorsal columns next to the dorsal root entry zone usually on the left side of the cord (though sometimes recordings were also made from the opposite side).

Recordings of CDPs were made while stimulating either the radial nerve or within the pyramids at supramaximal stimulus intensity (Figure 2-4B). The stimulus repetition rate was approximately 2Hz and recordings of 25 sweeps were typically collected and averaged at each recording position for radial nerve stimulation while 50 sweeps were averaged for the smaller potentials produced by pyramidal stimulation.

Throughout the recording of CDPs, great care was taken to remove fluid from the surface of the cord. The accumulation of cerebrospinal fluid tends to short circuit the recording electrodes and therefore results in smaller potentials than when precautions are taken to remove the fluid. This is an important potential source of inaccuracy and fluid was therefore removed before moving the cord dorsum recording electrode to each new recording position and also during recording if a decline in the amplitude of the CDPs was observed while collecting records from the same location.

All recordings of electrical potentials were digitised (Cambridge Electronic Design 1401+ interface, Cambridge, UK) and stored on a computer at a sampling rate of 20 kHz, without filtering. Averaging and measurements of the amplitudes and latencies of electrical potentials were performed using Signal software (Cambridge Electronic Design, Cambridge, UK).

#### 2.2.3.13 Conditioning of radial CDPs with pyramidal stimulation

As an additional way of assessing the function of the corticospinal projection below the level of a lesion we applied conditioning stimuli in the pyramids and looked at their effect on CDPs evoked by radial-nerve afferents below the level of the lesion (Figure 2-5).

Test potentials were evoked by electrical stimulation of the radial nerve (single shock, 0.2ms duration, supraximal intensity). Responses to test stimuli were conditioned by prior application of stimuli within the pyramids (5 shocks at 300 Hz, 0.2ms duration, supramaximal intensity). The tests were carried out using intervals between the first conditioning stimulus and the test stimulus (conditioning-test interval) of 20ms, 25ms and 30ms. In case the conditioning stimulus evoked potentials that interfered with the test potential, recordings were also made of the conditioning stimulus-evoked potentials on their own. Stimuli were applied in an alternating fashion in order to avoid changes over time (i.e. drift of the recording conditions over time due to e.g. build up of fluid) that could affect the results if sequential averaging of responses to test stimuli were collected, followed by collection of responses to conditioning plus test stimuli and then conditioning stimuli alone. For each test, the pattern of stimulation was therefore in an alternating cycle consisting of 1) test stimulus alone, 2) conditioning stimulus followed by test stimulus, 3) conditioning stimulus alone. To avoid possible interaction (e.g. inhibition) between each application of the condition-test paradigm, the repetition rate between each stimulus was 1 second. A total of 75 sweeps were collected, 25 sweeps for each of the stimulus conditions. This procedure was repeated for recordings made at 3mm, 4mm, 5mm and 6mm below the C4/5 reference position. Each of the conditioning-test intervals (20ms, 25ms, and 30ms) was tested at each position (see result).

For normal animals it was sometimes necessary to subtract records obtained during application of conditioning stimuli alone from those obtained with both conditioning and test stimuli. The resulting record of the conditioned potential was then compared to that obtained with the test stimulus alone. After dorsal column lesions, the pyramidal-evoked potentials below the lesion were much smaller so that this was not necessary. Measurements of the peak amplitude of test and conditioned potentials were made off-line and the conditioned amplitude expressed as a percentage of the test amplitude.

#### 2.2.3.14 Perfusion

Most of the animals were transcardically perfused with mammalian Ringer's solution followed by paraformadehyde fixative at the end of the

electrophysiological experiment for histology. Animals were perfused through the left ventricle with mammalian Ringer's solution containing 0.1% lidocaine (to help dilate the blood vessels) followed by 500 ml 4% paraformaldehyde in 0.1MPB, pH 7.4. Brain stem and cervical spinal cord were then carefully removed without damaging the marking electrode if present. Post fixation of the cord was achieved by placing the cord in the same fixative solution overnight in which 30% sucrose was added for the purpose of cryoprotection.

### *2.2.4 Histological processing*

#### 2.2.4.1 Histological processing of brainstem for stimulation sites

After washing in 0.1MPB, the electrode tracks in the brainstem were identified. Blocks containing the electrode tracks were carefully prepared. Blocks were notched at the ventral aspect of the spinal cord on the left side (usually electrode tracks were on right side) and sectioned transversely at 70µm using a freezing microtome (Ernst Leitz wetzlar, Germany). Sections with electrode tracks were mounted on plain glass slides in Vectashield mounting medium (Vector Laboratories, UK) and then coverslipped and the edges of the coverslip sealed with nail varnish. Slides were stored at -20°C.

#### 2.2.4.2 Histological processing of spinal cord for lesions

After washing in 0.1MPB, lesion sites were identified. Blocks containing the whole lesion were prepared. Dorsal and ventral roots were removed without damaging the lesion site. A notch was made at the ventral aspect of the cord on the right side. 70µm sections were transversely (occasionally parasagitally) cut on a freezing microtome (Ernst Leitz Wetzlar, Germany). Sometimes, where the lesion was extensive, it was difficult to cut whole sections or sections fell apart after cutting. A note was made of any sections which were lost in the cutting process so that they could be taken into account when quantifying the lesion size. Sections were washed in phosphate buffered saline 0.3M (PBS double salt), and then incubated for 30 min in 50% ethanol. After washing 3 times 10 minutes each in PBS sections were treated with fluorescence histochemistry techniques. 72h incubation of sections with anti-NF200 (1:1000 Sigma) and anti-GFAP (1:1000) primary antibodies at 4°C which label respectively the axons and the

astrocytes (lesion boundaries) was followed by appropriate species secondary antibodies conjugated to fluorophores (Alexa 488 1:500, Rhodamine 1:100) (2 hours at room temperature or overnight at 4°C). After washing 3 times for 10 minutes in PBS, sections were mounted on plain glass slides in anti-fade medium (Vectashield; Vector Laboratories, UK), and coverslipped and the edges of the coverslip sealed with nail varnish and then stored at –20°C.

## *2.2.5 Microscopy*

### 2.2.5.1 Reconstruction of stimulation sites in the Pyramids

Sections containing stimulating electrode tracks were reviewed under microscopy (Zeiss Axioplan 2 Imaging). The stimulating electrode tracks were reconstructed by using Camera lucida drawings.

### 2.2.5.2 Verification of dorsal column lesion

Sections containing the lesion cavity were observed using phase contrast light microscopy to determine the perimeter of the cavity and the relationship to the boundaries between grey and white matter. The same sections were sometimes viewed using epifluorescence microscopy to observe neurofilament immunolabelling and/or GFAP immunolabelling in the section.

### 2.2.5.3 Quantification of lesion size

Because we have previously found that the lesion elongates rostro-caudally but does not increase significantly in cross sectional area over time, we have measured the length of cavity to indicate the lesion volume. For parasagital sections, length of cavity for the section with the longest cavity from each animal was measured using a camera lucida attachment with a calibrated setting. For transverse sections, length of cavity = (the number of sections with lesion + any sections lost during cutting) X 70μm (section thickness).

## *2.2.6 Off-line analysis of electrophysiology*

### 2.2.6.1 Off-line analysis of CDPs

Average records were inspected offline using Signal software. The amplitudes of CDPs recorded at each location were measured by using Signal software. The data was noted in excel spreadsheets then imported to Prism 4 software (GraphPad Software Inc, USA) to create potential plots.

### 2.2.6.2 Off-line analysis of CDP conditioning

Average records were inspected offline using Signal software. The amplitudes of radial-evoked CDPs at different test intervals (i.e. 20ms, 25ms, and 30ms) at each recording location were measured by using Signal software. The amplitudes of radial-evoked CDPs after subtracting pyramidal conditioning were also measured for each recording. The data were entered on excel spreadsheets. Conditioned CDPs were expressed as a percentage of control CDPs. Average percentages of each recording location at different conditioning-test intervals in each group were calculated.

## *2.2.7 Statistical analysis*

The following statistical tests were carried out on the electrophysiological data (GraphPad Software Inc, USA). Analysis of variance (ANOVA), The Dunnett Post-hoc test, and Student's t-test were used to reveal the differences among different groups.

# 2.3 Results

## *2.3.1 Spinal cord function assessed by electrophysiology*

In this study, cord dorsum potentials (CDPs) evoked by stimulating the corticospinal tract and/or radial nerve were used to assess function in the cervical spinal cord.

Recordings were made from normal animals (n=24) and animals with dorsal column (DC) lesions (n=37). Animals with dorsal column lesions were investigated at three time points: immediately after the lesion (n=7), one week following the lesion (n=19), and three months following the lesion (n=18).

### 2.3.1.1 Components of surface potentials evoked by pyramidal stimulation

When the stimulating electrode was lowered into the brain stem using the appropriate stereotaxic co-ordinates (see methods), a potential could be detected with an electrode on the surface of the spinal cord. The potentials were recorded with a silver ball electrode positioned on the dorsal columns at 1mm intervals from 8mm rostral to 8mm caudal to the C4/5 segmental border (Figure 2-4). Examples of pyramidal-evoked CDPs are shown in Figure 2-6. The surface recordings consist of a stimulus artefact which indicates the onset of stimulation. This is followed after a brief interval by a short duration wave called an afferent volley which represents the action potentials travelling along fibres in the CST. Immediately following this is a longer duration wave called a CDP. This represents the synaptic activity generated by connections between the collaterals of the CST fibres and spinal cord neurons in the grey matter and provides a measure of the strength of these connections. The recordings in Figure 2-6 were made at different rostro-caudal locations. The afferent volley is clearest and largest at locations close to the stimulation site, becomes dispersed further from the stimulation site and eventually merges with the CDP at more caudal locations.

### 2.3.1.2 Conduction velocity of corticospinal fibres

To obtain a value for the conduction velocity of the corticospinal fibres, the latency between the onset of the stimulating pulse and the onset of the afferent volley (as is indicated for the recording in Figure 2-6) was measured in two normal animals. The latencies were measured for all recordings from 8mm rostral to 8mm caudal of the C4/5 border. The latencies were then plotted against recording locations as shown in Figure 2-7. The plots were fitted with lines using linear regression. The slopes of these lines give the conduction velocity of the fastest conducting corticospinal fibres which are as indicated on the plots in Figure 2-7.

In each case the plots were best fitted by two separate lines of different slopes indicating a change in conduction velocity. The fibres appeared to conduct more rapidly (20.3$ms^{-1}$ and 21.2$ms^{-1}$) in the upper cervical segments and to slow within the C4-7 segments (10.3$ms^{-1}$ and 14.5$ms^{-1}$). This slowing presumably reflects the more extensive branching of the fibres within these segments and the resultant thinning of the parent branches. The conduction velocities of the CST measured between +3 and -8mm are similar to those reported by others (Alstermark et al. 2004; Mediratta and Nicoll, 1983).

### 2.3.1.3 Technical problems associated pyramidal stimulation

In order to obtain a quantitative measure of the strength of actions of the corticospinal pathway which can be compared between animals, it is necessary to be able to activate the corticospinal pathway consistently, i.e. to the same extent, from animal to animal. Using a supra-maximal stimulus intensity is a convenient way of achieving this. The pyramids consist of compact bundles of corticospinal fibres and therefore provide an anatomically convenient location at which to activate the whole of the corticospinal tract. In principle, with an electrode placed in the middle of a pyramid, it should be possible to increase the stimulating current intensity until it is sufficient throughout the pyramids to activate the whole of the tract. In practice there are several potential problems. 1) The stimulus intensity has to be raised sufficiently to achieve a current density that activates fibres at the outer edge of the pyramids; 2) At the same time, there should not be current spread beyond the outer edge of the pyramids

that would activate reticulospinal fibres in the adjacent reticular formation; 3) the stimulus current should also activate fibres at the edge of the pyramids before reaching a density close to the electrode tip that would produce anodal block of fibres at the centre (Ranck 1981); 4) The pyramids are bilateral structures which lie very close to one another at the midline. If the electrode is not optimally placed in the target pyramid (e.g. too close to the midline), then there is the possibility that partial activation of the opposite pyramid may occur before activation of the target pyramid is fully achieved. This could be a problem depending on the type of recordings being made.

#### 2.3.1.4 Method for supramaximal activation of the corticospinal tract unilaterally

To determine whether it was possible to fully activate the pyramidal tract on one side only, careful stereotaxic placement of the electrode was combined with investigation of the stimulus-recruitment curve and subsequent histological determination of the position of the electrode tip. Figure 2-8 illustrates this process. First the electrode was lowered to the position where the threshold for evoking a CDP at the +5 mm position was lowest and a careful note made of this threshold intensity. In Figure 2-8A, a CDP was just evident at an intensity of 8μA. Recordings were then made while the stimulus intensity was increased incrementally (as shown by in Figure 2-8A) and a note was made of the point at which the CDP was maximal. Measurements of the CDP amplitude at different stimulus intensities were later plotted as shown in Figure 2-8B. This procedure was followed in all experiments in which pyramidal stimulation was used to determine an appropriate supramaximal stimulus intensity for use in the experiment. After the experiment, the electrode track was identified in histology of the brain stem (Figure 2-8C) and its position reconstructed (Figure 2-8D).

In order to determine the conditions under which stimulation within the pyramids could safely be considered to have maximally activated the target pyramid without stimulus spread to the opposite pyramid, a systematic comparison was made of the stimulus-recruitment curves and electrode position for all animals where this was obtained. For this exercise, data from experiments reported in this chapter has been pooled with that from

experiments described in Chapter 3. Table 2-1 shows the different experimental groups from which these animals were drawn. The comparison is based on 40 F344 animals for which histological reconstruction of one or more stimulating electrode sites was performed.

The animals were divided into four groups based on the position of the stimulating electrode determined histologically: a “Middle” group where the electrode was located in the middle third of the target pyramid, a “Lateral” group where the electrode was located in the lateral third of the target pyramid, a “Medial” group where the electrode was within the medial third of the target pyramid, and a “Midline” group where the electrode was at the extreme medial end of the target pyramid and/or very close to the midline. Note that animals in this later group were excluded from further study but are reported here for the purpose of validating the pyramidal stimulation conditions. The numbers of animals and stimulation sites in each of these groups is shown in Table 2-2.

#### 2.3.1.5 Comparison of stimulus-recruitment curves and electrode position

***Threshold stimulus intensity***

Table 2-2 shows data for the threshold stimulus intensities for animals in each of these groups. As can be seen, when the electrode was placed in the middle or lateral third of the target pyramid the mean threshold was around 10μA and when in the medial third less then 20μA. However, when the electrode was off target and lay close to the midline, the mean threshold was just above 30μA, three times higher than at the centre (bottom line of Table 2-2). When each of the animal groups is considered as a whole, irrespective of the electrode position (but excluding animals where the electrode was off target i.e. midline), the mean threshold values are quite similar, being between 8 and 17μA. In particular, there is no difference between the normal animal group and the three month survival dorsal column lesioned animals. This suggests that the dorsal column lesion has little effect on the excitability of the corticospinal fibres being investigated.

***Pattern of recruitment***

The pattern of recruitment of corticospinal fibres as stimulus intensity was raised above threshold was evaluated in three ways. 1) by visually inspecting the shape (steepness and position of plateau) of the stimulus-recruitment curves; 2) by determining the stimulus intensity evoking a CDP 95% of maximum amplitude and 3) by noting the maximal amplitudes of CDPs at a fixed recording location.

Examples of stimulus-recruitment curves obtained with the stimulating electrode positioned in the middle third of the target pyramid are shown in Figure 2-9. The stimulus-recruitment curves obtained from this group were generally very steep and plateaued abruptly. The mean stimulus intensity at which CDPs in this group were 95% of maximal was 226μA (Figure 2-13) and the mean amplitudes of maximal CDPs were 0.3mV (see Table 2-3). Once the stimulus-recruitment curve had reached a plateau there was minimal change in amplitude as the stimulus intensity was increased several fold above maximal. Not only was there rarely much of an increase in the amplitude of CDPs but usually there was little or no decrease in amplitude as might be expected if anodal block was a problem.

Examples of stimulus recruitment curves obtained with the stimulating electrode positioned in the lateral third of the pyramids are shown in Figure 2-10. The stimulus recruitment curves obtained from this group were quite similar to the "middle third" group being steeply rising and arriving abruptly at a plateau. The mean stimulus intensity at which CDPs in this group were 95% of maximal was 136μA (see Figure 2-13) and the mean amplitudes of the maximal CDPs were 0.42mV (see Table 2-3). Minimal change in amplitude occurred even when the stimulus intensity was increased several fold above maximal.

Examples of stimulus recruitment curves obtained with the stimulating electrode positioned in the medial third of the pyramids are shown in Figure 2-11. The picture was broadly similar to the previous two groups except that some of the stimulus recruitment curves were less steep and approached a plateau level less abruptly. Consistent with this the mean stimulus intensity at which CDPs in this group were 95% of maximal was a little higher at 310μA (see Figure 2-13). However, the mean amplitudes of the maximal CDPs was similar at 0.34mV (see Table 2-3). Again, once the stimulus response curve had reached a plateau, there was minimal change in amplitude as the stimulus intensity was increased several fold beyond maximal.

Examples of stimulus recruitment curves obtained with the stimulating electrode positioned close to the midline are shown in Figure 2-12. The picture here was quite different from when the stimulating electrode more accurately targeted a pyramid. In this case, the stimulus-recruitment curves were always more gently sloping and more gradual in their approach to a plateau level. This was reflected in the mean stimulus intensity at which the CDPs evoked from these locations were 95% maximal which was much higher than at the other locations at 497μA (see Figure 2-13). Furthermore the maximal amplitudes of CDPs evoked by stimuli near the midline were considerably greater than at all the other locations, in some cases up to twice as large (mean 0.58mV, see Table 2-3).

The results show that stimulation within the middle and lateral thirds of the pyramids produces steep stimulus recruitment curves which reach a maximum and do not grow further when the stimulus intensity is raised to several multiples of maximal. Stimulation within the medial third can also result in complete activation of the target pyramidal tract without significant stimulus spread provided that the electrode tip is not too close to the midline. Stimulation throughout these sites results in CDPs of broadly similar amplitudes. However, when the stimulation site is too close to the midline, it appears that stimulus can spread to activate fibres in both pyramids resulting in larger CDPs at the spinal level.

Histological verification of the position of the stimulating electrode relative to the pyramids was obtained only for a proportion of the animals (40 out of 112; 36%). It was therefore necessary to have a method of filtering out those animals where the pyramidal electrode was too medially placed but the electrode position not determined histologically. This was done by inspecting the stimulus recruitment curve for the following features: 1) a relatively high threshold stimulus intensity (i.e. 20 μA or more); 2) a gradual and rounded slope; 3) a relatively high maximal stimulus intensity 4) a relatively high maximal CDP amplitude. Where these features were seen the animals were omitted from the study.

Although for purposes of comparison we have divided animals into “medial” and “midline “ groups, in practice there must be a continuum in the distribution of stimulating positions moving progressively more medially to approach the

midline. To check how effective the use of the above electrophysiological exclusion criteria were in the selection of animals, we compared the amplitudes of maximal CDPs recorded from animals for which histological verification of the stimulation site was obtained with that for the population of animals as a whole. As can be seen in Table 2-4 these proved to be closely similar so validating the approach.

The ideal placement for the electrode is in the middle third of the pyramids though the results show that placement within the medial or lateral third of the pyramids can also be compatible with selective and full activation of the target pyramid. The histological reconstructions of electrode tracks showed that in 43% of animals the electrode tip lay within the middle third and in a further 45% within the lateral or medial third of the pyramids. In only 12% of animals was the electrode tip close to the midline and therefore unsuitable for obtaining valid results. Furthermore, in some of these cases, it was possible to re-position the electrode to obtain valid results. This shows that the method can be used with a fairly high success rate.

#### 2.3.1.6 Cord dorsum potentials generated unilaterally can be recorded bilaterally

Recording from the surface of the spinal cord is a convenient way of recording population synaptic activity generated at synapses between spinal cord neurones and the afferent pathways terminating on them. However, synaptic activity generated by activity on one side of the cord can be detected at varying positions on the cord surface including on the contralateral side. For recordings of CDPs evoked by peripheral nerve stimulation there is usually some attenuation of the contralateral potential. However, for CDPs evoked by stimulation in the pyramids, even under conditions where we were confident the stimulation was unilateral, CDPs recorded from the two sides of the cord were often closely similar in amplitude. Figure 2-14 shows examples of CDPs recorded from both sides of the cord in 3 different animals where the stimulating electrode was located close to the middle of the target pyramid. Figure 2-15 shows stimulus recruitment curves recorded contralateraly and ipsilaterally to the stimulated side when the electrode was placed in the lateral half of the target pyramid. The close similarity of the curves indicates that they are generated by activation

of the same population of fibres. It is evident from this that being sure that pyramidal stimulation results in the activation of the pyramids on one side only is important to the validity of using cord dorsum potentials as a measure of the effectiveness of the corticospinal tract.

#### 2.3.1.7 Assessment of pyramidal-evoked CDPs

Pyramidal-evoked CDP recordings were made from normal animals (n=18), acutely lesioned animals (n=7), one week survival lesioned animals (n=14), and three month survival lesioned animals (n=15).

***Normal animal group***

CDPs evoked by pyramidal tract stimulation were investigated in 18 normal animals. Examples of CDPs recorded from three representative animals of this group are shown in Figure 2-16. The recordings show that clear surface potentials are evoked by pyramidal stimulation at all of the recording locations examined. This is from 8mm rostral to 8mm caudal to the C4/5 border of the cervical segments. Cervical segments are about 3mm long in the rat so that this corresponds to approximately C2 to C7. The recordings show clear afferent volleys rostrally which become more dispersed and show a longer latency at progressively more caudal recording locations due to the longer conduction distance. The amplitudes of the CDPs were often quite similar at all of the recording locations as shown in Figure 2-16. However, sometimes the amplitudes of the CDPs were smaller at particular locations perhaps because of blood vessels. The mean CDP amplitude for all animals in this group at each recording location is shown in Figure 2-17. This plot confirms that in normal animals, pyramidal-evoked CDPs are on average of similar amplitude at all recording sites from 8mm rostral to 8mm caudal of the C4/5 segmental border. The average amplitudes are around 0.25-0.3 mV, though as the error bars indicate, there was some variation from animal to animal.

***Repeatability of CDP recordings***

To test the repeatability of CDP recordings, multiple mappings of pyramidal-evoked CDPs were performed in two animals while the stimulating electrode remained at exactly the same location in the right pyramid. Other conditions

such as the stimulus intensity also remained the same. The mapping was performed from 8mm above to 8mm below the C4/5 segmental border and each mapping was performed sequentially. Recordings at each location were separated by between 15 to 20 minutes since this is the time it takes to complete one mapping. An example of the recordings made from one of these animals is shown in Figure 2-18. As can be seen, the amplitudes of the CDPs recorded in each mapping are closely similar showing that the recording method is quite consistent and the CDPs quite stable over time.

### *Acute lesion group*

The effect of acutely lesioning the dorsal columns on CDPs evoked by pyramidal stimulation were investigated in 7 animals. Recordings were made both before and after lesioning the dorsal columns and the first recordings began between 10 and 25 minutes after making the lesion. Examples of CDPs recorded from two representative animals of this group are shown in Figure 2-19. As expected, CDPs recorded below the level of the lesion were virtually abolished due to the axotomy of the main component of the corticospinal tract on which these potentials largely depend. CDPs remained, however, above the lesion site. The rostro-caudal distribution of CDPs for this group is shown in Figure 2-20, which shows the mean CDP amplitude for all animals in this group at each recording location. This confirms that CDPs below the lesion are almost undetectable but also shows that the lesion did not change the amplitudes of CDPs above the lesion (from +3 to +8mm).

### *One week survival DC lesioned group*

CDPs evoked by stimulation in the pyramidal tract were investigated in 14 animals one week after a dorsal column lesion. Examples of CDPs recorded from two representative animals of this group are shown in Figure 2-21. The rostro-caudal distribution of CDPs for this group is shown in Figure 2-22. As in the acutely lesioned group, CDPs below the lesion were almost abolished. At some positions close to the lesion, the CDPs appeared to be slightly larger than following acute lesions but this was not significant (Table 2-5). Above the lesion, the CDPs persisted and in fact tended to be of larger amplitude (by 20-40%) than those recorded from normal animals and acutely lesioned animals. This tendency was significant at most locations when compared to normal animals but did not

reach significance for acutely lesioned animals because of the small number of animals investigated (Table 2-5).

***Three months survival DC lesioned group***

CDPs evoked by stimulation in the pyramidal tract were investigated in 15 animals three months after a dorsal column lesion. Examples of CDPs recorded from two representative animals of this group are shown in Figure 2-23. The rostro-caudal distribution of CDPs for this group is shown in Figure 2-24. Although CDPs below the lesion were much smaller than those recorded in normal animals, they were two to five times larger at all recording locations than those recorded in animals one week after a dorsal column lesion. This difference was significant at all recording sites (-2 to -8mm) except those closest to the lesion (Table 2-5). Above the level of the lesion, CDPs were significantly larger than in normal animals (Table 2-5) and virtually the same as those recorded in animals one week after a dorsal column lesion.

#### 2.3.1.8 Cord dorsum potentials evoked by radial nerve stimulation

Recordings were made from normal animals (n=22), acutely lesioned animals (n=7), one week survival lesioned animals (n=17), and three month survival lesioned animals (n=18).

Potentials evoked by radial nerve stimulation were recorded with a silver ball electrode positioned on the dorsal columns at 1mm intervals from 8mm rostral to 8mm caudal to the C4/5 segmental border as for pyramidal-evoked potentials (Figure 2-4). Examples of radial nerve-evoked CDPs are shown in Figure 2-25. Electrical stimulation of the radial nerve typically produces an afferent volley followed by a distinct negative CDP from the dorsal surface of the spinal cord. The recordings in Figure 2-25 were made at different rostro-caudal locations. The afferent volley is clearest and largest at locations close to the segment of entry of the stimulated root, becomes dispersed at more rostral and caudal locations. The CDPs represent the synaptic activity generated by connections between the collaterals of the primary afferent fibres and spinal cord neurons and provide a measure of the strength of these connections.

To test the contribution of each spinal dorsal root to the amplitude of radial nerve-evoked CDPs, dorsal roots were sequentially sectioned following a different order in two animals, while recording the CDPs at a fixed position. The amplitudes of CDPs following dorsal root sectioning were expressed as percentages of the CDPs before lesioning. The percentages are shown in Table 2-6. In the first animal, CDPs were recorded from the middle of C6 (about 4mm below the C4/5 segmental border). The amplitude of this CDP was substantially reduced to 35.2% after C6 dorsal root sectioned and almost abolished after sectioning both C6 and C7 dorsal roots. Similar results were obtained from the second animal. CDPs were recorded from the middle of C7 (about 7mm below the C4/5 segmental border). When the C7 dorsal root was sectioned, the amplitude of the CDP was reduced to 63.9%. Sectioning both C7 and C6 almost abolished the CDP. Therefore, C6 and C7 dorsal roots contribute most to the CDPs.

***Normal animal group***

CDPs evoked by radial nerve stimulation were investigated in 22 normal animals. Examples of CDPs recorded from three representative animals of this group are shown in Figure 2-26. The recordings show that clear surface potentials are evoked by radial nerve stimulation at all of the recording locations examined. Afferent volleys are seen especially close the entry of the radial afferent which was 3 to 4 mm below C4/5 segmental border.

The rostro-caudal distribution of CDPs for this group as a whole is shown in Figure 2-27, which shows the mean CDP amplitude for all animals in this group at each recording location. In normal animals, the biggest radial-evoked CDPs were recorded at around 3 to 4mm below the C4/5 segmental border. The amplitudes of the biggest CDPs were around 0.7mV. CDPs of gradually declining amplitude could be recorded for several segments above and below the C4/5 segmental border. Small CDPs were still detected at 8mm above the C4/5 segmental border.

***Acute lesion group***

CDPs evoked by radial nerve stimulation were investigated in 7 acutely lesioned animals. Examples of CDPs recorded from two representative animals of this

group are shown in Figure 2-28. As anticipated, CDPs were virtually absent above the lesion due to axotomy of the ascending branches of primary afferent fibres on which these potentials largely depend. CDPs remained, however, below the lesion site. The rostro-caudal distribution of CDPs for this group is shown in Figure 2-29. Surprisingly, CDPs recorded below the lesion tended to be smaller following the acute lesion compared to those recorded in normal animals but this was not significant (Table 2-7).

### *One week survival DC lesioned group*

CDPs evoked by radial nerve stimulation were investigated in 17 animals one week after a dorsal column lesion. Examples of CDPs recorded from two representative animals of this group are shown in Figure 2-30. The rostro-caudal distribution of CDPs for this group as a whole is shown in Figure 2-31. CDPs tended to be larger than those recorded in acutely lesioned animals at every recording location. However, this was only significant for certain sites below the lesion probably because of the small number of animals in the acute lesion group (Table 2-7). Interestingly, CDPs recorded below the lesion tended to be larger than those recorded in the normal animals group between -3 and -8 and the difference was significant at some locations (Table 2-7).

### *Three months survival DC lesioned group*

CDPs evoked by radial nerve stimulation were investigated in 18 animals three months after a dorsal column lesion. Examples of CDPs recorded from two representative animals of this group are shown in Figure 2-32 and the rostro-caudal distribution of CDPs for this group as a whole is shown in Figure 2-33. In three month survival animals, CDPs recorded above the lesion were very similar in amplitude to those recorded in one week lesioned animals. Below the lesion, CDPs recorded from three month survival animals were significantly larger at all locations than those recorded for the acute lesion group except -2mm (Table 2-7). CDPs differed in a more complex way from those recorded at one week. Close to the lesion (0 to -2mm) the CDPs in three month animals tended to be smaller than those recorded in one week animals and this difference was significant (Table 2-7). Farther away from the lesion, however, CDPs in three month animals were the same or larger than those recorded at one week after lesioning though the difference was only significant at -6mm.

#### 2.3.1.9 Conditioning

Activity in the corticospinal tract leads to inhibition of transmission at the terminals of sensory afferents in the spinal cord and this can be detected using a conditioning-test paradigm where stimulation in the pyramids precedes stimulation of sensory afferents (see methods, Figure 2-5).

In order to test whether the significantly larger amplitude pyramidal-evoked CDPs seen at the caudal locations in the three month dorsal column lesioned animals compared to the one week animals also leads to a change in the strength of the inhibition, conditioning was performed while recording at -3, -4, -5, and -6mm using conditioning-test intervals of 20ms, 25ms, and 30ms. Conditioning was performed in 7 normal animals, 8 one week dorsal column lesioned animals and 9 three month survival animals.

An example of conditioning in a normal animal is shown in Figure 2-34. Here a radial nerve-evoked CDP recorded at -3 is conditioned by applying stimuli in the pyramids at a conditioning-test interval of 20ms. A train of 4 shocks within the pyramid was applied as this has previously been found to evoke maximal inhibition. The effects of the inhibition were clear in a normal animal (Figure 2-34B). The percentages of inhibition produced at different conditioning-test intervals at different position are shown in Figure 2-35. In normal animals, the radial-evoked CDPs were inhibited by between 13% and 17%. The inhibition was similar at different conditioning-test intervals i.e. 20ms, 25ms, and 30ms and tended to be slightly stronger more rostrally.

An example of conditioning in a lesioned animal is shown in Figure 2-36 and the results from all animals in the lesioned animal groups are summarized in Figure 2-35. The percentages of inhibition detected in each of the lesion groups (between 6%-12%) was much lower than in normal animals as expected following axotomy of the main component of the corticospinal tract. The remaining conditioning effect may be due either to the minor corticospinal component travelling in the lateral funiculus or propriospinal actions. However, there was little difference between any of the lesioned animal groups. In particular, the inhibition seen in three month survival animals did not differ significantly from the one week survival animals.

### *2.3.2 Lesion*

The appropriate locations of the dorsal column lesions (C4/5 segmental border) were confirmed in all the lesioned animals included in this study. The lesions made by the wire knife were accurate and consistent across and within groups of animals.

Examples of sections containing lesion cavities from different animal groups are presented in Figure 2-37. In the acute lesion group, the lesion was contained within only a few sections. The wire knife lesion interrupted the full width of the dorsal columns, while the dorsal horn of the grey matter was almost intact. The one week survival dorsal column lesioned animals developed a cavity and some parts of the dorsal horns were evidently damaged together with the dorsal columns. The lesion cavities were typically observed in about 20-30 sections since the cavity developed mainly rostro-caudally. The lesion site of the three months survival animals appeared similar to that of one week survival animals. The cavities occupied the dorsal columns and varying amounts of the grey matter but were more extensive rostro-caudally than those in the one week survival animal group.

A quantitative comparison of the lengths of the lesion cavities which developed following a dorsal column lesion in the one week and three month survival animal groups is shown in Table 2-8. The lengths of the lesion cavities in the one week survival group ranged from 1330-2100μm with a mean length of 1788μm. The cavities in the three month survival group were more variable with a range of 1260-3920μm, and the mean of length of the cavity was 2511μm which is significantly larger than in the one week animal group ($P=0.0081$) (Table 2-8).

## 2.4 Discussion

### *Methodological considerations*

In this thesis an electrophysiological approach has been used to investigate plasticity in the spinal cord following injury and following potential treatments. The main approach has been to maximally activate the pathways of interest and then to record the massed activity produced at connections within the spinal cord in order to quantify the efficacy of the pathways. The reliability of the results reported depend on the consistency with which the sensory and corticospinal pathways are activated and the accuracy with which the recordings made reflect their connectivity. The stimulation and recording protocols used are therefore crucial to the validity of the quantitative comparisons between different animal groups.

### *Maximal activation of afferent systems*

Electrical stimulation of peripheral nerves or sites within the brain is a standard electrophysiological technique which has been widely used for several decades to investigate the connectivity of neuronal pathways in the CNS *in vivo.* In studies designed to demonstrate connections it is not essential to achieve maximal activation of a given afferent pathway since activation of a significant proportion is usually sufficient. Furthermore, submaximal stimulation is usually preferred in order to avoid the problem of stimulus spread to nearby neurones or fibres of passage which if activated could be misidentified as connections form the intended target of the stimulation. Stimulating an afferent system in a manner that leads to activation of all of the neurones or fibres comprising the system, whilst at the same time avoiding any “contamination” of the recordings by inadvertent activation of other afferent systems, is a technically more challenging requirement especially for systems originating within the brain.

### *Maximal activation of sensory afferents*

Throughout this thesis, electrical stimulation of the superficial radial nerve has been used to activate sensory afferents. The superficial radial nerve was chosen

in part because sensory fibres from the nerve were found to terminate and therefore produce CDPs in a convenient location within the cervical segments. In addition the radial nerve is one of the few forelimb nerves for which it is possible to form a paraffin pool which is the optimum method for fully controlling stimulation (Ranck 1981; Swett and Bourassa, 1981). Although it is possible to stimulate forelimb afferents by inserting needle electrodes percutaneously, it is difficult to control their location relative to the nerves or precisely target individual nerve branches. It is not therefore a suitable method of achieving maximal stimulation of a selected nerve branch that is reproducible from one experiment to another. Placing the nerve in a cuff electrode (Swett and Bourassa, 1981) would be an alternative approach but cuffs are prone to problems of fluid collection or pressure block of the nerve. Mounting the cut end of the nerve on electrodes in a paraffin pool allows maximum control over the stimulation conditions because the nerve is insulated from surrounding tissues. This means that all of the stimulus current applied flows through the nerve and the stimulus intensity can be raised to very high values without any stimulus spread.

The superficial radial nerve innervates predominantly skin. In addition, group I muscle afferents do not produce CDPs on the dorsal surface of the rat spinal cord and group II muscle afferents produce only small CDPs at specific locations (Riddell and Hadian, 1998). Most of the sensory primary afferent fibres contributing to the CDPs recorded following radial nerve stimulation are therefore of cutaneous origin. There are however, several populations of cutaneous sensory fibres; large/medium diameter myelinated (A-beta) fibres which innervate mainly low threshold mechanoreceptors in skin, small diameter myelinated (A-delta) fibres which are mainly nociceptive or thermoreceptive and unmyelinated C-fibres (Willis and Coggeshall, 2004). These populations of fibres differ with respect to their conduction velocity, electrical excitability and terminations within the spinal cord. In this study the aim was to maximally activate the A-beta fibres in order to detect any changes in their central actions following spinal cord injury and following potential treatments. This is comparatively easy because the A-beta fibres, being the largest diameter fibres are the most easily excited by electrical stimulation. Furthermore, although a few A-delta fibres may be activated when the stimulus intensity is raised

sufficiently to activate the whole population of A-beta fibres in the nerve, the population of A-delta fibres as a whole require much greater stimulus intensities. The small overlap that occurs in electrical threshold between A-beta and A-delta fibres is not a problem because A-delta fibres conduct more slowly than A-beta fibres and produce much smaller CDPs even when maximally activated. The CDPs produced by the small number of A-delta fibres activated by stimuli that are maximal for A-beta fibres therefore make no difference to the peak amplitude of the A-beta evoked CDP. Maximal activation of A-beta sensory afferents and selective detection of their synaptic actions is therefore a relatively straight forward procedure.

### *Maximal activation of the corticospinal tract*

Maximal activation of the corticospinal projection represents a greater problem. Although corticospinal neurones can be activated by stimulation within the sensorimotor cortex (Donoghue and Wise, 1982; Hummelsheim and Wiesendanger, 1985; Adamson et al. 1989; Neafsey et al. 1986), it is difficult to activate all corticospinal fibres this way because the corticospinal neurones are spread over a large area. A more commonly used method for activating the corticospinal tract is to take advantage of the compact projection of corticospinal fibres as they course through the brain stem forming the ventral midline structure called the pyramids. Placement of stimulating electrodes within the pyramids can be achieved using a dorsal approach and stereotaxic techniques and this has been widely used to investigate the functional connectivity of the corticospinal tract in monkeys (Porter and Lemon, 1993) and rats (Alstermark et al. 2004). There are, however, several potential difficulties in achieving maximal selective activation of this projection suitable for quantitative comparisons. Firstly, the pyramids are bilateral structures and although smaller than the cortex, would be difficult to activate bilaterally. Furthermore, even when activation of the corticospinal tract is limited to one side only, CDPs can be detected anywhere over the dorsal surface of the spinal cord, not just on the side to which the corticospinal fibres project. This means that it is necessary to develop an approach that allows the corticospinal tract on one side to be fully activated but without activation of any of the cortiospinal tract on the opposite side. The anatomical proximity of the left and right

corticospinal projections at the midline makes this a challenge. Secondly, the pyramids are surrounded dorsally and laterally by the reticular formation and reticulospinal projections originate from the nucleus reticularis gigantocellularis in particular (Hermann et al. 2003). Activation of these projections by spread of stimulus from the pyramidal electrode is a further potential complication. Thirdly, when the stimulating current density reaches a certain multiple of threshold anodal block occurs. Current density is greatest near the electrode tip and falls off with distance (Ranck 1981). There is therefore the possibility that fibres near the electrode tip would be subject to anodal block before fibres at the periphery of the tract had become activated.

To minimise these problems, in this study we used a concentric bipolar stimulating electrode which concentrates the current density at the tip of the electrode and so minimises current spread. Use of these electrodes was combined with careful stereotaxic placement within the pyramids, the accuracy of which could be assessed during the experiment from the very low threshold for evoking CDPs and from the stimulus-recruitment curve. Histological determination of the actual position of the stimulating electrode relative to the pyramids showed that they could be targeted quite reliably. Comparison of stimulus-recruitment curves in animals where the position of the stimulating electrode was known allowed interpretation of the curves. It was concluded that stimuli applied within the lateral and middle thirds of the pyramid could fully activate the target pyramid without spread to the opposite pyramid. However, when the electrode was very medially located, the maximal amplitudes of evoked CDPs were usually considerably larger suggesting bilateral activation of corticospinal fibres. Instances where this occurred could also be recognised by high thresholds and gentler, more rounded stimulus-recruitment curves. These characteristics enabled animals with non-optimally placed pyramidal electrodes to be omitted from the study, even where the electrode position was not histologically confirmed.

Although the stimulus intensities used in the study are relatively low and did not lead to activation of the contralateral pyramidal tract, we cannot rule out the possibility of stimulus spread sufficient to activate reticulospinal axons. Reticulospinal axons are faster conducting than corticospinal fibres in the rat (Shapovalov and Gurevitch, 1970) and will therefore also be more readily

excitable by electrical stimuli. It is therefore likely, particularly where the electrode was located in the lateral third of the pyramids, that some activation of reticulospinal fibres will occur when using stimuli which are sufficient to activate the thinner corticospinal fibres on the farthest perimeter of the pyramids. However, field potential recordings made in the ventral horn while stimulating in the pyramids (described in the next chapter) show that any such activation of the reticulospinal projection is quite minimal because field potentials were small and infrequent within the ventral horn where the reticulospinal projection terminates. Furthermore, because of the predominantly ventral termination of reticulospinal fibres, like muscle afferents, they do not produce CDPs (Riddell, Enriquez-Denton and Toft unpublished). This is evident from the results obtained in animals with acute lesions of the dorsal columns where stimulation in the pyramids resulted in a virtual abolition of CDPs below the lesion, even though the reticulospinal projection through the lateral and ventral white matter is unaffected by the lesion.

Anodal surround block is a potential issue when applying electrical stimuli in the brain if the stimulus intensity used is well above threshold for activating fibres. For example, when stimulating primary afferent fibres in the dorsal columns, anodal block occurs when the stimulus intensity is raised to approximately 20 times threshold. If corticospinal fibres have a similar blocking factor then, since thresholds for pyramidal evoked CDPs were mostly of the order of 10 – 20 μA, anodal block might be expected to begin to occur at between 200 and 400μA. If anodal block had occurred at these and higher stimulus intensities then it would be expected that once the maximal stimulus intensity was reached, further increases in stimulus intensity would result in a reduction in the amplitude of the CDP as fibres near to the tip of the electrode became blocked rather than excited. Several of the stimulus-recruitment plots do in fact show a reduction in amplitude at higher stimulus intensities, however, these reductions are very modest (see Figures 2-9 to 2-12). Anodal block does not therefore appear to be a problem. In theory it is possible that fibres near the electrode tip could be blocked while fibres at the most distant perimeter of the pyramid were still being recruited so masking the anodal block. However, this seems unlikely to have occured since this would be expected to create a rounded stimulus recruitment curve while for the most part they are quite steep and show a sharp

deflection when reaching a plateau. We therefore conclude that anodal block occurs only infrequently and where it might have occurred does not greatly affect the amplitude of the recorded CDP. We therefore considered it safe to stimulate at a supramaximal intensity which should avoid any problems of drift of threshold due to changes in stimulation conditions over time.

We are therefore confident that the pyramidal stimulation protocol we have used is valid for quantitative analysis of corticospinal actions because: 1) it maximally activates the corticospinal tract on one side, 2) it can achieve this without activation of the contralateral corticospinal projection but where this does occur it can be recognised and excluded from the study 3) activation of reticulospinal projections does not complicate interpretation of the results.

### *Does axotomy affect the excitability of corticospinal fibres in the pyramids?*

For a valid comparison of CDPs in injured and non injured animals, the effectiveness of the protocol for maximally activating the corticospinal projection should not be affected by the lesioning. Injury to a neurone or its axon is known to trigger many changes, including changes that affect the electrical properties of the neurone. For example, after section of a peripheral nerve, the surviving proximal length of the axon becomes gradually thinner and its myelin sheath also thins. This means that the fibres conduct more slowly but also that they become less excitable to electrical stimulation so that greater stimulus intensities are required to activate them (Cragg and Thomas, 1961). The effects of axotomy on central axons are less well documented but it is well established that axotomy can cause hypertrophy of surviving neurones including of pyramidal neurones within the sensorimotor cortex following a dorsal column lesion (Giehl and Tetzlaff, 1996; Carter et al. 2008).

In the present study, electrical stimulation in the pyramids activates the whole population of fibres in the pyramid but different populations of fibres will be differently affected by the lesion. 1) Those corticospinal fibres projecting caudally to the lumbar and thoracic segments are likely to be completely disconnected from their target neurons. These might be expected to undergo the

greatest atrophy. 2) Most corticospinal fibres projecting to the cervical enlargement are likely to retain some connections with neurones above the level of the lesion, though they may be partly disconnected if they projected in part to neurones in segments below the lesion level. Since this group of pyramidal neurones retain some or all of their connections, they are likely to be less affected by the axotomy 3) the corticospinal fibres forming the minor components projecting in the contralateral lateral funiculus and ipsilateral ventral funiculus will not be axotomised at all and their excitability should not be changed. In our investigations we examined normal animals and animals with lesions of the main corticospinal projection at midcervical level. However, thresholds for evoking CDPs above the lesion level using stimulation in the pyramids were very similar in both groups of animals. This suggests that axotomy has little effect at least on the corticospinal fibres responsible for CDPs recorded above the dorsal column lesion.

### *Validity of using CDPs as a measure of the strength of synaptic connections in spinal pathways*

Cord dorsum potentials provide a reflection of the current flow generated at active synapses between afferent pathways and spinal cord neurones. They can be considered analogous to population post-synaptic potentials although in part they also reflect the firing of spinal cord neurones. CDPs therefore provide a convenient means of measuring the strength of connections between a given set of afferent connections and spinal cord neurones. One of their advantages is that they are relatively quick to record and the electrode can be moved progressively along the cord so allowing assessment over a relatively long section of the cord in the same experiment. They can also be used to assess spinal cord function several times in the same experiment; before and after a dorsal column lesion for example. Cord dorsum potentials are biased towards revealing connections that occur more dorsally within the grey matter. This makes them particularly suitable for measuring the synaptic actions of cutaneous sensory fibres and corticospinal fibres both of which terminate predominantly in the dorsal horn (Willis and Coggeshall 2004; Casale et al. 1988). In the case of pyramidal evoked CDPs it also helps ensure the selectivity of the measurements since even if reticulospinal fibres are inadvertently activated by pyramidal stimuli, their

connections are too ventrally located to produce detectable CDPs. Measurements of maximal CDPs also appear to be repeatable and stable over time provided the animal is maintained in a healthy state. They are not affected by topping up anaesthetic. However, they are very sensitive to accumulation of CSF on the surface of the cord which short circuits the recording and reduces the amplitude of the recorded potential. Frequent checking and removal of this fluid is crucial to the accuracy of the recordings.

The use of CDPs as a recording method does have limitations. The spatial resolution of CDPs is poor. CDPs generated on one side of the cord can be detected on the opposite side of the cord so that it is crucial that when stimuli are applied in the pyramids, for example, care is taken to ensure activation of corticospinal fibres is limited to one side. The poor spatial resolution also means that no information can be obtained about the distribution of synapses in the grey matter, so that changes in the strength or number of connections in a given area or the appearance of connections in new areas of the grey matter cannot be determined by this approach. Field potential recording is a potential alternative to the recording of CDPs but is a much more time consuming process and can therefore only be carried out at a limited number of sites. It provides greater spatial resolution and can provide information on the distribution of potentials in different areas of the grey matter of the spinal cord. Neither CDPs nor field potentials are suitable methods for determining the specificity of connections. Intracellular recording is required for this but is technically difficult, limited to the largest neurones and involves very small samples at best.

## *Evidence for spontaneous plasticity of the corticospinal tract after dorsal column lesions*

In normal animals, CDPs evoked by stimulation in the pyramids could be recorded at all segmental levels of the cervical spinal cord as has been reported previously (Alstermark et al. 2004). Pyramidal-evoked CDPs showed more variability than sensory CDPs. This may be a technical issue. CDPs evoked by pyramidal stimulation are relatively small (at least half the amplitude of radial nerve CDPs) so that they are more susceptible to any factors (e.g. fluid accumulation) that affect the amplitude of the recordings. However, it is also

possible that much of the variation is biological as there is considerable evidence for activity-dependent plasticity in the spinal cord (Wolpaw and Tennissen, 2001)

### *Corticospinal tract plasticity above a dorsal column lesion*

When CDPs evoked by the corticospinal tract were investigated, acute lesions of the dorsal columns were found to have minimal effect on CDP amplitudes except at those sites closest to the lesion. Axotomy of corticospinal fibres at the C4/5 level does not therefore lead to any immediate change in function at their more rostral connections within the spinal cord. However, when examined one week after a dorsal column lesion, CDPs evoked at sites above the lesion were significantly larger than those seen in normal animals indicating a potentiation of corticospinal actions in this region. There was little difference between 1 week and 3 month survival animals showing that the plasticity is close to maximal within 7 days but also that it persists for at least 3 months following injury.

This enhancement of corticospinal actions was not an acute effect triggered by axotomy or due to release from tonic inhibitory influences as a result of the dorsal column lesion because the CDPs were not changed following an acute lesion. The mechanisms could involve sprouting of fibres so that they form more connections within the grey matter after lesioning, or an increase in the efficacy of the same compliment of connections that existed before the lesion. The relatively rapid time course of the enhancement (less than 7 days following axotomy) might be considered to support synaptic plasticity since it is less likely that a process involving anatomical plasticity would be complete within this time.

As discussed above, stimulation in the pyramids activates corticospinal fibres projecting from the forelimb area to the cervical segments, from the hindlimb area to the lumbar enlargement and a trunk area projecting to the thoracic segments. We cannot therefore determine from our results which of these populations are involved in the plasticity. However, corticospinal fibres with a hindlimb projection form few if any connections with neurones in the cervical segments so that if these contribute to the enhanced CDPs then anatomical

plasticity is certainly involved. This issue could be resolved either by further electrophysiological experiments in which microstimulation in the forelimb and hindlimb areas was compared or by tracing the corticospinal tract.

Sprouting of the corticospinal tract above a dorsal column lesion has been reported previously (Fouad et al. 2001). In this case the dorsal columns were lesioned at a midthoracic (T8) level and microstimulation in the cortex centred on the forelimb and hindlimb area carried out while observing muscle twitches under very light anaesthesia. The threshold stimulus required to elicit responses in forelimb and hindlimb muscles before lesioning was compared before and 4 weeks after lesioning. A shift in the motor map was reported such that stimulation in the hindlimb area, which did not evoke responses before lesioning, began to produce twitches in the forelimbs after lesioning. Anterograde labelling from the hindlimb area revealed more collaterals entering the cervical segments following lesioning suggesting that sprouting of the hindlimb corticospinal projection was the mechanism responsible for the responses in forelimb muscles on stimulation of the former hindlimb area.

### *Corticospinal tract plasticity below a dorsal column lesion*

CDPs recorded below the level of the lesion, were very much reduced in amplitude in all lesioned animals. This is to be expected since the great majority of fibres (90%) forming the corticospinal tract travel in the dorsal columns and will have been severed by the lesion (Rouiller et al. 1991; Hicks and D'Amato 1975; Miller 1987). After acute lesions of the dorsal columns, CDPs below the lesion were barely detectable. At seven days after lesioning there was little change, but 3 months following the lesion, the potentials at most positions below the lesion, though still very small compared to normal, were significantly larger than at the 1 week time point. Corticospinal fibres do not regenerate and grow around a dorsal column lesion in the absence of any intervention in rats (Lu et al. 2006), although there is a report that they may do so in mice (Steward et al. 2008). Similarly, remyelination of axons (Yang et al. 2006) is not an explanation because transaction models do not result in demyelinated fibres to any significant extent (Siegenthaler et al. 2007).

There are two potential explanations for plasticity below the lesion. One involves plasticity in the spared minor components of the CST which course in the lateral and ventral funiculi and are unaffected by the dorsal column lesion. The other involves a strengthening of propriospinal connections originating above the lesion and terminating below.

The longer time course for the expression of the plasticity below the lesion compared to that seen above the lesion tends to suggest an entirely different process from that operating above the lesion, although it is conceivable that sprouting of non-axotomised fibres proceeds on a much slower time scale than for axotomised fibres. Weidner et al. (2001) reported that sprouting of ventral corticospinal fibres into medial motoneurone columns could be seen 6 weeks following a cervical dorsal column lesion in rats. However, if sprouting is the explanation for the enhanced CDPs we have observed, then it is more likely they are due to the minor lateral component as the ventral component projects ipsilaterally and sprouting into motonuclei is unlikely to be detected with dorsally sited recording electrodes. It should be possible to confirm this mechanism using tract tracing techniques.

There are known to be numerous priopriospinal interneurones at various levels within the cervical spinal cord. Some of these have descending axons within white matter other than the dorsal columns (Jankowska et al. 1974; Giovanelli Barilari and Kuypers, 1969). Strengthening of connections between corticospinal fibres and existing propriospinal interneurones above the lesion cannot be the whole explanation because plasticity above the lesion is seen at 1 week while that below the lesion is not evident at this time point. It has been suggested that following cervical level hemisection lesions the corticospinal fibres sprout onto propriospinal neurones above the lesion and that these in turn form new connections in the motonuclei below the lesion (Bareyre et al. 2004). It is unlikely that this is responsible for the enhanced CDPs below the lesion because again, this involves connections in the motonuclei. However, it is possible that a similar strengthening of propriospinal connections from neurones contacted by corticospinal fibres above the dorsal column lesion but terminating on more dorsally located targets below the lesion can occur.

## *Spontaneous plasticity in sensory circuits below the level of a dorsal column lesion*

Spontaneous plasticity in sensory systems is much less well investigated than that in the corticospinal tract. In this study, evidence of plasticity of the connections formed by large diameter sensory fibres in the radial nerve was seen following dorsal column lesions. CDPs evoked by radial nerve stimulation 1 week after a dorsal column lesion were significantly larger below the level of the lesion than those recorded from normal animals at the same location. This effect was similar if not greater at the 3 month survival period. This is the first time that spontaneous changes of transmission at the central terminal of primary afferent fibres have been demonstrated. As for the corticospinal tract, the underlying mechanism may involve either synaptic plasticity or sprouting. Injection of a tract tracer into the radial nerve and quantification of the central terminals of afferent fibres before and after a dorsal column lesion would be one way of investigating this question.

**Table 2-1 Summary of the number of animals of each group for which histological verification of the pyramidal electrode position was obtained**

For some animals stimulation in the pyramid was performed at more than one position so that the number of stimulating electrode tracks is also given. Note that the 'OEC above' and 'Medium' animal groups are fully described in chapter 3.

| Animal group | Number of animals | Number of stimulation sites |
|---|---|---|
| Normal | 7 | 8 |
| 1 week | 4 | 6 |
| 3 month | 9 | 11 |
| OEC above | 14 | 15 |
| Medium | 6 | 9 |
| Total | 40 | 49 |

**Table 2-2 Threshold stimulus intensities for evoking CDPs on stimulation in the pyramids**

The table shows the mean thresholds (μA) for each group of animals arranged according to the position of the stimulating electrode relative to the target pyramid: middle = middle third, medial = medial third, lateral = lateral third. Midline = between the left and right pyramids. The mean threshold for each of these sites considering all animals is shown in the bottom row. The mean threshold for animals in each of the treatment groups, omitting animals where the electrode was off target (midline), is shown in the right hand column. Note that the 'OEC above' and 'Medium' animal groups are fully described in chapter 3.

| Animal group | Electrode location | | | | | | | | Mean of (1+2+3) | |
|---|---|---|---|---|---|---|---|---|---|---|
| | Middle (1) | | Medial (2) | | Lateral (3) | | Midline (4) | | | |
| | n | mean | n | mean | n | mean | n | mean | n | mean |
| Normal | 4 | 6.8 | 2 | 27.5 | 1 | 6.0 | 1 | 50.0 | 7 | 12.6 |
| 1 week | 1 | 5.0 | 2 | 27.5 | 1 | 6.0 | 2 | 25.0 | 4 | 16.5 |
| 3 month | 2 | 10.0 | 6 | 14.2 | 3 | 9.3 | 0 | 0 | 11 | 12.1 |
| OEC above | 10 | 9.6 | 4 | 20.0 | 0 | 0 | 1 | 40.0 | 14 | 12.6 |
| Medium | 4 | 7.0 | 2 | 11.0 | 1 | 5.0 | 2 | 25.0 | 7 | 7.86 |
| Mean of each column | 21 | 10.4 | 16 | 18.2 | 6 | 11.4 | 6 | 31.7 | | |

**Table 2-3 Amplitudes of maximal corticospinally-evoked CDPs following stimulation at different locations**

The table shows the numbers of animals of different groups for which the position of the stimulating electrode aimed at the pyramids was histologically verified. The animals are grouped according to stimulating electrode location relative to the target pyramid: middle third, medial third, lateral third, or midline. The mean maximal amplitude (mV) of CDPs evoked by stimulation in each animal group and each location is shown. Means for all animals stimulated at a given location are shown in the bottom row and means for maximal CDPs recorded from all animals of the group at all stimulation locations within the target pyramid (middle, medial, and lateral) are shown in the far right column.

| Animal group | Middle (1) | | Medial (2) | | Lateral (3) | | Midline (4) | | Mean of (1+2+3) | |
|---|---|---|---|---|---|---|---|---|---|---|
| | n | mean | n | Mean | n | mean | n | mean | n | mean |
| Normal | 4 | 0.33 | 2 | 0.22 | 1 | 0.45 | 1 | 0.50 | 7 | 0.31 |
| 1 week | 1 | 0.42 | 2 | 0.38 | 1 | 0.68 | 2 | 0.63 | 4 | 0.47 |
| 3 month | 2 | 0.27 | 6 | 0.34 | 3 | 0.29 | | | 11 | 0.31 |
| OEC above | 10 | 0.25 | 4 | 0.37 | 0 | 0 | 1 | 0.53 | 14 | 0.29 |
| Medium above | 4 | 0.39 | 2 | 0.31 | 1 | 0.54 | 2 | 0.60 | 7 | 0.40 |
| Mean of each column | 21 | 0.30 | 16 | 0.34 | 6 | 0.42 | 6 | 0.58 | | |

**Table 2-4 Summary of mean maximal amplitudes of CDPs evoked by pyramidal stimulation and recorded at +5mm**

The data is presented for each animal group and is given separately for those animals for which histological verification of the electrode position was performed and for all animals in each group. Note that there is a close correspondence between the CDP amplitudes of the histologically verified animals and the group as a whole. Note that the 'OEC above' and 'Medium' animal groups are fully described in chapter 3.

| Animal group | Mean of maximal CDP amplitudes (mV) | |
|---|---|---|
| | Histology animals | All animals |
| Normal | 0.31 | 0.32 |
| 1 week | 0.47 | 0.43 |
| 3 month | 0.31 | 0.32 |
| OEC above | 0.29 | 0.31 |
| Medium | 0.40 | 0.40 |
| All | 0.36 | 0.35 |

**Table 2-5 Statistical analysis of the differences between pyramidal-evoked CDPs recorded in different animal groups at each recording location**

ANOVA with post-hoc Dunnett's test was first applied and where a significant difference was found the P value threshold is given. Where no significance was detected with ANOVA, Student's t-test was used and where a significant difference was detected the P-value is given. Comparisons where no significance was detected with either test are indicated by NS.

| | Normal Acute | Normal 1 week | Normal 3 month | Acute 1 week | Acute 3 month | 1 week 3 month |
|---|---|---|---|---|---|---|
| +8 | NS | P=0.0192 | P=0.0017 | NS | P=0.0173 | NS |
| +7 | NS | P=0.0082 | P=0.0066 | NS | NS | NS |
| +6 | NS | P=0.0006 | P=0.0045 | NS | NS | NS |
| +5 | NS | P=0.0036 | P=0.023 | NS | NS | NS |
| +4 | NS | P=0.0061 | P=0.0307 | NS | NS | NS |
| +3 | NS | NS | P<0.05 | NS | P<0.05 | NS |
| +2 | NS | NS | NS | NS | P=0.0135 | NS |
| +1 | P<0.01 | P<0.01 | P<0.01 | NS | P=0.0285 | NS |
| 0 | P<0.01 | P<0.01 | P<0.01 | NS | P=0.0376 | NS |
| -1 | P<0.01 | P<0.01 | P<0.01 | NS | P=0.0126 | NS |
| -2 | P<0.01 | P<0.01 | P<0.01 | NS | P=0.0027 | P=0.0113 |
| -3 | P<0.01 | P<0.01 | P<0.01 | NS | P<0.05 | P=0.0097 |
| -4 | P<0.01 | P<0.01 | P<0.01 | NS | P=0.0133 | P<0.05 |
| -5 | P<0.01 | P<0.01 | P<0.01 | NS | P=0.0371 | P=0.0021 |
| -6 | P<0.01 | P<0.01 | P<0.01 | NS | P=0.0362 | P=0.0093 |
| -7 | P<0.01 | P<0.01 | P<0.01 | NS | P=0.0313 | P=0.0055 |
| -8 | P<0.01 | P<0.01 | P<0.01 | NS | P=0.011 | P<0.05 |

**Table 2-6 Contribution of spinal dorsal roots to CDPs**

To test the contribution of each spinal dorsal root to the amplitude of CDPs, dorsal roots were sequentially sectioned following different orders in two animals, and CDPs were recorded immediately. The amplitudes of CDPs following roots sectioning were expressed as percentages of the previous amplitudes of CDPs. The percentage was 100% with CDP recorded when all the roots were intact. In the first animal (A), the amplitude of CDP was substantially reduced to only 35.2% after C6 dorsal root sectioned. After sectioning both C6 and C7 dorsal roots, only a small percent of CDP was left. Similar result has also been observed in the second animal (B). C7 dorsal root was firstly sectioned. The amplitude of CDP was reduced to 63.9%. After sectioning both C7 and C6, CDP was almost abolished. Therefore, C6 and C7 dorsal roots contribute to most of CDPs.

A

| Roots sectioned | Percentage of amplitudes (%) |
|---|---|
| Intact | 100 |
| C6 | 35.2 |
| C6+C7 | 10.7 |
| C6+C7+C5 | 8.4 |
| C6+C7+C5+C8 | 0.3 |

B

| Roots sectioned | Percentage of amplitudes (%) |
|---|---|
| Intact | 100 |
| C7 | 63.9 |
| C7+C6 | 4.5 |
| C7+C6+C5 | 0.3 |

**Table 2-7 Statistical analysis of the differences between radial nerve-evoked CDPs recorded in different animal groups at each recording location**

ANOVA with post-hoc Dunnett's test was first applied and where a significant difference was found the P value threshold is given. Where no significance was detected with ANOVA, Student's t-test was used and where a significant difference was detected the P-value is given. Comparisons where no significance was detected with either test are indicated by NS.

| | Normal Acute | Normal 1 week | Normal 3 month | Acute 1 week | Acute 3 month | 1 week 3 month |
|---|---|---|---|---|---|---|
| +8 | P<0.01 | P<0.01 | P<0.01 | NS | NS | NS |
| +7 | P<0.01 | P<0.01 | P<0.01 | NS | NS | NS |
| +6 | P<0.01 | P<0.01 | P<0.01 | NS | NS | NS |
| +5 | P<0.01 | P<0.01 | P<0.01 | NS | NS | NS |
| +4 | P<0.01 | P<0.01 | P<0.01 | NS | NS | NS |
| +3 | P<0.01 | P<0.01 | P<0.01 | NS | NS | NS |
| +2 | P<0.01 | P<0.01 | P<0.01 | NS | P=0.026 | NS |
| +1 | P<0.01 | P<0.01 | P<0.01 | P<0.01 | P=0.0004 | NS |
| 0 | P<0.01 | P<0.01 | P<0.01 | P<0.05 | NS | P=0.0163 |
| -1 | P<0.01 | P<0.01 | P<0.01 | NS | P=0.0455 | P<0.01 |
| -2 | NS | NS | P<0.01 | NS | NS | P=0.0167 |
| -3 | NS | NS | NS | NS | P=0.0379 | NS |
| -4 | NS | P=0.0316 | P=0.0019 | P<0.01 | P<0.01 | NS |
| -5 | NS | NS | P<0.05 | P<0.05 | P<0.01 | NS |
| -6 | NS | NS | P<0.01 | NS | P<0.01 | P=0.039 |
| -7 | NS | NS | P<0.01 | P<0.05 | P<0.01 | NS |
| -8 | NS | P=0.017 | P<0.05 | NS | P<0.05 | NS |

**Table 2-8 Quantification of lesion cavity size in the one week survival and three month survival groups**

The lengths of the cavities in both one week and three month survival groups were assessed and compared (see methods) using Students' t-test which showed a significant difference in mean cavity length (P=0.0081). The cavities in the three month survival group were more variable compared to those in the one week survival group.

| | 1 week group (n=14) | 3 month group (n=15) |
|---|---|---|
| Length of cavity (Range) | 1330-2100 µm | 1260-3920 µm |
| Length of cavity (Mean) | 1788 µm | 2511 µm |

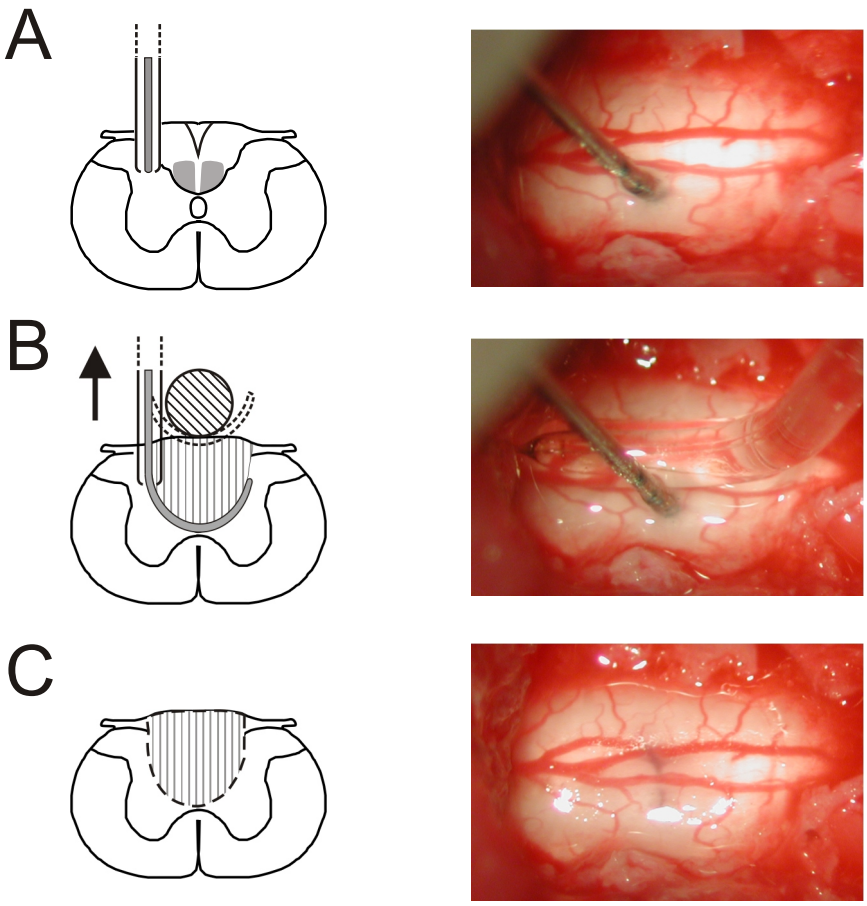


**Figure 2-1 Procedure for making dorsal column lesions using wire knife**
A, the relevant segment of the spinal cord is exposed by laminectomy and the guide cannula containing the wire knife lowered into the spinal cord at an appropriate position and to an appropriate depth. B, the wire knife is then extruded and a glass rod lowered to the surface of the cord. The wire knife is then raised against the glass rod in order to cut through the dorsal columns. C, The glass rod is raised, the wire knife retracted and the guide cannula removed. The lesion can be seen through the intact dura. Note that the blood vessels remain undamaged.

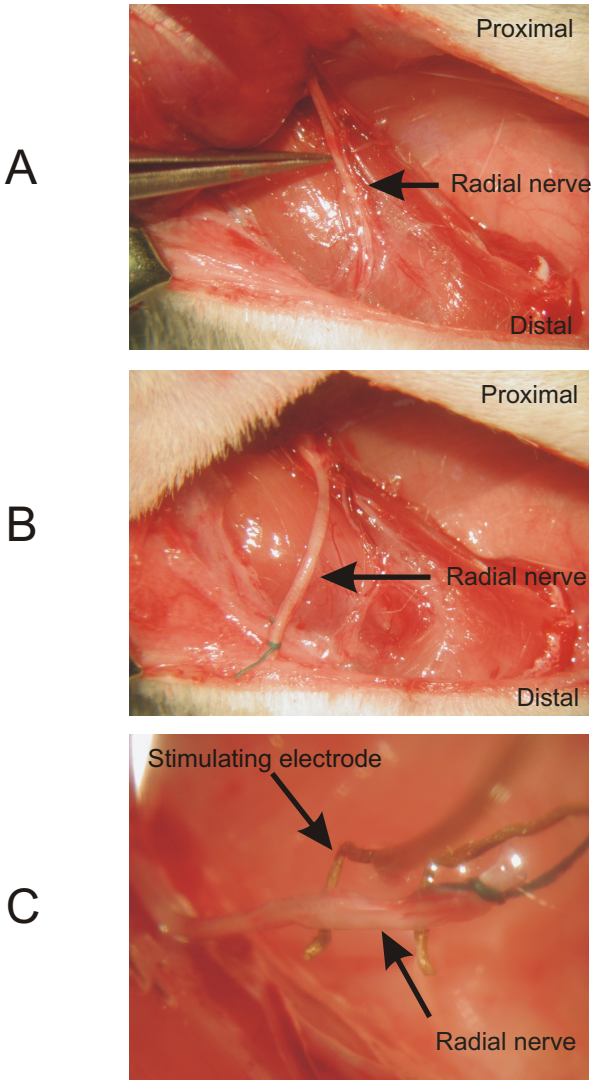


**Figure 2-2 Radial nerve dissection and stimulation**
A, the superficial branches of the radial nerve are exposed and identified. B, the branches of the radial nerve are dissected free and sectioned distally, a suture loop is tied to the end of the branches in order to lift it without damage. C, the branches of the radial nerve are placed on bipolar silver wire electrodes immersed in the paraffin pool.

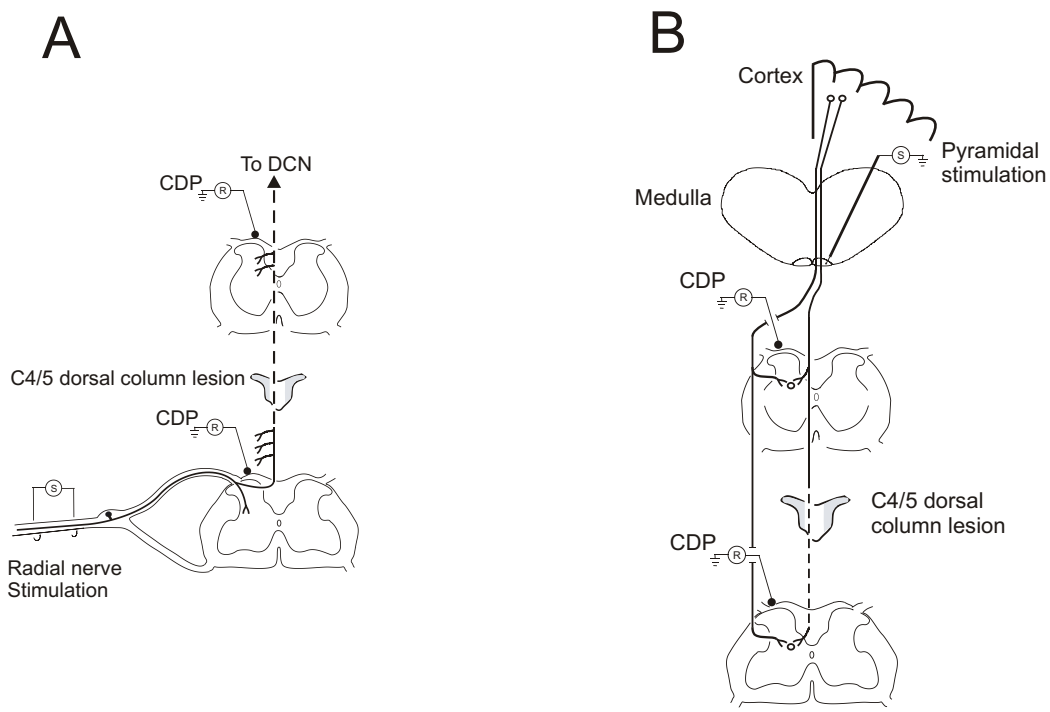


**Figure 2-3 Schematic diagram of preparation of electrophysiological experiments for assessing CDPs**

Schematic diagrams show location of lesion and of stimulating and recording electrodes for assessing radial nerve-evoked (A) and corticospinally-evoked (B) CDPs. The dorsal columns were lesioned bilaterally at the C4/C5 junction interrupting the main component of the corticospinal tract which runs in the ventral aspect of the dorsal columns and the ascending dorsal column pathway more dorsally.

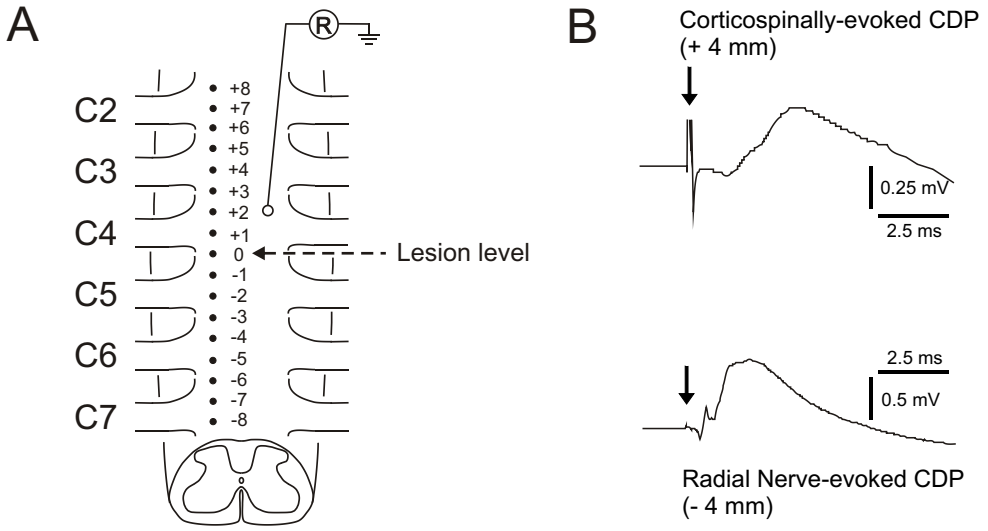


**Figure 2-4 Schematic diagram showing recording locations for CDPs and examples of CDPs**

Cord dorsum potentials (CDPs) evoked by electrical stimulation of the radial nerve and/or corticospinal tract were recorded to assess spinal cord function in the region of the lesion. Recordings were made at 1mm intervals for 8 mm above and below the C4/5 reference level (the lesion site in the lesioned animal group) (A). Typical radial nerve-evoked and corticospinally-evoked CDPs were showen in B.

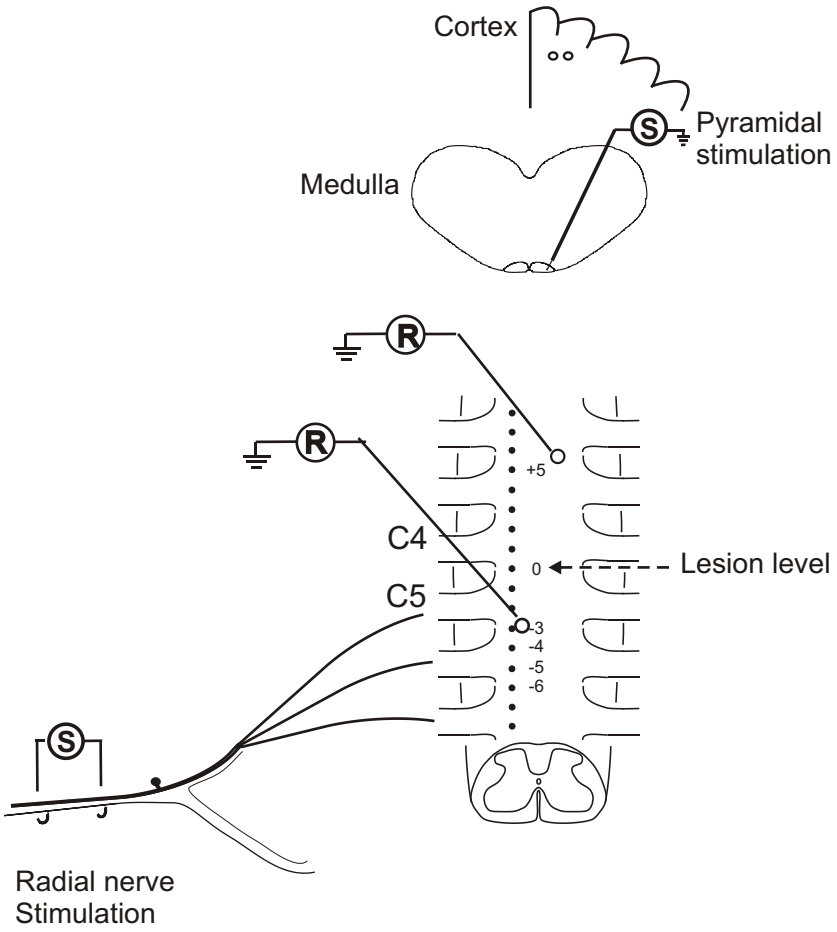


**Figure 2-5 Conditioning of radial CDPs with pyramidal stimulation**
Schematic diagram shows the experimental arrangement. The effects of conditioning stimuli in the pyramids on CDPs evoked by radial nerve afferents below the level of the lesion were investigated to assess the function of the corticospinal projection. The recordings were made at 3mm, 4mm, 5mm and 6mm below the C4/5 reference position at different conditioning test intervals (20ms, 25ms, and 30ms). Another recording electrode was placed at 5mm above the C4/5 reference position to monitor the efficacy of appropriate pyramidal stimulation.

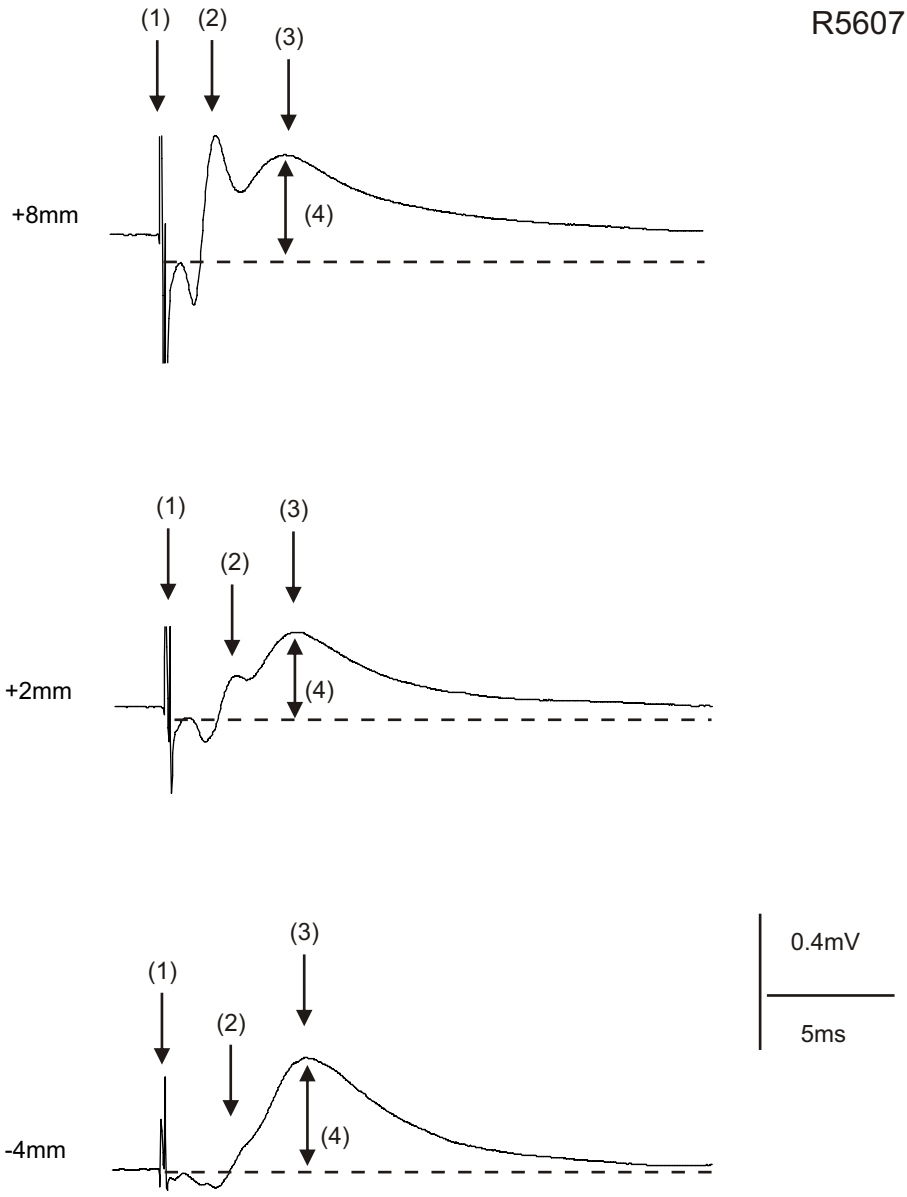


**Figure 2-6 Examples of CDPs evoked by pyramidal stimulation**
Examples of surface recordings made at different locations on the cervical spinal cord in a normal animal. All recordings are averages of 50 sweeps. The numbered arrows point to different components of the surface recordings: (1) stimulus artefact, which indicates the timing of the stimulation; (2) afferent volley, which represents the action potentials travelling along CST fibres; (3) CDP, which represents the synaptic activity generated by connections between the collaterals of the CST fibres and spinal cord neurons and provides a measure of the strength of these connections; (4) the peak amplitude of these CDPs was measured at each recording location using Signal software. The afferent volley is clearest and largest at locations close to the stimulation site (top trace), becomes dispersed further from the stimulation site and eventually merges with CDP recordings at more caudal locations (bottom trace).

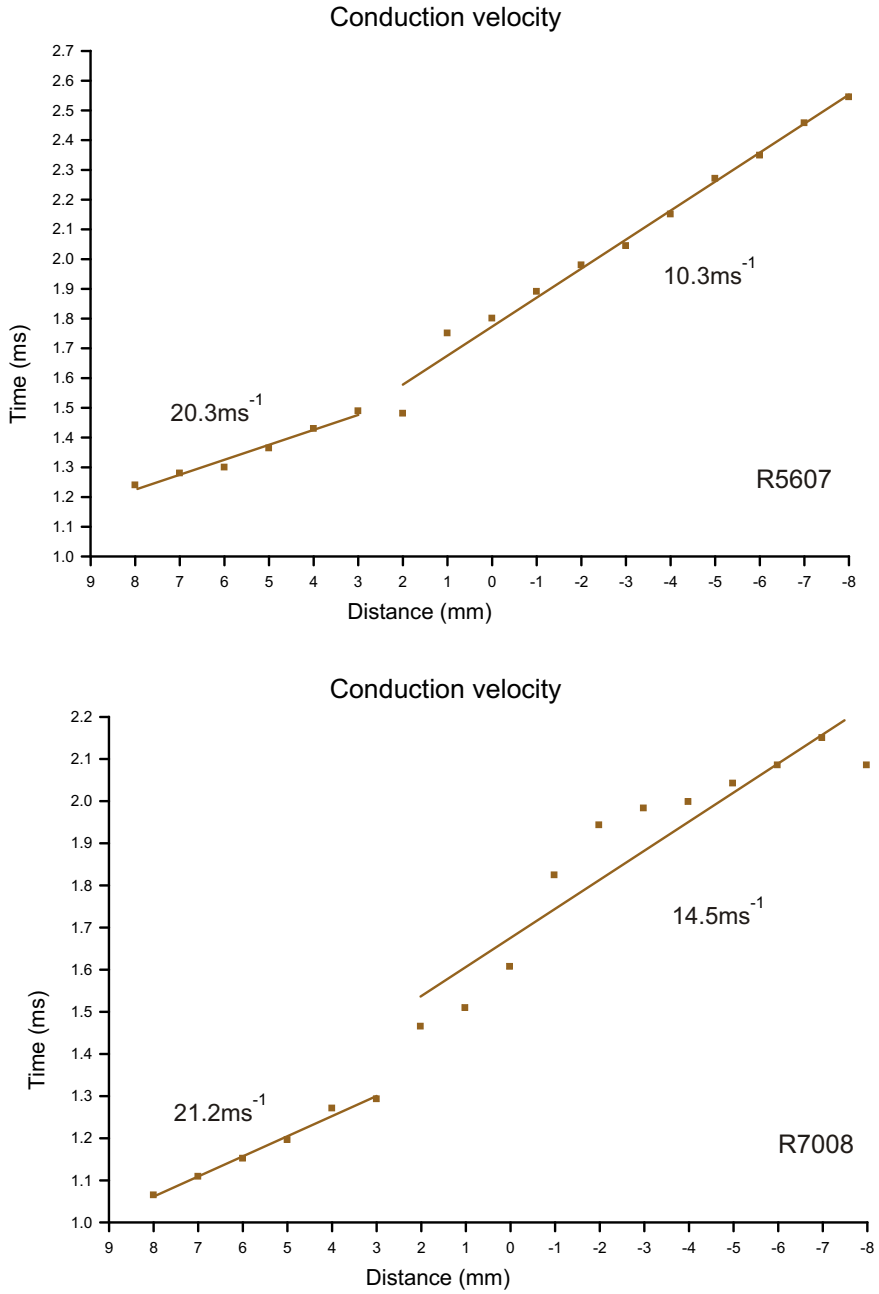


**Figure 2-7 Determination of CST conduction velocity in two normal animals**
The latencies of volleys recorded from 8mm rostral to 8mm caudal were measured and plotted against recording locations. Lines were fitted using linear regression and the slopes of the plots represent the conduction velocity of the CST. In these two animals, the conduction velocity is faster in the rostral cervical segments (C2-3); ($20.3ms^{-1}$ and $21.2ms^{-1}$ respectively) than more caudally (C4-7); ($10.3ms^{-1}$ and $14.5ms^{-1}$).

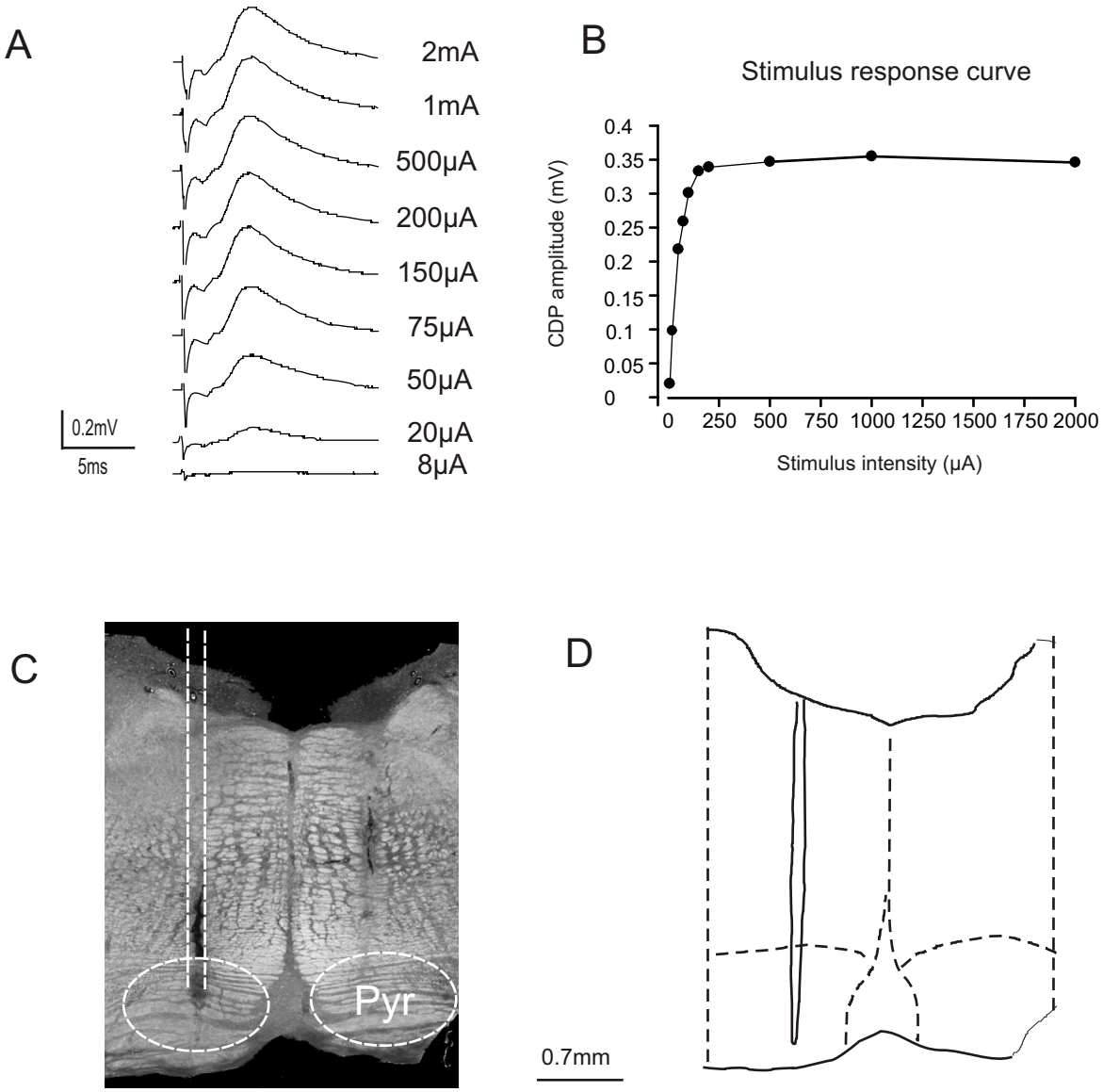


**Figure 2-8 Electrical stimulation of the pyramids**
A, CDPs evoked by stimuli of graded intensity applied to the pyramids using the electrode which made the track shown in C and D; B, stimulus-response curve obtained using the records illustrated in A. C, histological verification of the correct positioning of a stimulating electrode in the right pyramid. Scale bar=0.7mm; D, schematic diagram of the outline of the section and stimulating electrode track was reconstructed by using Camera lucida drawings. Scale bar=0.7mm;

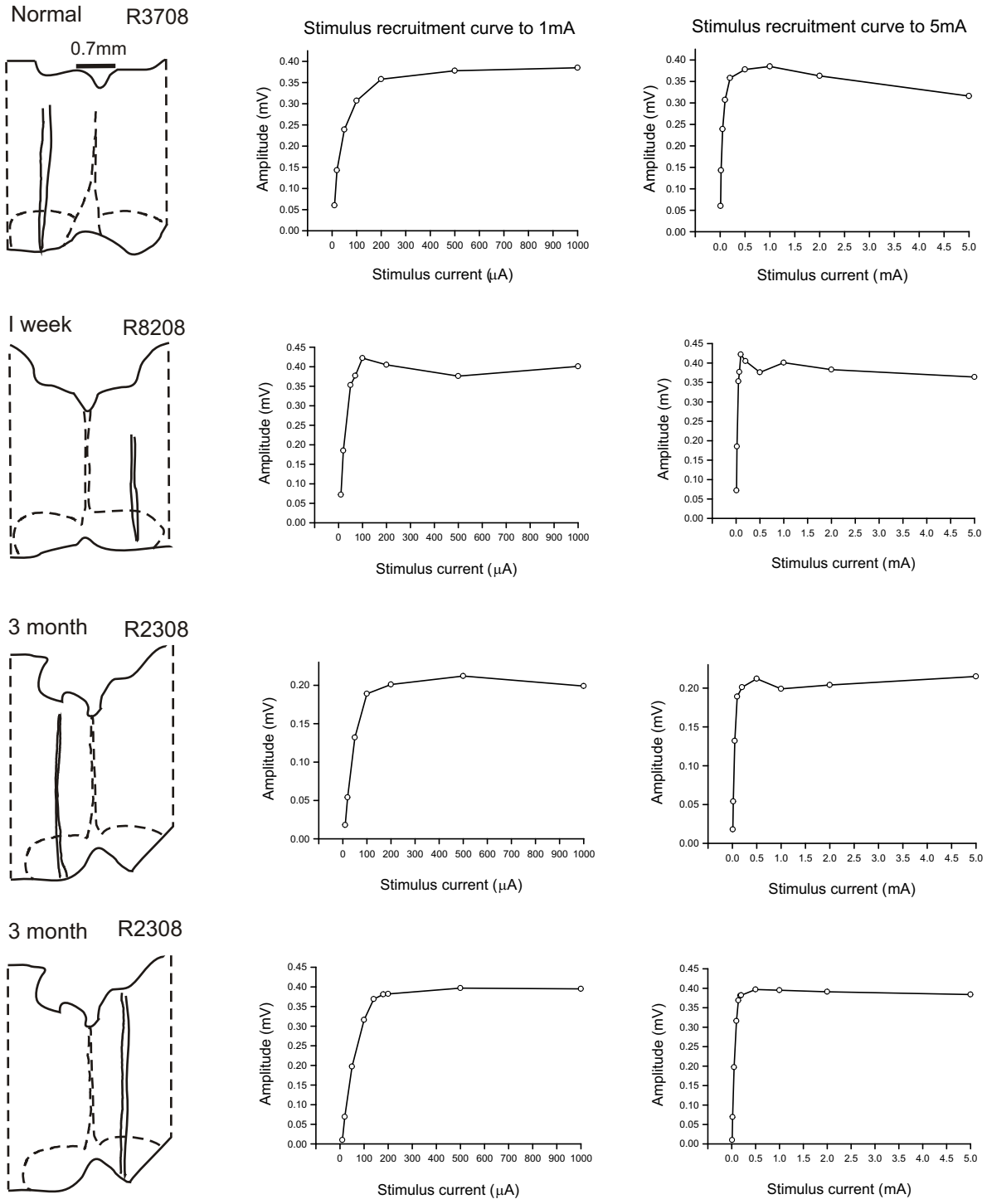


**Figure 2-9 Stimulus-recruitment curves for animals of the 'Middle' electrode placement group**

The diagrams to the left show reconstructions of the stimulating electrode tracks. The plots to the right show corresponding stimulus-recruitment curves, one for stimulation up to 1mA and another up to 5mA. The animal group is indicated above each histological reconstruction. Note that this figure includes two pages.

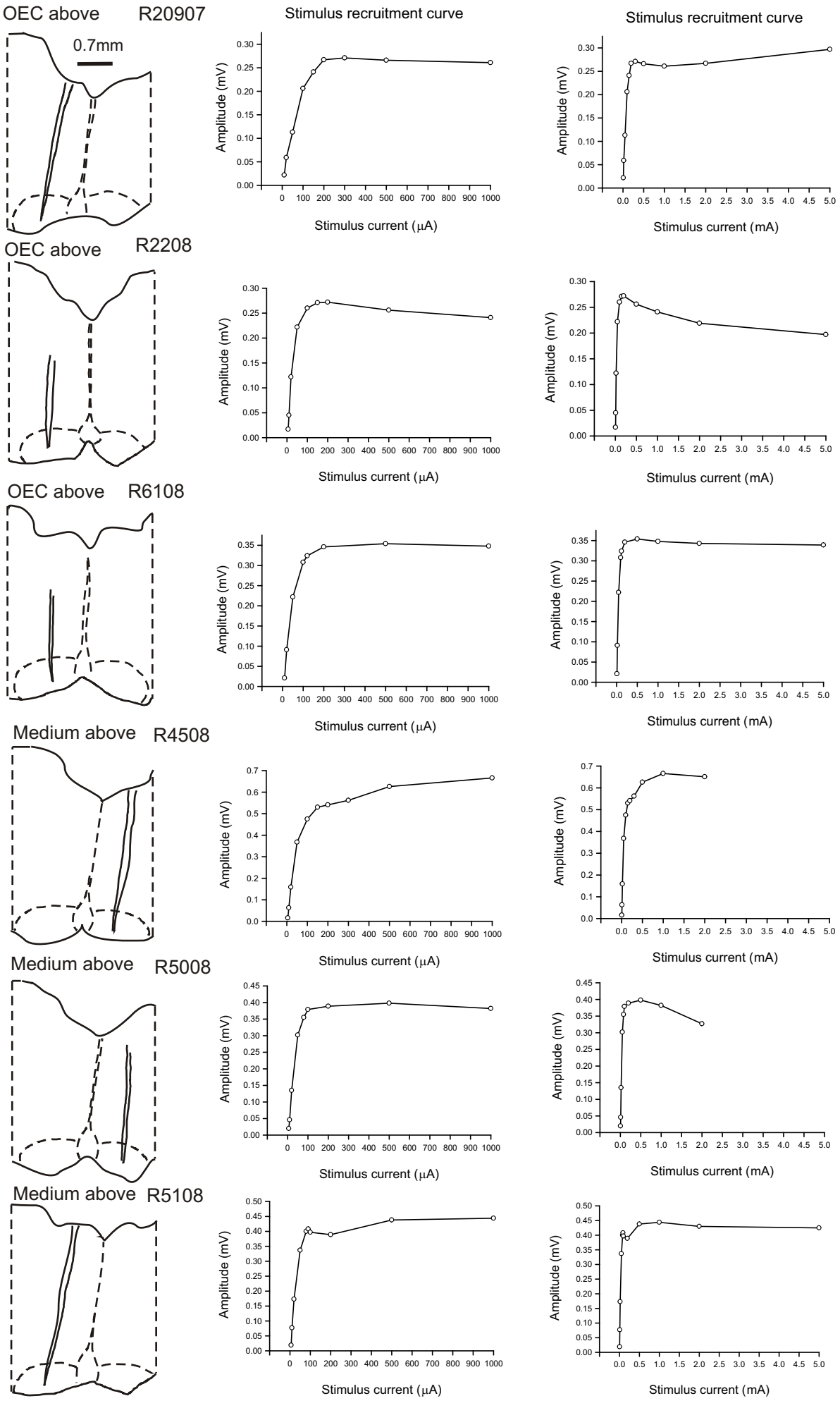
OEC above R20907
0.7mm
Stimulus recruitment curve
Amplitude (mV)
Stimulus current (μA)
Stimulus recruitment curve
Amplitude (mV)
Stimulus current (mA)
OEC above R2208
Amplitude (mV)
Stimulus current (μA)
Amplitude (mV)
Stimulus current (mA)
OEC above R6108
Amplitude (mV)
Stimulus current (μA)
Amplitude (mV)
Stimulus current (mA)
Medium above R4508
Amplitude (mV)
Stimulus current (μA)
Amplitude (mV)
Stimulus current (mA)
Medium above R5008
Amplitude (mV)
Stimulus current (μA)
Amplitude (mV)
Stimulus current (mA)
Medium above R5108
Amplitude (mV)
Stimulus current (μA)
Amplitude (mV)
Stimulus current (mA)

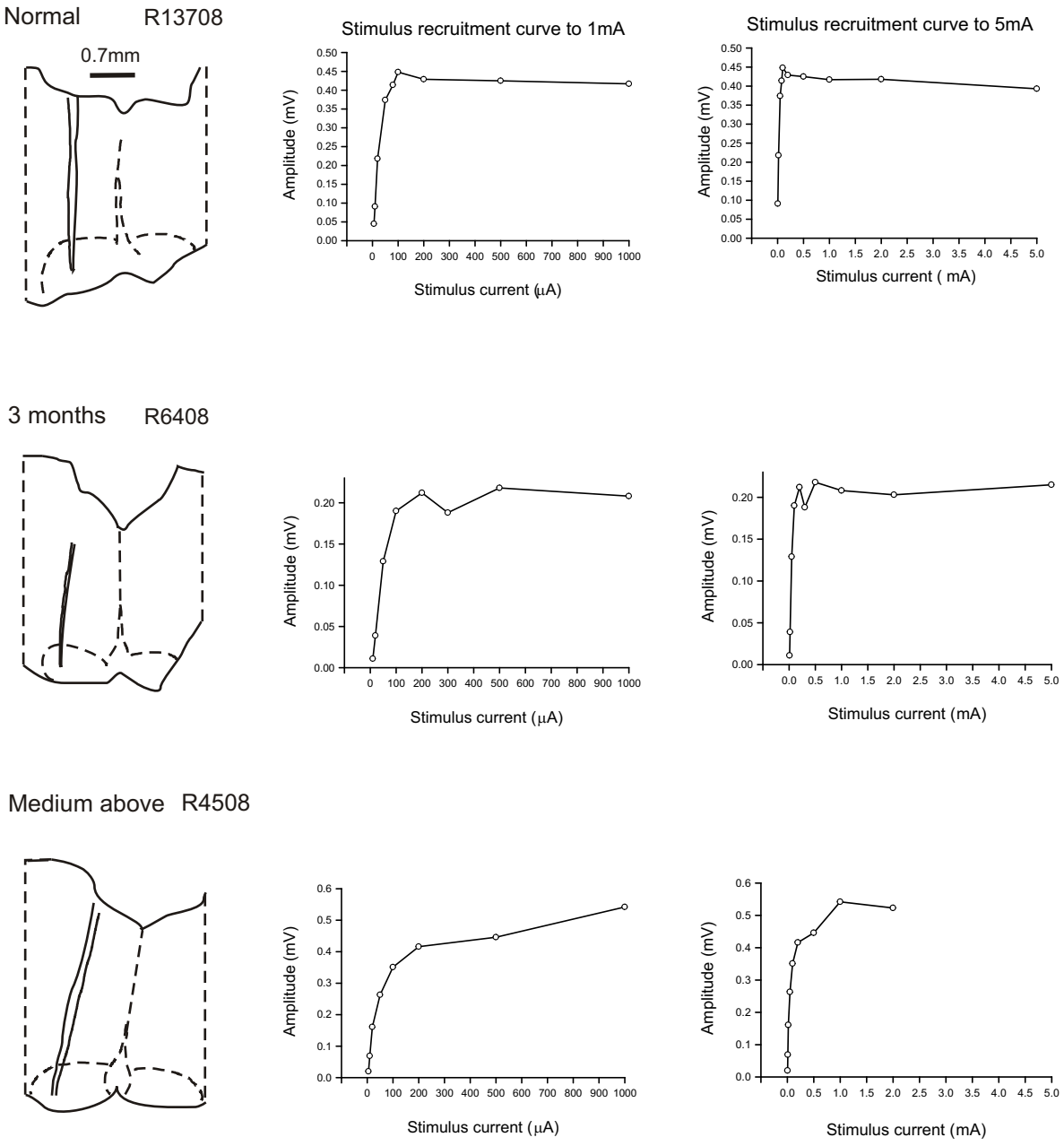


**Figure 2-10 Stimulus-recruitment curves for animals of the 'Lateral' electrode placement group**

The diagrams to the left show reconstructions of the stimulating electrode tracks. The plots to the right show corresponding stimulus-recruitment curves, one for stimulation up to 1mA and another up to 5mA. The animal group is indicated above each histological reconstruction.

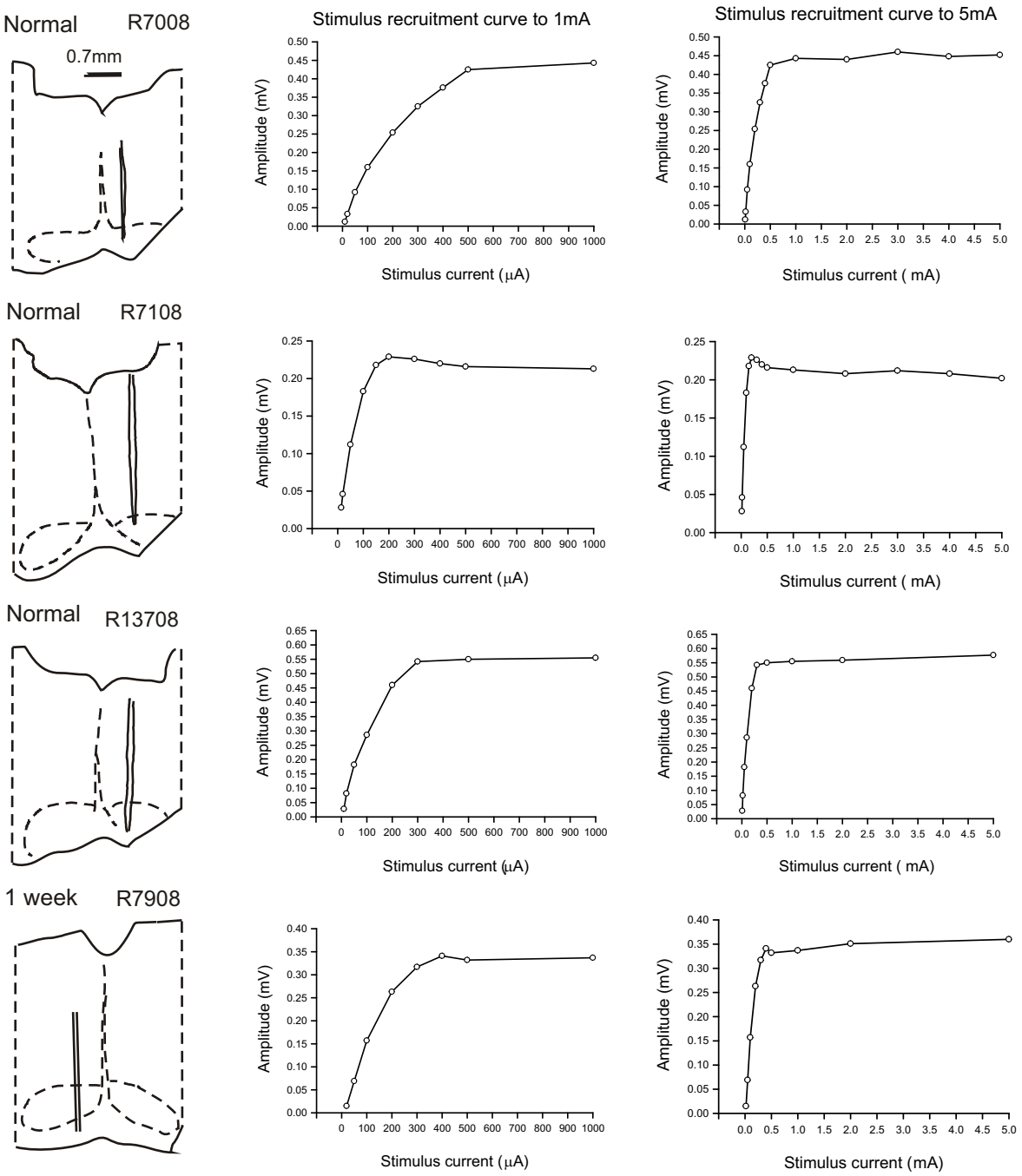


**Figure 2-11 Stimulus-recruitment curves for animals of the 'Medial' electrode placement group**

The diagrams to the left show reconstructions of the stimulating electrode tracks. The plots to the right show corresponding stimulus-recruitment curves, one for stimulation up to 1mA and another up to 5mA. The animal group is indicated above each histological reconstruction. Note that this figure includes two pages.

3 months R1608

0.7mm

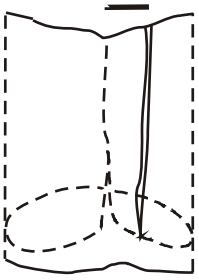

Stimulus recruitment curve

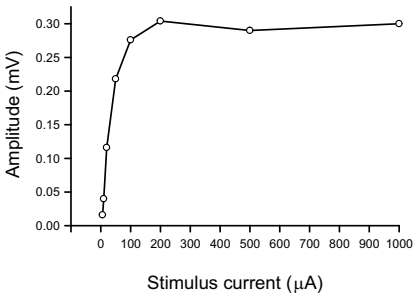


Stimulus recruitment curve

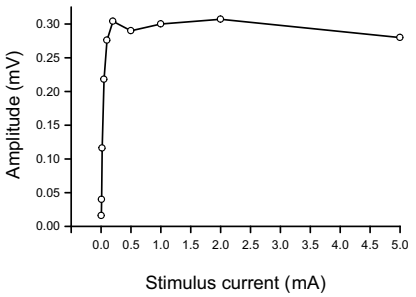


3 months R2408

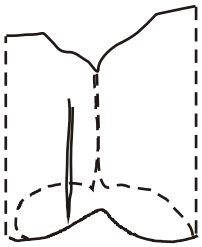

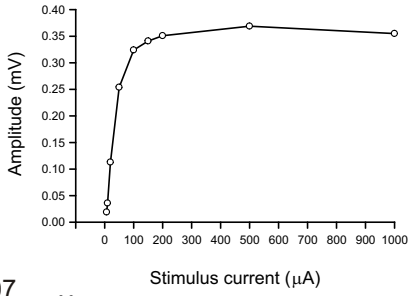


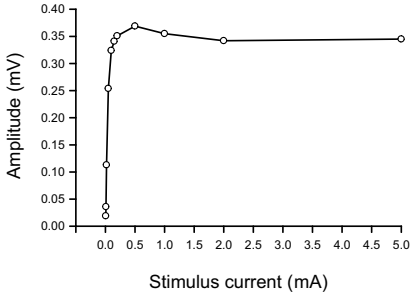


OEC above R20607

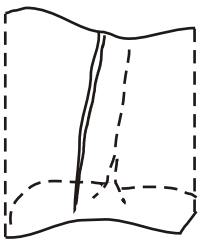

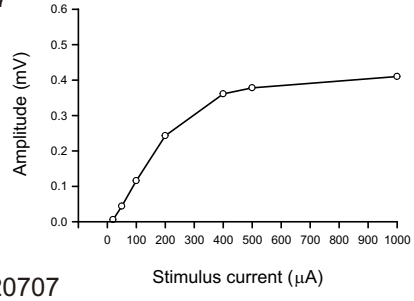


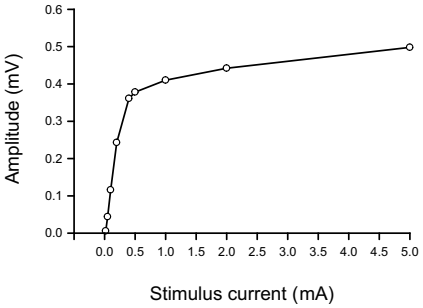


OEC above R20707

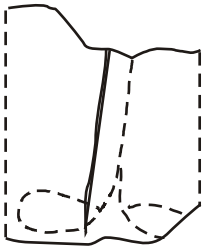

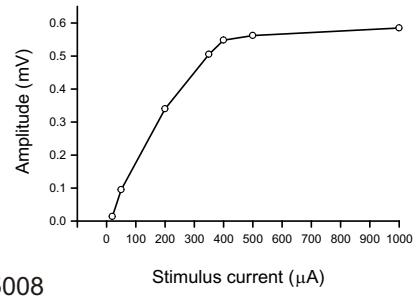


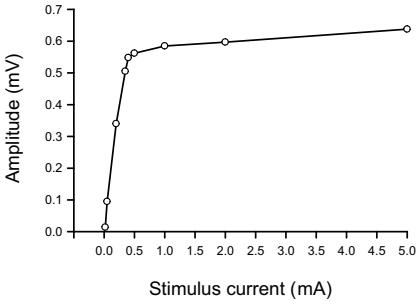


Medium above R5008

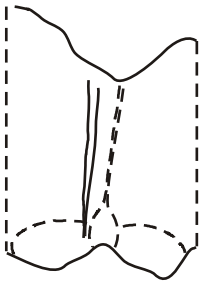

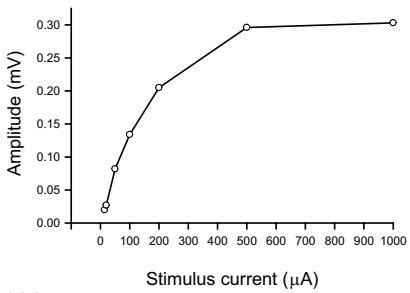


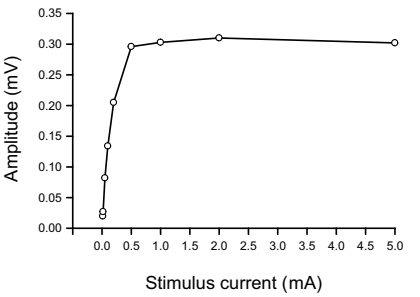


Medium above R5108

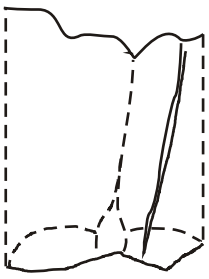

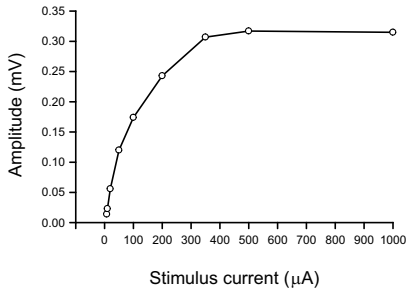


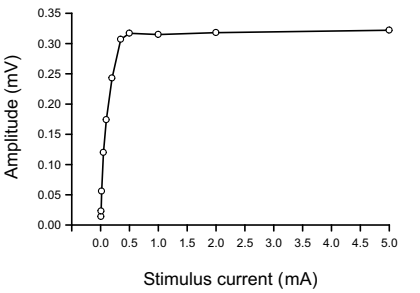

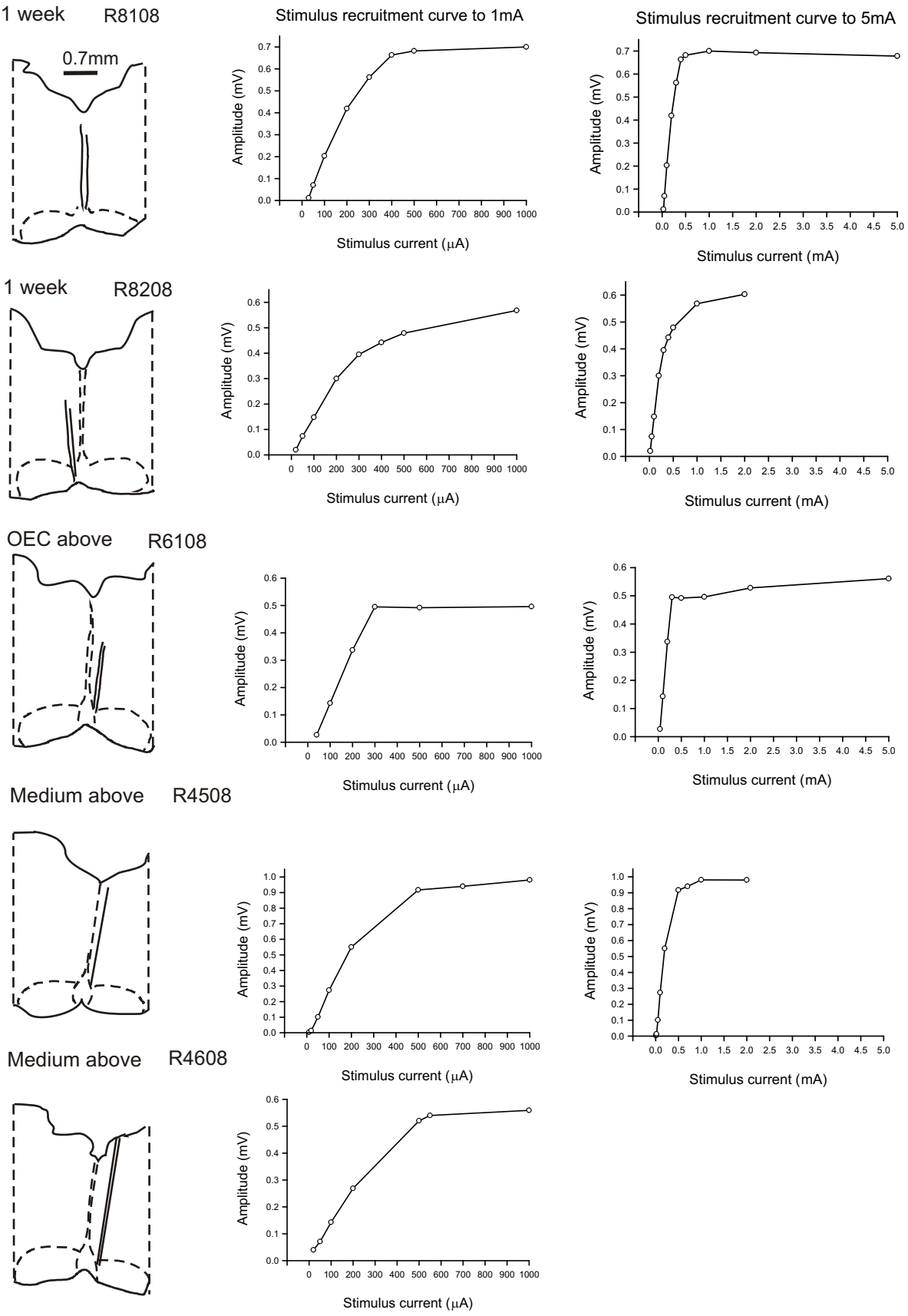


**Figure 2-12 Stimulus-recruitment curves for animals of the 'Midline' electrode placement group**

The diagrams to the left show reconstructions of the stimulating electrode tracks. The plots to the right show corresponding stimulus-recruitment curves, one for stimulation up to 1mA and another up to 5mA. The animal group is indicated above each histological reconstruction.

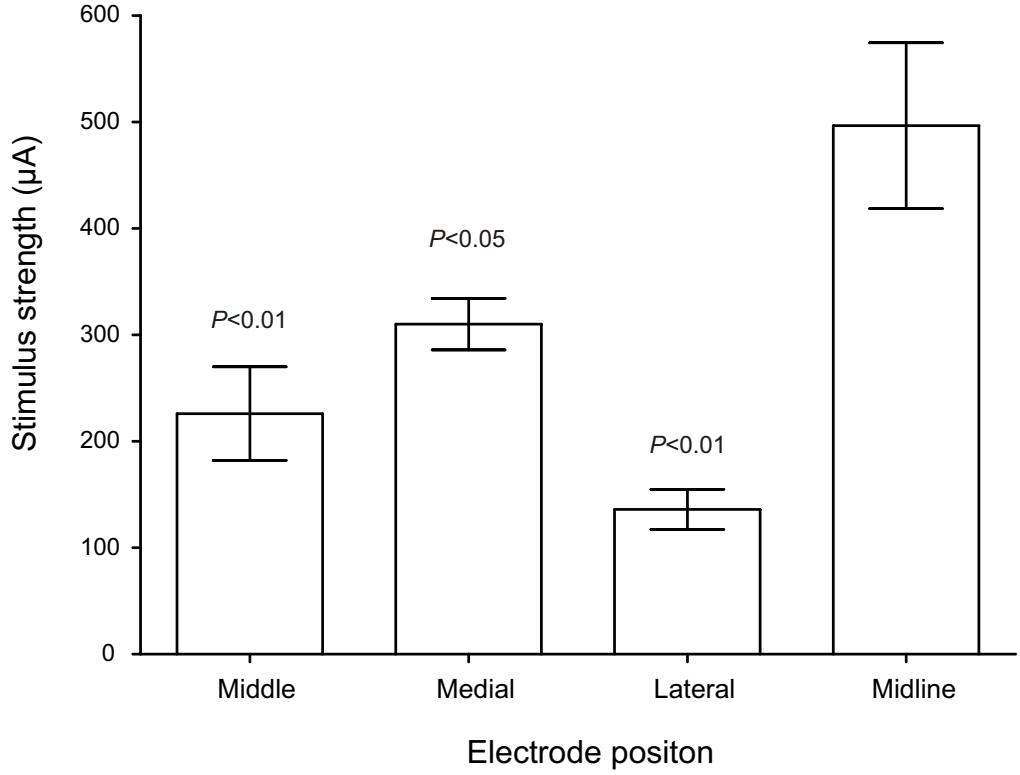


**Figure 2-13 Stimulus intensities required to evoke CDPs 95% of maximal at different stimulus locations**

The bar chart shows the average stimulus intensities required to evoke CDPs 95% of maximal amplitude for each of the groups of animals that were organized according to the location of the stimulating electrode. The error bars show +/- SD. ANOVA and Dunnett post-hoc test were used to compare the different stimulus intensities. There was no statistically significant difference between the 'Middle', 'Medial', or 'Lateral' groups but the 'Midline' group required a significantly higher stimulus intensity than each of the other groups (*P* value is labelled on the top of the relevant column).

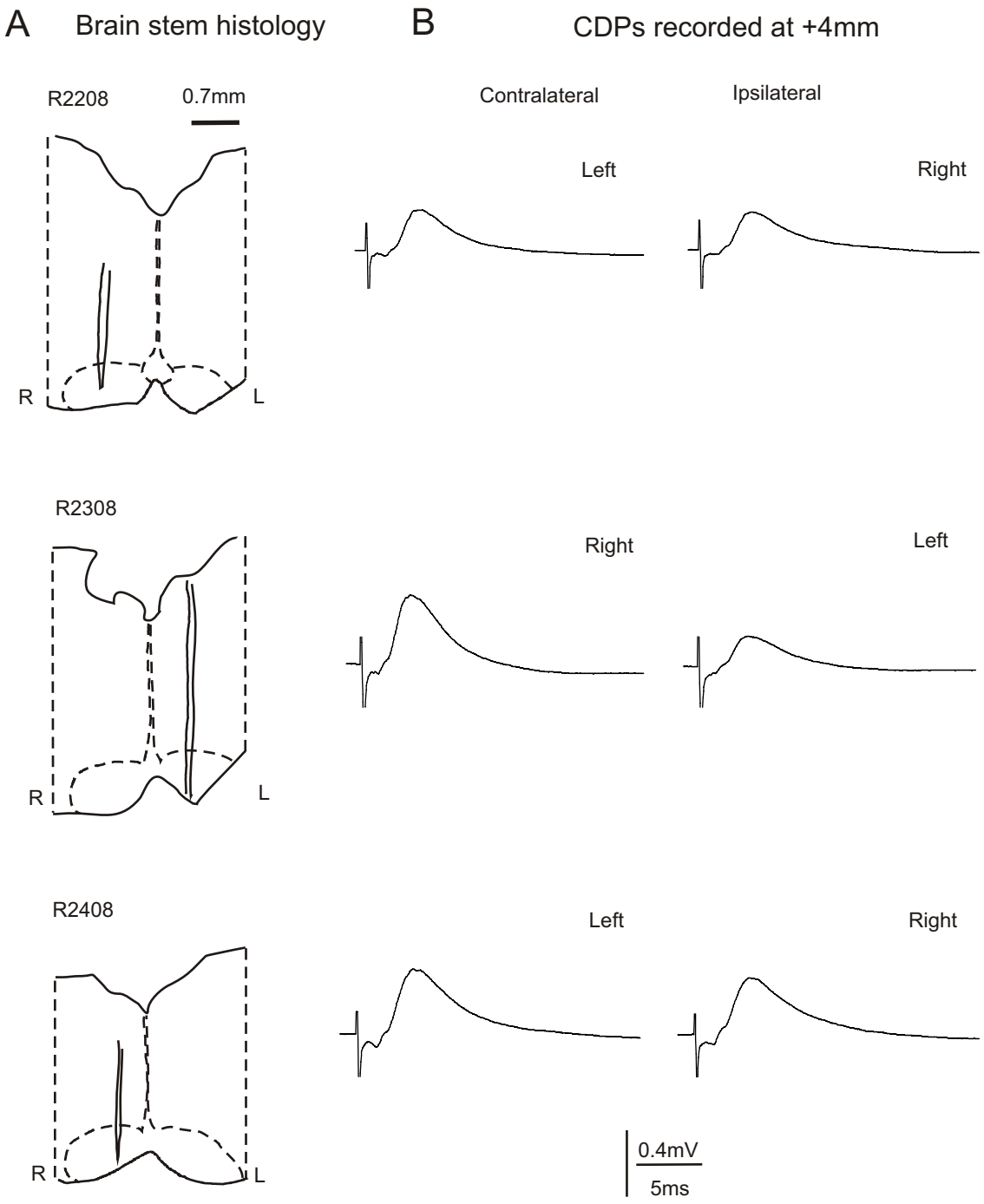


**Figure 2-14 Pyramidal-evoked CDPs recorded from the left and right sides of the spinal cord**

A, reconstructions of the stimulating electrode tracks for three animals where the electrode targetted the middle of a pyramid on one side. Scale bar=0.7mm; B, pyramidal-evoked CDPs recorded at 4mm above the C4/5 segmental border from both sides of the spinal cord. Note that CDPs can be detected from both sides of the spinal cord while stimulating unilaterally. The relative amplitudes of CDPs recorded on the two sides vary and may be closely similar or larger on the side contralateral to the stimulating electrode.

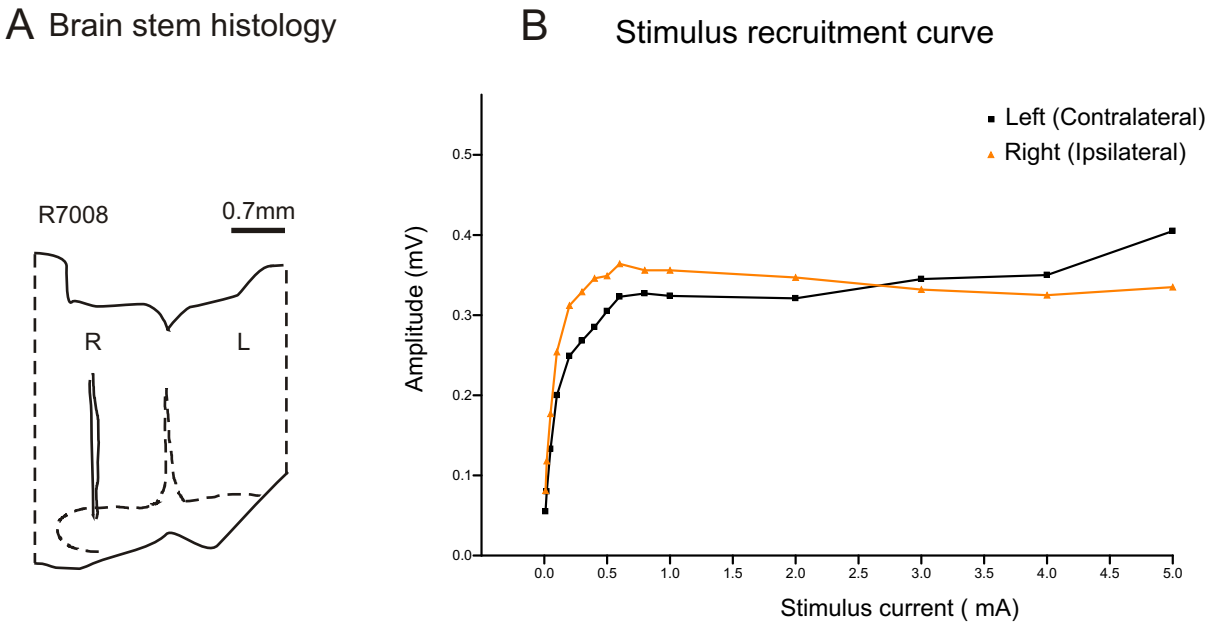


**Figure 2-15 Stimulus-recruitment curves for CDPs recorded from the left and right sides of the spinal cord while stimulating the pyramids on one side are similar**
A, shows a reconstruction of the stimulating electrode positioned in the middle of the right pyramid. Scale bar=0.7mm; B, shows the stimulus-recruitment curve recorded from the left (contralateral) and right (ipsilateral) sides of the spinal cord while stimulating at the position shown in A.

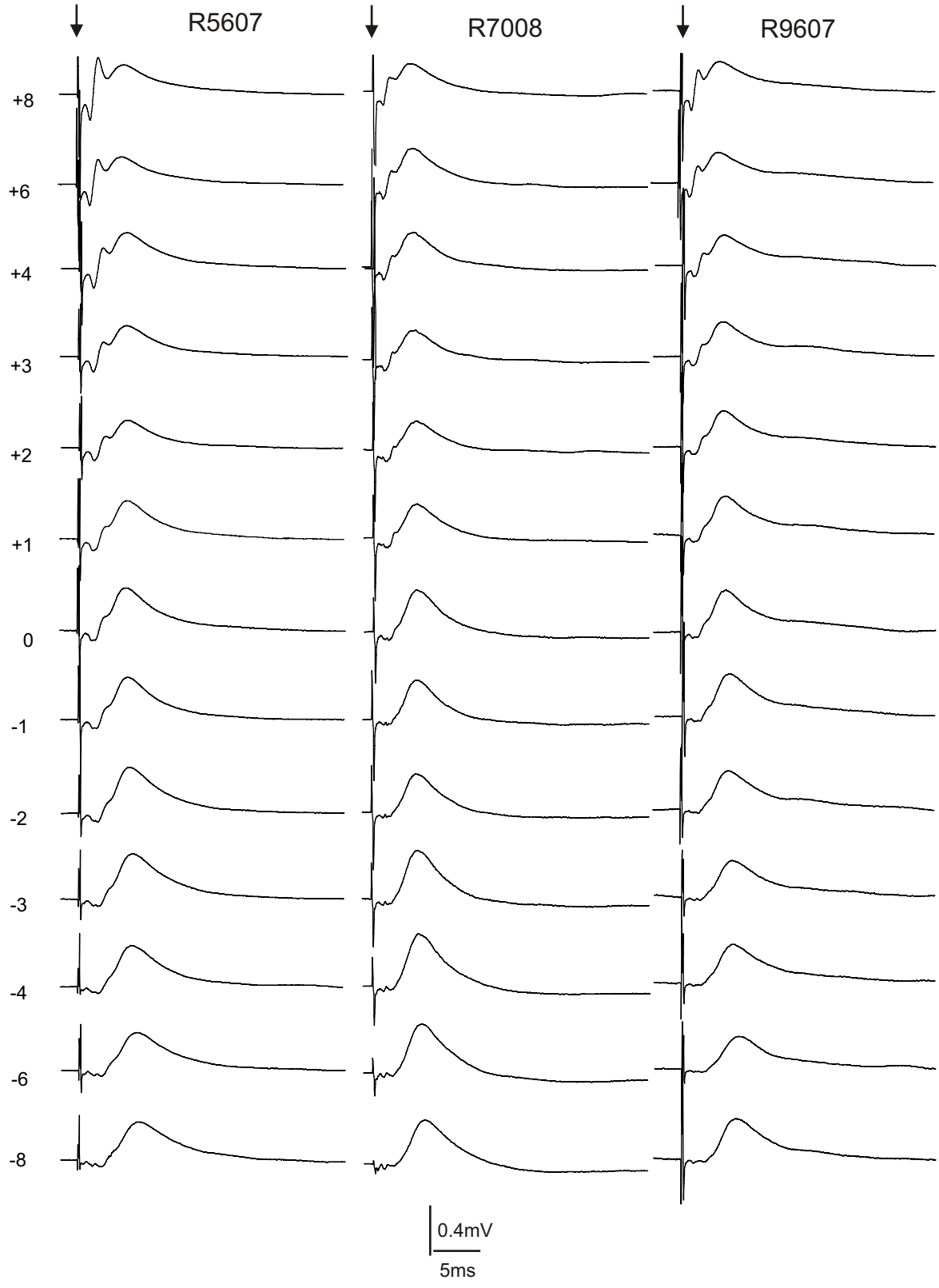


**Figure 2-16 Examples of CDPs evoked by pyramidal stimulation in normal animals**
Each column of traces shows recordings made from one animal. The recordings were made at 1mm intervals from 8mm rostral to 8mm caudal to the C4/5 segmental border as indicated to the left of each trace. Some traces (recorded at +7, +5, -5, -7mm) are omitted. The traces represent averages of 50 sweeps and the calibrations apply to all traces. The arrows indicate stimulus artifacts.

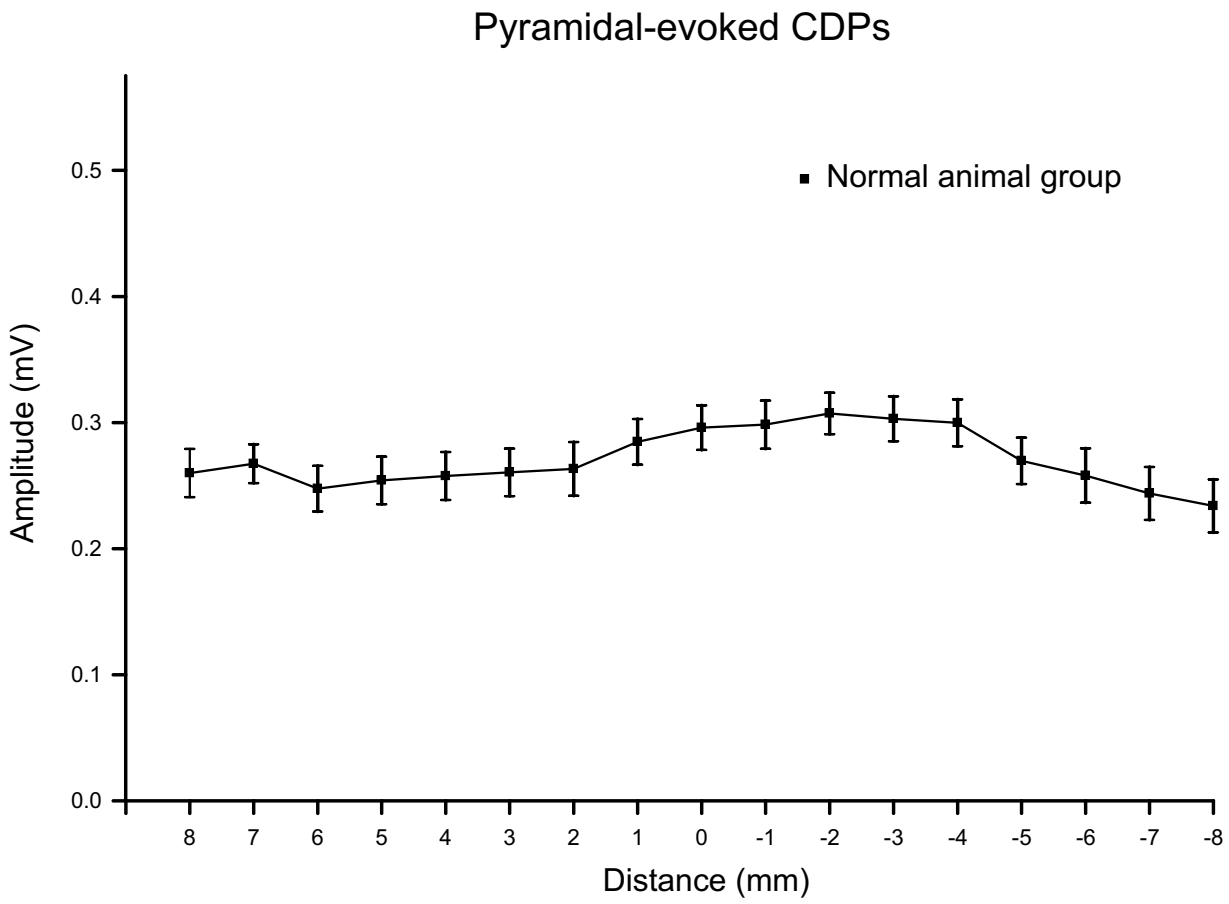


**Figure 2-17 Amplitudes of pyramidal-evoked CDPs recorded in normal animals**
Each data point is the mean CDP amplitude for all animals (n=18) in this group. The error bars show +/- SEM. The recordings were made over the cervical spinal cord and are shown relative to the C4/5 border (0 mm) where dorsal column lesions were made in the lesioned groups. In normal animals, pyramidal-evoked CDPs were on average of similar amplitudes at all recording sites from 8mm rostral to 8mm caudal of the C4/5 segmental border.

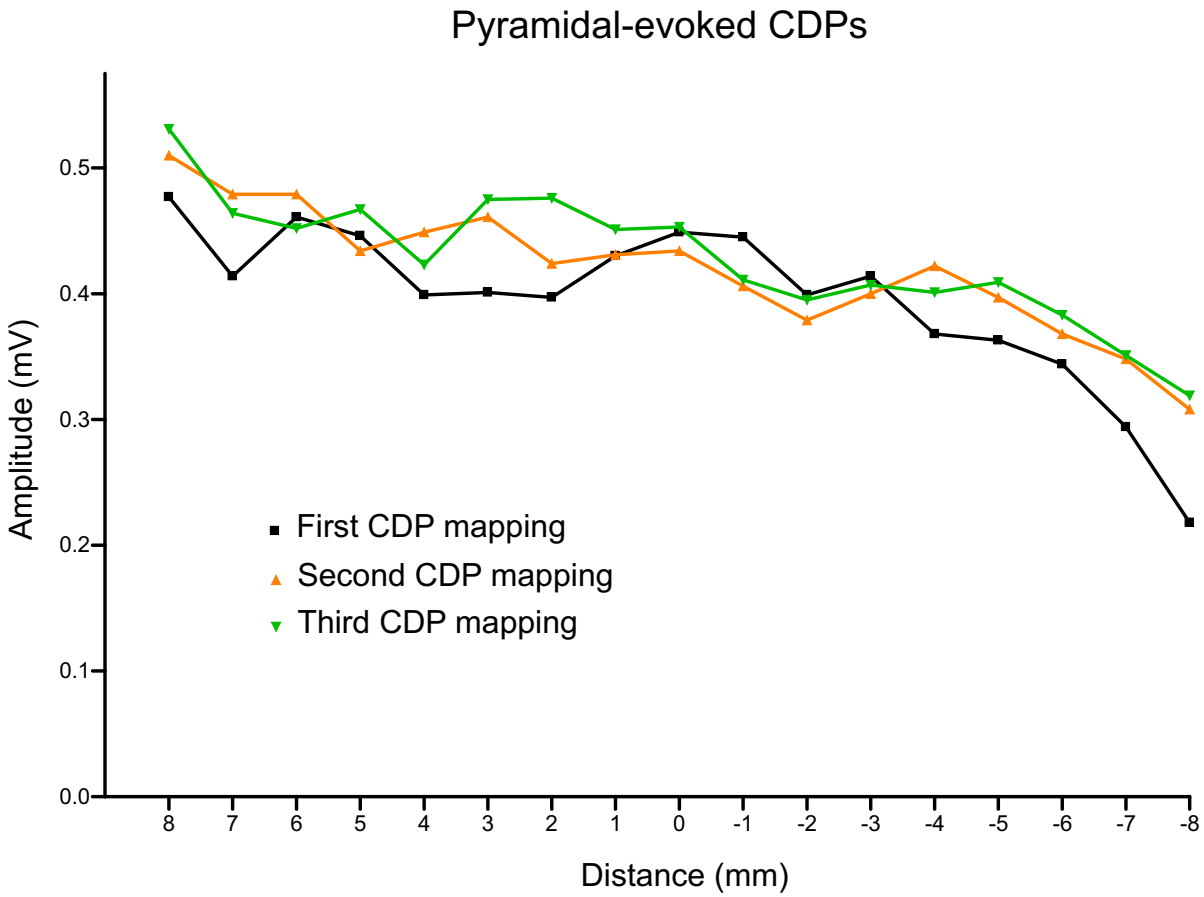


**Figure 2-18 Plots showing the repeatability of CDP recordings**
Plots of CDPs recorded from 8mm above to 8mm below the C4/5 segmental border. Each individual plot represents a separate mapping of the CDPs. The order in which the mapping was performed is shown in the key. Note that the three plots were made sequentially from the same animal while the stimulating electrode remained at the same location. Recordings at each location were separated by 15 to 20 minutes since this is the time it takes to complete one mapping. Note that the amplitudes of the CDPs in each of the plots is very similar.

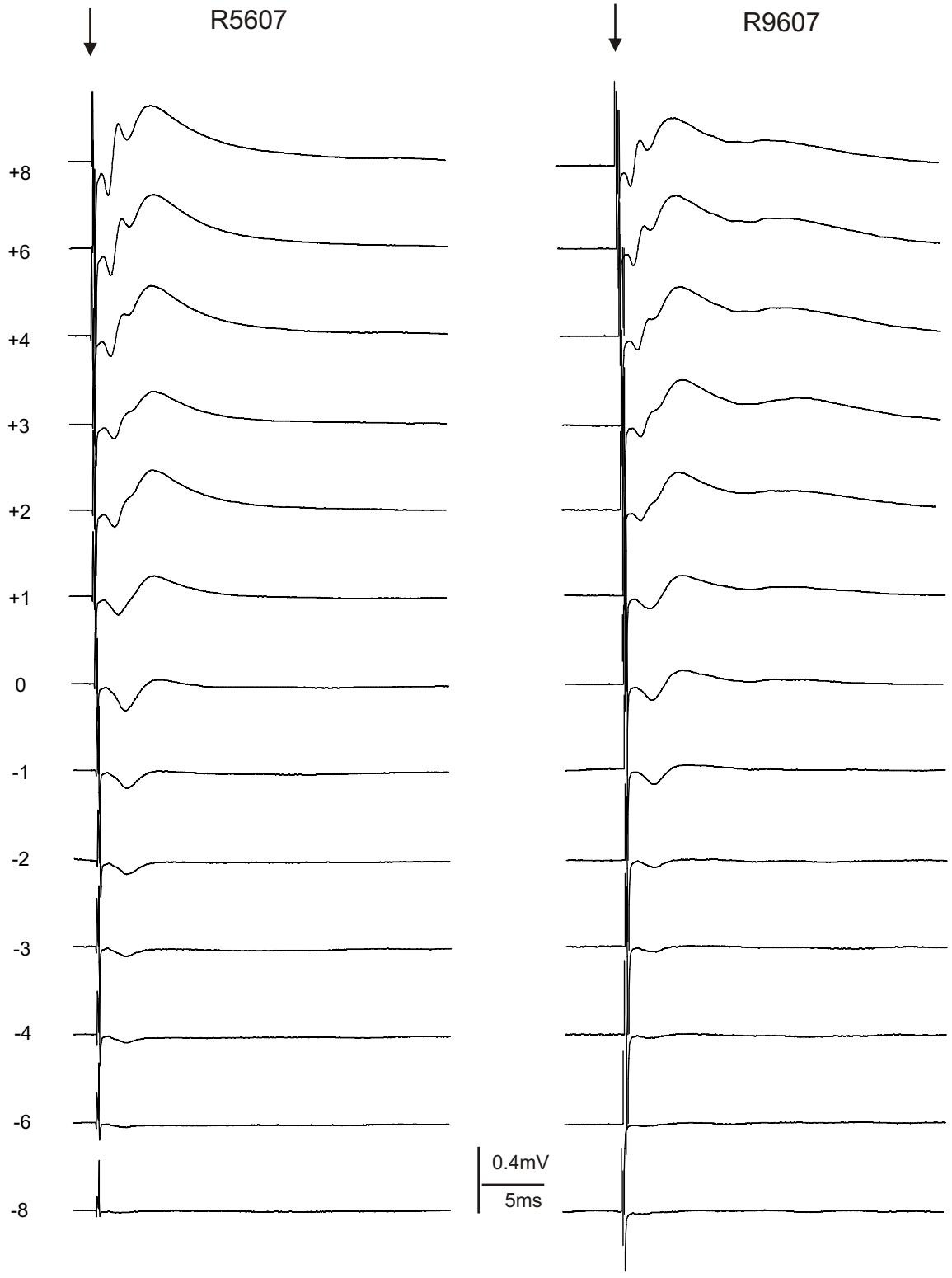


**Figure 2-19 Examples of CDPs evoked by pyramidal stimulation in acutely lesioned animals**

Each column of traces shows recordings made from one animal. The recordings were made at 1mm intervals from 8mm rostral to 8mm caudal to the C4/5 segmental border as indicated. Traces recorded at +7, +5, -5, and -7mm are omitted. The traces represent averages of 50 sweeps and the calibrations apply to all traces. The arrows indicate stimulus artifacts. Note that CDPs are virtually absent caudal to the lesion but remain above the lesion.

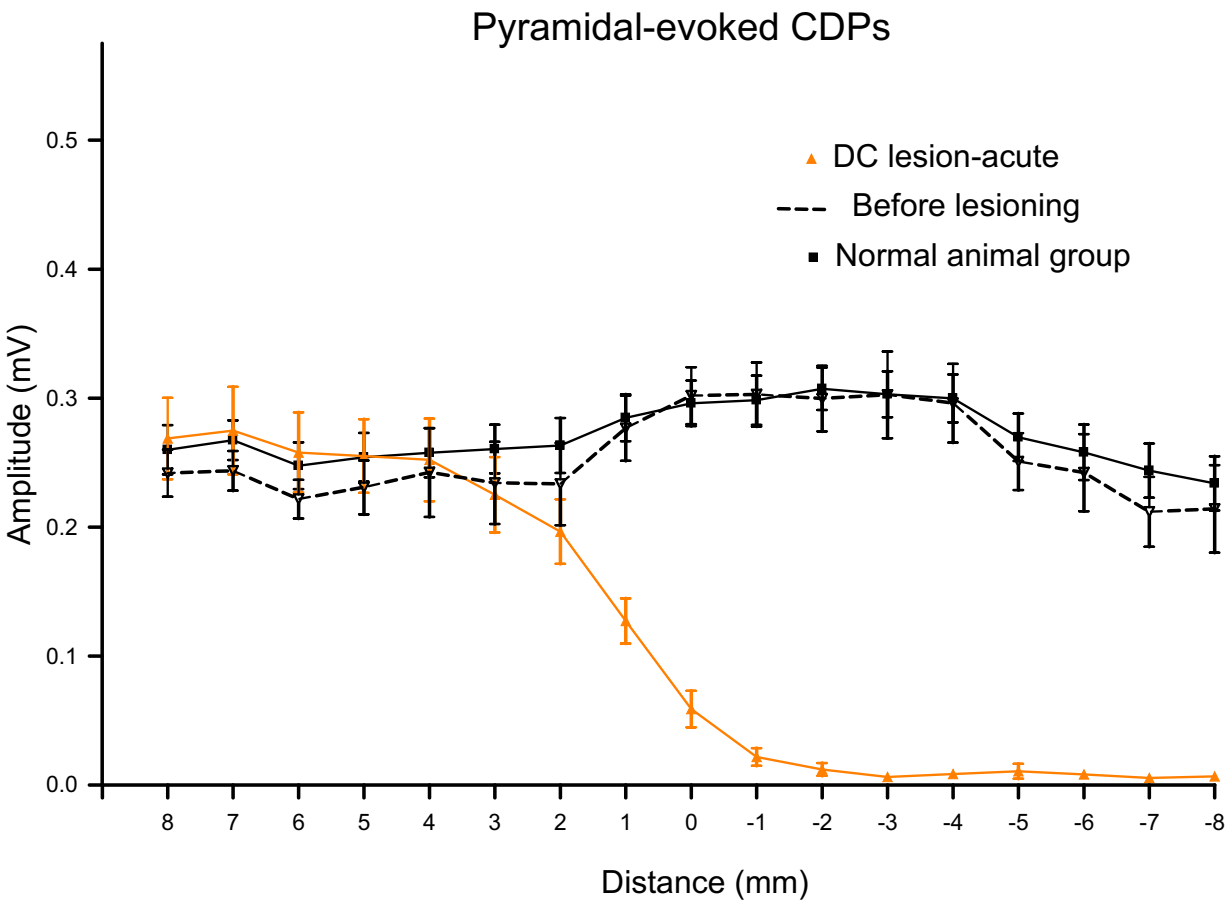


**Figure 2-20 Amplitudes of pyramidal-evoked CDPs recorded in acutely lesioned animals**

The plot shows the amplitudes of CDPs recorded from the acutely lesioned animal group (n=7) as a whole. The amplitude of CDPs recorded from these same 7 animals before making the lesion is indicated by the dashed line. The previous plot for normal animals is also shown for comparison. Each data point is the mean CDP amplitude for all animals from each group. The error bars show +/- SEM. The recordings were made over the cervical spinal cord and are shown relative to the C4/5 border (0 mm) where dorsal column lesions were made in lesioned animals. In acutely lesioned animals, pyramidal-evoked CDPs below the lesion (from -1 to -8mm) were virtually absent, while CDPs above the lesion (from +3 to +8mm) were not affected.

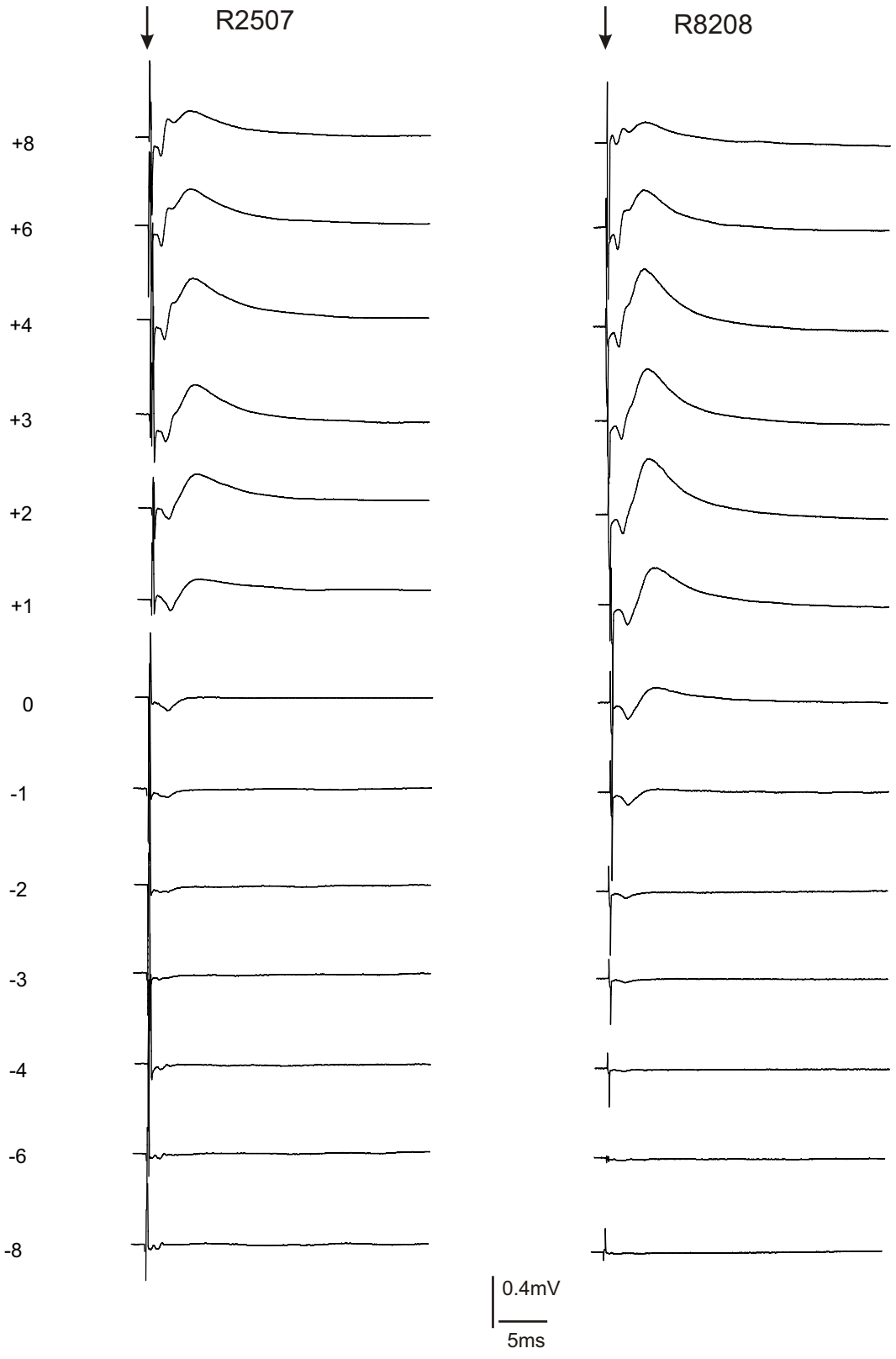


**Figure 2-21 Examples of CDPs evoked by pyramidal stimulation in one week survival DC lesioned animals**

Each column of traces shows recordings made from one animal. The recordings were made at 1mm intervals from 8mm rostral to 8mm caudal to the C4/5 segmental border as indicated. Traces recorded at +7, +5, -5, and -7mm are omitted. The traces represent averages of 50 sweeps and the calibrations apply to all traces. The arrows indicate stimulus artifacts. Note that tiny CDPs were observed at some caudal locations, especially close to the lesion site.

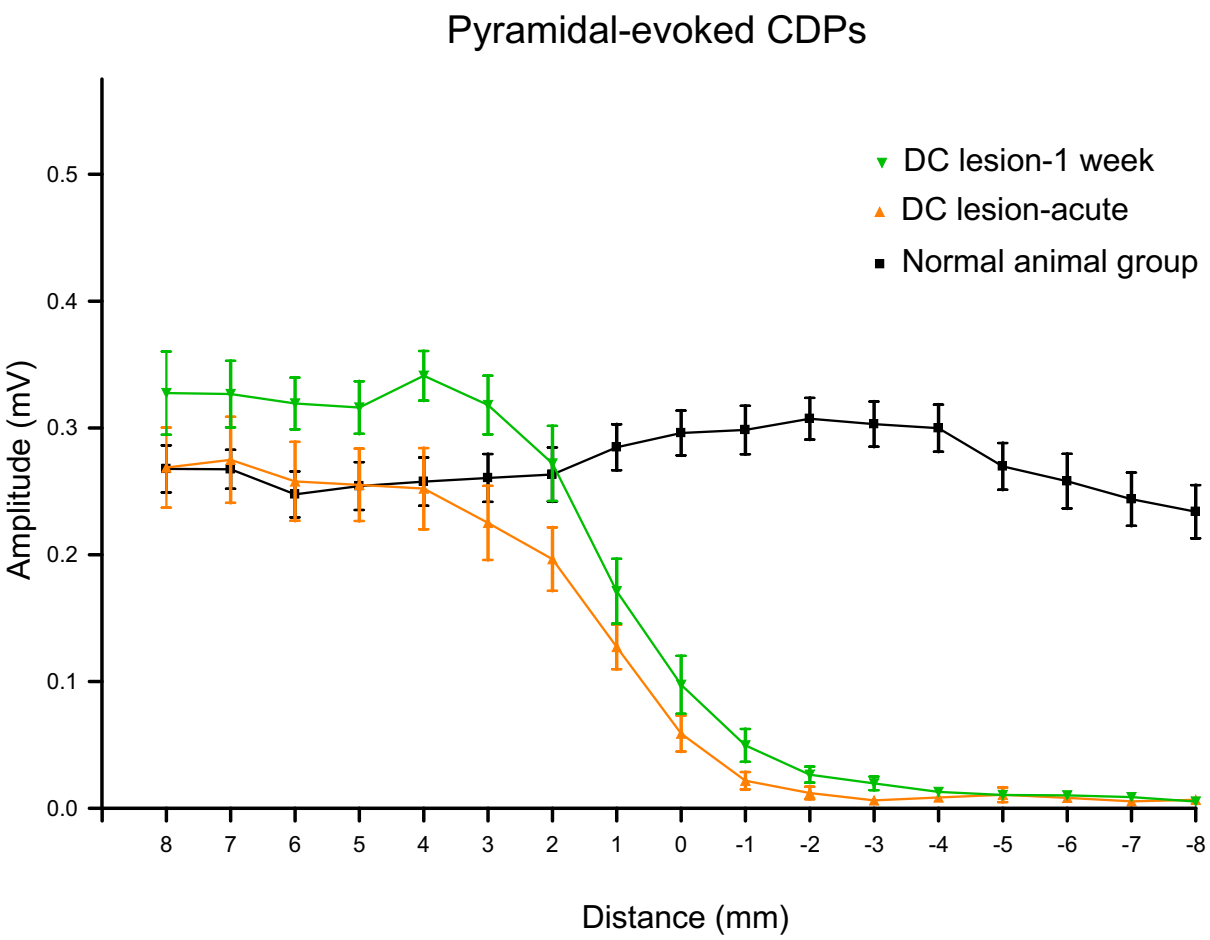


**Figure 2-22 Amplitude of pyramidal-evoked CDPs recorded in one week survival DC lesioned animals**

The plot shows the amplitudes of CDPs recorded from the one week survival lesioned animal (n=14) group as a whole. The previous plots for the normal group and for the acutely lesioned animal group are also shown for comparison. Each data point is the mean CDP amplitude for all animals from each group. The error bars show +/- SEM. The recordings were made over the cervical spinal cord. Recording positions are shown relative to the C4/5 border (0 mm) where dorsal column lesions were made in lesioned animals. In one week survival animals, CDPs below the lesion (from -8mm to -2mm) were almost abolished as in the acutely lesioned group. At some positions close to the lesion, CDPs were larger than those in acutely lesioned animals, but not significantly different. Above the lesion, the CDPs remained and in fact tended to be of larger amplitudes than those recorded from normal animals and acutely lesioned animals. This difference was significant only in comparison to the normal group.

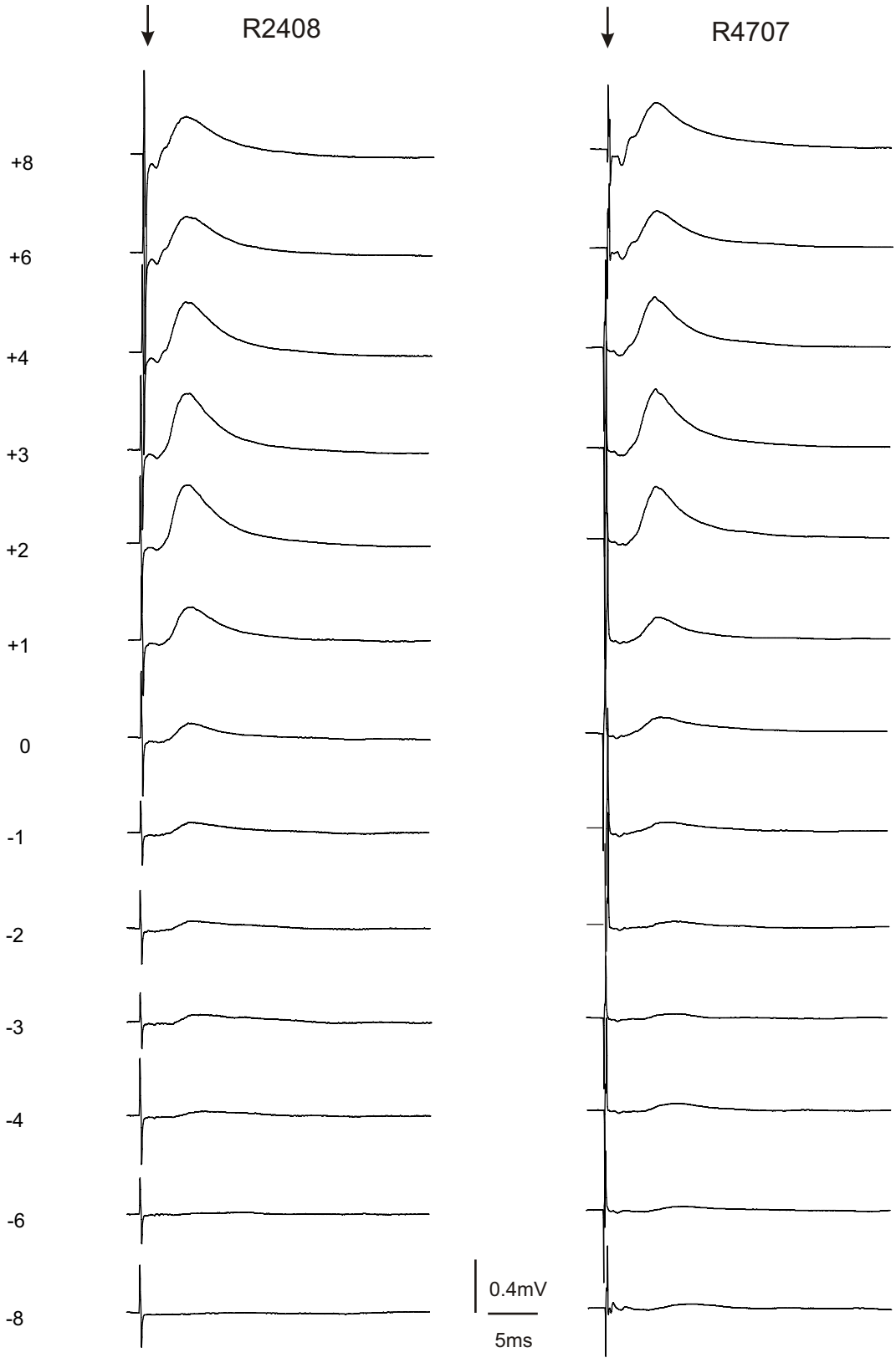


**Figure 2-23 Examples of CDPs evoked by pyramidal stimulation in three months survival DC lesioned animals**

Each column of traces shows recordings made from one animal. The recordings were made at 1mm intervals from 8mm rostral to 8mm caudal to the C4/5 segmental border as indicated. Traces recorded at +7, +5, -5, and -7mm are omitted. The traces represent averages of 50 sweeps and the calibrations apply to all traces. The arrows indicate stimulus artifacts. Note that small but obvious CDPs were observed at the caudal locations of the lesion site.

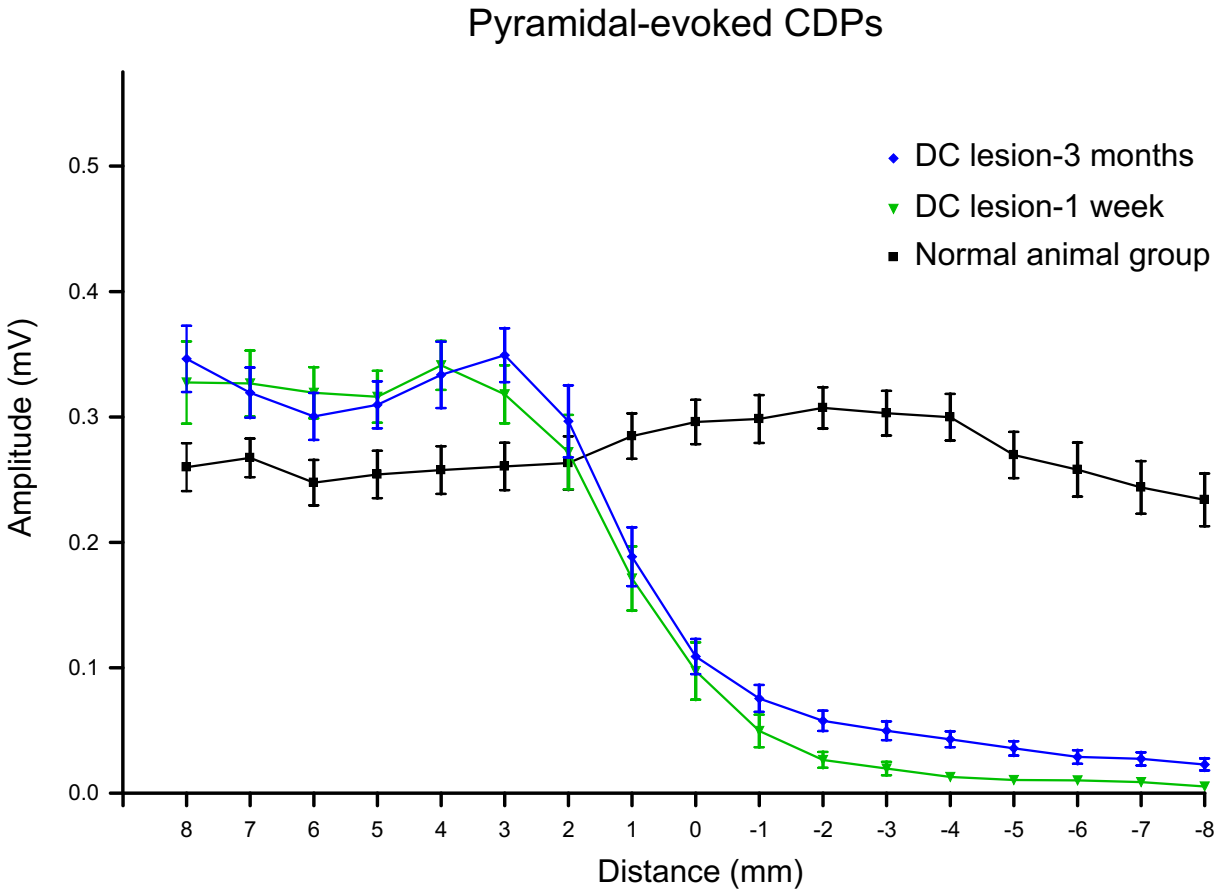


**Figure 2-24 Amplitudes of pyramidal-evoked CDPs recorded in three month survival DC lesioned animals**

The plot shows the amplitudes of CDPs recorded from three month survival lesioned animals (n=15). The previous plots for the normal group and for the one week survival group are also shown for comparison. Each data point is the mean CDP amplitude for all animals from each group. The error bars show +/- SEM. The recordings were made over the cervival spinal cord. Recording positions are shown relative to the C4/5 border (0 mm) where dorsal column lesions were made in lesioned animals. In the three months group, CDPs below the lesion were larger at all recording locations than those recorded in animals one week after a dorsal column lesion. This difference was significant at all recording sites (-2 to -8mm) except those closest to the lesion. Above the level of the lesion, CDPs were significantly larger than in normal animals and virtually the same as those recorded in animals one week after a dorsal column lesion.

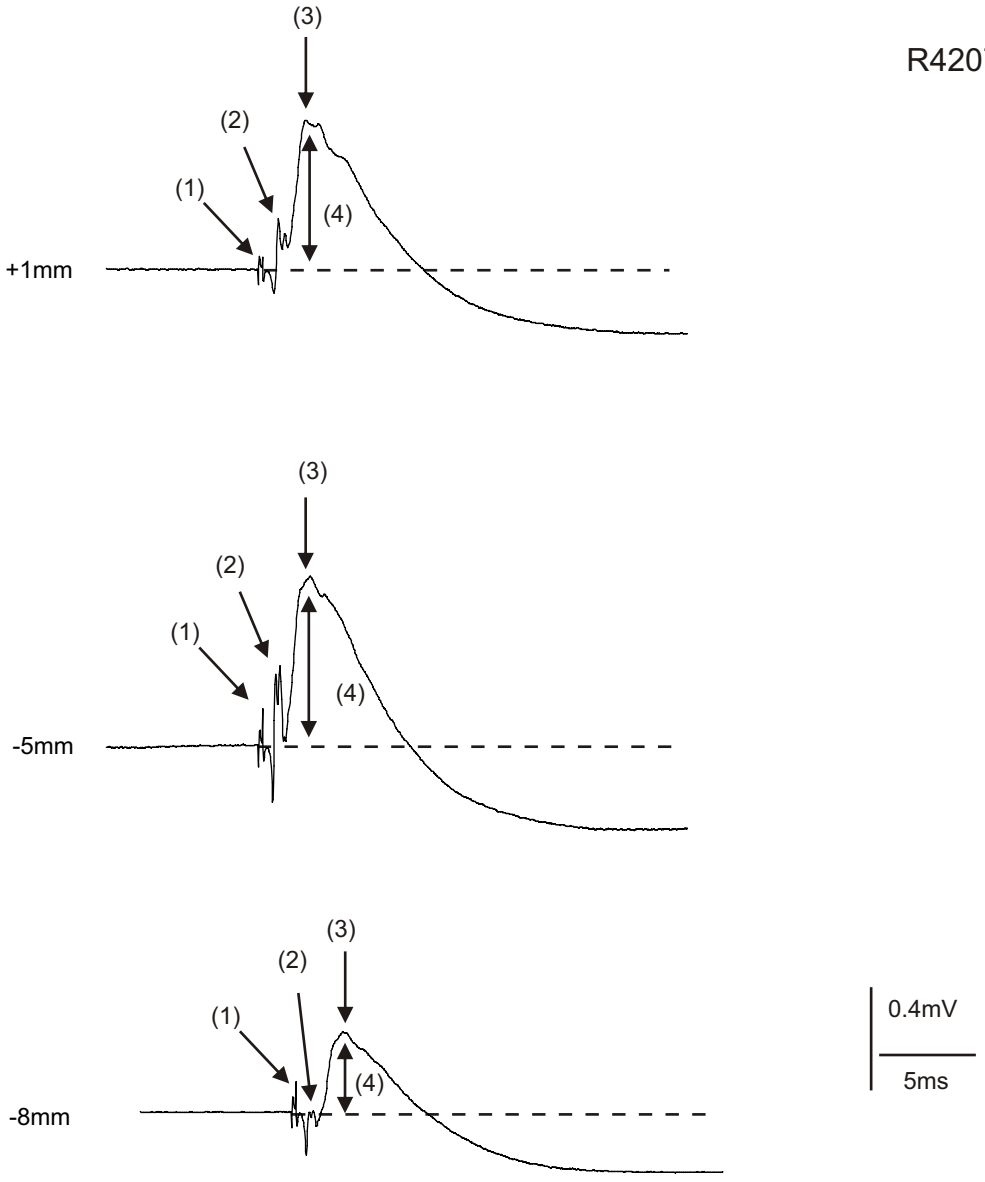


**Figure 2-25 Examples of CDPs evoked by radial nerve stimulation**
Examples of surface recordings made at different locations on the cervical spinal cord in a normal animal (R4207). All recordings are averages of 25 sweeps. The numbered arrows point to different components of the surface recordings: (1) stimulus artefact, which indicates the timing of the stimulation; (2) afferent volley, which represents the action potentials travelling along the afferent fibres; (3) CDP, which represents the synaptic activity generated by connections between the collaterals of the primary afferent fibres and spinal cord neurons and provides a measure of the strength of these connections; (4) the peak amplitude for CDPs, which was measured at each recording location using Signal software. The afferent volley is clearest and largest at locations close to the segment of entry of the stimulated root (middle trace), becomes dispersed at more rostral and caudal locations.

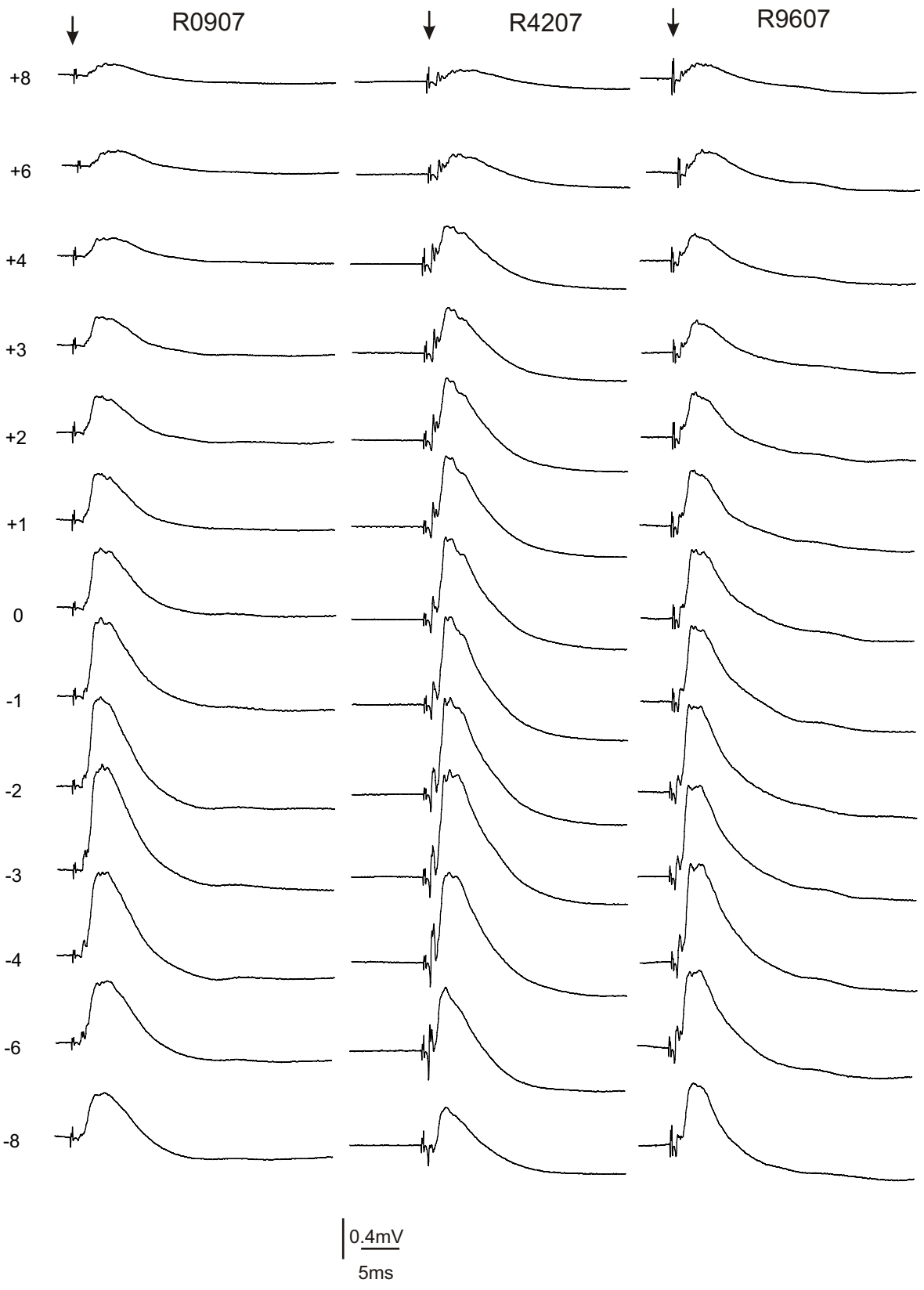


**Figure 2-26 Examples of CDPs evoked by radial nerve stimulation in normal animals**
Each column of traces shows recordings made from one animal. The recordings were made at 1mm intervals from 8mm rostral to 8mm caudal to the C4/5 segmental border as indicated. Traces recorded at +7, +5, -5, and -7mm are omitted. The traces represent averages of 25 sweeps and the calibrations apply to all traces. The arrows indicate stimulus artifacts. Note that the largest CDPs were recorded at -3/-4mm.

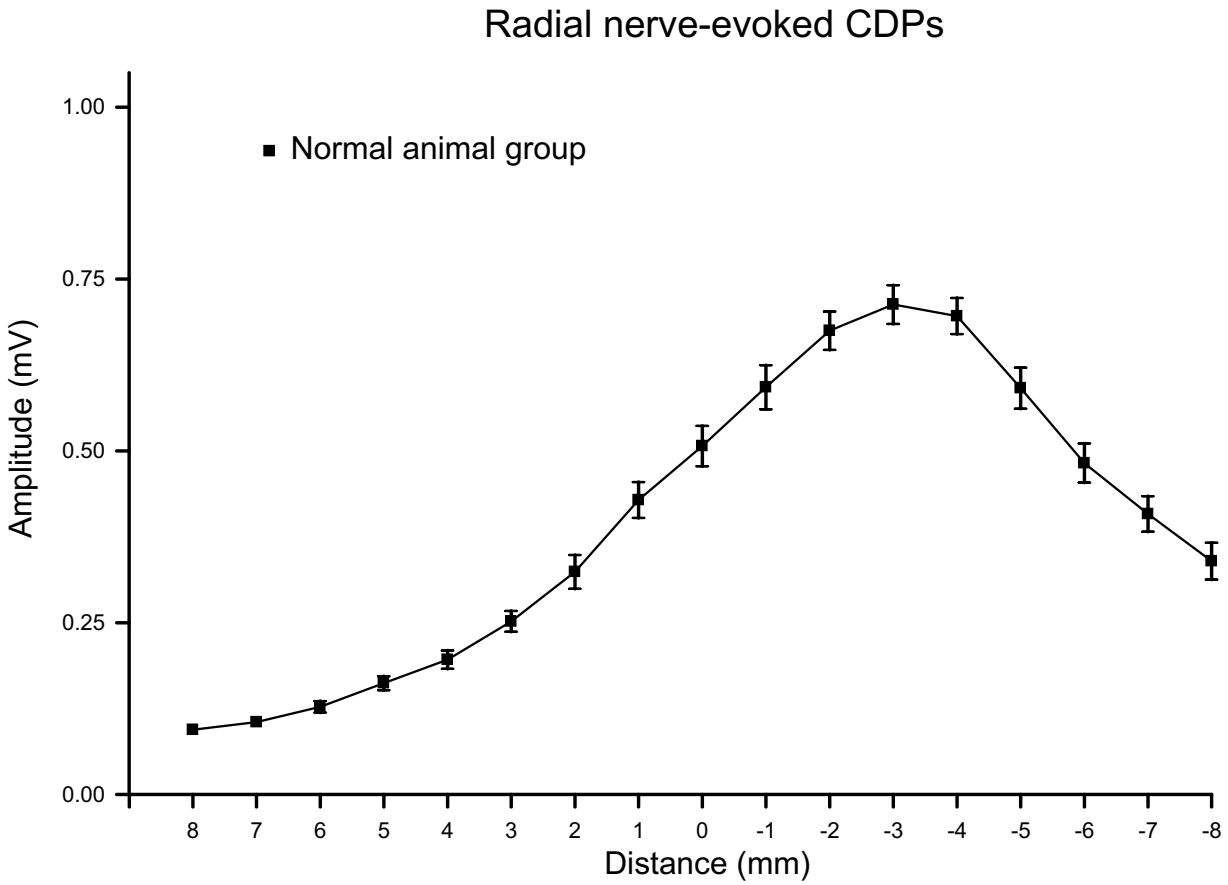


**Figure 2-27 Amplitudes of radial nerve-evoked CDPs recorded in normal animals**
The plot shows the amplitudes of CDPs recorded from the normal animal group as a whole (n=22). Each data point is the mean CDP amplitude for all animals in the group. The error bars show +/- SEM. The recordings were made over the cervical spinal cord. Recording positions are shown relative to the C4/5 border (0 mm) where dorsal column lesions were made in the lesioned groups. In normal animals, the biggest radial-evoked CDPs were recorded around 3 to 4mm below C4/5 border. The amplitudes of the biggest CDPs were around 0.7mV. CDPs decreased in amplitude more rostrally and caudally. Small CDPs were still detected at 8mm above the C4/5 border.

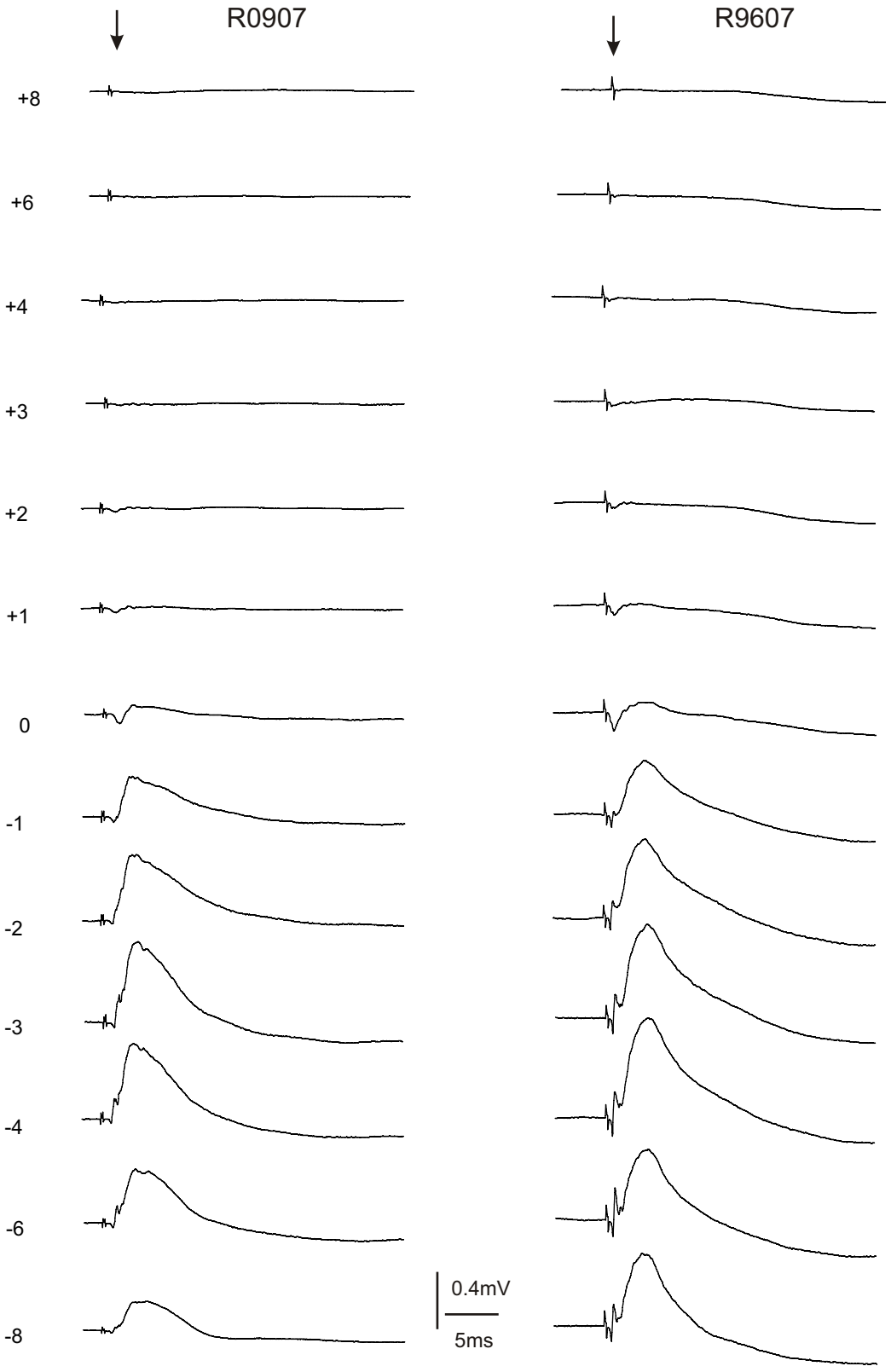


**Figure 2-28 Examples of CDPs evoked by radial nerve stimulation in acutely lesioned animals**

Each column of traces shows recordings made from one animal. The recordings were made at 1mm intervals from 8mm rostral to 8mm caudal to the C4/5 segmental border as indicated. Traces recorded at +7, +5, -5, and -7mm are omitted. The traces represent averages of 25 sweeps and the calibrations apply to all traces. The arrows indicate stimulus artifacts. Note that CDPs were virtually absent rostral to the lesion.

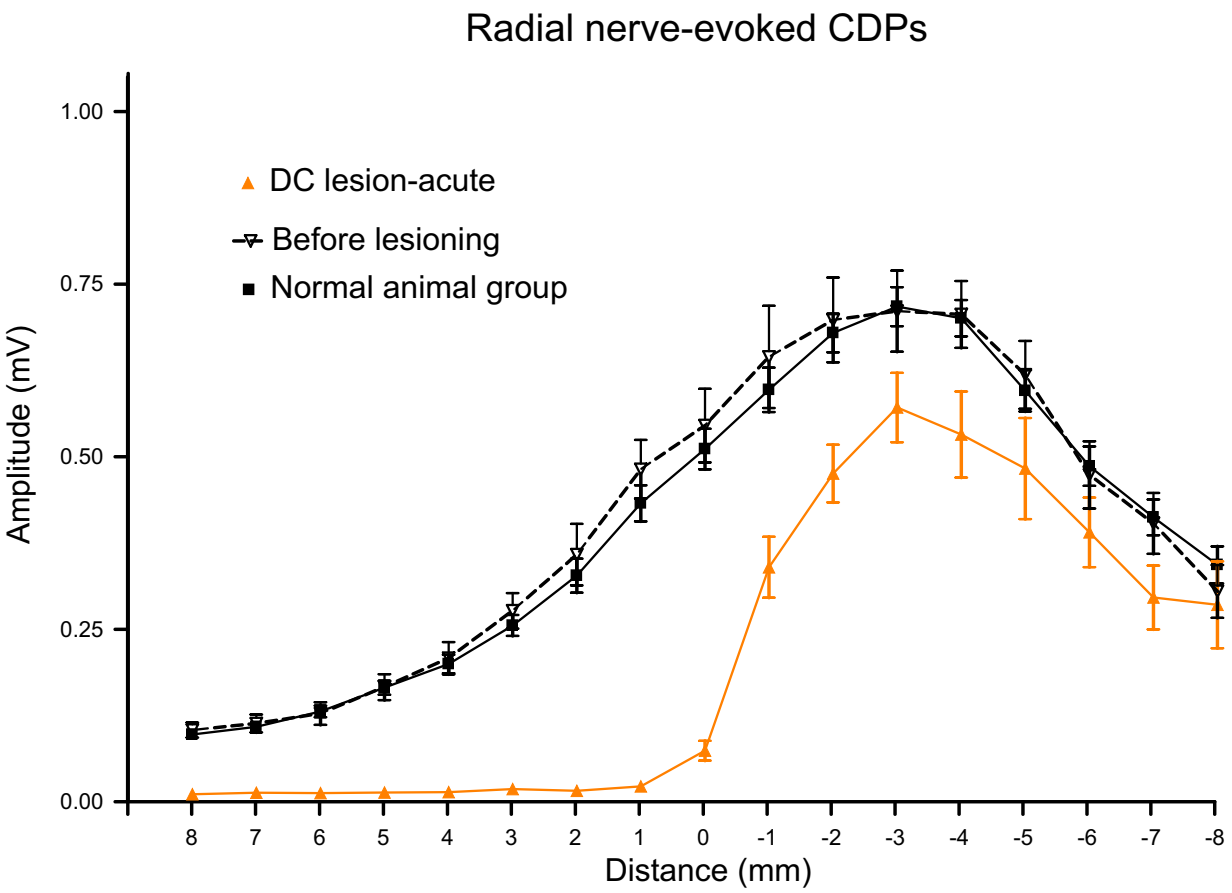


**Figure 2-29 Amplitude of radial nerve-evoked CDPs recorded in acutely lesioned animals**

The plot shows the amplitudes of CDPs recorded from acutely lesioned animals (n=7). The plot for normal animals is also shown for comparison as is the plot for CDPs recorded from the seven animals prior to lesioning. Each data point is the mean CDP amplitude for all animals from each group. The error bars show +/- SEM. The recordings were made over the cervical spinal cord. Recording positions are shown relative to the C4/5 border (0 mm) where dorsal column lesions were made in lesioned animals. After lesioning, CDPs above the lesion site (from 1 to 8mm) were virtually absent, while CDPs below the lesion (from -2mm to -8) were also smaller compared to those recorded in normal animals but not significantly.

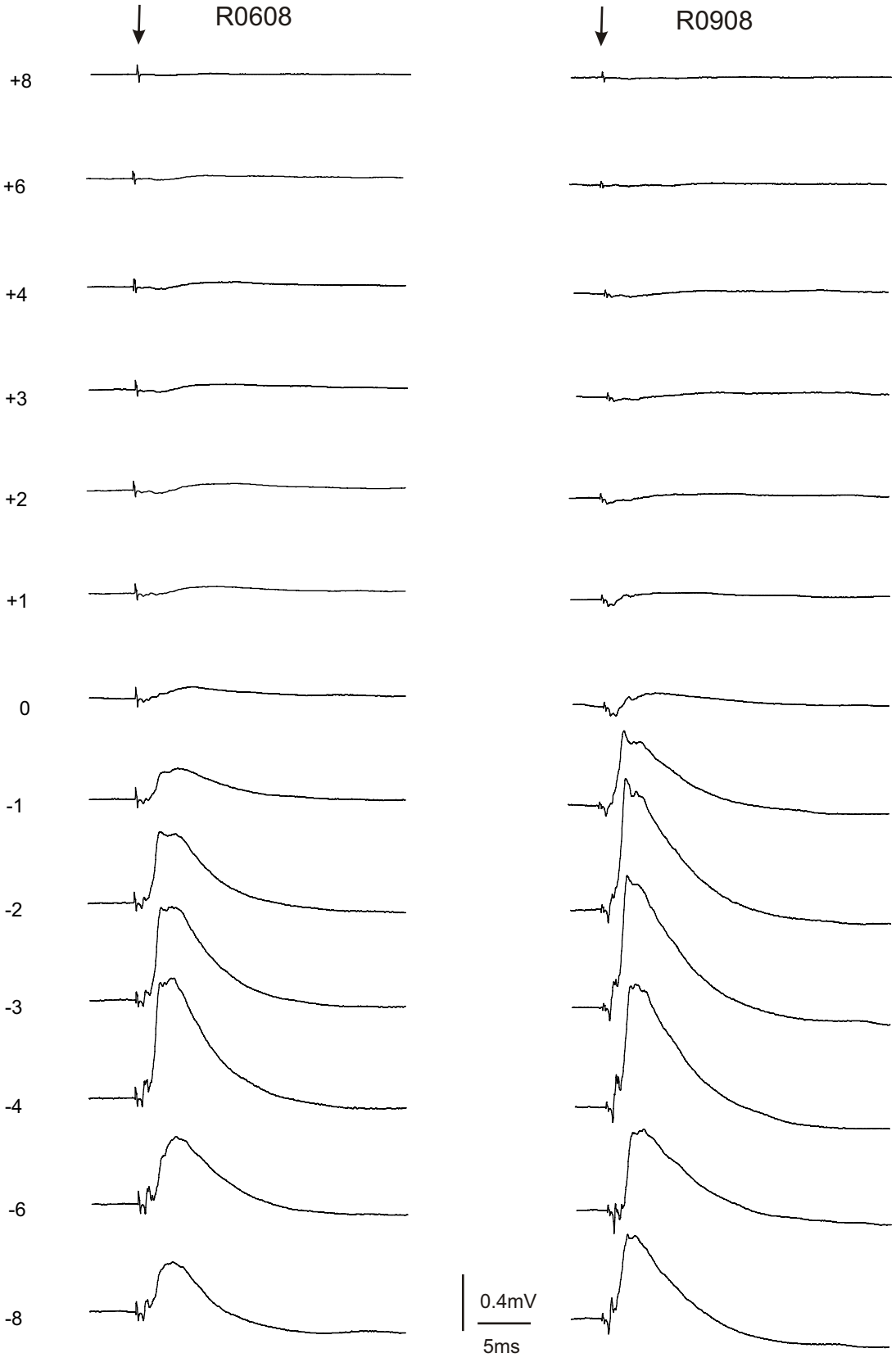


**Figure 2-30 Examples of CDPs evoked by radial nerve stimulation in one week survival DC lesioned animals**

Each column of traces shows recordings made from one animal. The recordings were made at 1mm intervals from 8mm rostral to 8mm caudal to the C4/5 segmental border as indicated. Traces recorded at +7, +5, -5, and -7mm are omitted. The traces represent averages of 25 sweeps and the calibrations apply to all traces. The arrows indicate stimulus artifacts. Note that small CDPs were observed at locations rostral to the lesion site.

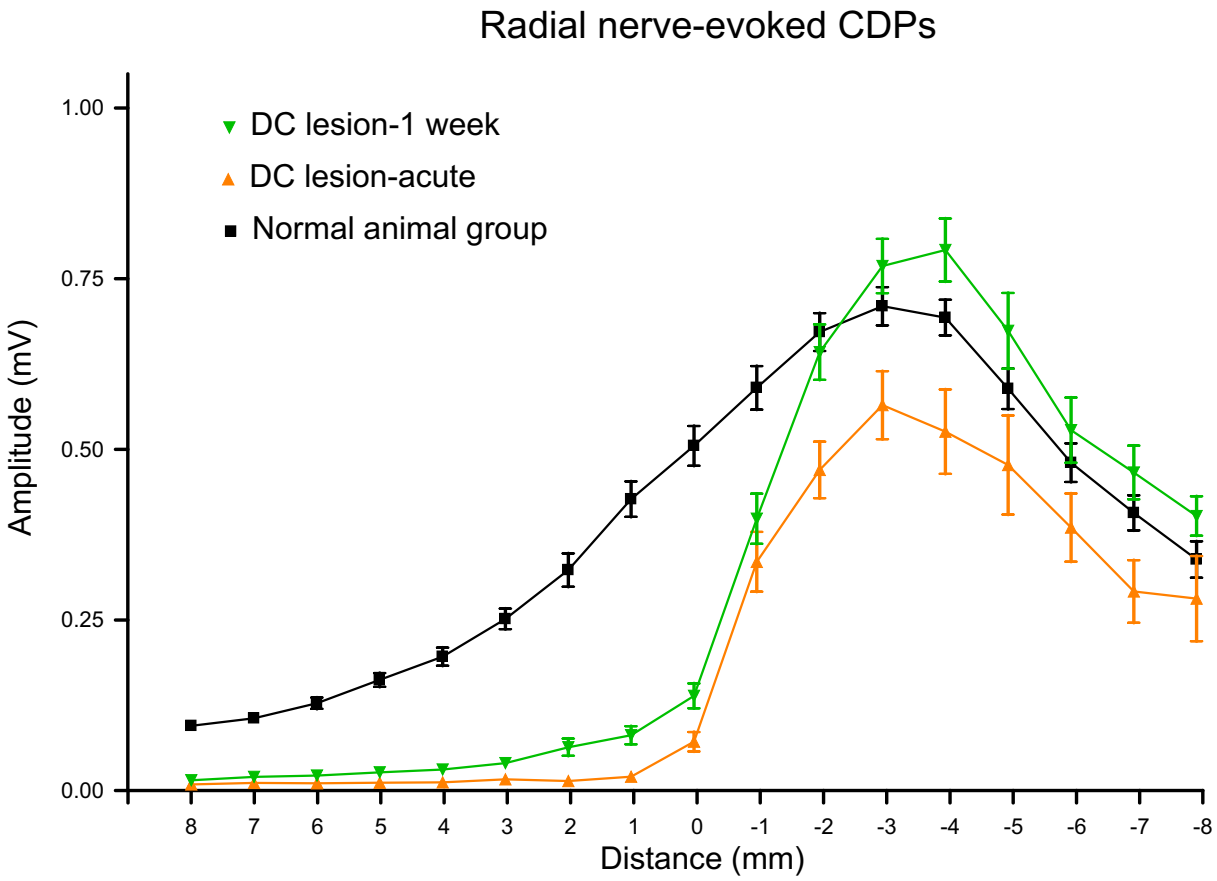


**Figure 2-31 Amplitude of radial nerve-evoked CDPs recorded in one week survival DC lesioned animals**

The plot shows the amplitudes of CDPs recorded from the one week survival lesioned animal group (n=17). The previous plots for normal animals and acutlely lesioned animals are also shown for comparison. Each data point is the mean CDP amplitude for all animals from each group. The error bars show +/- SEM. The recordings were made over the cervical spinal cord. Recording positions are shown relative to the C4/5 border (0 mm) where dorsal column lesions were made in lesioned animals. In the one week group, radial-evoked CDPs were bigger at all recording locations than those recorded in the acutely lesioned group. CDPs at some caudal locations (-4mm and -8mm) were even significantly larger than those recorded in normal animals.

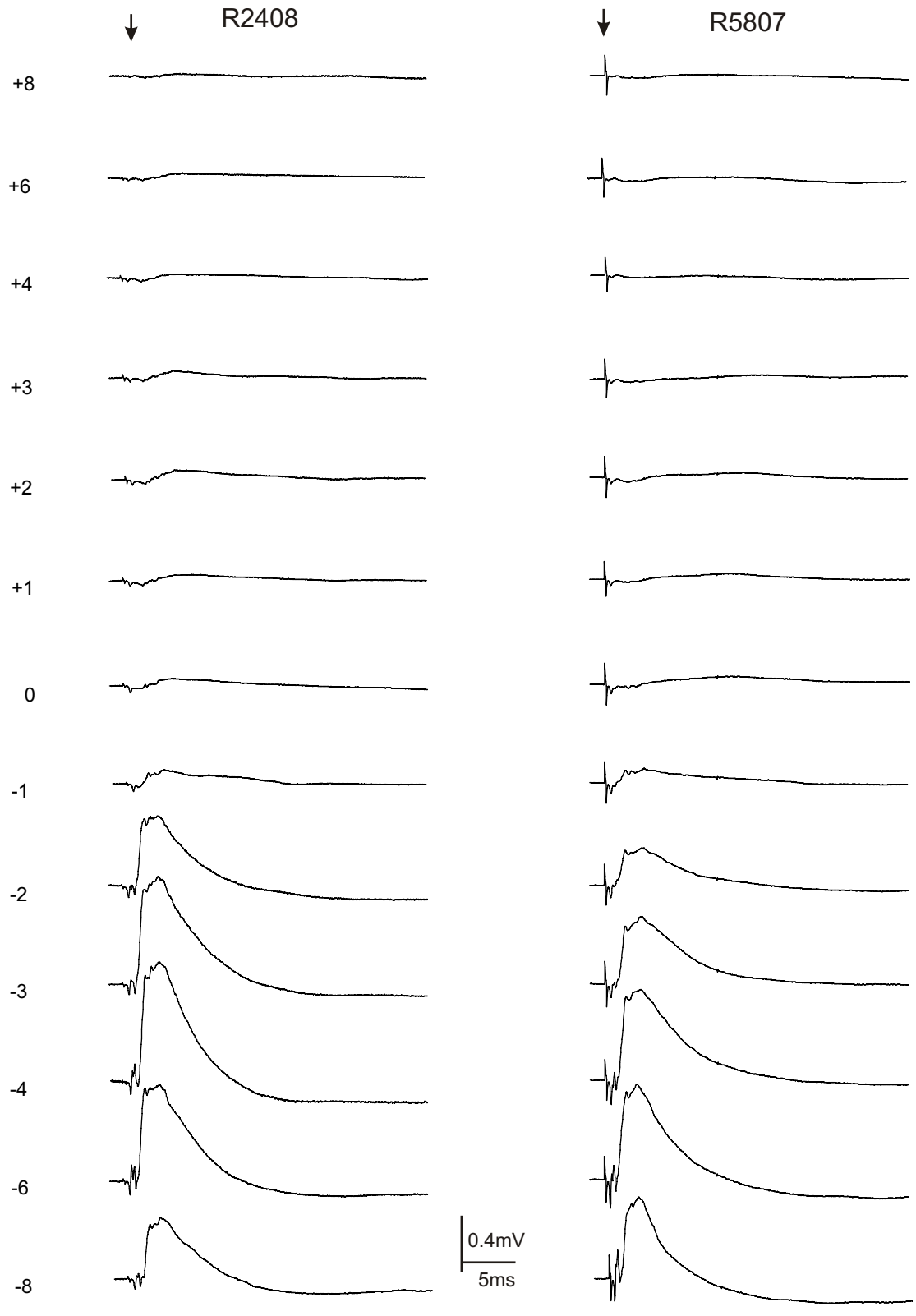


**Figure 2-32 Examples of CDPs evoked by radial nerve stimulation in three month survival animals**

Each column of traces shows recordings made from one animal. The recordings were made at 1mm intervals from 8mm rostral to 8mm caudal to the C4/5 segmental border as indicated. Traces recorded at +7, +5, -5, and -7mm are omitted. The traces represent averages of 25 sweeps and the calibrations apply to all traces. The arrows indicate stimulus artifacts. Note that small CDPs were obeserved at locations rostral of the lesion site.

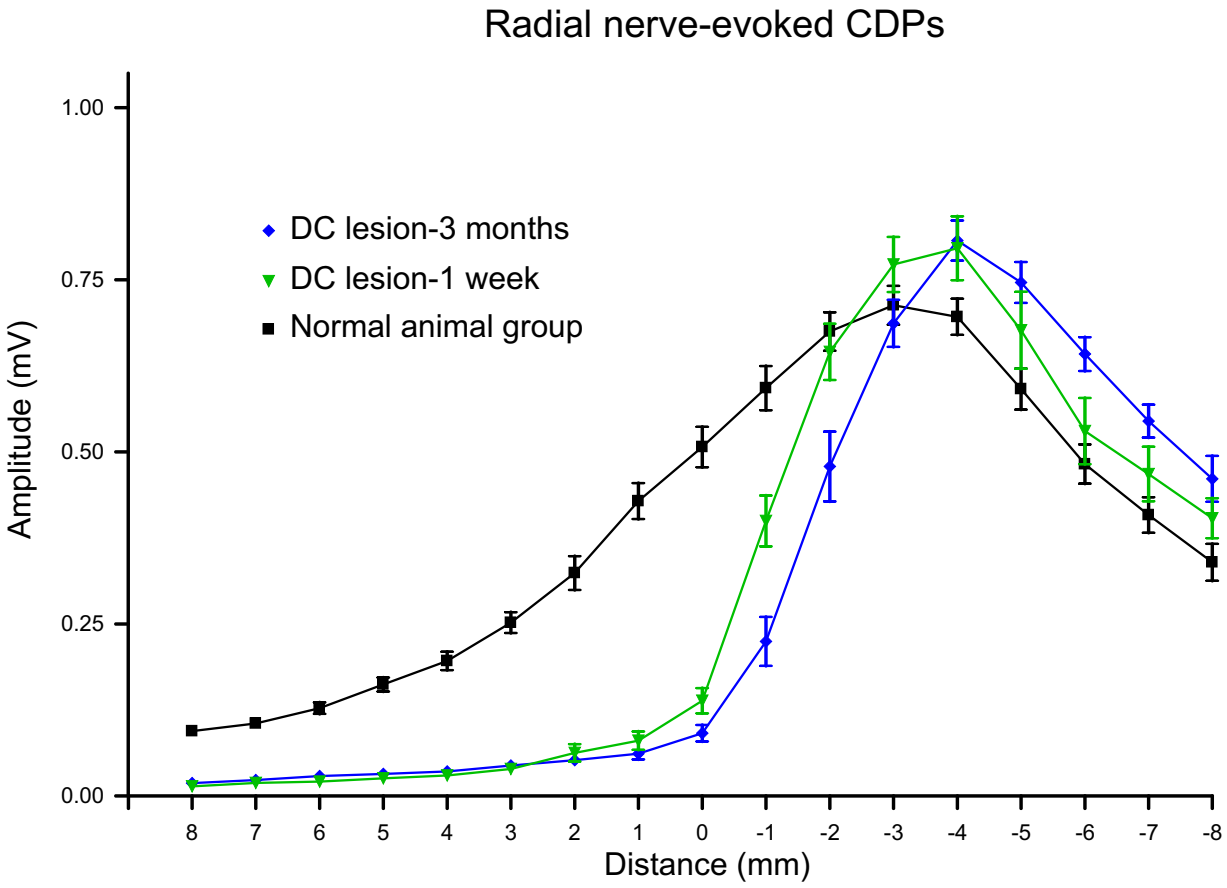


**Figure 2-33 Amplitudes of radial nerve-evoked CDPs recorded in three month survival DC lesioned animals**

The plot shows the amplitudes of CDPs recorded from the 3 month survival group (n=18). The previous plots for normal animals and one week survival lesioned animals are also shown for comparison. Each data point is the mean CDP amplitude for all animals from each group. The error bars show +/- SEM. The recordings were made over the cervical spinal cord. Recording positions are shown relative to the C4/5 border (0 mm) where dorsal column lesions were made in lesioned groups. CDPs above the lesion were very similar in amplitude to those in 1 week lesioned animals. Below the lesion, CDPs differed in a more complex way from those recorded at 1 week. Close to the lesion (0 to -2mm) the CDPs in 3 month animals tended to be smaller than in 1 week animals and this difference was significant. Farther away from the lesion, however, CDPs were the same or larger than those recorded at 1 week after lesioning though the difference was only significant at -6mm.

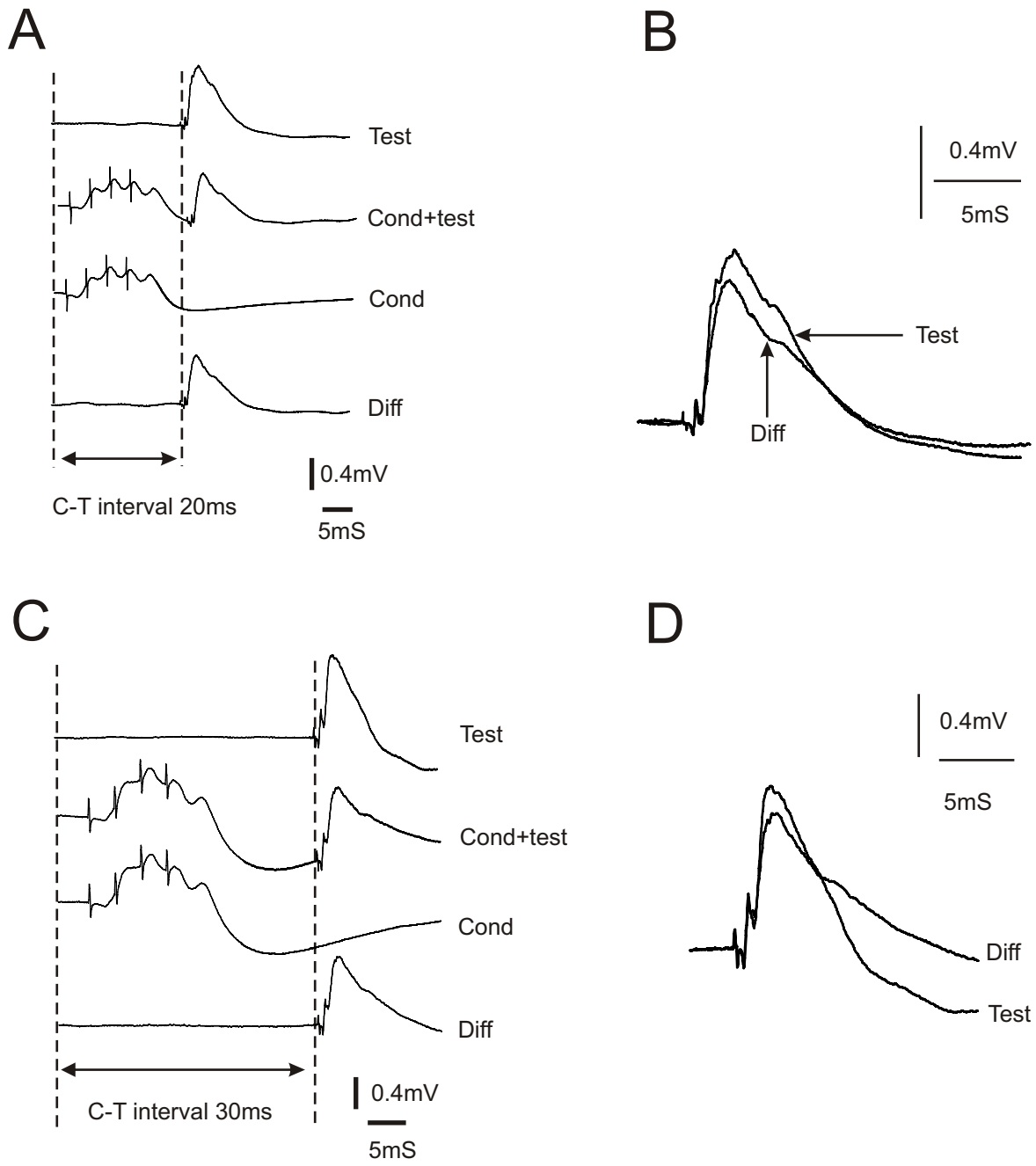


**Figure 2-34 Inhibitory control of sensory transmission by the corticospinal tract from a normal animal**

A, CDP recordings evoked by radial nerve afferents with conditioning stimuli in the pyramid were recorded at 3mm below the C4/5 reference location in a normal animal (9308). The top trace (test) shows a cord dorsum potential evoked by radial nerve stimulation. The second trace (cond + test) shows the effect of preceding the stimulus to the peripheral nerve with a train of 4 shocks within the pyramid. Note the strong inhibition (reduction in amplitude) of the cord dorsum potential. The next trace (cond) shows the effect of stimulation in the pyramids alone and the bottom trace (diff) shows cond + test minus cond. B, the radial nerve-evoked potential from the top trace (test) and the bottom trace (diff) are shown superimposed in order to illustrate the degree of inhibition (reduction in amplitude) produced by the corticospinal tract. The interval between the first conditioning stimulus and the test stimulus (C-T interval) is 20ms. C and D show an example recorded at 4mm below the C4/5 border with a conditioning-test interval of 30ms.

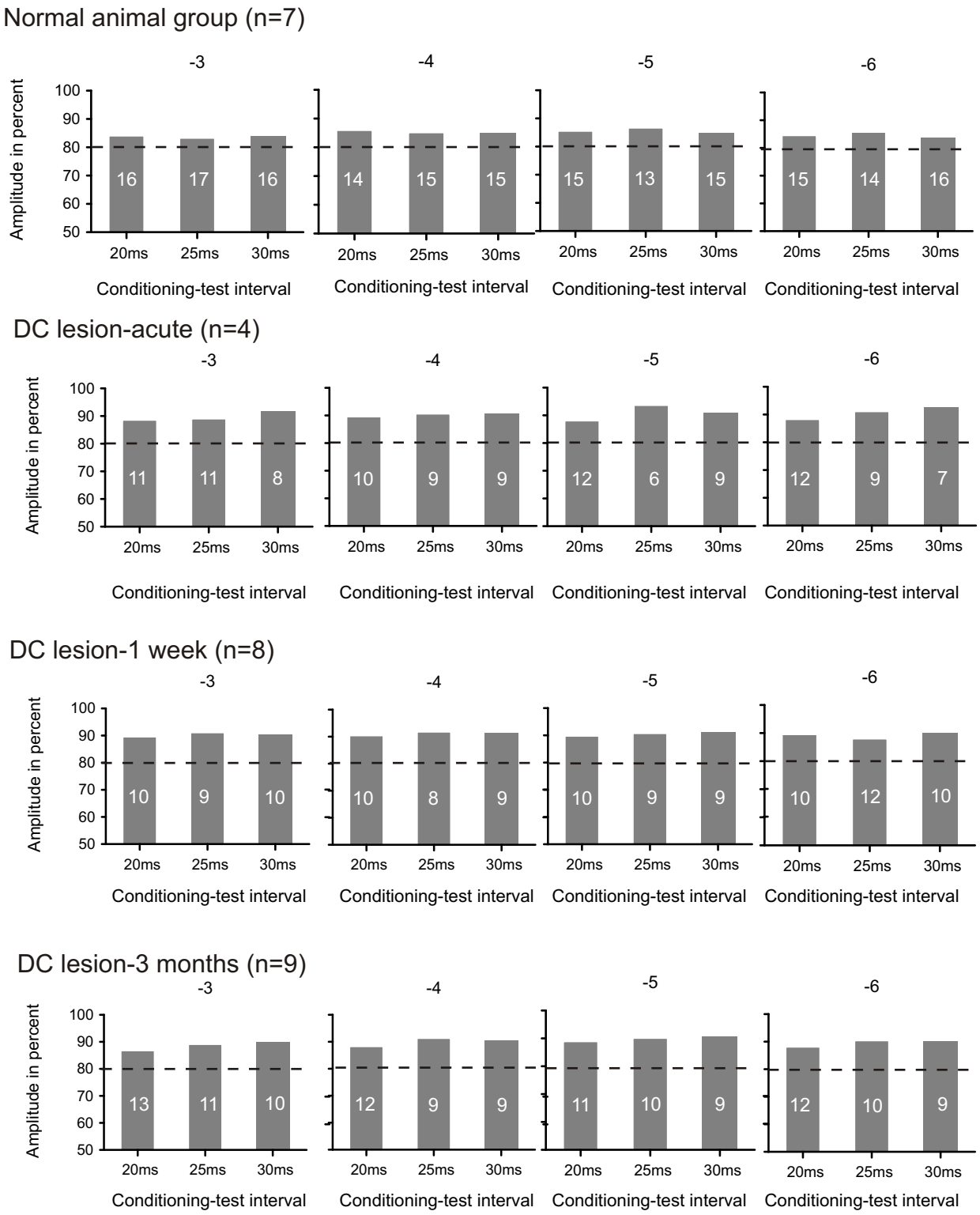


**Figure 2-35 Inhibitory control of sensory transmission by the corticospinal tract in different groups**

Inhition was tested in normal animals (n=7) and lesioned animals (acute n=4; 1 week n=8; 3 months n=9). The data are presented as groups. The recording locations are shown on the top of each column. Conditioning intervals are shown at the bottom. The percentages of inhibition were leballed in the columns as white numbers. As expected, the inhibition in normal animals were stronggest compared to lesioned animals. There is a tendency that more inhition was presented in three month survival animals compared to those in one week lesioned animals. However, it was not significantly different. Note that the data were collected from small number of animals.

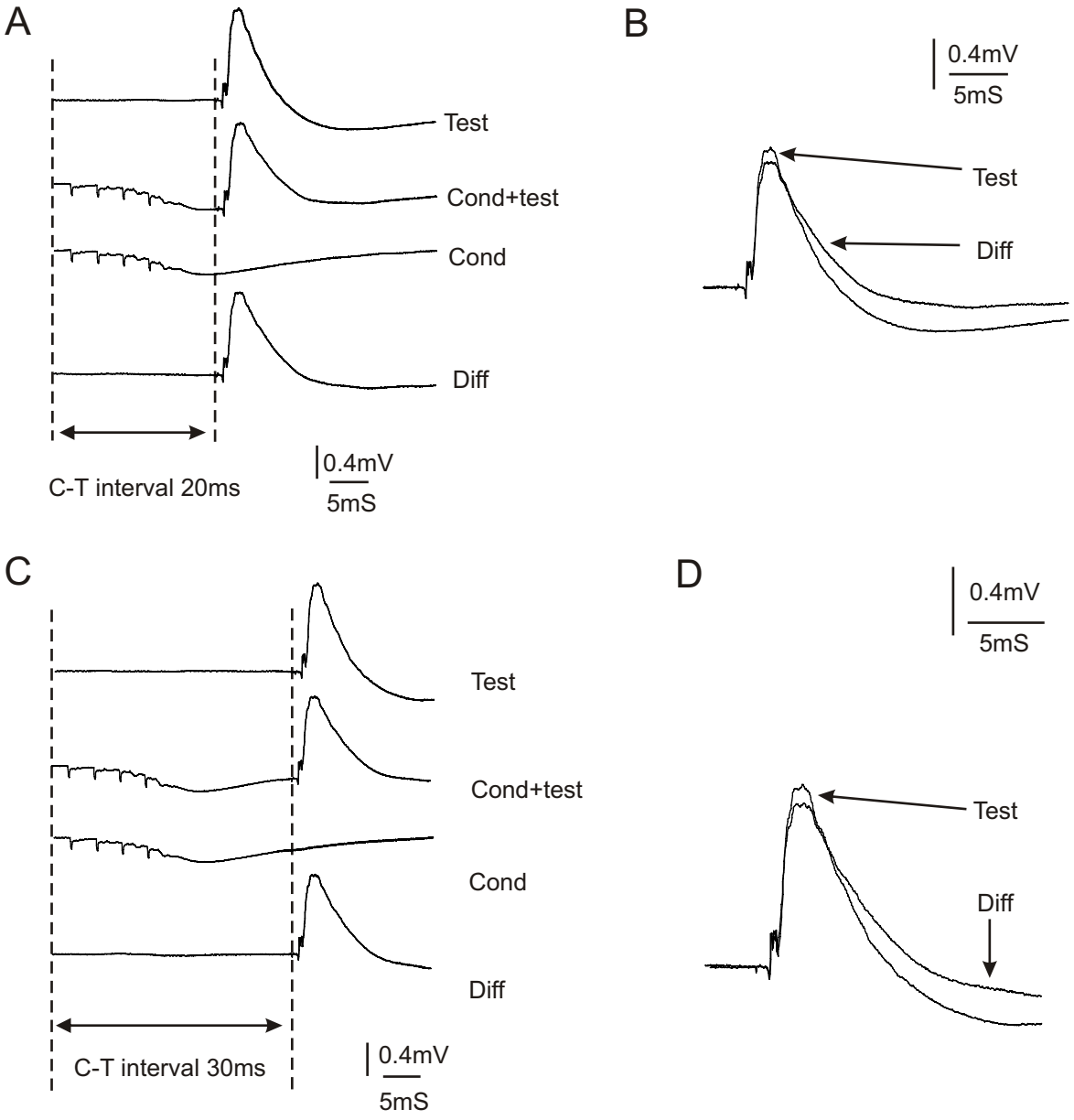


**Figure 2-36 Inhibitory control of sensory transmission by the corticospinal tract from a lesioned animal**

A, surface recordings from the cervical spinal cord close to where radial CDPs are largest (-4mm) in a lesioned animal (R8008). The top trace shows a cord dorsum potential evoked by radial nerve stimulation (test). The second trace shows the effect of preceding the stimulus to the peripheral nerve with a train of 4 shocks within the pyramid (cond + test). Note the small inhibition (reduction in amplitude) of the cord dorsum potential. The third trace shows the effect of stimulation in the pyramids alone (cond). The bottom trace shows cond + test minus cond (diff). B, the radial nerve-evoked potential from the top trace (test) and the bottom trace (diff) are shown superimposed in order to illustrate the degree of inhibition (reduction in amplitude) produced by the corticospinal tract. The interval between the first conditioning stimulus and the test stimulus (C-T interval) is 20ms. C and D show an example with C-T interval of 30ms.

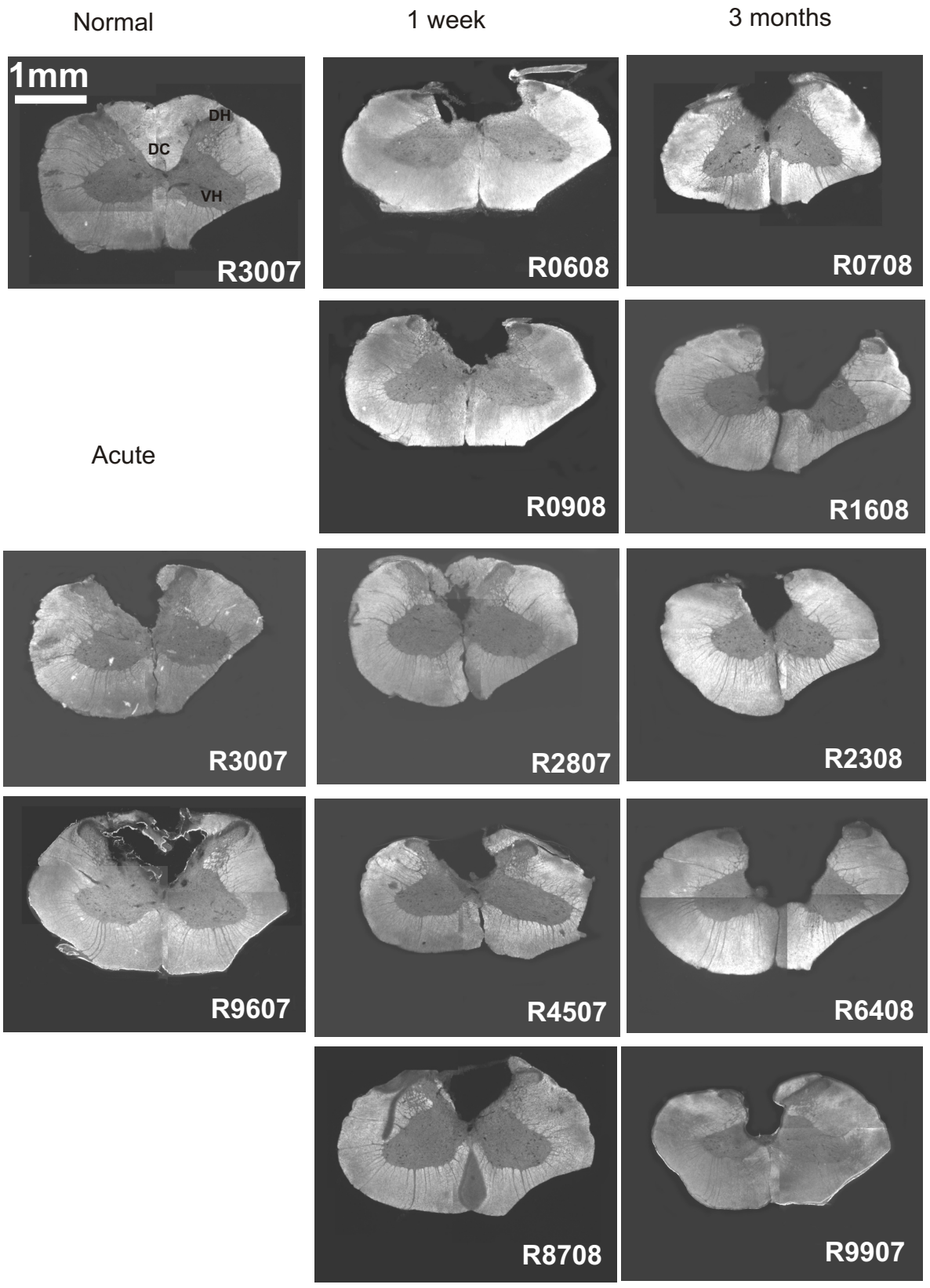


**Figure 2-37 Lesion morphology**
Light microscope images taken with a dark field condenser from transvers sections of the C4/5 spinal cord of different animal groups. A section from a normal animal is shown top left. The lesion interrupted the whole dorsal columns in acutely lesioned animals (bottom left). Lesion cavities were observed in 1 week and 3 month survival lesioned animals (middle and right columns respectively). Varying amounts of the dorsal horn grey matter were also affected by the lesion. Scale bar 1mm applies to all images.

# Effects of OEC transplants on sensorimotor pathways following injury

## 3.1 Introduction

OECs, which are glia from the olfactory system, have become a promising candidate for transplant-mediated repair after SCI on the basis that they operate in both PNS and CNS environments to support the ongoing axonal growth, ensheathment, and targeting of olfactory neurons throughout life. Although unique in function, they share many properties with Schwann cells, including antigenic and morphologic profiles, growth factor response, and transcription factor expression during myelination. However, OECs evoke a less-severe astrocytosis after transplantation (Santos-Sliva et al. 2007).

Evidence for improved functional recovery after OEC transplants is mixed and is derived from the use of various behavioural tests of sensorimotor function. For example, OEC transplants have been reported to improve performance in a reaching task following lesions of the corticospinal tract (Li et al. 1997) and to improve ladder climbing and other motor tasks following complete transection (Ramon-Cueto et al. 2000; Lu et al. 2001; Lopez-Vales et al. 2006). On the other hand, Steward et al. (2006) failed to see improved recovery following complete transection and following contusion injuries recovery has variously been reported to be absent (Takami et al. 2002) or modest (Plant et al. 2003). It therefore seems that OEC transplants may bring about some functional benefits following spinal cord injury in rodent models under appropriate conditions and/or with appropriate tests.

The mechanisms responsible for the functional improvements reported are equally contentious. There are numerous reports that OEC transplants support axonal regeneration. However, while it is evident that axonal regeneration is supported within the transplanted lesion itself, reports on the extent of axonal regeneration beyond the lesion are mixed. Some report long-distance regeneration across the injury (Li et al. 1998; Ramon-Cueto et al. 2000; Lu et al. 2001) while others report that regeneration is restricted to the transplant site (Andrews and Stelzner, 2004; Ruitenberg et al. 2003, 2005; Ramer et al. 2004a, b; Lu et al. 2006). In our own lab, regeneration of the ascending dorsal column pathway has been studied after OEC transplantation and although a small numbers of fibres have been seen growing for very short distances beyond the

lesion we have concluded that OEC transplants alone promote very limited long distance axonal regeneration (Toft et al. 2007).

Apart from promoting axonal regeneration, transplants of OECs could contribute to improved function following injury by several other mechanisms. These include reducing cavitation (Takami et al. 2002; Ramer et al. 2004a, b), improving vascularisation (Lopez-Vales et al. 2004; Ramer et al. 2004a, b), remyelinating axons with a damaged myelin sheath (Franklin et al. 1996; Sasaki et al. 2004), neuroprotection of long projection neurones (Sasaki et al. 2006) or the promotion of sprouting (Chuah et al. 2004) or other forms of plasticity.

In a recent study from our lab an electrophysiological approach was used to investigate the effect of OECs transplanted into dorsal column lesions on the function of sensory pathways in spinal cord segments adjacent to the lesion (Toft et al. 2007). The actions of sensory afferents on spinal cord neurones in the vicinity of the lesion were found to be better in OEC transplanted animals than in lesioned controls without the cells. Furthermore, this improved function at the spinal level appeared to translate into improved transmission of sensory information to the sensorimotor cortex. Two potential mechanisms were suggested to explain the improved function in transplanted animals, these were neuroprotection and plasticity. It was recognised that both of these mechanisms might operate together but it was not possible to distinguish between their respective contributions. The aim of the work described in this chapter was to determine whether OEC transplants induce plasticity following a spinal cord lesion. This requires a situation where any potential plasticity inducing actions are not complicated by the neuroprotective actions of OECs. When OEC transplants fill a lesion cavity they have been shown to prevent expansion of the lesion with time and to have neuroprotective actions. To test whether sprouting is also induced by OEC transplants therefore requires that the cells are distributed within the spinal cord above and/or below the lesion but not within the lesion itself. Fortuitously, we had previously found when transplanting OECs into a cervical level dorsal column lesion, that very few cells remained within the lesion cavity, but numerous cells became distributed within the spinal cord below the level of the lesion. We therefore made use of this situation, together with injection of OECs directly into the spinal cord above the lesion, to test whether plasticity was induced in regions containing OECs. The method of

assessment was the same as that described in the previous chapter. Lesions of the dorsal columns were made at the C4-C5 level and electrophysiological assessment of the actions of the corticospinal pathway and sensory afferents from the radial nerve were performed to determine whether transmission in these pathways was enhanced by the presence of OECs.

## 3.2 Methods

### *3.2.1 Animals*

The observations reported in this chapter are based on investigation of 51 male Fischer 344 rats (Harlan, Loughborough, UK, 200-250g). Fischer 344 rat was chosen because this inbred strain can avoid the problem of immunological rejection after cell transplantation. Forty two rats were subjected to dorsal column lesions and were allowed to recover for 3 months. Of these, olfactory ensheathing cells (OECs) were transplanted into the lesion site in 16 animals (OEC below group) and into the cord above the lesion in 14 animals (OEC above group). A further group of 12 animals was injected with similar volumes of medium as a control (medium above group). The remaining 9 animals were used to check cell distribution at different time points after transplantation. Of the 9 animals, OECs were transplanted into the lesion site in 3 animals and into the cord above the lesion in 6 animals after lesioning.

Results obtained using field potential recording include fields recorded from some normal animals described in the previous chapter.

### *3.2.2 Cell culture*

#### 3.2.2.1 Preparation of olfactory ensheathing cells

All cell culture was carried out by Mr. Thomas Sardella in Professor Sue Barnett's laboratory in the Beatson Institute, University of Glasgow.

OECs for transplantation were prepared from the olfactory bulb. The olfactory bulb consists of a mixture of cell types including oligodendrocytes, astrocytes, OECs, and neurons. To purify OECs from this mixture, fluorescence activated cell sorting (FACS) and appropriate antibodies were used. The FACS machine applies an electromagnetic field to deviate the cell trajectory and redirect the selected cells to a specific collecting tube, while excluding all other cells, dead cells, debris and auto-fluorescent material.

Franceschini and Barnett have shown that OECs express the O4 antibody in vivo (Franceschini and Barnett 1996). However, the O4 antibody is also expressed by oligodendrocytes (Sommer et al. 1981). Galactocerebroside is the major galactosphingolipid in myelin; and it has been shown that anti-galactocerebroside antibody is expressed by oligodendrocytes but not by OECs (Ranscht et al. 1982). Therefore it is possible to discriminate and purify OECs from the other cell types present in the olfactory bulbs by using FACS coupled with the O4 antibody and monoclonal antibodies to GalC (Barnett et al. 1993). The protocol followed to purify the OECs was a modification of that designed by Barnett and colleagues (1993) and is described below.

### *Dissection*

OECs were purified from the olfactory bulbs of post natal day 7 Fisher 344 rats. Rats were sacrificed with an overdose of Euthatal (sodium pentobarbital, 200 mg/ml, Vericore Ltd, UK) in accordance with UK Animals Scientific Procedures Act of 1986 under the restrictions and regulations of the schedule 1 killing method. Rats were placed on ice to maintain cell viability. The dissection was carried out on a polystyrene box top covered with tin foil. Using forceps and scissors the olfactory bulbs were exposed, excised and placed in a 7ml bijou tube containing 1-2ml of L15 and 25µg/ml gentamicin. Samples were then transported from the animal house to the tissue culture facility in the Beatson. From this step onwards all procedures were carried out in a vertical laminar flow bench with the use of sterile material.

### *Dissociation*

The sample containing the olfactory bulbs was maintained on ice as much as possible throughout the purification procedure in order to promote cell viability. Within 2 hours from dissection the olfactory bulbs were transferred to a 90mm Petri dish and all media removed with a Pasteur pipette. The tissue was dissociated by chopping it into small pieces using a scalpel, followed by enzymatic dissociation by placing the sample in a 7ml bijou tube containing 0.5ml of a 1.33% collagenase solution for 30 min at 37$^{o}$C. Subsequently 0.5ml of a mix (SD) of soya been trypsin inhibitor (0.52mg/ml) and DNAse1 (0.04mg/ml) were added mainly to prevent cell clumping from the DNA released from dead cells.

The sample was finally fully dissociated into a cell suspension using a syringe attached to needles of decreasing diameter: starting with a needle sized 18 gauge, switching to a needle sized 23 gauge and ending with a needle sized 26 gauge. It was vital during this second step of mechanical dissociation to be gentle and not to pull or push the syringe plunger too hard as this would have produced strong negative or positive pressures that would have had a detrimental effect on cell viability.

Subsequently the sample was transferred into a 15ml falcon centrifuge tube and washed in 4ml of Dulbecco's modified eagle medium (DMEM, Gibco, 21885) containing sorting media and centrifuged at 306m/sec$^2$, discarding the supernatant and leaving the pellet in a small volume of liquid. This allowed the pellet to be easily resuspended in the remaining solution by flicking the tip of the tube.

***Cell purification step***

The sample contained in the tube was gently resuspended in filtered primary antibodies and left 30 minutes on ice: the solution of primary antibodies was a mixture comprised of the O4 antibody (mouse monoclonal IgM, 1:4) and anti-galactocerebroside (mouse monoclonal IgG3, 1:2) antibodies, diluted in sorting media to a final volume of 2ml.

The excess of primary antibodies was removed by two washes and the sample was resuspended and incubated with a mix of secondary antibodies for 15 minutes on ice: goat anti-mouse IgM Phycoerythrin (1:100, Southern Biotech) and goat anti mouse IgG3 Fluorescein (1:100, Southern Biotech) or the inverse, diluted in sorting media to a final volume of 2ml. The excess of secondary antibodies was removed with 2 washes. The resulting cell sample was finally resuspended in 1ml of sorting media, filtered through a 40µm sieve and transferred to a FACS machine purification tube. The filtration process was necessary in order to remove cell clumps which would block the nozzle of the FACS machine.

A negative control to set up and standardise the FACS machine was a small aliquot of cells taken from the sample before incubation with the secondary

antibodies. Once the FACS machine settings were optimized the cells were separated as O4 positive and Galc negative cell population and collected in a new tube. The cells were centrifuged, the supernatant discarded and the sample centrifuged again for 1 second at 306m/sec$^2$ to get rid of the thin film of sorting media present on the tube inner side surface (as this can occasionally cause bacterial or fungal contamination). A Gilson pipette was inserted in the tube and the sample was transferred to a 12.5 cm$^2$ poly –L-lysine (PLL, 13μg/ml) coated flask. The flask was placed into a 37$^o$C incubator in a humidified atmosphere of 7% CO2 and 93% air. After 10 minutes, the time required for viable cells to adhere to the flask surface, the flask was topped up with cell culture media.

The FACS machine was fully operated by Thomas Gilbey and occasionally by Margaret O'Prey, two specialized technicians in the Beatson Institute.

All centrifuging steps in the 15ml falcon tubes involving OECs were carried out at g-force of 306m/sec$^2$ for a time that was determined by multiplying the sample volume (ml) by 30sec/ml.

***GFP lentiviral transduction***

One or two days after OEC purification, if cell numbers and viability looked good the cells would be transduced with a lentiviral vector expressing a gene that encodes the enhanced green fluorescent protein (EGFP, virus kindly donated by Dr George Smith, University of Kentucky, USA); which will be referred to as GFP for simplicity). The procedure was carried out in a category 2 hood and involved adding concentrated GFP lentivirus to the cultured cells and leaving for 1-2 days. This time allowed the GFP gene to become integrated into the nuclear DNA of a high proportion of cells. Media was then changed and the transduction efficacy was confirmed by placing the flask under an inverted UV microscope (Olympus, CKX41) with the appropriate filter set and counting the number of GFP expressing cells.

***OEC propagation***

After the GFP lentiviral transduction procedure, cells were passaged every 2-3 days once they reached confluency. To passage OECs the culture media was removed from the tissue culture flasks and washed with PBS. This step was

repeated once more and a PBS solution containing 0.025% trypsin was added, the flask placed in the incubator at 37°C and monitored under the phase microscope to confirm cell detachment. To stop the trypsin reaction a solution containing foetal bovine serum (DMEM-10% FBS) was added and the cells transferred to a centrifuge tube and placed on ice. At this point cells were often counted with a haemocytometer (Weber Scientific). Then the sample was centrifuged and the supernatant discarded; and the cells resuspended in cell culture media and diluted (1:2 or 1:3) into a new flask. The amount of media used to plate cells in the 12.5 $cm^2$ flasks, 25 $cm^2$ flasks and 75 $cm^2$ flasks was approximately 0.12ml/$cm^2$ of flasks surface area (3ml, 5ml, and 12ml respectively).

The daily growth rate of OECs calculated on 19 populations of OECs, each deriving from different animals and different purification dates, equalled 0.85 (StErr=0.06). This means that the number of OECs doubled on average every 57 hours.

The number of OECs per cultured surface area were calculated when the cells were fully confluent on cell populations from 19 independent olfactory bulb purifications: OEC density was of 21080 cells/$cm^2$ (StErr=1347 cells/$cm^2$).

***Long-term freezing of OECs in the liquid nitrogen***

During cell culture unpredictable and uncontrollable events could affect the growth of OECs: e.g. 7 day old rats were not necessarily available at the appropriate time, the cells plated after an olfactory bulb sort were not always viable, fungal or bacterial infections were unexpected and unwanted guests. These unpredictable events were incompatible with planning in advance for the surgical procedures in the knowledge that a source of cells could be available at any time. It proved to be more convenient and certainly more controllable to make the timing of cell purification independent from the timing of cell transplantation; this was possible by freezing a stock of purified GFP positive cells. After purification and GFP infection of OECs, once cells had reached a sufficient number, cells were frozen in liquid nitrogen to be retrieved and cultured when needed. It has been reported that no obvious differences in morphology or antigenic phenotype were found in cultured mouse OECs before and after storage in liquid nitrogen (Ramer et al. 2004a). Furthermore,

transplanted cryopreserved OECs from canine olfactory bulb were shown to retain their ability to myelinate demyelination axons in vivo (Smith et al. 2002).

***Cell freezing***

Cells were detached from the culture flasks with trypsin, DMEM-10% FBS was then added to inactivate trypsin and a cell count was made with a haemocytometer. Following centrifugation, the supernatant was discarded and cells were resuspended in freezing media that contained Dimethyl sulfoxide (DMSO) and aliquoted in cryotubes (this was completed as quickly as possible because DMSO is toxic to cells). Cryotubes were covered with cotton wool and placed in the -80$^{o}$C freezer for a few hours or up to a few days prior to storage in the liquid nitrogen freezer for an indefinite amount of time.

***Cell thawing***

Cells were normally thawed about a week before they were required for transplantation. A cryotube was collected from the liquid nitrogen and placed in a 37$^{o}$C water bath to thaw the cells quickly prior to centrifugation in a falcon centrifuge tube containing DMEM-10% FBS to dilute residue DMSO. Following centrifugation the supernatant was discarded and the cells were resuspended in culture medium and plated at the required confluency.

### 3.2.2.2 Cell preparation for transplantation

The phase contrast microscope was used to assess the general appearance and confluency of the cells and to check lack of bacterial or fungal infection. The FBS present in the media was removed from the flasks and a PBS solution containing trypsin added. The flasks were placed in the 37$^{o}$C incubator and monitored until cell detachment took place. The trypsin reaction was stopped by incubation in DMEM-10% FBS also containing approximately 2µg/ml DNAse: DNAse prevented the cells from forming clumps that would block the injection cannula during the transplantation process. The content of the flasks was transferred into a 15ml falcon centrifuge tube and placed on ice. After counting the cells with a haemocytometer the tubes were centrifuged and the supernatant discarded. A second but brief centrifugation was necessary to get rid of any medium present on the inner surface of the falcon tube and to avoid

contamination when inserting the Gilson to transfer the concentrated cells to a 0.2ml PCR sterile tube. The tube was placed inside a larger tube in ice, transported from the Beatson institute to the University main campus animal house. Before starting the transplantation, the tube containing the cells was centrifuged on a bench centrifuge to remove excess medium. The average density of the OECs at the time of transplantation was of 229322 cells/µl (StErr=10544 cells/µl). OECs were cultured for an average time of 29 days and passaged on average 8 times before being transplanted.

#### 3.2.2.3 Cell purity and GFP labelling

Cultured OECs possess a characteristic morphology when viewed under the phase contrast microscope giving an indication of cell type. However to check for purity we used the marker $P75^{NTR}$ that characterises OECs. OECs were seeded on PLL-coated cover slips for 2-3 days and then immunolabelled with antibody to P75 neurotrophin receptor ($P75^{NTR}$, hybridoma supernatant, 1:2, IgG1). Coverslips were incubated with the primary antibody diluted in DMEM for 15min at room temperature, rinsed in PBS and then incubated in the goat secondary class specific antibody diluted 1:100 (Southern Biotechnologies) for 15min at room temperature. Coverslips were rinsed in PBS and mounted in anti-fade containing DAPI (Vectashield, Vector Laboratories, Peterborough, UK) to identify nuclei. On a few occasions OECs were incubated with Thy1.1 to quantify fibroblast contamination. $P75^{NTR}$ expression was always detected on more than 98% of the cells in OECs cultures (Figure 3-1).

The presence of GFP expressing cells was determined on all cell populations before transplant by placing the tissue culture flask under a UV inverted microscope (Olympus, CKX41) and switching between the UV and the plain light source to confirm the expression of GFP in a reasonable proportion of cells. A more precise quantification was achieved on all cell populations that were transplanted by labelling the cells with a rabbit anti-GFP antibody (1:1000 AbCam). Cells were plated on PLL coated coverslips and fixed 2-3 days later with a solution of 4% paraformaldeyde; membranes were then permeabilised in a PBS 0.5% triton (Sigma) solution and non-specific antibody binding sites blocked with a PBS 0.2% porcine skin gelatine (Sigma) solution for 30 minutes. The GFP antibody was incubated with the cells for 30 minutes followed by donkey anti

rabbit or anti goat Alexa 488 secondary antibody incubation for 10 minutes (Molecular Probes). Primary and secondary antibodies were incubated in a PBS solution 0.1% Triton X-100 and 0.2% gelatine. Coverslips were mounted with DAPI containing Vectashield (Vector laboratories, Peterborough, UK) to visualize the nuclei. GFP expression varied between individual OEC cultures and was generally between 20% and 80%.

Images for both cell surface and intracellular staining were taken by fluorescence microscopy (Zeiss Axioplan2) coupled with ISIS software (MetaSystems). Colour levels were adjusted with Photoshop (Adobe) and cell counting was performed with the Cell Counter plug-in on ImageJ (NIH, USA).

#### 3.2.2.4 Cell culture materials

All cell culture formulations were filtered to reduce microbial contamination. Regular mycoplasma screening was performed to reduce the possibility mycoplasma infections.

***OECs Media***
OECs media is made up by adding to DMEM (see below): 5% FBS, 48% DMEM-BS media, 25 ng/ml fibroblast growth factor (PeproTech, 100-18b), 25ng/ml Heregulin (R&D systems, 396-HB) and 2.1µg/ml Forskolin (Sigma, F-6886).

***Bottenstein-Sato's Media (DMEM-BS)***
This media was composed of DMEM, 5ng/ml insulin (bovine pancreas, Sigma), 50ng/ml transferrin (Sigma), 0.022% SATO mix (see below) and 100mM glutamine (GIBCO, 25030) and was stored at $4^{o}C$.

***DMEM-10% FBS***
Made up of 90% DMEM and 10% foetal bovine serum (FBS).

***Sorting Media***
Made up of 99% DMEM and 1% FBS.

***DMEM***

Once Dulbecco's Modified Eagle Medium (Gibco, 21885) was opened 25µg/ml gentamicin (Gibco, 15750) was added to reduce risk of bacterial infections and stored at 4°C.

***Leibovitz's L-15 Medium (L15)***

Once Leibovitz's L-15 Medium (Gibco, 11415) was opened, 25ug/ml gentamicyn (Gibco, 15750) was added and stored at 4°C.

***Collagenase***

Collagenase was made up of L15 and 13.3mg/ml collagenase (MP Biomedicals, 195109) and stored at -20°C.

***Soya been trypsin inhibitor and DNAse (SD)***

Made up of L15, 3.0mg/ml bovine serum albumin (BSA) (Sigma A2153), 0.52mg/ml Soya been trypsin inhibitor (Sigma T-9003), 0.04mg/ml bovine pancreas DNAse (Sigma D-4263); storage at -20°C.

***Polylisine (PLL) coated flasks and coverslips***

PLL (Sigma, MW>80,000) was dissolved to a final concentration of 13.3µg/ml. 4 ml, 1 ml and 1 ml of this PLL solution were added to a 75 $cm^2$, a 25 $cm^2$ and a 12.5 $cm^2$ flask respectively, while 0.5ml was added to each well containing a 13mm diameter coverslip in a 24 multi-well plate. These were agitated to get PLL all over the surface. After incubation at 37°C for 30 min PLL was removed and washed away (as free PLL is toxic for cells) with sterile water. It is not necessary to completely dry the flasks or coverslips before plating the cells.

***Freezing media***

Made up of 50% FBS, 40% DMEM and 10% DMSO (Fisher Chemicals, D/4121/PB08) and stored at 4° C.

***O4, GalC and $p75^{NTR}$ hybridoma cell lines***

O4 and GalC monoclonal antibodies were produced from the O4 and the Galactocerebroside cell lines which were kindly donated by Professor Mark

Noble, University of Rochester. Hybridomas for the O4 antibody and Galactocerebroside and $P75^{NTR}$ antibodies were maintained in liquid nitrogen in 1ml cryotubes. Cryotubes were rapidly thawed in a 37°C water bath and transferred to a 15ml falcon centrifuge tube. 10ml of Optimem-50% FBS was added and the sample was centrifuged. The supernatant was discarded and the cells were resuspended in 5ml of Optimem-50% FBS and counted with a haemocytometer. Cells were plated in non-poly-lysine coated flasks at 30% of full confluency (full confluency is approximately $2x10^5$ cells/$cm^2$) in a final volume of approximately 0.25ml/$cm^2$ of Optimem-50% FBS. Two or three days later cells would be confluent and others formed floating clumps. The flasks were tapped strongly and any cell clumps dissociated using a pipette and then passaged. The cells in each flask were then transferred to new flasks and the volume of media adjusted to approximately 0.25ml/$cm^2$ of Optimem-10% FBS in order to gradually reduce the FBS concentration from 50% to 10%.

***Antibody production***

Following 2-3 more days in culture, cells were dissociated and transferred to a centrifuge tube. Following the centrifugation step the supernatant was discarded and cells were resuspended in Optimem-10% FBS and plated in new flasks. Three days later cells were dissociated and centrifuged. The supernatant was filtered, aliquoted and placed in the -20°C freezer for long storage. The titre of the hybridoma supernatant was tested on unpurified cultured olfactory bulb cells or on other CNS derived cultured cells.

An aliquot of the hybridoma was re-frozen for future use into cryotubes. Each cryotube, containing approximately $2.5x10^6$ hybridoma cells, was wrapped in cotton wool and placed in the -80°C freezer for a few hours or up to a few days and finally placed in liquid nitrogen for storage.

***Optimem-50% FBS***

Made up of 50% Optimem (Gibco 11415) with 25µg/ml gentamicin and 50% foetal bovine serum; stored at 4° C.

***Optimem-10% FBS***

Made up of 90% Optimem (Gibco 11415) with 25µg/ml gentamicin and 10% foetal bovine serum; stored at 4° C.

***SATO mix***

Made up of: 200 ml PBS + 5.72 ml BSA path-o-cyte 5 (Bovine albumin path-o-cyte, MP biomedicals 810111) mixed with 200 ml dH20 + 322 mg Putrescine (Sigma P7505), and with 20 ml ethanol + 8.0 mg thyroxine T4 (Sigma T-2501), and with 20 ml ethanol + 6.74 mg Tri-Iodo-Thyronine T3 (Sigma T-2752). Once the above solutions were combined, 2 ml of each of the following were added: 20 ml ethanol + 12.46 mg Progesterone (Sigma P-0130) and then 20 ml dH20 + 7.74 mg Selenium (Sigma S-1382). The resulting solution was filtered and stored at -20° C.

***Hybridoma freezing medium***

Made up of 90% FBS and 10% DMSO; stored at 4° C.

### 3.2.2.5 Pipettes for cell injection

To prepare pipettes with appropriate diameter tips for cell transplantation, glass capillary tubes (GC 100T-10, Harvard Apparatus Ltd, UK) were pulled using a vertical puller (Narishige PE-2, Narishige, Japan). The tip of pipette was cut by blunt micro-scissors to approximately 60-70µm internal diameter. After measuring the internal diameter under a microscope, the tip of the pipette was sharpened by using a beveller for approximately 5 minutes. And then, the tip was cleaned by blowing on it and by stroking it gently. The final internal and external diameters of the tip were measured and noted down. A permanent marker was used to mark gradations at 1.65mm apart from the neck of the pipette tip along the length of the pipette. These gradations approximated to a volume of 1µl and were used to keep tack of the volume of cells injected. Pipettes were securely stored in labelled glass containers and autoclaved before using.

#### 3.2.2.6 Cell preparation for transplantation

A phase contrast microscope was used to assess the general appearance and confluency of the cells and to exclude bacterial or fungal infection which would have unpredictable effects on the transplant outcome. The FBS present in the media was washed away from the flasks and a PBS solution containing trypsin was added. The flasks were placed in the 37$^{o}$C incubator and monitored until cell detachment took place. The trypsin reaction was blocked with a solution of 10%FBS also containing approximately 2µg/ml DNAse. The content of the flasks was transferred into 15ml falcon centrifuge tubes and placed on ice. After counting the cells with a haemocytometer the tubes were centrifuged and the supernatant discarded. A second but brief centrifugation was necessary to get rid of any medium present on the inner surface of the falcon tube and to avoid contamination when inserting the Gilson pipette tip to transfer the concentrated cells to a sterile PCR tube. The PCR tube was placed inside a larger tube in ice, transported from the Beatson institute to the main campus animal house and centrifuged again briefly on a bench centrifuge to get rid of any excess medium. The cell suspension was then carefully drawn into the pipette as required. Care was taken to avoid producing any air bubbles and/or damaging the tip of the pipette.

### *3.2.3 Lesioning*

All the dorsal column lesions and cell transplantations in this study were carried out by Dr. John Riddell.

The dorsal columns were lesioned bilaterally at the C4/C5 junction. The lesioning procedure used was the same as described in the methods section of chapter 2. Animals routinely received the peri-operative medication described previously in Chapter 2. OECs were transplanted into the animals immediately after lesioning.

### *3.2.4 Acute cell transplantation*

In order to test whether OECs are able to induce plasticity in sensorimotor pathways we aimed to transplant cells so that they were distributed within the

spinal cord above and below the lesion but not within the lesion site itself. Fortuitously, we found that following injection into a cervical dorsal column lesion, OECs spread caudally for more than 6mm along the dorsal columns but did not remain within the lesion cavity. Animals transplanted with cells in this way were therefore used to investigate the effect of OECs on the function of sensory afferents terminating in this region. Since the cells did not spread rostrally in significant numbers, to investigate the effect of OECs on the function of corticospinal fibres terminating in this region, OECs were injected rostral (above) of the lesion site.

#### 3.2.4.1 Transplantation of OECs into the lesion

A pipette with appropriate diameters loaded with cells, was mounted on a stereotactic manipulator, and then inserted into the lesion at an angle of 28$^{o}$ on each side through a slit in the dura with the tip pointing to the lesion centre and was lowered to a depth of approximately 1000μm. Cells were then injected until they overflowed out of the lesion, which required injection of up to 10μl of cell suspension into each lesion. The injection was performed by applying brief (40ms) pressure pulses (Picoinjector, WPI, Sarasota FL, USA) over the course of several minutes, during which the pipette was gradually raised to the surface. Three animals with OECs transplanted into the lesion were sacrificed at 3 weeks, 4 weeks, and 6 weeks to investigate the distribution of the transplanted cells at different time points.

#### 3.2.4.2 Transplantation of OECs above the lesion

A pipette loaded with cells was mounted on a stereotactic manipulator, and then vertically inserted into the cord approximately 250μm to the left of the midline through a slit in the dura and was lowered to a depth of approximately 1100μm. Approximately 1μl cells were then injected by applying brief (40ms) pressure pulses (Picoinjector, WPI, Sarasota FL, USA) over the course of several minutes, during which the pipette was gradually raised to a depth of approximately 750μm. The pipette was then slowly removed from the cord. OECs were injected into the cord between the lesion site and 4mm rostral of the lesion at a depth corresponding to the main component of the corticospinal tracts. Cells were injected at between 4 and 5 sites in order to produce a

relatively even distribution. Six animals with OECs transplanted above the lesion were sacrificed at different time points (1 day, 2 days, 1 week, 2 weeks, 3 weeks, and 4 weeks) to investigate the distribution of the transplanted cells.

#### 3.2.4.3 Medium injected above the lesion

As a control for the animals in which cells were injected above the lesion, a further group of animals were injected with the same medium as was used to suspend the cells. Injections were made of similar volumes and with a similar distribution as for the OECs.

A suture was placed in the dura over the lesion at a known location so that it could be identified at the later electrophysiological experiment and the segmental level could be confirmed at the end of the experiment. The wound was closed and analgesia, antibiotics and s.c. saline routinely administered as mentioned before. Animals recuperated in a warm environment in which easy access to food and water was provided. Animals were allowed to survive for approximately 3 months before electrophysiological assessment.

### *3.2.5 Electrophysiology*

#### 3.2.5.1 Anaesthesia

Animals were anaesthetised as described in Chapter 2 during the preparatory surgery and electrophysiological assessment.

#### 3.2.5.2 Preparatory surgery

The preparations for surgery and electrophysiological assessment were exactly the same as described in Chapter 2.

#### 3.2.5.3 Recordings of cord dorsum potentials

To assess spinal cord function in the region of the lesion and the effect of OEC transplants, CDPs evoked by electrical stimulation of the radial nerve and/or corticospinal tract were recorded. Recordings of CDPs were made while

stimulating either the radial nerve or within the pyramids at supramaximal stimulus intensity. The procedures for stimulation and recording were the same as described in chapter 2. Throughout the recording of CDPs, great care was taken to remove fluid from the surface of the cord to avoid inaccuracy of recordings.

All recordings of electrical potentials were digitised (Cambridge Electronic Design 1401+ interface, Cambridge, UK) and stored on a computer at a sampling rate of 20 kHz, without filtering. Averaging and measurements of the amplitudes of electrical potentials were performed using Signal software (Cambridge Electronic Design, Cambridge, UK).

#### 3.2.5.4 Conditioning of radial CDPs with pyramidal stimulation

As an additional way of assessing the function of the corticospinal projection below the level of a lesion we applied conditioning stimuli in the pyramids and looked at their effect on CDPs evoked by radial-nerve afferents below the level of the lesion. The detailed procedure was described in Chapter 2.

#### 3.2.5.5 Field potential recording

To assess possible changes in the areas of terminations of corticospinal fibres, systematic mapping of the field potentials evoked by pyramidal stimulation was performed in cervical segments above and below the dorsal column lesion.

The recordings were made using microelectrodes attached to a stepping motor which was mounted on a micromanipulator. In early experiments a carbon fibre electrode was used (Carbostar-1, tip size 5μm, impedance 0.5-2MΩ, Kation Scientific, USA) but this was found to be affected by the stimulus artefact leading to distortion of the early part of the record. We therefore changed to using glass microelectrodes (Tip size of 1-2μm; impedance 2MΩ) which were pulled from 1mm diameter filamented glass capillary tubing (GC 150TF-10, Harvard Apparatus LTD, UK) using a microelectrode puller (PE-2, Narishige, Japan), and then filled with 2M sodium chloride. The glass microelectrodes provided less distorted recordings than the carbon fibre electrodes. Recordings from both types of microelectrodes provided reliable information but the

recordings made using the carbon fibre electrodes required more careful interpretation.

Recordings of field potentials were made in normal animals and in lesioned animals both above and below the level of the lesion (Figure 3-2). For lesioned animals, recordings above the lesion were made at sites as close as possible to where the largest pyramidal-evoked CDPs had been recorded earlier in the experiment. This was generally from 2.5 mm to 4 mm above the level of the lesion. Recordings in normal animals were made within comparable locations. Recordings below the lesion were usually made within a few mm of the lesion where small pyramidal-evoked CDPs were often recordable. In lesioned animals where recordings were to be made below the lesion there was little to record. Therefore, before recording below the lesion, recordings were first made with the same electrode at a position above the lesion to make sure that the electrode and other equipment and settings were appropriate and everything was in working order.

The electrode was mounted with the tip pointing rostral 20 degrees in order to provide a clearer view of the spinal cord using the binocular microscope. Electrode tracks were then made using a vertical medio-lateral angle at regular intervals of 100 or 200μm to cover the full medio-lateral width of the grey matter (Figure 3-2B). Sometimes the spacing of the tracks had to be adjusted to avoid blood vessels. The first track was usually made at, or close to midline. Midline was identified by moving the electrode so that it was pointing directly to the left dorsal root entry zone and then the right dorsal root entry zone and noting the distance between them. This was then divided in two and this position taken as the midpoint.

A small opening was made in the pia using watch makers forceps through which the electrode could be inserted. At each track location, recordings were made at regular intervals of 100μm from the surface to at least 2.4mm deep. The manipulator was zeroed at the surface of the first track and this setting was then kept throughout all subsequent tracks. That is, the manipulator was not reset for surface at the top of each recording track. This was done in order that the depth would be aligned in all electrode tracks so forming a grid which could be used for subsequent reconstruction of the field potential maps (Figure 3-2B).

Recordings at each location were made while stimulating the pyramids with single shocks (0.2ms duration up, usually supramaximally). Between 25 and 50 sweeps were recorded and averaged at each position. Sometimes several recordings were made at the same position using different strengths of stimulation to obtain further information about the strength of pyramidal stimulation required to elicit the response. The recordings were made using an Axoprobe-1A microelectrode amplifier (Axon Instruments, UK). They were further amplified and filtered (NL824, Digitimer Ltd, UK). The signals were then digitised using a CED 1401 interface (Cambridge Electronic Design Ltd, UK) for off line analysis.

At the end of the experiment, empty glass microelectrodes were inserted into the spinal cord to mark the position at which field potentials were recorded. The electrodes were mounted on the stepping motor and driven into the spinal cord at a known position relative to the electrode tracks. The blank electrodes were cut and left in the cord and their position noted. The positions of these marking electrodes were determined histologically and used to align the map of the field potential recordings with the outline of the grey matter at the recording level.

#### 3.2.5.6 Perfusion

Most of the animals were transcardically perfused at the end of the electrophysiological experiment for histology as described in chapter 2.

### *3.2.6 Histological processing*

#### 3.2.6.1 Histological processing of spinal cord for lesion and cell distribution

Animals receiving transplants of OECs the sections were cut sagittaly in order to preserve information about the distribution of OECs in the rostro-caudal axis. Three 4mm blocks were prepared carefully from each animal: rostral block (from 6mm to 2mm above lesion), lesion block (from 2mm above lesion to 2mm below lesion), and caudal block (from 2mm to 6mm below lesion). A rostro-ventral notch was made on each block. Blocks were cut into 70μm parasagittal sections on a freezing microtome, washed in phosphate buffered saline 0.3M (PBS double salt), and then incubated for 30min in 50% ethanol. After washing 3 times for 10

minutes each in PBS sections were treated with fluorescence histochemestry techniques. 72h incubation of sections with anti-NF200 (1:1000 Sigma), anti-GFP (1:1000) and anti-GFAP (1:1000 Sigma) primary antibodies at 4°C which label respectively the axons, the OECs, and the astrocytes (lesion boundaries) was followed by secondary antibodies of appropriate species conjugated to fluorophores (Alexa 488 1:500, Cy5 1:100, Rodamine 1:100) (2 hrs at room temperature or overnight at 4°C). After washing 3 times for 10 minutes in PBS, sections were mounted on plain glass slides in anti-fade medium (Vectashield; Vector Laboratories, UK), and coverslipped and the edges of the coverslip sealed with nail varnish and then stored at –20°C.

#### 3.2.6.2 Histological processing of brainstem for stimulation sites

Brainstem tissue containing the stimulating electrode tracks were carefully processed as described in chapter 2. Slides were stored at -20°C.

#### 3.2.6.3 Histological processing of spinal cord for field potential recording sites

After washing in 0.1MPB, the marking electrodes or recording sites were identified. Blocks containing the marking electrodes or encompassing the recording sites were carefully prepared to avoid damaging the electrode tracks if present. A notch was made at the ventral aspect of the cord on the right corner. Sections were cut transversely (approximately parallel with marking electrode if present in order to reconstruct a clear electrode track) at 70µm using a freezing microtome (Ernst Leitz Wetzlar, Germany). Sections were mounted on plain glass slides in Vectashield mounting medium, coverslipped and the edges of the coverslip sealed with nail varnish, and then stored at -20°C.

### *3.2.7 Microscopy*

#### 3.2.7.1 Reconstruction of stimulation sites in the Pyramids

Sections containing the stimulating electrode tracks were reviewed under microscopy (Zeiss Axioplan 2 Imaging), and the stimulating electrode tracks were reconstructed by using Camera lucida drawings as described in chapter 2.

#### 3.2.7.2 Verification of dorsal column lesion

Sections containing the lesion cavity were observed using phase contrast light microscopy to determine the perimeter of the cavity and the relationship to the boundaries between grey and white matter as described in chapter 2.

#### 3.2.7.3 Quantification of lesion size

The length of the lesion cavity was measured as described in chapter 2.

#### 3.2.7.4 Distribution of OECs

Sections from animals transplanted with OECs were examined using epifluorescence microscopy (Nikon Eclipse E600) to confirm the survival of the transplanted cells and to document their distribution. Confocal microscope images of sagittal sections through dorsal column lesions and cell transplants were taken to illustrate the distribution of transplanted cells.

#### 3.2.7.5 Reconstruction of field potential recording sites

Sections containing tracks left by the marking electrodes or, if the marking electrode was not located, sections from close to the recording sites were reviewed by microscopy with a dark field condenser, and then photographed using a digital camera (4X objective Axiocam Zeiss, Germany). 4 photos were taken if necessary to show the whole field view of the section, and then montaged using Adobe Photoshop CS2 software. Each montaged image of the section from the recording site was then traced using a graphics tablet (Wacom pen tablet, Japan) to outline the section and grey and white matter border together with the position of the electrode track if present.

### *3.2.8 Off-line analysis of electrophysiology*

#### 3.2.8.1 Off-line analysis of CDPs

CDP recordings were inspected and analysed by using Signal software as described in chapter 2. The data was noted in excel spreadsheets then imported to Prism 4 software (GraphPad Software Inc, USA) to create potential plots.

#### 3.2.8.2 Off-line analysis of CDP conditioning

Averaged records were inspected and analysed offline using Signal software as described in chapter 2.

#### 3.2.8.3 Off-line analysis of field potentials

Averaged records were inspected offline using Signal software. The amplitudes of field potentials at each location were measured by using Signal software. The measurement of field potential of each location was noted in excel spreadsheets, and then imported to 3D field software to create potential plots.

An outline of the section from field potential recording site and isopotential plots were both imported into a graphics program (Coreldraw version 12; Corel USA) and properly scaled (adjusted to matching scale). No adjustment was made for shrinkage of tissue after perfusing. The Isopotential plot was then accurately overlaid on the outline of the spinal cord using information about the electrode surface, midline, and visible marking electrode tracks.

### *3.2.9 Statistical analysis*

The following statistical tests were carried out on the electrophysiological data (GraphPad Software Inc, USA). Analysis of variance (ANOVA), the Dunnett Post-hoc test, and Student’s t-test were used to reveal the differences among different groups.

## 3.3 Results

### *3.3.1 Distribution of OECs in cervical spinal cord*

OECs were transplanted into the cervical spinal cord using two methods: by injecting into the lesion cavity made by the wire knife or by injecting directly into the spinal cord above the lesion. A cavity surrounded by an area of spinal cord tissue containing reactive astrocytes (labelling densely for GFAP) developed at the wire knife lesion site as described in chapter 2.

Figure 3-3 shows examples of confocal images obtained from three representative animals of the group which received transplants of cells into the lesion cavity. Very few cells remained within the lesion cavity apart from a few distributed around the rim. However, there was an extensive distribution of cells caudal to the lesion in the form of a continuous track occupying the ventral half of the dorsal columns and medial most aspects of the dorsal horns. The cells were extended for at least 6mm below the lesion and therefore provided a convenient region within which to test sensory pathways using radial nerve afferents. Relatively few cells were observed rostral to the lesion in these animals.

Figure 3-4 shows examples of confocal images obtained from three animals which received OEC transplants made at separate injection sites spanning from 0.5 to 5mm above the lesion. Labelled cells were observed throughout the dorsal columns and medial most aspects of the dorsal horn but were less dense than the caudally distributed cells in animals with cells injected into the lesion cavity. However, a lower proportion of the cells injected into these animals expressed GFP so that the precise distribution and density of cells is also more difficult to judge than in the lesion transplanted animals.

### *3.3.2 Spinal cord function assessed by electrophysiology*

CDPs evoked by stimulating the corticospinal tract and/or radial nerve were used to assess function in the cervical spinal cord as in the previous chapter. Recordings were made from animals with OECs transplanted into the lesion site

(n=16), OECs transplanted into the cord above the lesion site (n=14), and medium injected into the cord above the lesion site (n=12). Recordings from normal animals (n=24) and animals in the three month survival lesioned group (n=18) presented in chapter 2 are also referred to for comparison.

#### 3.3.2.1 Cord dorsum potentials evoked by pyramidal stimulation

Potentials evoked by pyramidal stimulation were recorded with a silver ball electrode positioned on the dorsal columns at 1mm intervals from 8mm rostral to 8mm caudal to the C4/5 segmental border as described in chapter 2.

***OEC below group***

CDPs evoked by stimulation in the pyramidal tract were investigated in 10 lesioned animals three months after OECs were transplanted into the lesion site resulting in caudally distributed cells. Examples of CDPs recorded from two representative animals of this group are shown in Figure 3-5 and the distribution of averaged CDPs in all animals of this group is shown in Figure 3-6. In the OEC below group, CDPs recorded both above and below the lesion were similar to those in three month survival animals which were lesioned but did not receive any treatment. At some locations above the lesion, CDPs had a tendency to be larger than in the 3 month animals. CDPs above the lesion were significantly larger than those recorded in normal animals, as in the 3 month survival animals (Table 3-1).

***Medium above group***

CDPs evoked by stimulation in the pyramidal tract were investigated in 10 lesioned animals three months after medium was injected into the cord above the lesion site. Examples of CDPs recorded from two representative animals of this group are shown in Figure 3-7 and the distribution of averaged CDPs in all animals of this group is shown in Figure 3-8. CDPs recorded both above and below the lesion were similar in amplitude to those recorded in the 3 month survival dorsal column lesioned animals and did not differ significantly at any location. Like the 3 month animals, CDPs recorded above the lesion were significantly larger than those recorded in normal animals.

***OEC above group***

CDPs evoked by stimulation in the pyramidal tract were investigated in 14 lesioned animals three months after OECs were transplanted into the cord above the lesion site. Examples of CDPs recorded from two representative animals of this group are shown in Figure 3-9 and the distribution of averaged CDPs in all animals of this group is shown in Figure 3-8. CDPs recorded both above and below the lesion did not differ significantly from those recorded from animals injected with medium above the lesion or 3 month dorsal column lesioned animals (Table 3-1). There was some tendency for potentials recorded in the OEC above group to be slightly smaller between +2 and +4mm where the cells were injected, but this was not significant.

#### 3.3.2.2 Cord dorsum potentials evoked by radial nerve stimulation

Potentials evoked by radial nerve stimulation were recorded with a silver ball electrode positioned on the dorsal columns at 1mm intervals from 8mm rostral to 8mm caudal to the C4/5 segmental border as described in chapter 2.

***OEC below group***

CDPs evoked by radial nerve stimulation were investigated in 16 lesioned animals three months after OECs were transplanted into the lesion site leading to subsequent spread of the cells up to 6mm caudal to the lesion. Examples of CDPs recorded from two representative animals of this group are shown in Figure 3-11 and the distribution of averaged CDPs in all animals of this group is shown in Figure 3-10. CDPs recorded in this group were almost identical to those recorded in the three month survival animals which received dorsal column lesions only. CDPs recorded above the lesion were still very small while CDPs recorded below the lesion were significantly larger than those recorded in normal animals from -4mm to -8mm (Table 3-2).

***Medium above group***

CDPs evoked by radial nerve stimulation were investigated in 12 lesioned animals three months after medium injected into the cord above the lesion site. Examples of CDPs recorded from two representative animals of this group are shown in Figure 3-12 and the distribution of averaged CDPs in all animals of this

group is shown in Figure 3-13. CDPs recorded in the animals with medium injected rostral of the lesion site were almost identical to those in three month survival animals which were not transplanted.

***OEC above group***

CDPs evoked by radial nerve stimulation were investigated in 13 lesioned animals three months after OECs were transplanted into the cord above the lesion site. Examples of CDPs recorded from two representative animals of this group are shown in Figure 3-14 and the distribution of averaged CDPs in all animals of this group is shown in Figure 3-13. The CDPs recorded from this group were broadly similar to those of the 3 month survival dorsal column lesioned animals and those injected with medium above the lesion. However, the difference between the CDPs recorded below the lesion and those recorded from normal animals was less marked and failed to reach significance between -2 and -6mm.

### 3.3.2.3 Field potentials

Extracellular field potentials recorded within the spinal grey matter are negative potentials that reflect current flow at synapses between afferent systems and spinal cord neurones. They therefore reflect the same process as CDPs except that by recording at different locations in the grey matter information can be obtained about the spatial distribution of the synapses generating the fields. In order to assess the possible changes in the areas of termination of the corticospinal fibres, field potentials evoked by pyramidal stimulation were recorded above and below the C4/5 border in normal animals and above and below the lesion site in lesioned animals.

***Normal animals***

Recordings of field potentials evoked by pyramidal stimulation were made from 4 normal animals, all at a position 4mm above the C4/5 border. Examples of field potential recordings from a normal animal are shown in Figure 3-15. The field potentials were recorded 4mm rostral of the C4/5 border. Small negative field potentials usually appeared close to the surface and were usually distinct by 0.2mm. The biggest negative fields were observed at the medial edge of the deep dorsal horn at a depth of 1.0-1.2mm. At some locations, an afferent volley

could be detected before the onset of the field potential. The peak amplitudes were around 0.6mV-1.1mV. The field potentials started to reverse and become positive at a depth of about 1.4-1.5mm.

### *Dorsal column lesioned animals*

Recordings of field potentials evoked by pyramidal stimulation were made from 17 animals with dorsal column lesions; three 1 week survival animal, six 3 month survival animals, four animals with medium injected above the lesion, and four animals with OECs injected above the lesion. Recordings were made above the lesion in 8 animals and from below the lesion in 9 animals.

For recordings above the lesion the field potentials were recorded as close as possible to the location where the largest pyramidal-evoked CDPs were recorded, which was generally from 2.5mm to 4mm above the lesion site. Examples of field potential recordings made 3.5mm above the lesion in one of these animals are shown in Figure 3-16. The distributions of the fields in lesioned animals were broadly similar to that seen in normal animals. There was considerable variation in the shape, area, and size of the isopotential plots obtained from different animals in both normal and lesioned groups so that it was considered difficult to safely interpret this data.

Field potentials below the level of the lesion were often absent or very small. The fields were only large enough and common enough in two animals to allow full mapping and construction of an isopotential plot. Examples of field potential recordings made 3mm below the lesion from one of these animals is shown in Figure 3-17. Attempts to record field potentials below the lesion often failed to disclose any action at the locations sampled or resulted in very occasional recordings. Some of the potentials recorded below the lesion were located in more lateral and ventral parts of the grey matter and sometimes required stimulus intensities at the upper end of the range activating corticospinal fibres. They were also often shorter in latency than corticospinal evoked activity should be indicated that a small amount of spread to reticulospinal fibres had occurred.

### *3.3.3 Lesion size*

The appropriate locations of the dorsal column lesion (i.e. C4/5 segmental border) were confirmed in all the lesioned animals included in this study. The lesions made by the wire knife approach were consistent and accurate across and within groups of animals.

Examples of sections containing lesion cavities from different animal groups are presented in Figure 3-18. The wire knife lesion interrupted the full width of the dorsal columns. The lesion site of the transplanted animal groups appeared similar to that of three months survival animals. The lesion cavities were developed rostro-caudally and occupied the dorsal columns and varying amounts of grey matter.

Table 3-3 shows the quantitative comparison of the lengths of the lesion cavities in the lesioned animal groups: three month survival group, OEC below group, OEC above group, and medium above group. The ranges of the lengths of the cavities in all the groups vary. The means of the lengths of the cavity are similar among the groups.

## 3.4 Discussion

### *Cell transplants*

Previous studies from this lab using OECs have shown that when transplanted into lumbar level wire knife lesions of the dorsal columns the cells survive well within the lesion site and to a large extent fill the lesion cavity (Toft et al. 2007). When we attempted to make perform similar transplants (as described in Toft et al. 2007) into wire knife lesions at the cervical level the cells rarely remained within the lesion site in any significant numbers. The reason for this technical failure is not clear but may be related to a greater flow of cerebrospinal fluid from the cervical level lesions or to the greater movement that occurs at the cervical compared to lumbar region when the animals recover and become mobile again. Despite the absence of cells in the lesion cavity itself, inspection of blocks of spinal cord taken from below the lesion site showed that in nearly every case there was an extensive caudally directed distribution of the cells and that these cells remained 3 months after transplantation. The cells were so numerous that they formed a continuous column spread through out the ventral half of the dorsal columns and most lateral aspects of the dorsal horn. Earlier studies of olfactory ensheathing cell transplants suggested that these cells have migratory properties and that these were an important aspect of their ability to support extended axonal regeneration (Ramon-Cueto and Nieto-Sampedro, 1994; Li et al. 1997; 1998; Ramon-Cueto et al. 1998, 2000). However, at least in the case of wire knife lesions, it is likely that much of the spread of cells occurs as an artifact of the lesioning and injecting technique at the time of transplantation. In a detailed study by Lu et al. (2006), OECs and other cell types were transplanted both within the lesion and at nearby sites and the distribution of the cells studied at different time points by detection of GFP expressed in the transplanted cells. Extensive movement of the cells was seen within hours of the injections suggesting that most of the dispersion was explained by passive spread from the injection site, possibly along tears in the neuropil created by the lifting action of the wire knife.

Spread of cells from the injection lesion site rarely occurred in the rostral direction. For this reason cells were directly injected into the spinal cord above

the lesion. The cells spread from the injection sites with time so that this process also resulted in continuously distributed cells extending from the lesion to 4 or 5mm more rostral. However, the cells were less densely distributed than below the lesion where the distribution occurred by “natural” processes.

### *Lack of electrophysiological evidence for sprouting*

The rationale of the experiments reported in this chapter was to test whether enhancement of corticospinal and radial nerve-evoked actions matched the distribution of transplanted cells. That is, if the presence of OECs within the spinal cord adjacent to the lesion induced sprouting of ascending and descending pathways, then in animals with cells distributed above the lesion, CDPs evoked by corticospinal fibres above the lesion should be larger in lesioned controls. Similarly if the presence of OECs distributed below the lesion induced plasticity in sensory afferents, the CDPs evoked by the radial nerve should be larger below the lesion than in lesioned controls. However, in each case the actual results observed showed that the presence of OECs had little detectable effect on the amplitude of CDPs evoked by either ascending or descending fibre pathways. The electrophysiological evidence therefore suggests that OECs do not induce sprouting of either corticospinal or sensory afferent terminals after dorsal column lesions.

### *Sensitivity of electrophysiological recording for detecting plasticity*

This negative finding is not likely to be due to a lack of sensitivity of the electrophysiological assessment because it was shown in the previous chapter that changes in the amplitude of CDPs can be detected in response to lesioning and these involve not just detection of the direct interruption of ascending and descending fibres by axotomy but also the more subtle changes in function that occur in the intact proximal sections of the axotomised axons where collateral arbours form connections with spinal cord neurones. Furthermore, it will be shown in the next chapter that the same electrophysiological assessment procedures can detect changes in function induced by administration of antibodies that block myelin inhibitory proteins. It therefore seems reasonable

to presume that if OECs induced plasticity then this would have been detected using the electrophysiological methods adopted here.

### *Are the cells optimally located?*

Little is known about the extent to which OECs directly stimulate axonal growth or the mechanisms by which they do so. OECs promote neurite outgrowth from DRG neurones in culture. They have also been shown to support axonal regeneration of various fibre types in the spinal cord (Richter and Roskams, 2007). However, it is not clear from the *in vivo* experiments to what extent OECs actively promote axonal regeneration and to what extent they simply provide a growth supportive substrate. It has even been suggested that Schwann cells infiltrating the transplant may be responsible for most of the growth promoting effects (Lu et al. 2006). Nor is there much known about the mechanisms that are involved in any growth promoting effects that OECs might have. One possibility is that soluble factors are released by the transplanted cells (Au et al. 2007) and that these induce collateral sprouting. Signalling by this mechanism could potentially occur at some distance. Another possibility is that some form of contact signalling occurs either between OECs and the regenerating growth cones of axotomised fibres near the lesion site or by contact of parent fibres or their axon collaterals. In ongoing anatomical studies of OEC transplants in the lab, an association between transplanted cells and regenerating fibres is sometimes seen but is rather infrequent.

The distribution of the transplanted cells was assessed by microscopical examination of GFP labelled cells. In the spinal cord caudal to the lesion the cells were thickly distributed so that a continuous column of cells filled the dorsal columns and the adjacent lateral most aspect of the dorsal horn. These cells are well placed for inducing plasticity in radial afferent fibres by the release of soluble factors since they are close to the parent fibres in the dorsal columns and also adjacent to their termination site in the dorsal horn. However, they are arguably less well placed for any contact mediated actions since some radial afferents may be more dorsally located in the dorsal columns and the cells are not in the main area targeted by axon collaterals. The distribution of cells above the lesion was similarly targeted on the dorsal columns and adjacent

lateral white matter. In this case the cells are well placed in close proximity to the corticospinal fibres and their local axon collaterals. Sprouting of radial fibres above the lesion was not expected since few if any fibres are spared by the dorsal column lesion. Sprouting of corticospinal fibres below the lesion was also not expected because few if any of the main dorsal column fibres are spared by the dorsal column lesion and the transplanted cells are not in an appropriate location to interact with the minor components which project in the lateral and ventral funiculi (Casale et al. 1988; Rouiller et al. 1991; Brosamle and Schwab 1997).

### *Comparison with previous evidence for sprouting*

There has been only one previous direct investigation of the potential of OEC transplants to produce sprouting. Chuah et al. (2004) made lesions of the main dorsal column component of the corticospinal tract into which they then transplanted OECs. Examination of the density of tract-traced corticospinal fibre collateral branches below the level of the lesion revealed more in transplanted animals than in non-transplanted controls. Chuah et al attributed this to sprouting of the minor corticospinal components projecting through the ventral white matter. However, these observations would be equally consistent with a neuroprotective action of the OECs since the number of collateral branches in transplanted animals did not exceed that in normal animals. In this study we did not examine plasticity in spared fibres as in the Chuah et al. (2004) study. Instead we investigated whether OECs would induce sprouting in fibres that had been axotomised. The rationale for this was that axotomised fibres might be better primed for plasticity and that the actions of intact fibres would be easier to assess functionally than the much smaller populations of spared fibres. OECs have been reported to support regeneration of both corticospinal (Li et al. 1997; 1998) fibres and dorsal column fibres (Toft et al. 2007). To the extent that similar mechanisms may be involved in axonal regeneration and in sprouting, both fibres types are therefore suited to the study.

Several potential therapies for spinal cord injury, although originally devised with the intention of removing inhibitory influences on regenerating axons and so stimulating axonal regeneration, also appear to induce plasticity and may in

fact produce most of their functional effects by this mechanism (Bradbury and McMahon, 2006). However, the fact that OECs support regeneration of axotomised fibres within a transplant but do not promote sprouting of the undamaged collaterals of the same fibres is not necessarily a surprise. It is possible that entirely different signalling mechanisms are involved. It is also possible that OEC transplants *in vivo* have very little direct influence on the regeneration of axons and that rather than stimulating axonal regeneration they are mainly passive providers of a growth permissive scaffold. The regeneration of axotomised branches is driven by growth programmes and expression of various growth associated proteins (Bouquet and Nothias, 2007) so that these mechanisms alone may be sufficient to drive regeneration when OECs provide appropriate conditions within the lesion. In support of this possibility, ongoing work in the lab has shown that substantial axonal regeneration occurs in transplants of many different cells types in addition to OECs, including fibroblasts which are not considered to have specific axonal outgrowth promoting properties (Riddell, Barnett, Toft unpublished).

## *Does the injection process or presence of OECs have any detrimental effect?*

As a control for the possibility that the injection process itself might cause some damage to the spinal cord, a group of animals was injected with medium above the lesion and corticospinally-evoked CDPs assessed. When compared to lesioned animals without any injections above the lesion, CDPs from the medium injected animals were entirely comparable, suggesting that the injection process itself does not have any detrimental effect on the spinal cord. When corticospinally-evoked CDPs recorded in animals injected with OECs above the lesion were compared with the lesion only animals CDPs from the two animals were again very similar though there was a tendency towards smaller CDPs in the region (0 to +4mm) where OECs were injected. This suggests that OEC transplants may be associated with a very modest disruption of function and since the injection of medium alone had no effect, the cells themselves may be responsible. It is possible that damage simply results from the physical process of accommodating the volume (¾ to 1µl) of the cells within the normal spinal cord tissue where there is no natural space to accommodate them. It is known that the cells

themselves readily mingle with astrocytes and induce minimal astrocytic hypertrophy (Santos-Silva et al. 2007).

## *Significance of findings in relation to previous electrophysiological observations on OEC transplanted animals*

In previous work from the lab (Toft et al. 2007) OECs were transplanted into a lumbar dorsal column lesion similar to the cervical lesions used here. However, in this study the cells were shown to remain within the lesion cavity and to limit the usual expansion of the cavity which is seen with time. Electrophysiological assessment showed that this was associated with an enhancement of the CDPs evoked by sensory afferents in the region of the injury. It was suggested that this might be explained by OECs promoting sprouting of afferent fibres or neuroprotection of afferent fibre collaterals. The current results do not support the idea that OECs promote sprouting of damaged fibre systems and the explanation for the enhanced CDPs seen in the previous study therefore more likely involves neuroprotection. OEC transplants may reduce the die back of dorsal column axons and therefore preserve more of the local axon collaterals which branch profusely to provide connections with spinal cord neurones. Preservation of these connections is probably the main explanation for the larger potentials in OEC transplanted animals.

**Table 3-1 Statistical analysis of the differences between pyramidal-evoked CDPs recorded in different animal groups at each recording location**

ANOVA with post-hoc Dunnett's test was first applied and where a significant difference was found the P value threshold is given. Where no significance was detected with ANOVA, Student's t-test was used and where a significant difference was detected the P-value is given. Comparison where no significance was detected with either test is indicated by NS.

| | Normal | Normal | Normal | 3month | 3month | 3month | OEC above |
|---|---|---|---|---|---|---|---|
| | OEC below | OEC above | Medium | OEC below | OEC above | Medium | Medium |
| +8 | P=0.034 | P=0.0306 | P=0.003 | NS | NS | NS | NS |
| +7 | NS | NS | P=0.0131 | NS | NS | NS | NS |
| +6 | P=0.0366 | P=0.0083 | P=0.0006 | NS | NS | NS | NS |
| +5 | P<0.01 | P=0.0407 | P<0.05 | NS | NS | NS | NS |
| +4 | P<0.01 | NS | P<0.05 | NS | NS | NS | NS |
| +3 | P<0.05 | NS | P=0.0275 | NS | NS | NS | NS |
| +2 | P=0.0406 | NS | NS | NS | NS | NS | NS |
| +1 | NS | P<0.01 | P<0.01 | NS | NS | NS | NS |
| 0 | P<0.01 | P<0.01 | P<0.01 | NS | NS | NS | NS |
| -1 | P<0.01 | P<0.01 | P<0.01 | NS | NS | NS | NS |
| -2 | P<0.01 | P<0.01 | P<0.01 | NS | NS | NS | NS |
| -3 | P<0.01 | P<0.01 | P<0.01 | NS | NS | NS | NS |
| -4 | P<0.01 | P<0.01 | P<0.01 | NS | NS | NS | NS |
| -5 | P<0.01 | P<0.01 | P<0.01 | NS | NS | NS | NS |
| -6 | P<0.01 | P<0.01 | P<0.01 | NS | NS | NS | NS |
| -7 | P<0.01 | P<0.01 | P<0.01 | NS | NS | NS | NS |
| -8 | P<0.01 | P<0.01 | P<0.01 | NS | NS | NS | NS |

**Table 3-2 Statistical analysis of the differences between radial nerve-evoked CDPs recorded in different animal groups at each recording location**

ANOVA with post-hoc Dunnett's test was first applied and where a significant difference was found the P value threshold is given. Where no significance was detected with ANOVA, Student's t-test was used and where a significant difference was detected the P-value is given. Comparison where no significance was detected with either test is indicated by NS.

| | Normal OEC below | Normal OEC above | Normal Medium | 3month OEC below | 3month OEC above | 3month Medium | OEC above Medium |
|---|---|---|---|---|---|---|---|
| +8 | P<0.01 | P<0.01 | P<0.01 | NS | NS | NS | NS |
| +7 | P<0.01 | P<0.01 | P<0.01 | NS | NS | NS | NS |
| +6 | P<0.01 | P<0.01 | P<0.01 | NS | NS | NS | NS |
| +5 | P<0.01 | P<0.01 | P<0.01 | NS | NS | NS | NS |
| +4 | P<0.01 | P<0.01 | P<0.01 | NS | NS | NS | NS |
| +3 | P<0.01 | P<0.01 | P<0.01 | NS | NS | NS | NS |
| +2 | P<0.01 | P<0.01 | P<0.01 | NS | NS | NS | NS |
| +1 | P<0.01 | P<0.01 | P<0.01 | NS | NS | NS | NS |
| 0 | P<0.01 | P<0.01 | P<0.01 | NS | NS | NS | NS |
| -1 | P<0.01 | P<0.01 | P<0.01 | NS | NS | NS | NS |
| -2 | P<0.01 | NS | NS | NS | NS | NS | NS |
| -3 | NS | NS | NS | NS | NS | NS | NS |
| -4 | P=0.0296 | NS | NS | NS | NS | NS | NS |
| -5 | P<0.05 | NS | P<0.05 | NS | NS | NS | NS |
| -6 | P<0.01 | NS | P<0.01 | NS | NS | NS | NS |
| -7 | P<0.01 | P=0.0315 | P<0.05 | NS | NS | NS | NS |
| -8 | P<0.05 | P=0.022 | P<0.01 | NS | NS | NS | NS |

**Table 3-3 Quantification of lesion cavity size in different groups**

The lengths of the cavities in lesioned groups were assessed and compared (see methods) using Students' t-test which showed no significant difference in mean cavity length among the groups.

| | 3 month group (n=15) | OEC below group (n=18) | OEC above group (n=16) | Medium above group (n=12) |
|---|---|---|---|---|
| Length of cavity (Range) | 1260-3920µm | 1750-3360µm | 1050-3360 µm | 1820-2800µm |
| Length of cavity (Mean) | 2511µm | 2423µm | 2389µm | 2293µm |

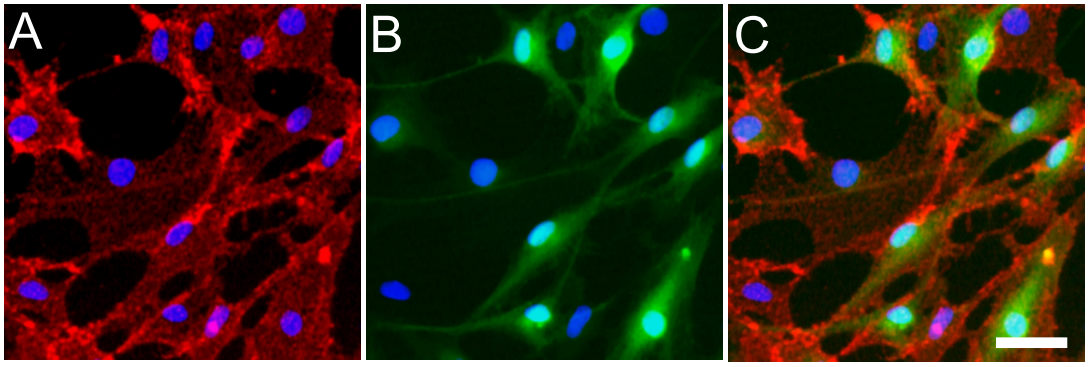


**Figure 3-1 18-day OECs in culture**
P75 (red, A), GFP (green, B) and merge (C). Blue is DAPI. Scale bar = 50μm.

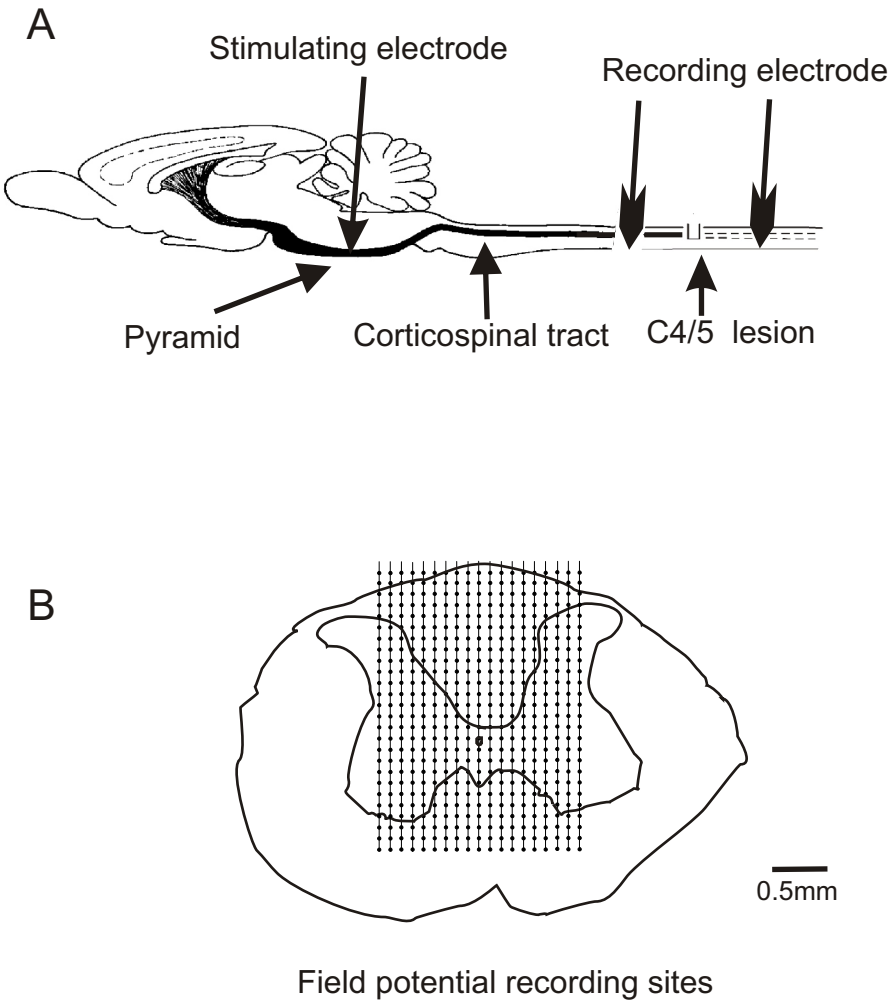


**Figure 3-2 Experimental setup for field potential recording**
Schematic diagram of experimental preparation show location of lesion and of stimulating and recording electrodes for assessing corticospinally-evoked field potentials. A, the dorsal columns were lesioned bilaterally at the C4/C5 junction which interrupts the main component of the corticospinal tract which runs in the ventral aspect of the dorsal columns. A stimulating electrode was inserted in the medullary pyramid dorsally and a micro-electrode was inserted into the spinal cord at locations above and below the C4/5. B, recordings were made at regular intervals of 100 or 200μm medio-laterally up to 900μm and normally 100μm intervals ventrodorsally from the surface to at least 2.4mm deep. In the transverse view of the spinal cord, dots represent recording sites.

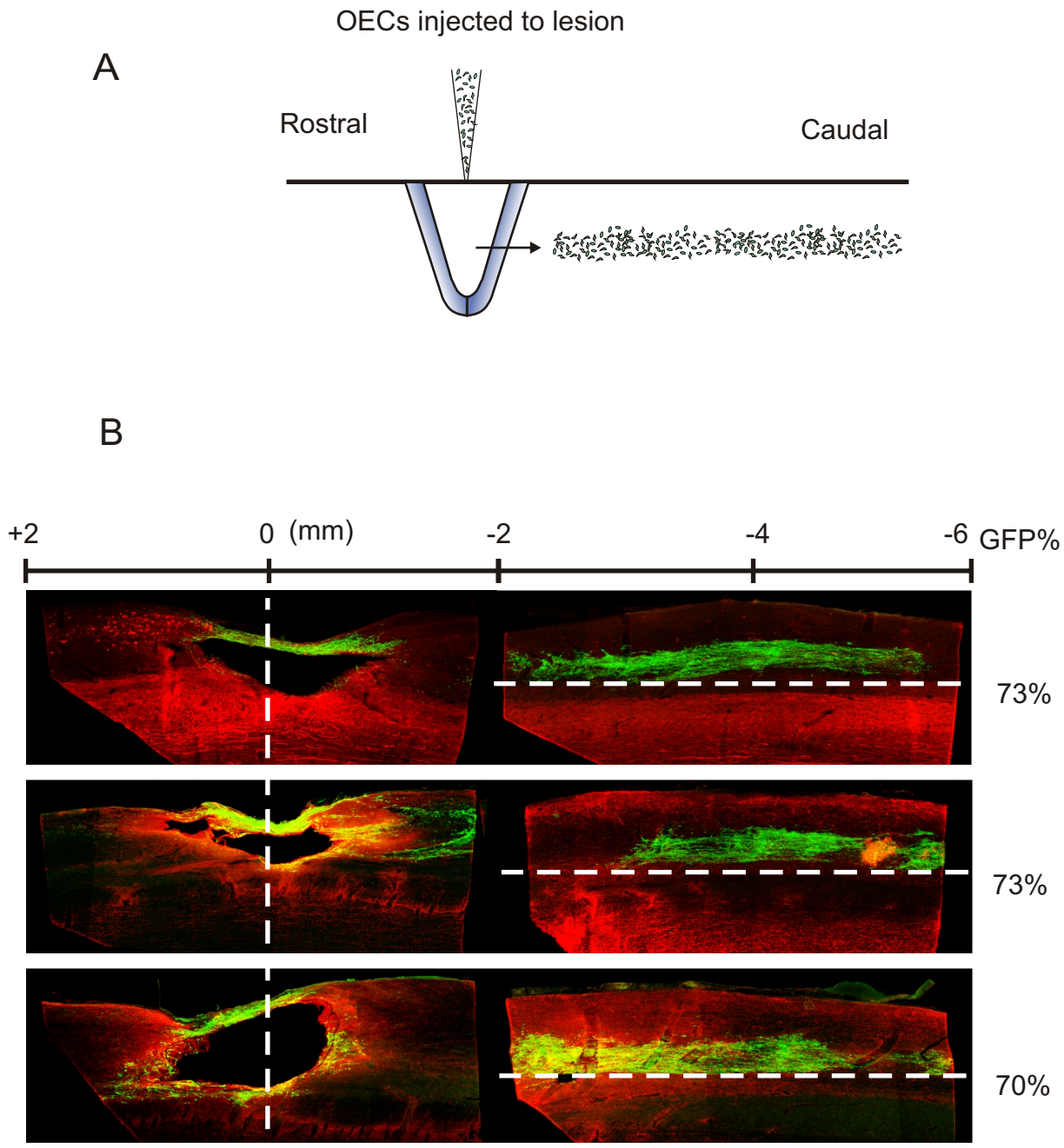


**Figure 3-3 Distribution of OECs 3 months after injections into the dorsal column lesion site**

A, schematic diagram of distribution of cells following injection into a dorsal column lesion. Few cells remained in the lesion cavity but a continous track of cells had formed in the dorsal column extending caudal from the injection site for 6mm; B, confocal images from three transplanted animals showing the lesion cavity largely devoid of cells and the extensive distribution of OECs (green) from 2mm above the lesion to 6mm below the lesion. The percentage of transplant cells that were GFP positive is indicated to the right.

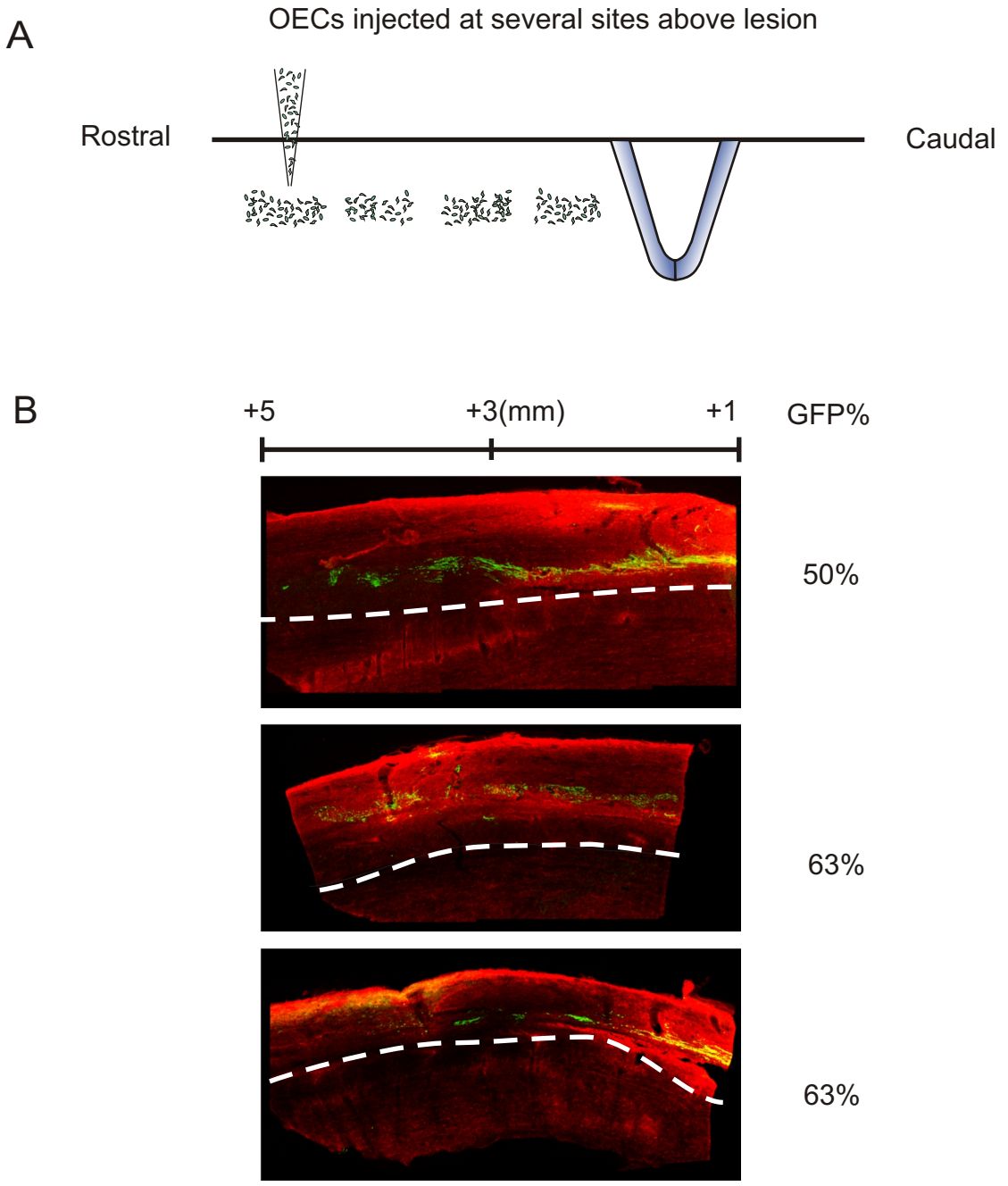


**Figure 3-4 Distribution of OECs 3 months after injections above the lesion site**
A, schematic diagram of the distribution of cells following injection above the lesion. The cells were transplanted in the cord at a depth corresponding to the corticospinal pathway at between 4 and 5 sites between the lesion and 4mm more rostrally. They were observed rostrally for more than 5mm along the dorsal columns; B, confocal images from three transplanted animals showing the distribution of OECs (green) from 1mm to 5mm above the lesion. The percentage of transplant cells that were GFP positive is indicated to the right.

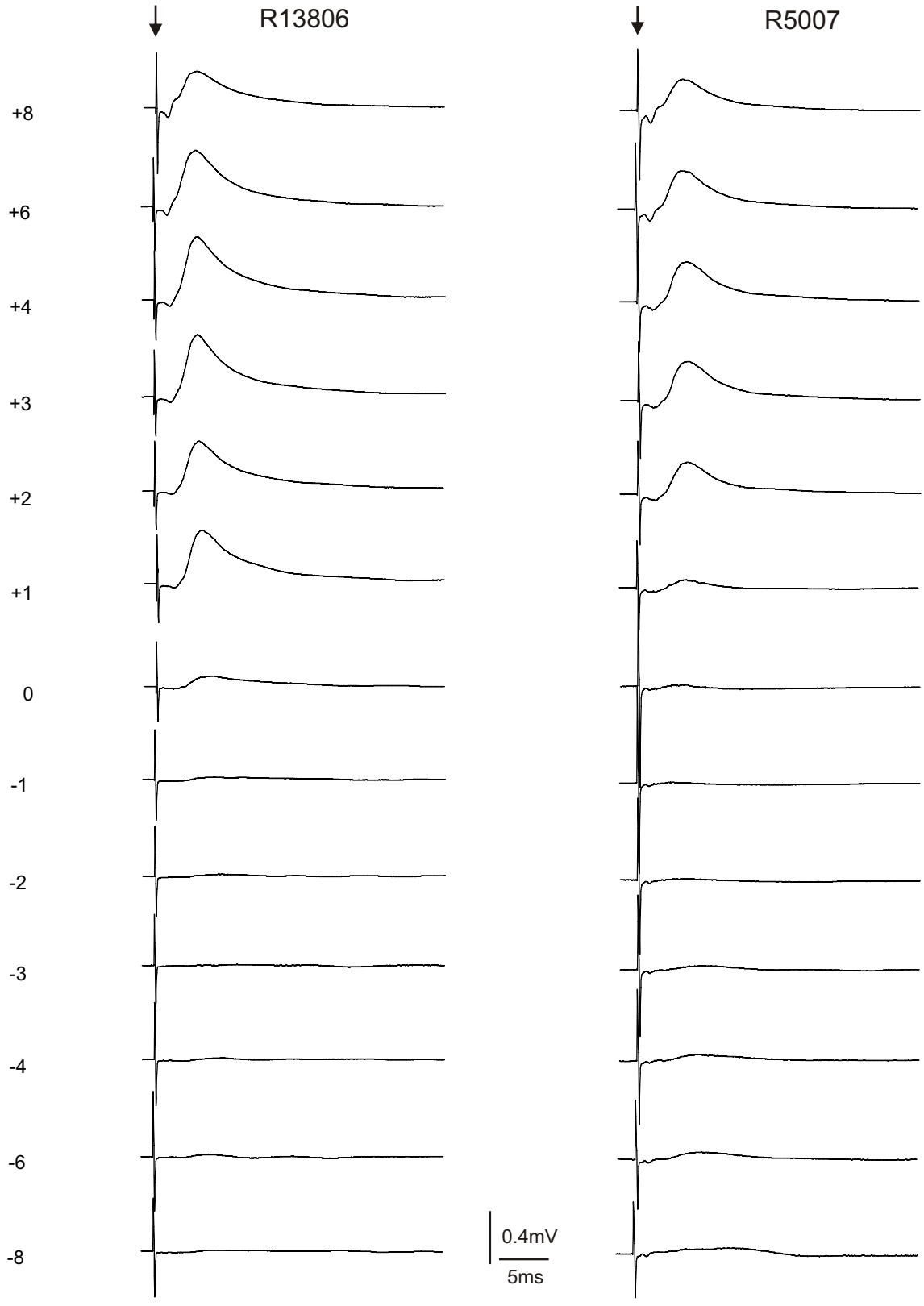


**Figure 3-5 Examples of CDPs evoked by pyramidal stimulation in the OEC below group**

Each column of traces shows recordings made from one animal. The recordings were made at 1mm intervals from 8mm rostral to 8mm caudal to the lesion level (C4/5 border) as indicated. Traces recorded at +7, +5, -5, and -7mm are omitted. The traces represent averages of 50 sweeps and the calibrations apply to all traces. The arrows indicate stimulus artifacts.

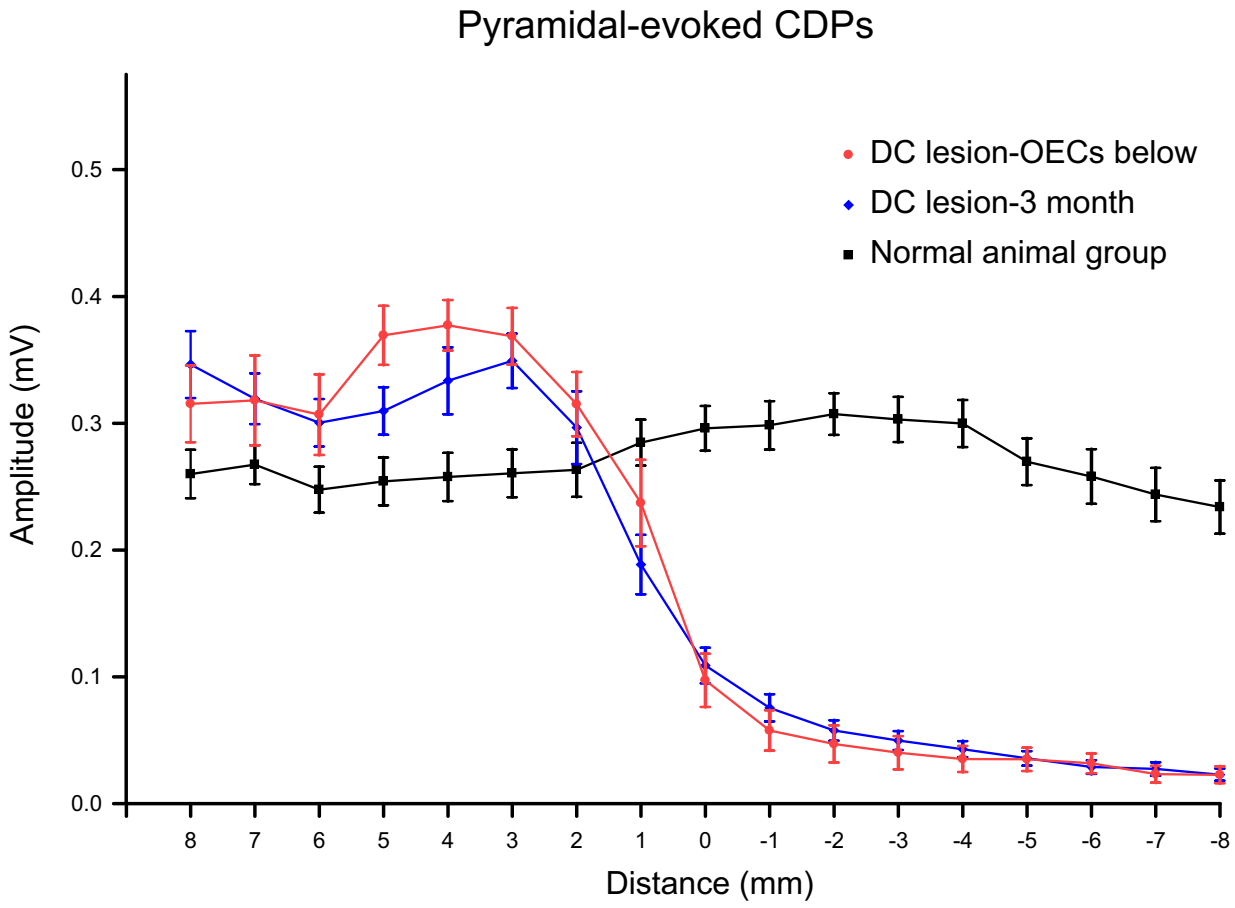


**Figure 3-6 Amplitudes of pyramidal-evoked CDPs recorded in the OEC below group**
The plot shows the distributions of the amplitudes of CDPs recorded from the OEC below group (n=10). The previous plots for the normal group and for the three month survival group are also shown for comparison. CDP amplitudes are averaged for all animals in each group, each data point showing mean +/- SEM. The recordings were made over the cervical spinal cord. Recording positions are shown relative to the C4/5 border (0 mm) where dorsal column lesions were made. CDPs recorded in the OEC below group were similar to those in three month survival animals both above and below the lesion. There is an increasing tendency from the lesion site to 5mm rostral of the lesion, but not statistically different from those recorded in the three month survival group.

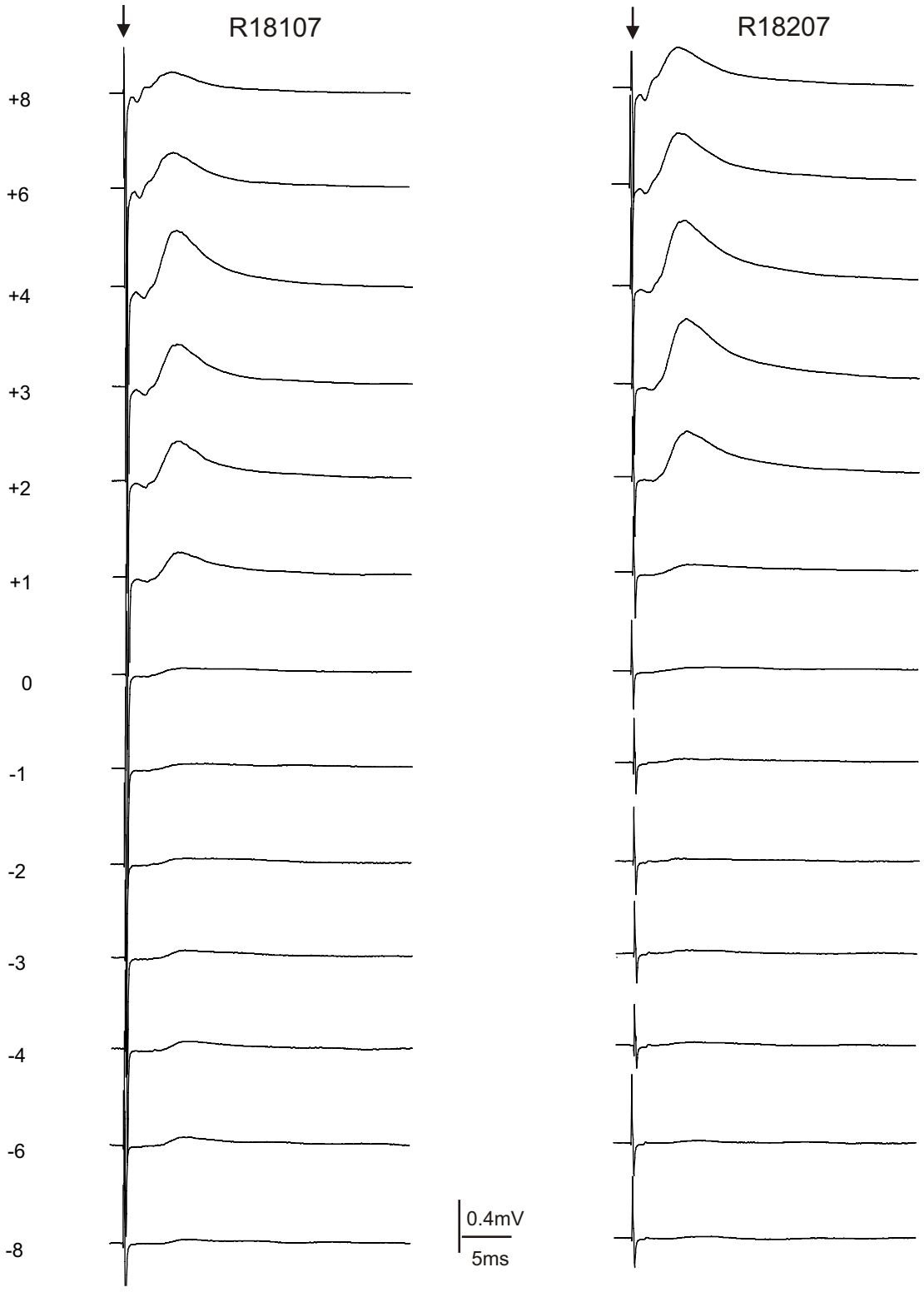


**Figure 3-7 Examples of CDPs evoked by pyramidal stimulation in the medium above group**

Each column of traces shows recordings made from one animal. The recordings were made at 1mm intervals from 8mm rostral to 8mm caudal to the lesion level (C4/5 border) as indicated. Traces recorded at +7, +5, -5, and -7mm are omitted. The traces represent averages of 50 sweeps and the calibrations apply to all traces. The arrows indicate stimulus artifacts.

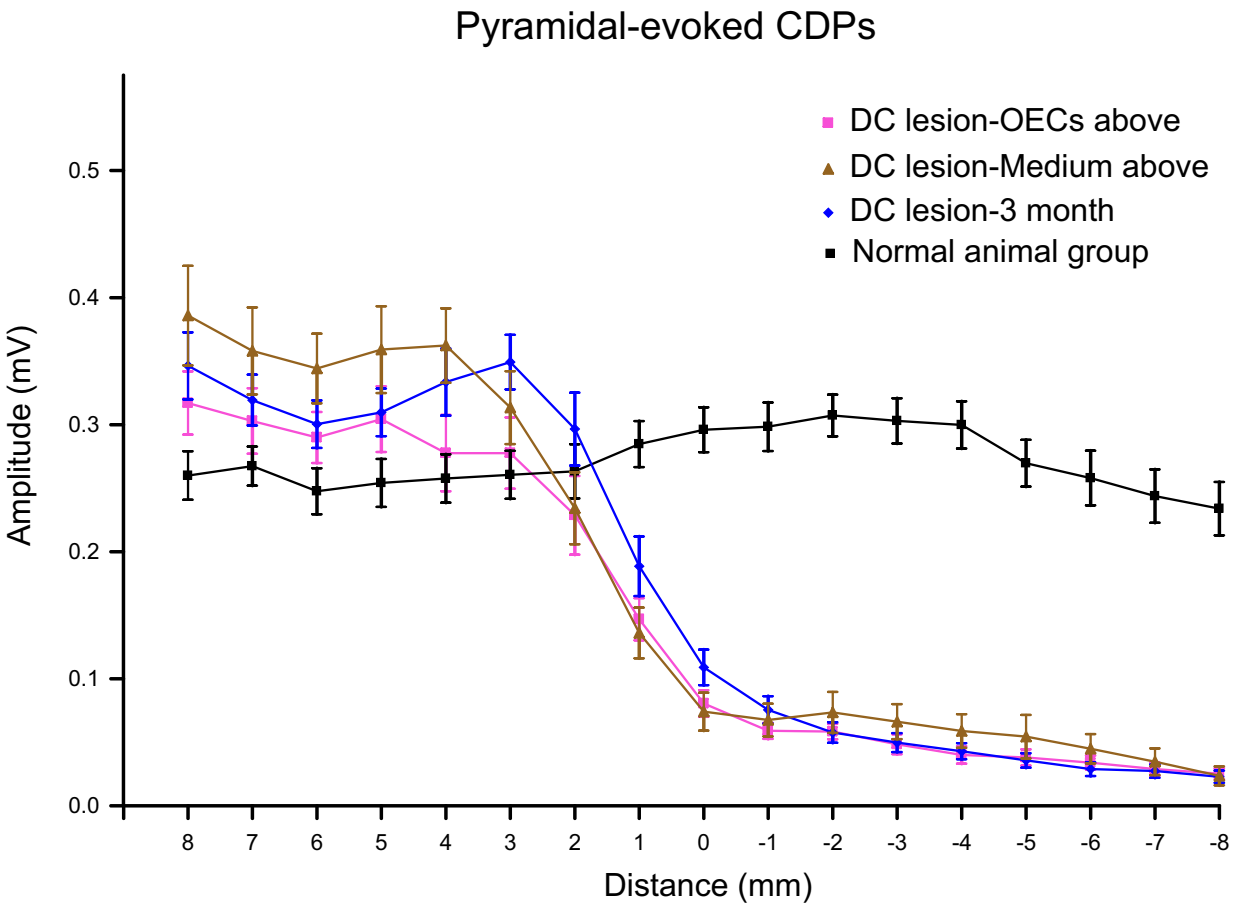


**Figure 3-8 Amplitudes of pyramidal-evoked CDPs recorded in the medium above and OEC above groups**

Plots show the amplitudes of CDPs recorded over the cervical spinal cord in response to pyramidal stimulation in the medium above (n=10) and OEC above (n=14) groups. The previous plots for the normal group and for the three month survival group are also shown for comparison. CDP amplitudes are averaged for all animals in each group, each data point showing mean +/- SEM. Recording positions are shown relative to the C4/5 border (0 mm) where dorsal column lesions were made. In the medium above group, CDPs below the lesion were larger than those recorded in three month survival lesioned animals but not significantly different. Compared to CDPs in the medium above group, CDPs recorded around the lesion were similar. Above the lesion, CDPs were smaller than those recorded in the medium above group but not significantly different.

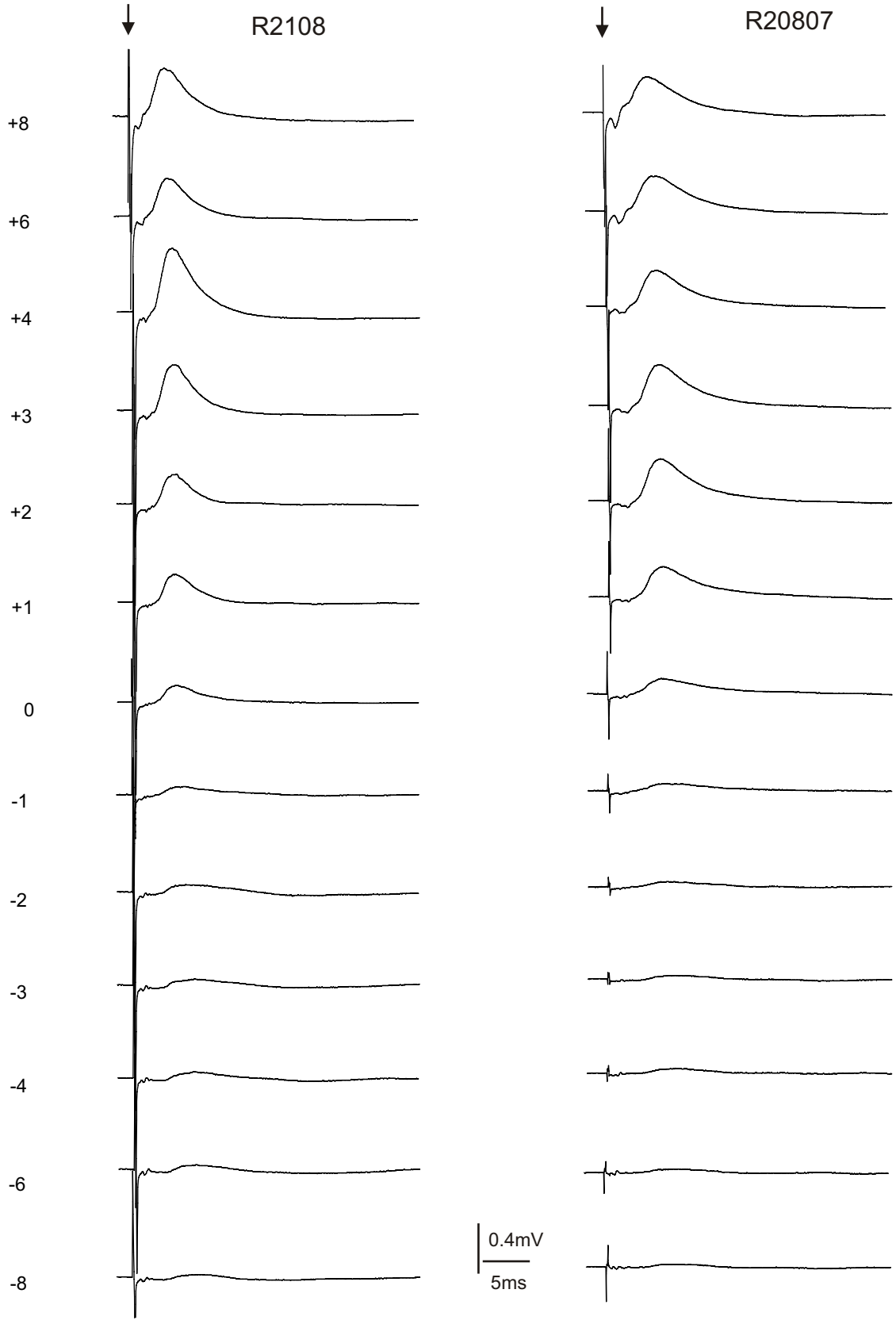


**Figure 3-9 Examples of CDPs evoked by pyramidal stimulation in the OEC above group**

Each column of traces shows recordings made from one animal. The recordings were made at 1mm intervals from 8mm rostral to 8mm caudal to the lesion level (C4/5 border) as indicated. Traces recorded at +7, +5, -5, and -7mm are omitted. The traces represent averages of 50 sweeps and the calibrations apply to all traces. The arrows indicate stimulus artifacts.

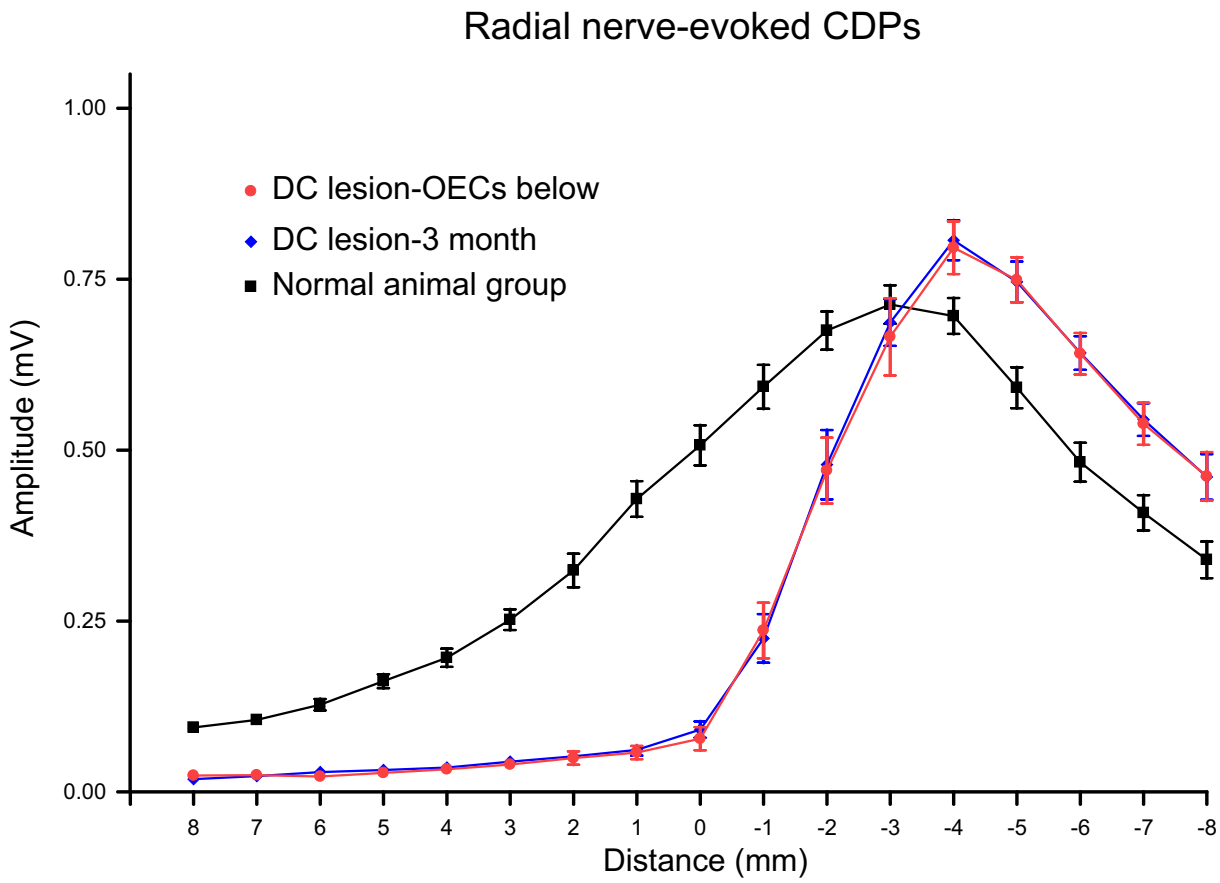


**Figure 3-10 Amplitudes of radial nerve-evoked CDPs recorded in the OEC below group**

The plot shows the amplitudes of CDPs recorded over the cervical spinal cord in response to radial nerve stimulation in the OEC below group (n=16). The previous plots for the normal group and for the three month survival group are also shown for comparison. CDP amplitudes are averaged for all animals in each group, each data point showing mean +/- SEM. Recording positions are shown relative to the C4/5 border (0 mm) where dorsal column lesions were made. CDPs recorded in the OEC below group were almost identical with those recorded in three month survival lesioned animals. CDPs recorded below the lesion were significantly larger than those recorded in normal animals from -4mm to -8mm.

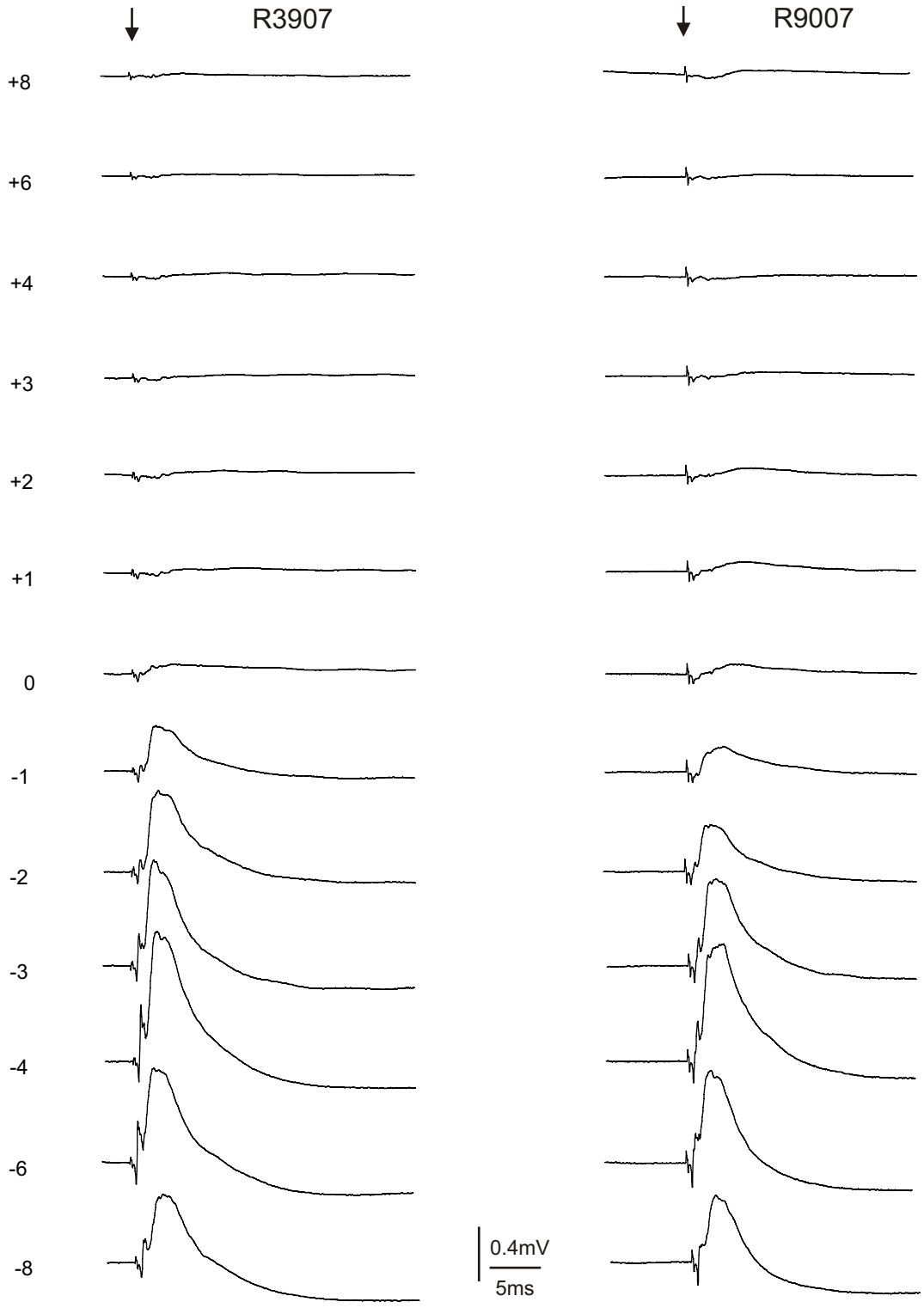


**Figure 3-11 Examples of CDPs evoked by radial nerve stimulation in the OEC below group**

Each column of traces shows recordings made from one animal. The recordings were made at 1mm intervals from 8mm rostral to 8mm caudal to the lesion level (C4/5 border) as indicated. Traces recorded at +7, +5, -5, and -7mm are omitted. The traces represent averages of 25 sweeps and the calibrations apply to all traces. The arrows indicate stimulus artifacts.

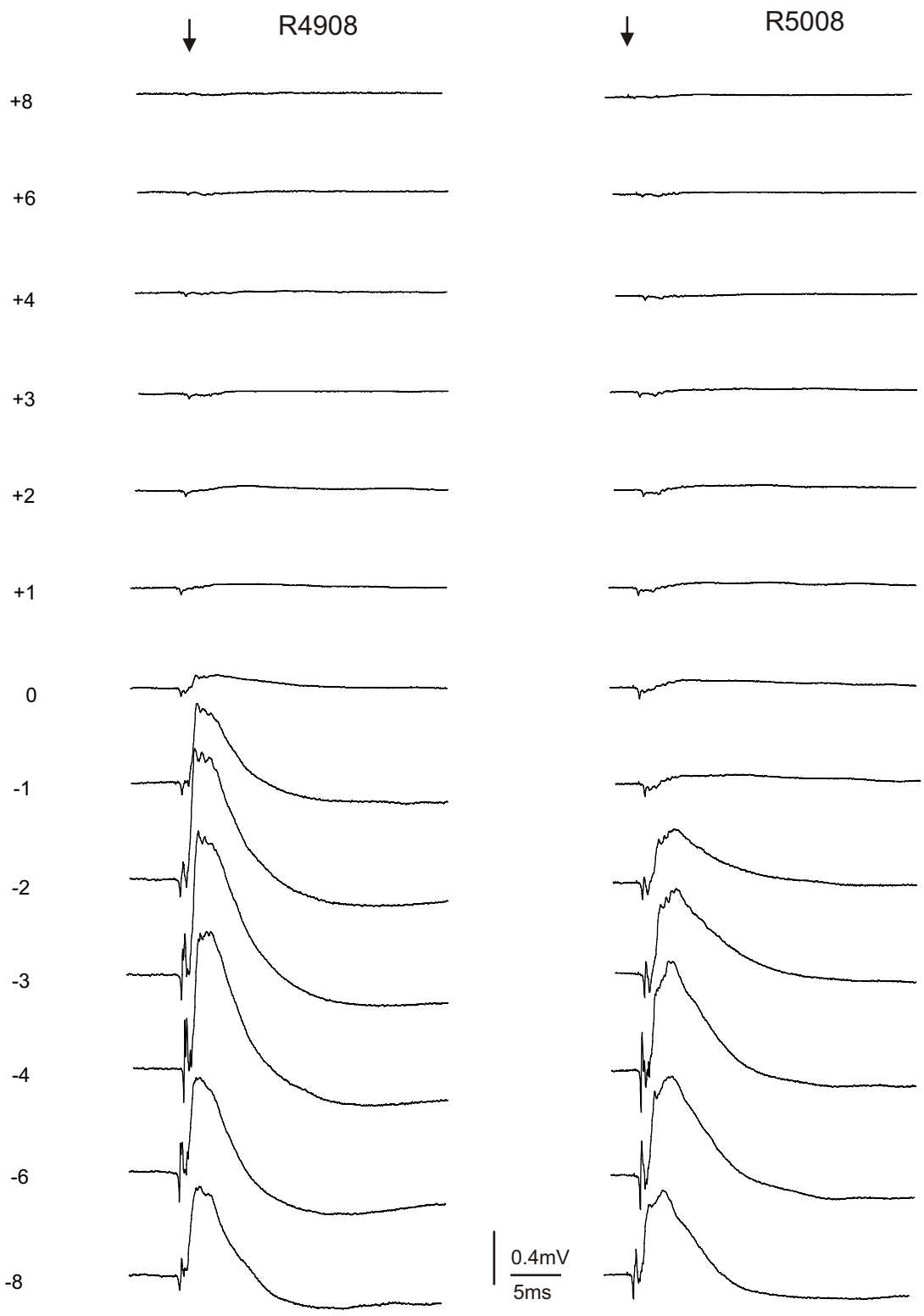


**Figure 3-12 Examples of CDPs evoked by radial nerve stimulation in the medium above group**

Each column of traces shows recordings made from one animal. The recordings were made at 1mm intervals from 8mm rostral to 8mm caudal to the lesion level (C4/5 border) as indicated. Traces recorded at +7, +5, -5, and -7mm are omitted. The traces represent averages of 25 sweeps and the calibrations apply to all traces. The arrows indicate stimulus artifacts.

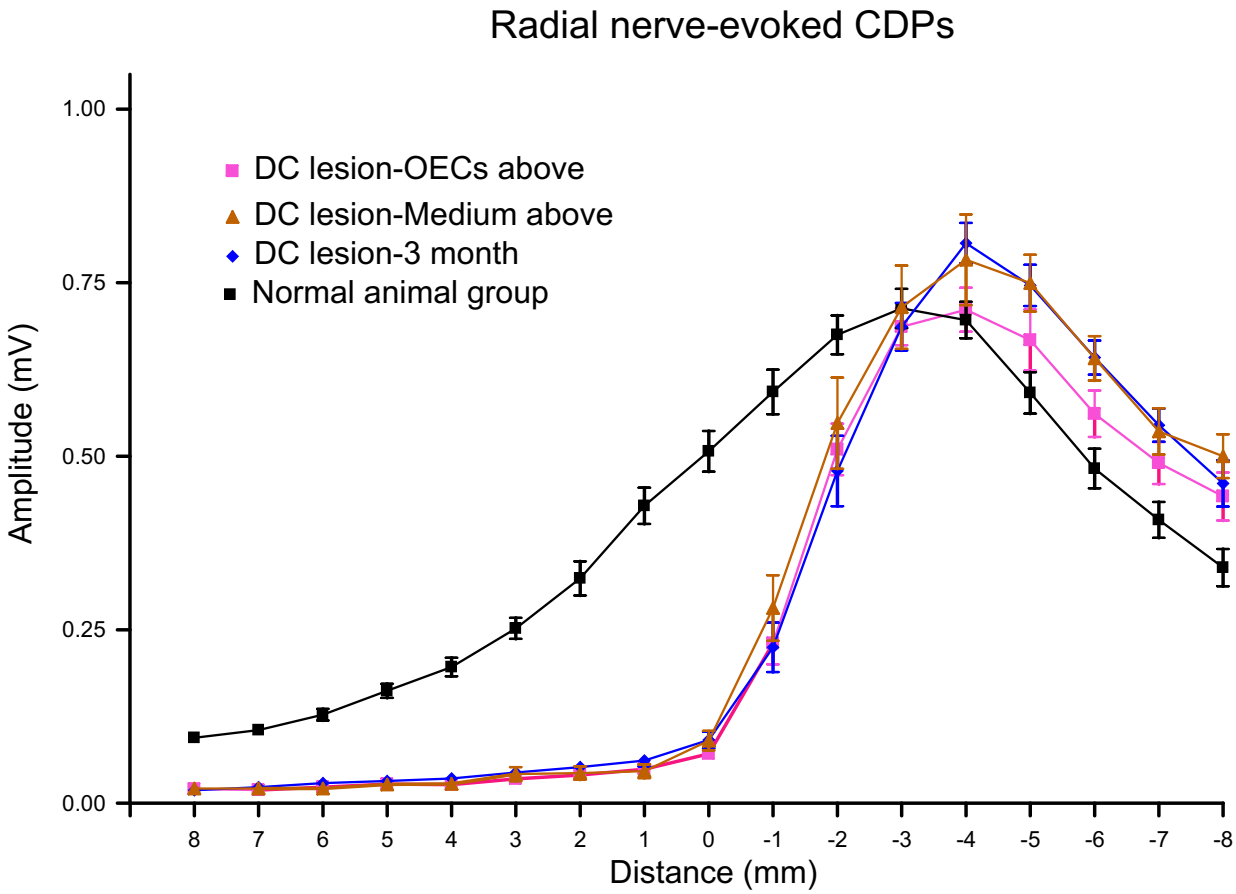


**Figure 3-13 Amplitudes of radial nerve-evoked CDPs recorded in the medium above and OEC above groups**

Plots show the amplitudes of CDPs recorded over the cervical spinal cord in response to radial nerve stimulation in the medium above (n=12) and OEC above (n=13) groups. The previous plots for the normal group and for the three month survival group are also shown for comparison. CDP amplitudes are averaged for all animals in each group, each data point showing mean +/- SEM. Recording positions are shown relative to the C4/5 border (0 mm) where dorsal column lesions were made. CDPs in the medium above group were almost identical to those in the three month group. In the OEC above group, CDPs recorded from 8mm to -3mm were similar to those recorded in the 3 month survival group. CDPs from -4mm to -8mm were smaller but not significantlly different.

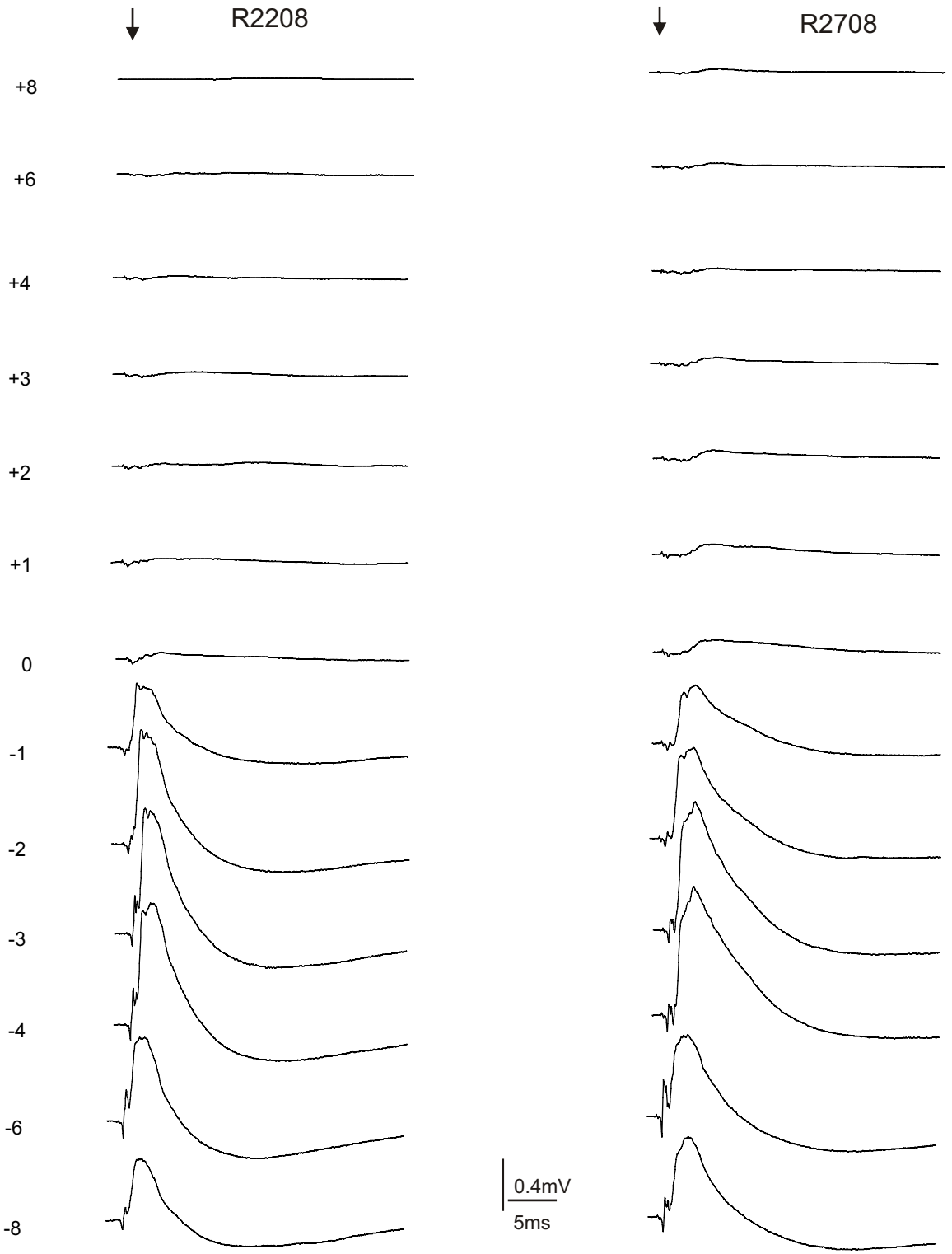


**Figure 3-14 Examples of CDPs evoked by radial nerve stimulation in the OEC above group**

Each column of traces shows recordings made from one animal. The recordings were made at 1mm intervals from 8mm rostral to 8mm caudal to the lesion level (C4/5 border) as indicated. Traces recorded at +7, +5, -5, and -7mm are omitted. The traces represent averages of 25 sweeps and the calibrations apply to all traces. The arrows indicate stimulus artifacts.

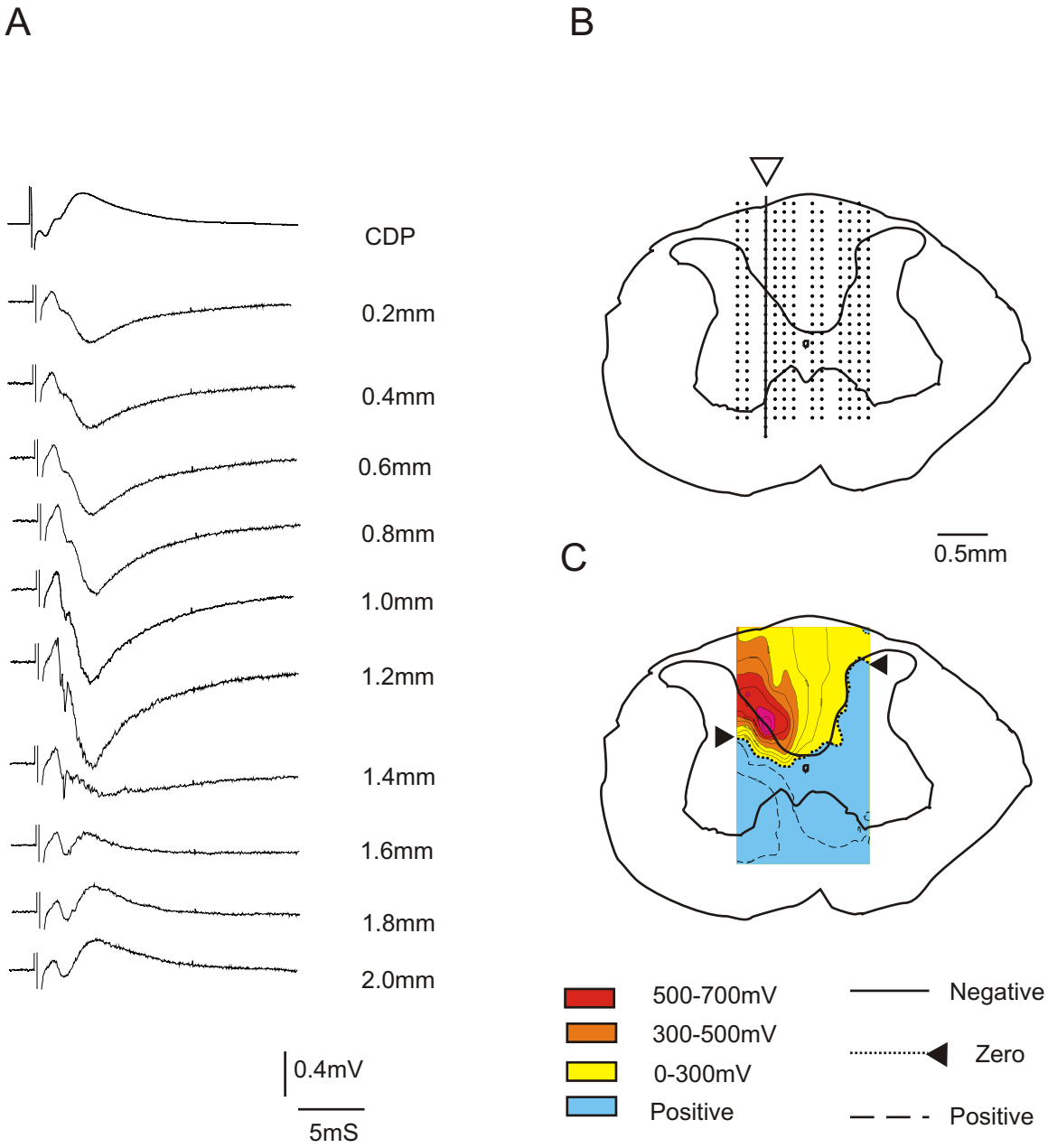


**Figure 3-15 Field potential recordings from a normal animal**
Field potential recordings were made at 4mm above the C4/5 reference location in a normal animal (9308). A, examples of field potential recordings made in the track indicated by an open arrow head in B (400µm to the left of midline). The top trace shows a CDP recording from the same level of the cord. The negative potential reached a peak amplitude at 1.2mm deep, then reversed; B, schematic diagram showing all recording sites. Solid line represents the track from which the recordings in A were made; C, isopotential plot computed from the recordings made at all locations and accurately overlaid on an outline of the spinal cord. Solid lines represent negative potentials, dashed lines represent positive potentials.

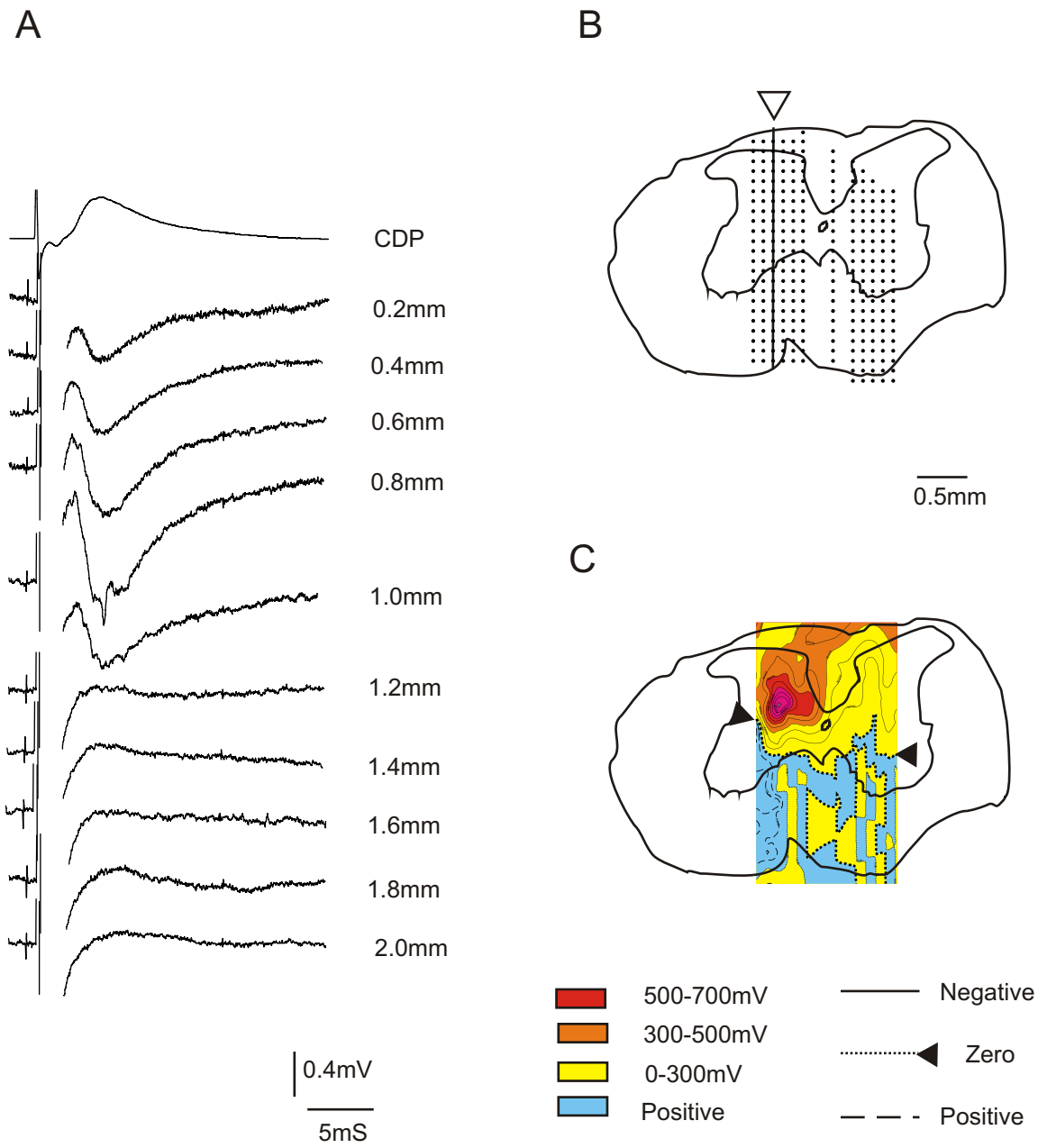


**Figure 3-16 Field potential recordings from above the lesion in a 3 month dorsal column lesioned animal**

Field potential recordings were made at 3.5mm above the lesion (C4/5 reference location) (R6508). A, examples of field potential recordings made in the track indicated by an open arrow head in B (500µm to the left of midline). The top trace shows a CDP recording from the same level of the cord. The negative potential reached a peak amplitude at 1.0mm deep, then reversed; B, schematic diagram showing all recording sites. Solid line represents the track from which the recording in A were made; C, isopotential plot computed from the recordings made at all locations and accurately overlaid on an outline of the spinal cord. Solid lines represent negative potentials, dashed lines represent positive potentials.

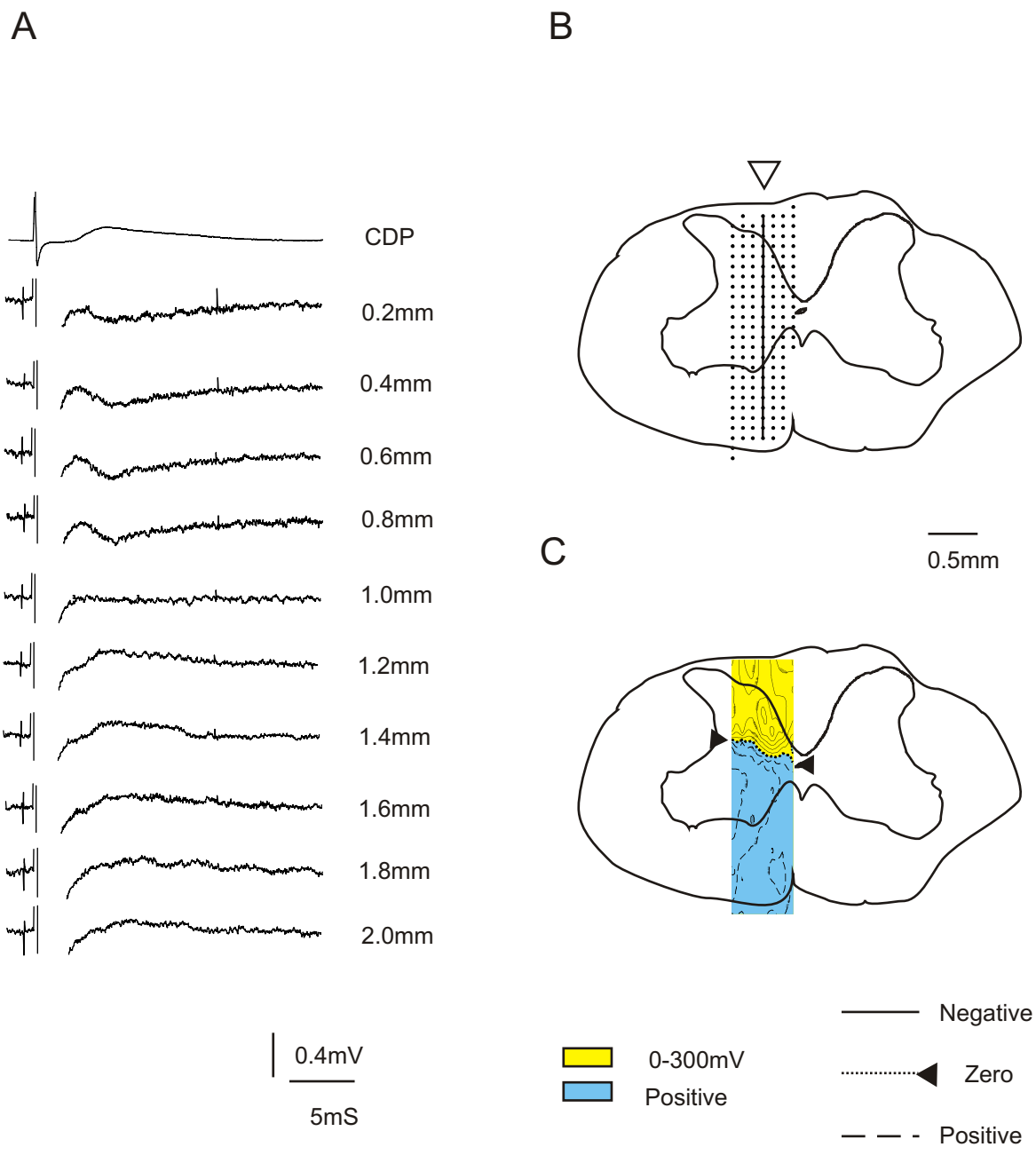


**Figure 3-17 Field potential recordings from below the lesion in a 3 month dorsal column lesioned animal**

Field potential recordings were made at 3mm below the lesion level (C4/5 reference location) (R6508). A, examples of field potential recordings made in the track indicated by an open arrow head in B (400µm to the left of midline). The top trace shows a CDP recording from the same level of the cord. The negative potential reached a peak amplitude at 0.8mm deep, then reversed; B, schematic diagram showing all recording sites. Solid line represents the track from which the recordings in A were made; C, isopotential plot computed from the recordings made at all locations and accurately overlaid on an outline of the spinal cord. Solid lines represent negative potentials, dashed lines represent positive potentials.

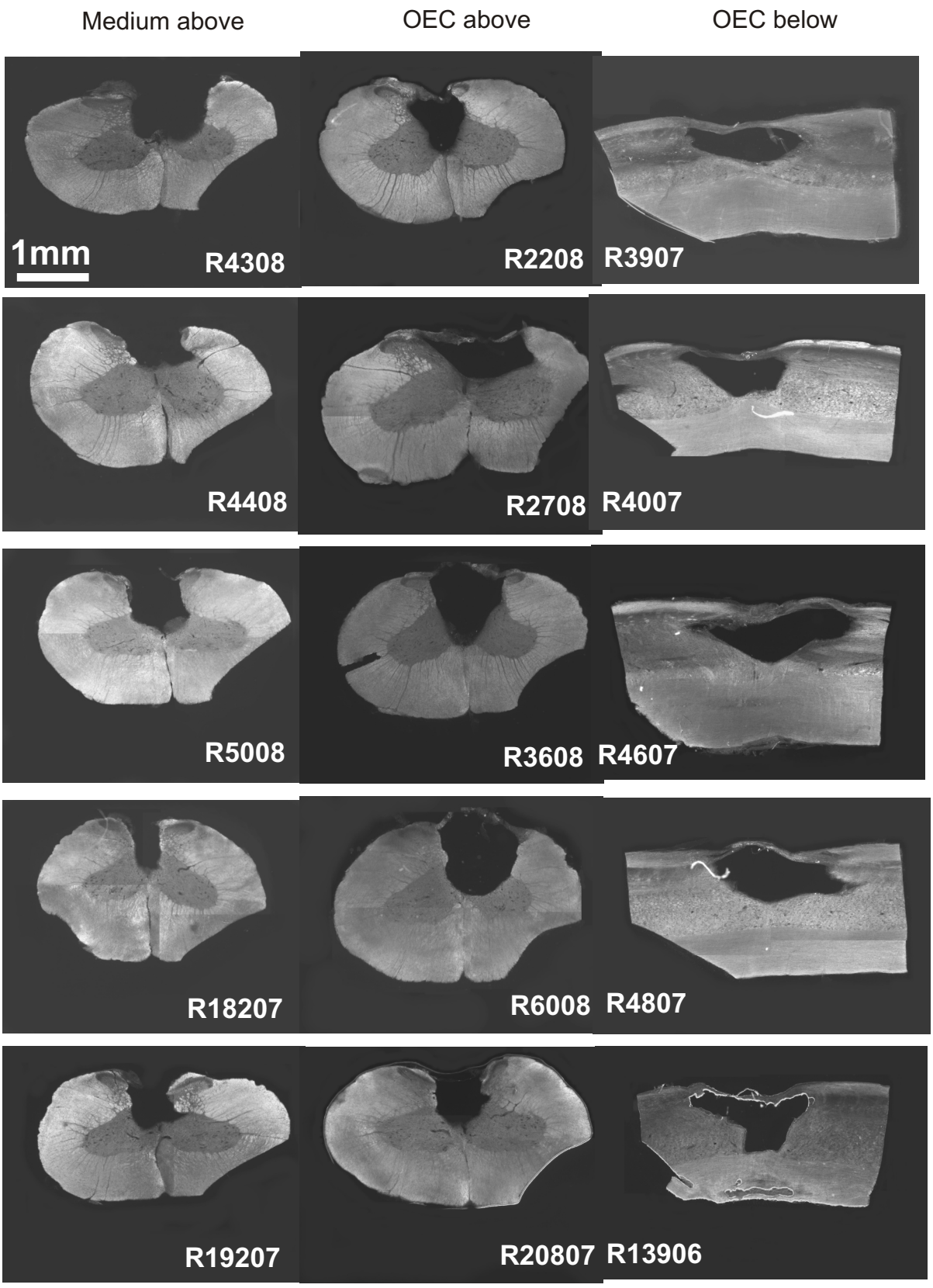


**Figure 3-18 Lesion morphology of transplanted animals**
Light microscopy images taken with a dark field view condenser from transvers/parasagittal sections of different animal groups. The lesion interrupted the whole dorsal columns. Lesion cavities were observed in all the transplanted groups. Varying amouts of the dorsal horn grey matter were also affected by the lesion. Scale bar 1mm applies to all images.

# Effects of anti-Nogo and anti-MAG on sensorimotor pathways following injury

## 4.1 Introduction

Axonal regeneration following injury is limited by neurite growth inhibitors present in CNS myelin such as Nogo-A and MAG. However, these proteins may normally serve to restrict axonal plasticity and sprouting in the adult nervous system once mature neuronal circuits have developed. Consistent with this hypothesis, treatment with antibodies directed at the NOGO-A-specific terminal of NOGO-A or interference with NOGO-R signalling has been shown to lead to sprouting in several fibres systems (Li et al. 2004; Schnell and Schwab 1990; Fouad et al. 2004; Liebscher et al. 2005; Freund et al. 2006; 2007) and to promote improved functional recovery (Liebscher et al 2005, Freund et al 2007). MAG also has the capacity to inhibit neurite outgrowth (McKerracher et al. 1994; Mukhopadhyay et al. 1994). Although its effects on plasticity have not been investigated, treatment with anti-MAG antibody is reported to have neuroprotective effects in a model of stroke. Improved functional recovery was accompanied by smaller lesion volumes and better tissue sparing in animals receiving anti-MAG antibody (Irving et al. 2005; Thompson et al. 2006).

The aim of this study was to use an electrophysiological approach to directly assess the effect of two antibodies targeting inhibitory myelin proteins on the function of sensorimotor pathways following spinal cord injury. The antibodies were supplied by GSK and included a mouse monoclonal antibody directed to a fragment of the amino terminal region of human NOGO-A (GSK577548) and a humanised antibody to MAG (GSK249320A).

## 4.2 Methods

### *4.2.1 Animals*

The observations reported in this chapter are based on investigation of 61 Sprague Dawley rats (Harlan, Loughborough, UK). Figure 4-1 shows the overall plan for this study. Twelve rats were naïve non-lesioned animals from which normal data was obtained in an acute electrophysiological experiment. Forty six rats were subjected to cervical dorsal column lesions and were allowed to recover for 8 weeks. Of these animals, 14 were implanted with pumps delivering vehicle, 10 animals with pumps delivering anti-Nogo antibody and 9 with pumps delivering anti-MAG antibody. The other 13 animals received lesions only to provide a control for any effects of the implanted intrathecal cannulae. Furthermore, three animals were sacrificed 5 weeks after lesioning and pump implantation in order to assess antibody distribution following intrathecal delivery (two animals for anti-Nogo antibody, one for anti-MAG antibody). Rats used for the naïve group weighed 380 –460g at the time of electrophysiology to approximately match the weight of animals which had been lesioned and allowed to survive for 8 weeks. At the time of surgery, rats used for the lesioned group weighed 243-295g.

### *4.2.2 Antibodies*

#### 4.2.2.1 Antibody preparation

Antibodies were prepared and supplied by GSK pharmaceuticals as part as a collaborative contract.

**Immunisation strategy** In order to generate monoclonal antibodies directed against the sequences unique to the CNS restricted Nogo-A isoform (A-splice) two female mice (SJL) were immunised subcutaneously with a mixture of human and rat NOGO-A-splice-GST proteins purified from *E.Coli* (5ug per injection). The RIMMS schedule used was designed to generate high affinity monclonal antibodies by rapid immunisation at multiple sites (day 0, 2 sites using CFA plus 4 sites using RIBI adjuvant, days 4 and 8, 4 sites using just RIBI). After three immunisations over 11 days, lymph node cells were harvested from 2 mice and

fused with Bcl2 expressing P3X myeloma cells. Cells were seeded into twenty 96 well plates. Wells displaying growing cells were progressed into the screening assay detailed below.

**Screening strategy** A large panel of anti-Nogo-A antibodies was generated. These antibodies were progressed on the basis of binding to cleaved human Nogo-A splice (to eliminate GST reactive clones) and then for cross-reactivity with both human and rat Nogo-A splice. Antibodies were further filtered using a competition assay with those antibodies showing the best inhibition of binding to immobilised Nogo-A following the addition of increasing quantities of soluble Nogo-A. These selected antibodies were screened as hybridoma supernatants for their ability to reverse the inhibitory activity of GST-human Nogo-A splice in neurite-outgrowth assays.

**Monoclonals selected for progression** These selected antibodies (53) were screened initially as hybridoma supernatants for their ability to reverse the inhibitory activity of GST-human Nogo-A splice in neurite-outgrowth assays. An automated neurite-outgrowth assay was configured using the Cellomics Arrayscan machine in which fluorescently labeled neuronal processes stained using anti-beta-tubulin are quantitated. Wells of poly-d-lysine coated 96 well plates were coated using a spot of recombinant purified protein at 3pmol/ul. Baseline growth was assessed by measuring neuronal growth on the GST alone protein, inhibition was assessed in wells coated with GST-Nogo-Asplice or GST-Nogo-A5+6 pretreated with HBSS. Reversal of inhibition was determined in wells coated with Nogo-A pretreated with hybridoma supernatant or purified IgG diluted in HBSS. Four antibodies were identified with function blocking activity in this assay (2A10, 2C4, 15C3 and 4E2). 4E2 could not be revived from frozen stocks but the remaining three lines were grown in Cell Factories under serum free conditions and antibodies were purified using immobilised Protein G columns. These purified antibodies were shown to be able to neutralise the inhibitory activity of GST-NogoAregion 5+6. From these purified antibodies 2A10 appeared to be the most efficacious antibody with both 2C4 and 15C3 requiring higher concentrations to inhibit Nogo. 2A10 was manufactured from the mouse hybridoma using standard tissue culture conditions. Antibody was purified using protein-A sepharose and further processed by ion-exchange chromatography. The identity of the antibody was confirmed by N-terminal sequencing and

activity was confirmed by ELISA and Biacore assays relative to a reference batch with neurite-outgrowth inhibition blocking activity.

#### 4.2.2.2 Pumps

Two different osmotic mini-pumps were used to deliver vehicle or antibodies in this study. The 2 week pumps (2ML2, ALZET, USA) were implanted into the animals, and then swapped for 4 weeks pumps (2ML4, ALZET, USA) after 2 weeks so that vehicle/antibody was delivered for 6 weeks in total.

#### 4.2.2.3 Dosing and antibody delivery

Pumps were filled and primed overnight in sterile saline at 35 $^{o}$C with the cannulae attached. For the vehicle treated animals the pumps were filled with Phosphate buffered saline (PBS, $Ca^{2+}$ and $Mg^{+}$ free, invitrogen, UK) diluent in which the Nogo antibody was prepared. For anti-Nogo treatment, 2 week pumps (2ML2) were filled with anti-Nogo antibody (anti-Nogo 2A10 mouse monoclonal) at a concentration of 3mg/ml. Since the 4 week pumps (2ML4) pump at a rate half that of the 2 week pumps, they were filled with anti-Nogo at a concentration of 6mg/ml. This concentration was chosen based on previous studies (Liebscher T et al. 2005). For anti-MAG treatment, 2-week pumps were filled with anti-MAG (GSK249320A humanised IgG1 antibody in phosphate buffer) at a concentration of 0.7mg/ml and 4-week pumps at a concentration of 1.4 mg/ml. This concentration was designed to deliver anti-MAG antibody at a dose of 100µg/24hrs and was chosen based on previous studies performed at GSK. The diluent used to prepare working strength solutions was the same as that in which the antibody was supplied.

### *4.2.3 Lesioning, intrathecal cannulation and pump implantation*

All the dorsal column lesions and pump implantations in this study were carried out by Dr. John Riddell.

#### 4.2.3.2 Dorsal column lesion procedure

The dorsal columns were lesioned bilaterally at the C4/C5 junction. The lesioning procedure was the same as described in the methods section of chapter 2. Surgical materials and instruments were sterilised and precautions were taken to minimise the risk of infection. Animals routinely received the peri-operative medication described previously in chapter 2.

#### 4.2.3.2 Intrathecal cannulation and pump implantation

At the same operation a fine cannula (ReCathco) was introduced through a slit in the dura at the atlanto-occipital junction and passed caudally until it appeared within the laminectomy opening (see Figure 4-2). The tip of the cannula was positioned just rostral to the lesion. The cannula was then secured to bone (C1 vertebra) with Vetbond cyanoacrylate adhesive and secured by suture thread more distally. The pump was placed in a subcutaneous pocket over the back at the thoraco-lumbar level. The positioning and continuity of intrathecal cannulae was determined at the electrophysiological experiment and the completeness of lesions after histological processing at the end of the experiment.

#### 4.2.3.3 Pump swap

Two weeks after the lesion operation, animals were re-anaesthetised with halothane and the 2 week pumps swapped for the 4 week pumps being careful not to introduce air bubbles when re-attaching to the cannula.

#### 4.2.3.4 Distribution of anti- Nogo and anti-MAG at 5 weeks and 8 weeks

To determine the distribution of the antibodies after intrathecal delivery, animals were lesioned and implanted with pumps exactly as for the electrophysiological experiments except that the animals were sacrificed at 5 weeks post-implantation. This time point was chosen because it is towards the end of the normal total delivery period of six weeks (3 weeks after implantation of the second minipump) and is before significant degradation of the antibodies would be expected. Two animals were implanted with pumps delivering anti-Nogo antibody and one animal with a pump delivering anti-MAG.

Immunolabelling for anti-Nogo (n=3) and anti-MAG (n=6) was also performed at the 8 week post-lesion time point i.e. 2 weeks after delivery of antibodies had ceased.

## *4.2.4 Electrophysiology*

### 4.2.4.1 Anaesthesia

Animals were anaesthetised as described in chapter 2 during the preparatory surgery and electrophysiological assessment.

### 4.2.4.2 Preparatory surgery

The preparation for surgery and electrophysiological assessment were exactly the same as described in chapter 2. During the surgery, the positioning and continuity of intrathecal cannulae were confirmed, and then the cannula was carefully removed.

### 4.2.4.3 Recordings of cord dorsum potentials

To assess spinal cord function in the region of the lesion and the effects of antibody treatments, cord dorsum potentials (CDPs) evoked by electrical stimulation of the radial nerve and/or the corticospinal tract were recorded. The procedures for stimulation and recording were the same as described in chapter 2. Recordings were made while stimulating the radial nerve or the pyramids at supramaximal intensities (typically 50-100μA for radial nerve and 200-350μA for pyramidal stimulation). Responses to 25 stimuli were recorded at each recording location and averaged using a CED 1401+ interface and Signal software.

### 4.2.4.4 Perfusion

Most of the animals were transcardically perfused at the end of the electrophysiological experiment for histology as described in chapter 2.

## *4.2.5 Histological processing*

### 4.2.5.1 Histological processing of brainstem for stimulation sites

Brainstem tissue containing the stimulating electrode tracks were carefully processed as described in chapter 2. Slides were stored at -20°C.

### 4.2.5.2 Histological processing of spinal cord for lesions

The procedure for the histological processing of tissue containing the lesion cavity was the same as described in chapter 2. Slides were stored at -20°C.

## *4.2.6 Microscopy*

### 4.2.6.1 Reconstruction of stimulation sites in the Pyramids

Sections containing stimulating electrode tracks were reviewed under microscopy (Zeiss Axioplan 2 Imaging), and the stimulating electrode tracks were reconstructed by using Camera lucida drawings as described in chapter 2.

### 4.2.6.2 Verification of dorsal column lesion

Sections containing the lesion cavity were observed using phase contrast light microscopy to determine the perimeter of the cavity and the relationship to the boundaries between grey and white matter as described in chapter 2.

## *4.2.7 Off-line analysis of electrophysiology*

CDP recordings were inspected and analysed by using Signal software as described in chapter 2. The data was noted in excel spreadsheets then imported to Prism 4 software (GraphPad Software Inc, USA) to create potential plots.

## *4.2.8 Statistical analysis*

The following statistical tests were carried out on the electrophysiological data (GraphPad Software Inc, USA). Analysis of variance (ANOVA); Tukey-Kramer Post-hoc; The Dunnett Post-hoc test; Student's t-test was used to reveal the differences among different groups.

## 4.3 Results

### *4.3.1 Distribution of antibodies*

The distribution of the antibodies following intrathecal delivery was investigated using immunocytochemistry and fluorescence and confocal microscopy.

#### 4.3.1.1 Anti-Nogo antibody at 5 weeks

Anti-Nogo immunolabelling could be detected at high levels around the rim of the lesion cavity and within the neuropil of the dorsal spinal cord above and below the lesion (Figure 4-3). Labelling was strongest within the more superficial aspects of the dorsal columns above the lesion, close to where the cannula tip was located (Figure 4-3D). Anti-Nogo labelling of blood vessels within the spinal cord, both in the dorsal aspects and the ventral aspects was also common (arrows in Figure 4-3B, C and D). There was no obvious co-localisation with neurofilament labelled structures (Figure 4-3) or with GFAP (not illustrated).

One of the anti-Nogo treated animals examined in this way appeared to have an unusually high density of large calibre blood vessels within the spinal cord close to the delivery site. This observation may reflect an angiogenic effect of the Nogo antibody or may simply be a response to the presence of an intrathecal cannula.

#### 4.3.1.2 Anti-MAG antibody at 5 weeks

Humanized anti-MAG immunolabelling could be detected at high levels within the spinal segments close to the intrathecal delivery. The immunolabelling was strongest around the edge of the lesion cavity but penetrated deep into the spinal cord parenchyma and was evident particularly in the dorsal columns (see Figure 4-4). There was evidence for preferential binding within degenerating white matter. The dotted white lines in Figure 4-4A indicate the upper and lower borders of the corticospinal tract within the ventromedial dorsal columns. As can be seen, above the lesion (left hand end of section), immunolabelling is seen mainly dorsal to the corticospinal tract within the degenerating white matter of the ascending dorsal column system. This pattern was also evident in

transverse sections taken from a block rostral to the parasaggital section (Figure 4-4E): immunolabelling here is seen particularly in the ascending dorsal column tract, avoiding the intact corticospinal tract. On the other hand, below the lesion (Figure 4-4A, right hand end of section) the immunolabelling was mainly within the degenerating corticospinal tract in the ventral aspect of the dorsal columns. Some evidence of binding to dorsal roots was also observed (Figure 4-4E and G). Co-localisation with APC was investigated but none seen (Figure 4-4F). Humanized MAG antibody labelling was, however, seen in blood vessels (Figure 4-4B) and in occasional cells (Figure 4-4C and D). Anti-MAG labelling was occasionally co-localised with endogenous MAG (arrows in Figure 4-4D) though endogenous MAG was not obviously increased around the lesion site or in degenerating white matter tracts at 5 week post-lesion in MAG antibody treated animals.

#### 4.3.1.3 Anti-Nogo and anti-MAG at 8 weeks

Immunolabelling for anti-Nogo (n=3) and anti-MAG (n=6) was also performed at the 8 week post-lesion time point i.e. 2 weeks after delivery of antibodies had ceased. Immunolabelling at this time point was very much reduced compared to the 5 week time point and was only detectable in the most superficial aspects of the cord and around the lesion cavity where the intensity was also greatest at 5 weeks (see Figure 4-5).

### *4.3.2 Spinal cord function assessed by electrophysiology*

As in the previous chapters, CDPs evoked by stimulating the corticospinal tract and/or radial nerve were used to assess function in the cervical spinal cord. Because Sprague-Dawley rats were used for this study rather than the F344 strain of the earlier studies, recordings were made again from normal animals (n=12). A further 33 animals were subjected to dorsal column lesions and implanted with a pump and intrathecal cannula. These were divided into three groups: one treated with vehicle (n=14), one with anti-Nogo (n=10), and one with anti-MAG (n=9).

#### 4.3.2.1 Cord dorsum potentials evoked by pyramidal stimulation

Potentials evoked by pyramidal stimulation were recorded with a silver ball electrode positioned on the dorsal columns at 1mm intervals from 8mm rostral to 8mm caudal to the C4/5 segmental border as described in chapter 2.

Because of the use of a different strain of animals for the work in this chapter, and the possibility of anatomical or other differences that could affect the protocol we developed for maximal unilateral pyramidal stimulation, brain stem stimulation sites were histologically verified for 6 animals. Figure 4-6 shows reconstructions of the electrode positions and the corresponding stimulus-recruitment curves for 4 of these animals. These showed the same characteristic features as the F344 animals so that the same protocol was used to select animals.

***Normal animal group***

CDPs evoked by pyramidal tract stimulation were investigated in 11 normal animals. Examples of CDPs recorded from two representative animals of this group are shown in Figure 4-7. The recordings show that clear surface potentials are evoked by pyramidal stimulation at all of the recording locations examined. This is from 8mm rostral to 8mm caudal to the C4/5 border of the cervical segments. Cervical segments are about 3mm long in the rat so that this corresponds to approximately C2 to C7. The recordings show clear afferent volleys rostrally which become more dispersed and show a longer latency at progressively more caudal recording locations due to the longer conduction distance. The mean CDP amplitude for all animals in this group at each recording location is shown in Figure 4-8. In normal SD rats, the distribution of CDP amplitudes evoked by pyramidal stimulation was fairly flat over most of the cervical cord but declined in amplitudes at further caudal locations. Compared to the amplitudes in normal F344 rats, the amplitudes tended to be higher at around 0.35mV, but these were not statistically significantly different (Table 4-1).

***Vehicle group***

CDPs evoked by pyramidal stimulation were investigated in 13 animals implanted with a pump delivering vehicle. Examples of CDPs recorded from two representative animals of this group are shown in Figure 4-9 and the distribution of averaged CDPs in all animals of this group is shown in Figure 4-10. CDPs below the lesion were greatly reduced compared to those in normal animals as expected following interruption of the main component of the corticospinal tract. However, small CDPs were detectable at these levels. On average these were about half the size seen in F344 animals 3 months following a dorsal column lesion. CDPs above the lesion were also smaller than those recorded in normal animals (by some 25-40%). The amplitudes above the lesion were around 0.25mV in vehicle treated animals compared to around 0.35mV in normal animals and this is significantly different (Table 4-1).

***Anti-Nogo group***

CDPs evoked by pyramidal stimulation were investigated in 10 animals with pumps delivering anti-Nogo antibody. Examples of CDPs recorded from two representative animals of this group are shown in Figure 4-11 and the distribution of averaged CDPs in all animals of this group was shown in Figure 4-12. CDPs below the lesion tended to be larger than those recorded in the vehicle group but this difference was not significant (Table 4-1). CDPs above the lesion also tended to be larger in the anti-Nogo treated animals than those in the vehicle group (by about 30%) and the difference was significant at some locations (Table 4-1). They were almost same as those recorded in normal animals. The amplitudes above the lesion level were larger than 0.3mV. Because intrathecal cannulation-vehicle treatments profoundly reduced the amplitudes of CDPs, the effect of the anti-Nogo treatment was to restore the CDPs to their normal amplitudes.

***Anti-MAG group***

CDPs evoked by pyramidal stimulation were investigated in 8 animals with pumps delivering anti-MAG antibody. Examples of CDPs recorded from two representative animals of this group are shown in Figure 4-13 and the distribution of averaged CDPs in all animals of this group is shown in Figure 4-14. The amplitudes of CDPs in the anti-MAG treated group were very similar to those recorded in the vehicle group.

#### 4.3.2.2 Cord dorsum potentials evoked by radial nerve stimulation

Potentials evoked by radial nerve stimulation were recorded with a silver ball electrode positioned on the dorsal columns at 1mm intervals from 8mm rostral to 8mm caudal to the C4/5 segmental border as described in chapter 2.

***Normal animal group***

CDPs evoked by radial nerve stimulation were investigated in 9 normal animals. Examples of CDPs recorded from two representative animals of this group are shown in Figure 4-15. The recordings show that clear surface potentials are evoked by radial nerve stimulation at all of the recording locations examined. The recordings show clear afferent volleys close to the entry of the stimulated root which was 3 to 4mm below C4/5 segmental border, and become more dispersed at progressively more rostral and caudal recording locations due to the longer conduction distance. The rostro-caudal distribution of averaged CDPs in all animals of this group is shown in Figure 4-16. In normal animals, the largest potentials were produced between 0 and -5 mm which corresponds to the C5 and C6 segments. CDPs of gradually declining amplitude were, however, evoked for several segments above and below this. The amplitudes of the biggest CDPs were around 0.8mV. The amplitudes of CDPs recorded in SD rats showed a slight tendency to be bigger than those recorded in F344 rats but the difference was not significant (Table 4-2).

***Vehicle group***

CDPs evoked by radial nerve stimulation were investigated in 14 animals with pumps delivering vehicle. Examples of CDPs recorded from two representative animals of this group are shown in Figure 4-17 and the distribution of averaged CDPs in all animals of this group is shown in Figure 4-18. Above the lesion level, CDPs in the vehicle treated group were almost abolished due to the dorsal column lesion. Below the lesion, CDPs recorded from vehicle treated animals were almost the same as those recorded in normal animals at positions between -3 and -8mm. Nearer to the lesion, however (-1 and -2mm) they were significantly smaller.

***Anti-Nogo group***

CDPs evoked by radial nerve stimulation were investigated in 10 animals treated with anti-Nogo. Examples of CDPs recorded from two representative animals of this group are shown in Figure 4-19 and the distribution of averaged CDPs in all animals of this group is shown in Figure 4-20. In the anti-Nogo group, CDPs above the lesion were of negligible amplitudes as in the vehicle treated group. However, CDPs below the lesion were larger than those recorded in the vehicle group (by 35-40%) and the difference was significant at some locations (Table 4-2). They also tended to be larger even when compared to CDPs in normal animals although in this case the difference did not reach significance (Table 4-2).

***Anti-MAG group***

CDPs evoked by radial nerve stimulation were investigated in 9 anti-MAG treated animals. Examples of CDPs recorded from two representative animals are shown in Figure 4-21 and the distribution of averaged CDPs in all animals of this group is shown in Figure 4-22. CDPs recorded in these animals were very similar to those of the vehicle treated group.

## 4.4 Discussion

### *Distibution of antibodies*

The dose chosen for the delivery of anti-Nogo was the same as has been used previously for the intrathecal delivery of similar anti-Nogo antibodies to that used here (Liebscher et al. 2005; Maier et al. 2009). The duration of the treatment was, however, prolonged beyond the four weeks delivery used in previous studies by swapping osmotic pumps to provide a total delivery period of six weeks. When the distribution of the antibody was investigated after 5 weeks of administration, it was found to be distributed mainly superficially within the neuropil and was enriched in the region of the lesion cavity as has been reported for similar antibodies directed against the Nogo-A-specific region of Nogo-A delivered icv (Weinmann et al. 2006). The choice of concentration for anti-MAG was based on previous studies performed by GSK in a stroke model (Irving et al. 2005). In this earlier study anti-MAG was given as bolus injections by icv or iv administration within a period of 72 hours following the induction of stroke but the distribution of the antibody was not examined. In the current study the antibody was delivered intrathecally for a continuous period of 6 weeks as for the anti- Nogo. When the distribution of the antibody was investigated after 5 weeks of administration, it was found to be distributed mainly within the dorsal half of the neuropil and was enriched around the lesion cavity but also in regions corresponding to degenerating white matter tracts in the dorsal columns.

### *Corticospinal and sensory CDPs in Sprague-Dawley compared to Fisher 344 animals*

For investigation of the effect of anti- Nogo and anti-MAG antibodies, Sprague-Dawley animals were preferred to Fischer 344s because SDs are more robust, less nervous animals and use of an inbred strain was not required. Because we were using a different strain and strain related differences are know to occur it was necessary to repeat recordings from normal animals. Corticospinally and sensory-evoked CDPs were very similar in both strains of animals although corticospinal CDPs tended to be slightly, though not significantly, bigger in SD animals. This may be related to reports of differences in the area of the sensorimotor cortex

in different strains of rats described by Whishaw and colleagues (Whishaw et al. 2003).

### *Effect of intrathecal cannulae and vehicle treatment*

One surprising finding was that pyramidal-evoked CDPs above the lesion in animals in which vehicle alone was delivered via an implanted intrathecal cannula were smaller in amplitude than those recorded from normal animals. This contrasts with the results obtained with F344 animals where at both 1 week and 3 months following a dorsal column lesion CDPs were larger than in normal animals of the same strain. CDPs evoked below the lesion by radial nerve afferents were not as affected since they were similar in size to normal animals, but this again contrasts with enhanced CDPs seen in F344 animals 1 week and 3 months after a dorsal column lesion. These observations suggest that either the presence of the cannula or the delivery of the vehicle from the pump had a detrimental effect on the spinal cord. Even though the cannula used was of the smallest possible diameter it was evident during placement that it was a tight fit between the pia and the dura. It was also sometimes possible to see a groove in the dorsal surface of the spinal cord where the cannula had rested. There have been previous reports of inflammation around chronically indwelling intrathecal cannulae. However, this is the first time that a functional assessment of the effect of an intrathecal cannula has been made. The result suggests that it would be preferable to use an alternative method of drug delivery where possible.

### *Effect of anti- Nogo treatment*

The results obtained from animals treated with anti- Nogo show a significant enhancement of both corticospinal and sensory afferent evoked CDPs compared to vehicle treated controls. Interpretation of the effects of anti- Nogo on corticospinal CDPs above the lesion are complicated by the negative effects of vehicle/intrathecal cannulation which meant that the CDPs following anti- Nogo treatment were increased towards that seen in normal animals rather than exceeding them. Corticospinally–evoked CDPs below the lesion also tended to be larger in anti-Nogo treated animals but this effect did not reach significance.

The results for CDPs evoked by sensory afferents of the radial nerve were clear cut. Treatment with anti-Nogo resulted in CDPs that exceeded not just those of the vehicle treated controls but also of normal animals. This evidence strongly suggests that anti-Nogo enhances plasticity in sensorimotor pathways, the functions of which are thereby enhanced.

### *Effect of anti-MAG treatment*

The results obtained from animals in which anti-MAG was delivered over the spinal cord are unequivocal. Anti-MAG treatment had no effect on either corticospinally evoked or sensory afferent evoked CDPs. The CDPs evoked by both pathways were neither suppressed nor enhance but remained almost identical to those of the vehicle treated controls. The fact that CDPs recorded from anti-MAG treated animals are so similar to the vehicle treated animals does, however, provide reassurance the CDP assessment method employed is consistent and therefore that the enhanced CDPs observed in the anti-Nogo treated controls are genuine.

The lack of effect of anti-MAG is not likely to be due to poor penetration of the antibody since immunocytochemical detection of the antibody showed it to be distributed throughout the relevant area of the spinal cord as discussed above. It therefore seems unlikely that anti-MAG treatment has any plasticity promoting effect, at least in this laceration model of spinal cord injury. This does not preclude the possibility that anti-MAG may have a neuroprotective function as has been reported in a stroke model (Irving et al. 2005) and suggested recently by *in vitro* studies (Nguyen et al. 2009). The wire knife dorsal column lesion model used in this study is not a model suited to disclosing neuroprotective actions as axons in the white matter are acutely axotomised and there is minimal collateral damage to neurones in the grey matter. Studies in a contusion injury model will be necessary to determine whether anti-MAG treatment has any neuroprotective actions following spinal cord injury.

## *Mechanisms of Nogo-induced plasticity - anatomical vs synaptic plasticity*

This study shows an increased efficacy of corticospinal and sensory pathways in response to anti-Nogo treatment. Previous investigations using similar antibodies to the amino-Nogo terminal have suggested that some axonal regeneration can occur (Brosamle et al. 2000; Freund et al. 2009) but also that there is widespread anatomical sprouting (Raineteau and Schwab, 2001; Raineteau et al. 2002; Bareyre et al. 2002). Sprouting has been reported for a number of different fibre systems including the corticospinal tract after interruption within the spinal cord or by pyramidotomy (Bareyre et al. 2002), in the rubrospianl tract after corticospinal tract lesions (Raineteau et al. 2002). The larger amplitude potentials seen below the lesion on stimulation of the pyramidal tract in Nogo-ab treated animals could theoretically be due either to regeneration or to sprouting. However, clearly the enhancement of corticospinal actions above the dorsal column lesion and the enhancement of sensory transmission below the lesion cannot be explained by axonal regeneration since they are the "wrong side" of the lesion. This, together with the fact that the CDPs evoked by sensory afferents are actually larger following anti-Nogo treatment than in normal animals indicates that a mechanisms involving plasticity is involved. Given the evidence discussed above, anatomical sprouting of the corticospinal tract is a strong possibility. Sprouting of large diameter sensory fibres has not been reported following anti-Nogo treatment so the mechanism by which the efficacy of sensory pathways is enhanced remains to be investigated.

## *Does plasticity occur in spared fibres or only axotomised fibres?*

We have shown that anti-Nogo treatment produces an increase in the effectiveness of corticospinal actions above a dorsal column lesion and of sensory afferents below a dorsal column lesion. Although both the corticospinal and sensory potentials are produced by intact sections of these fibres proximal to the lesion, most are likely to have been axotomised more distally by the dorsal column lesion. Stimulation of the corticospinal tract also produces larger potentials below the level of the lesion. While these are likely to be produced by intact fibres belonging to the minor lateral component which pass the lesion,

this is not definitive since corticospinal connections above the lesion are made partly onto propriospinal neurones with axons passing the lesion. It therefore remains uncertain as to whether the plasticity-inducing effects of anti-Nogo treatment work only on axotomised fibres or also on non-damaged fibres. It is also possible that direct damage to the fibres in which plasticity is induced is not necessary but that some damage to the system as a whole is sufficient to render them responsive to anti-Nogo treatment (Raineteau et al. 2002). This would be important if anti-Nogo treatment was to enhance activity in spared pathways. As discussed earlier in the context of spontaneous plasticity, it is not possible to tell whether the plasticity induced by anti-Nogo treatment occurs in the corticospinal projection to the lumbar cord or the projection to the cervical segments but this could potentially be investigated further by using microstimulation in the forelimb and hindlimb areas of the sensorimotor cortext to determine the involvement of projections from these two areas or by tract tracing if anatomical sprouting is involved.

### *Does anti-Nogo treatment induce plasticity in contusion models of spinal cord injury?*

Transection models of spinal cord injury are the most suitable for investigating the mechanisms underlying experimental treatments for spinal cord injury but contusion injuries most closely model clinical injuries. The effect of anti-Nogo treatments have not yet been investigated in this model and this will be important to understand how effective the treatment is in maximising function following this type of injury and therefore how useful it may be clinically where most injuries are contusion type injuries.

### *Over what distance is plasticity induced following intrathecal delivery of anti-Nogo?*

Nogo-abs have been delivered by injections of hybridoma cells into the brain ventricles or icv injection (Bareyre et al. 2002) or intrathecally via osmotic minipumps (Liebscher et al. 2005; Maier et al. 2009). Intrathecal delivery of Nogo-ab is generally made with the tip of the cannula close to the site of injury. Sprouting of the corticospinal system has been reported within the spinal cord

but also for collateral branches within the brain. How this sprouting relates to function is not known since the behavioural changes usually used to assess recovery of function could result from plasticity at any level of the neuraxis and could involve systems not investigated anatomically. It is also unclear how close delivery of Nogo-ab would need to be to the terminals in which induction of plasticity is desired. Signalling of plasticity might be very local within the axon i.e. only terminals close to Nogo-ab binding may be induced to sprout) or binding of Nogo-ab at one set of terminals may induce plasticity in all of the terminals of that axon even where they are at some distance from the antibody binding.

In the treatment of spinal cord injury, inducing plasticity at all levels below the lesion, not just close to the lesion site would be of greatest potential benefit since spared fibres may travel for long distances below the lesion and many fibre types will give rise to collaterals connecting with spinal cord neurones over several segments. It would therefore be valuable to determine whether the plasticity we can detect electrophysiologically when testing pathways terminating close to the level at which the Nogo antibody is delivered would also occur at a greater distance from the delivery site or whether the effects of anti-Nogo diminish rapidly with distance. A better understanding of how Nogo-ab treatment induces plasticity at a molecular and cellular level may also illuminate these issues.

### *Is anti-Nogo treatment as effective after a delay?*

Treatments for spinal cord injury that depend critically on treatment commencing within a short time of the injury will be more difficult to implement than treatments that are not time-critical. Furthermore, treatments that are effective when initiated some time after the injury could be useful not only for the treatment of new injuries but also for chronic injuries. In this study the anti-Nogo treatment was administered acutely i.e. from the time the lesion was made. The question of whether plasticity is induced only in axotomised fibres o also in spared fibres has a bearing on this question. If only axotomised fibres are influenced then this implies a mechanism that interacts with signalling mechanisms triggered by axotomy. Since these change with time then the effect of anti-Nogo treatment might also be time limited. If on the other hand anti-

Nogo treatment induces plasticity in non-damaged fibres, and in the absence of collateral injury, then it is more likely that the plasticity inducing effects can be produced by treatment at any time point. Preliminary evidence from the Schwab group suggests that delayed treatment for spinal cord injury is less effective while delayed treatment remains effective in stroke models (Seymour et al. 2005). It is not clear why there should be such a discrepancy and further investigation of anti-Nogo effects at different time points may be useful.

### *Duration of anti-Nogo induced plasticity*

In the current experiments, electrophysiological assessment was performed two weeks after anti-Nogo delivery by the implanted pumps was exhausted. This indicates that, after a six 6 week treatment with anti-Nogo, the effects of the treatment persist for at least a further two weeks. Furthermore, this occurs despite a marked reduction in the amount of bound antibody detectable in the spinal cord at 8 weeks compared to 5 weeks. However, it remains uncertain as to whether the plasticity induced is permanent or reduces with time when treatment is stopped and if it reduces, how soon. The answers to these questions have clear implications for any treatment regime. If the plasticity induced is permanent then this would mean that only a single treatment would be necessary to bring about the desired plasticity and once the effects were maximised, treatment could be stopped. On the other hand it would also mean that any undesirable effects, once established would be permanent, and would not resolve if treatment were ceased. Studies using different durations of treatment and following the functional changes over a long time course would therefore be desirable.

### *Does Nogo-ab induced plasticity translate into improved sensorimotor function?*

Synaptic plasticity (strengthening existing connections) would enhance existing pathways while sprouting (new connections) may either enhance existing pathways or result in the formation of entirely new pathways. These new connections may or may not be functionally appropriate and integrated in a useful way. It is far from clear which, if either mechanism of plasticity, would

provide the best prospects for improving function after spinal cord injury but there are several reports that treatments with anti-Nogo antibodies or with agents that interfere with Nogo-R signalling can provide modest improvements in function. Functional recovery reported following IN-1 antibody treatment or delivery of other monoclonal antibodies directed against the Nogo-A-specific terminal of Nogo-A includes improvements of locomotion in rats (Liebscher et al. 2005) and of grasping movements in monkeys (Freund et al. 2006).

**Table 4-1 Statistical analysis of the differences between pyramidal-evoked CDPs recorded in different animal groups at each recording location**

ANOVA with post-hoc Dunnett's test was first applied and where a significant difference was found the P value threshold is given. Where no significance was detected with ANOVA, Student's t-test was used and where a significant difference was detected the P-value is given. Comparison where no significance was detected with either test is indicated by NS.

| | SD | Normal | Normal | Normal | Vehicle | Vehicle | Anti-Nogo |
|---|---|---|---|---|---|---|---|
| | F344 | Vehicle | Anti-Nogo | Anti-MAG | Anti-Nogo | Anti-MAG | Anti-MAG |
| +8 | NS | P=0.0040 | NS | NS | NS | NS | NS |
| +7 | NS | P=0.0083 | NS | NS | P=0.0500 | NS | P=0.0433 |
| +6 | NS | P=0.0327 | NS | P=0.0127 | NS | NS | NS |
| +5 | NS | P=0.0305 | NS | P=0.0015 | P=0.0416 | NS | P=0.0462 |
| +4 | NS | P=0.0124 | NS | P=0.0101 | NS | NS | NS |
| +3 | NS | P=0.0022 | NS | P=0.0090 | NS | NS | NS |
| +2 | NS | P<0.05 | P<0.05 | NS | NS | NS | NS |
| +1 | NS | P<0.01 | P<0.01 | P<0.01 | NS | NS | NS |
| 0 | NS | P<0.01 | P<0.01 | P<0.01 | NS | NS | NS |
| -1 | NS | P<0.01 | P<0.01 | P<0.01 | NS | NS | NS |
| -2 | NS | P<0.01 | P<0.01 | P<0.01 | NS | NS | NS |
| -3 | NS | P<0.01 | P<0.01 | P<0.01 | NS | NS | NS |
| -4 | NS | P<0.01 | P<0.01 | P<0.01 | NS | NS | NS |
| -5 | NS | P<0.01 | P<0.01 | P<0.01 | NS | NS | NS |
| -6 | NS | P<0.01 | P<0.01 | P<0.01 | NS | NS | NS |
| -7 | NS | P<0.01 | P<0.01 | P<0.01 | NS | NS | NS |
| -8 | NS | P<0.01 | P<0.01 | P<0.01 | NS | NS | NS |

**Table 4-2 Statistical analysis of the differences between radial nerve-evoked CDPs recorded in different animal groups at each recording location**

ANOVA with post-hoc Dunnett's test was first applied and where a significant difference was found the P value threshold is given. Where no significance was detected with ANOVA, Student's t-test was used and where a significant difference was detected the P-value is given. Comparison where no significance was detected with either test is indicated by NS.

| | SD | Normal | Normal | Normal | Vehicle | Vehicle | Anti-Nogo |
|---|---|---|---|---|---|---|---|
| | F344 | Vehicle | Anti-Nogo | Anti-MAG | Anti-Nogo | Anti-MAG | Anti-MAG |
| +5 | NS | P<0.01 | P<0.01 | P<0.01 | NS | NS | NS |
| +4 | NS | P<0.01 | P<0.01 | P<0.01 | NS | NS | NS |
| +3 | NS | P<0.01 | P<0.01 | P<0.01 | NS | NS | NS |
| +2 | NS | P<0.01 | P<0.01 | P<0.01 | NS | NS | NS |
| +1 | NS | P<0.01 | P<0.01 | P<0.01 | NS | NS | NS |
| 0 | NS | P<0.01 | P<0.01 | P<0.01 | NS | NS | NS |
| -1 | NS | P<0.01 | P<0.01 | P<0.01 | NS | NS | NS |
| -2 | NS | NS | NS | NS | NS | NS | NS |
| -3 | NS | NS | NS | NS | P<0.01 | NS | P=0.0321 |
| -4 | NS | NS | NS | NS | P<0.05 | NS | NS |
| -5 | NS | NS | NS | NS | NS | NS | P=0.0133 |
| -6 | NS | NS | NS | NS | NS | NS | P=0.0386 |
| -7 | NS | NS | NS | NS | NS | NS | NS |
| -8 | NS | NS | NS | NS | NS | NS | NS |

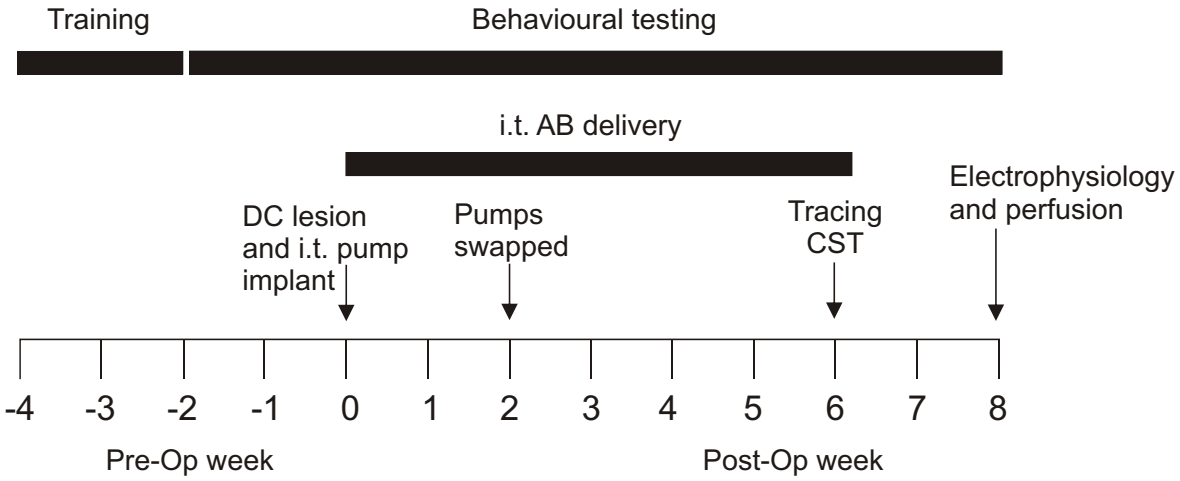


**Figure 4-1 Schematic diagram of study design**
Schematic diagram to show the overall plan of the experiment. The timing of individual experimental procedures is indicated relative to the operation to lesion the dorsal columns and implant pumps (Week 0). Behavioural testing although carried out, is not included in the present report.

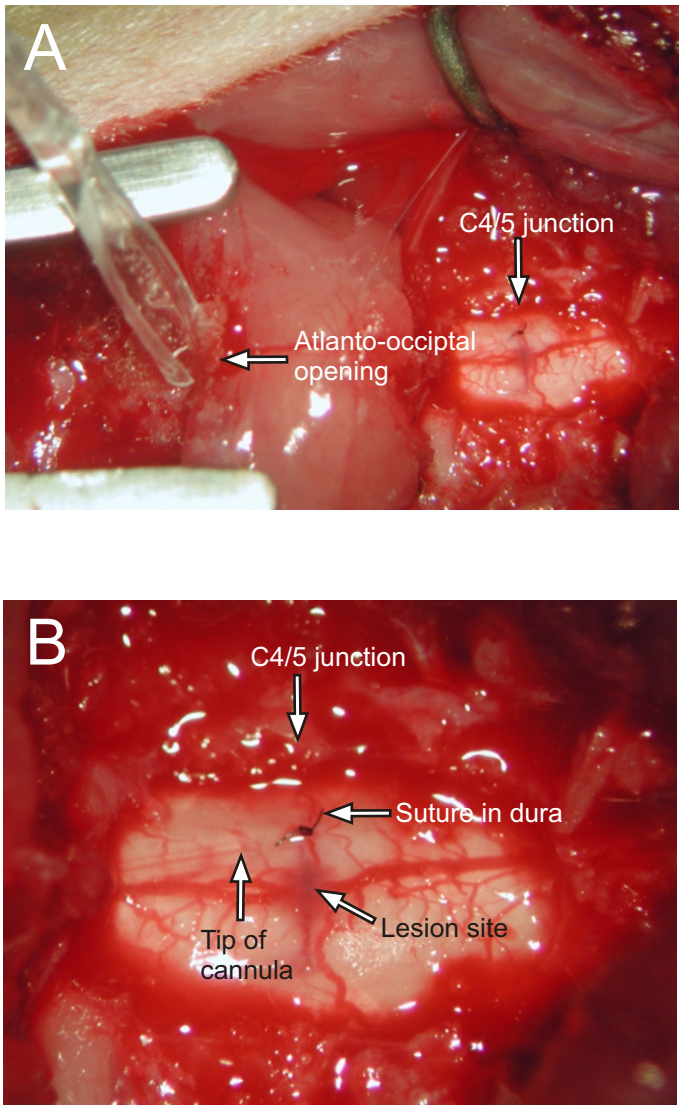


**Figure 4-2 Localisation of intrathecal cannulae for antibody delivery**
A, cannulae were inserted via the atlanto-occipital opening and routed intrathecally to localise the tip close to the C4/5 junction. B, the cannula tip was typically sited ca. 1 mm rostral of the C4/5 lesion site. A 10-0 surgical suture was stitched to the dura to mark the lesion site.

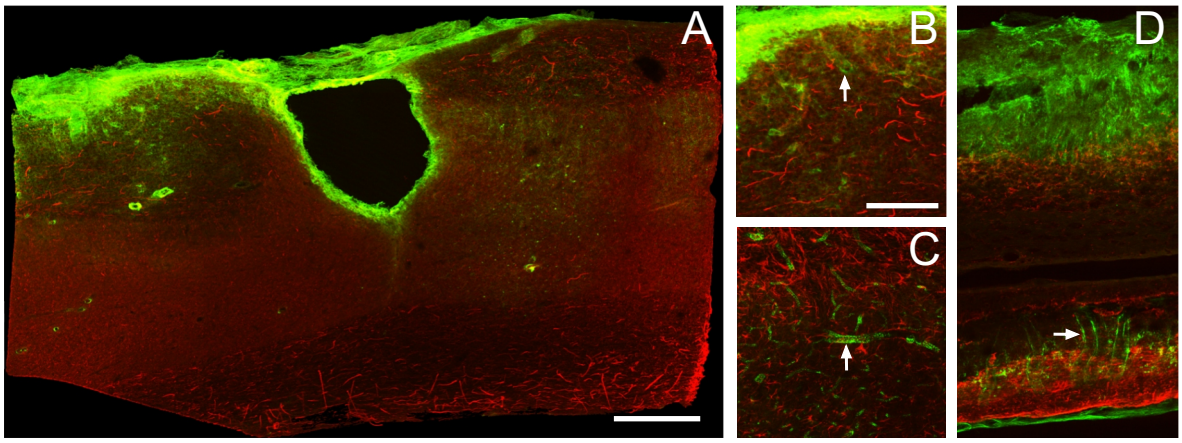


**Figure 4-3 Distribution of anti-Nogo within the spinal cord after intrathecal delivery at 5 weeks**

A, confocal microscope image of parasaggital section of spinal cord at the level of a dorsal column lesion where anti-Nogo was delivered intrathecally for five weeks. In this and other panels, immunolabelling for anti-Nogo is shown in green and immunolabelling for NF200 is shown in red. Anti-Nogo was detected mainly around the rim of the lesion cavity and dorsal surface of the cord but also penetrated into the dorsal aspects of the cord, especially rostral to the lesion where the cannula tip was situated; B, C, and D show selected areas from this and an additional section (D) to illustrate anti-Nogo binding to blood vessels (arrows), including within the ventral aspect of the cord (D). Scale bars: A, 500µm, B,C, D, 200µm.

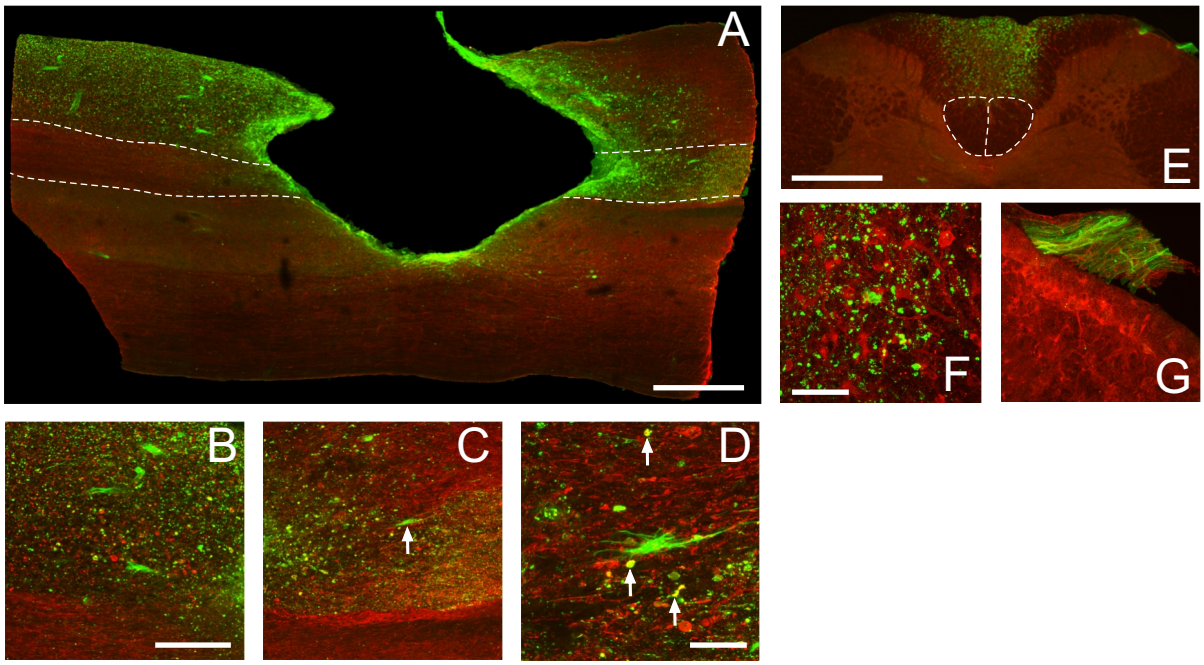


**Figure 4-4 Distribution of anti-MAG within the spinal cord after intrathecal delivery at 5 weeks**

A, confocal microscope image of parasaggital section of spinal cord at the level of a dorsal column lesion where anti-MAG was delivered for five weeks. Anti-MAG immunolabelling (green) is distributed around the periphery of the lesion cavity and dispersed more widely within the dorsal columns. Anti-MAG was distributed preferentially within areas of degenerating white matter: above the lesion (left hand side of section) immunolabelling occurs mainly dorsal to the intact corticospinal tract (dashed lines) within the degenerating ascending dorsal column tracts. Below the lesion (right hand side of section), immunolabelling is distributed mainly within the corticospinal tract (within dashed lines). E, transverse section from spinal cord several mm above the lesion showing the preferential distribution of anti-MAG within the region of dorsal columns containing degenerating ascending sensory fibres, and the absence of labelling within the corticospinal tract (within dashed lines); B and C show higher power views from an area of the ascending dorsal column (B) and the corticospinal tract (C). Note occasional anti-MAG labelled cells. The cellular labelling in C is shown in more detail in D where some examples of colocalisation of anti-MAG with structures labelled with endogenous MAG are also illustrated (arrows); F, high power image of an area of the dorsal columns (of the section shown in E) showing the anti-MAG was not co-localised with APC labelled cells; G, high power image of the dorsal root entry zone (from the section shown in E) showing the anti-MAG labelling within the dorsal root. Green = anti-MAG, Red (A-D) = endogenous MAG, (E-G) = APC. Scale bars: A, 500µm, B, C, E, 200µm, D, F, G, 50µm.

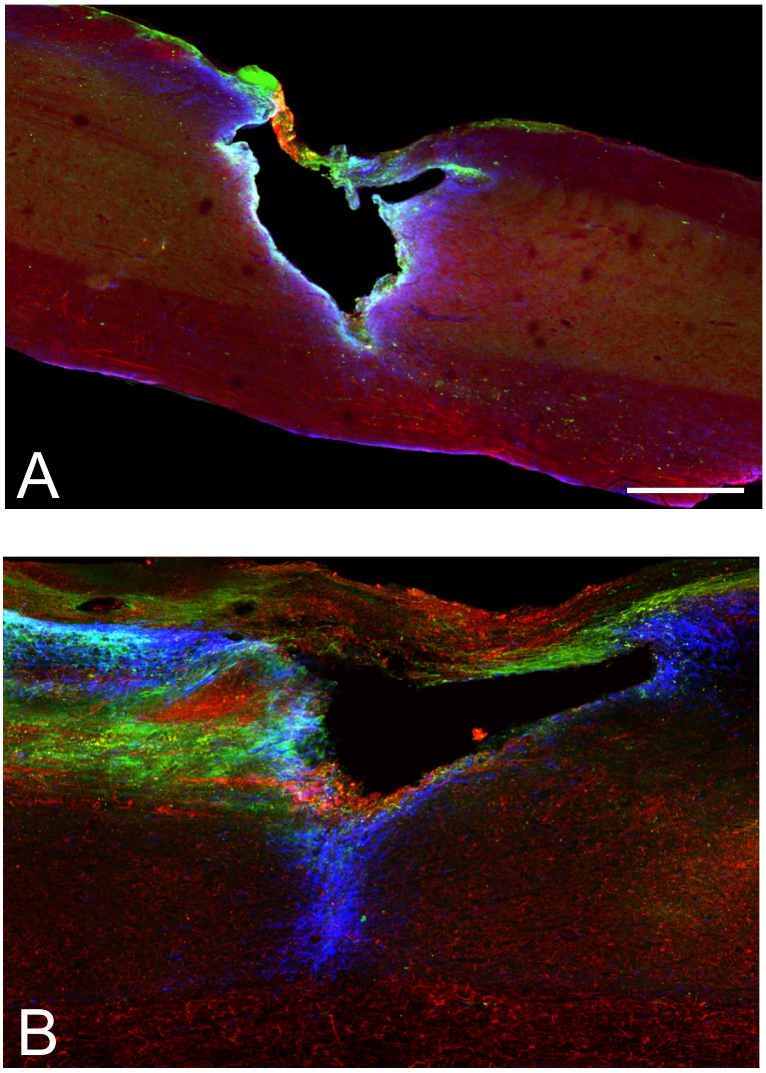


**Figure 4-5 Distribution of antibodies within the spinal cord at 8 weeks**
A and B, confocal images of parasaggital sections from animals treated with anti-Nogo (A) and anti-MAG (B). The antibodies were delivered continuously by intrathecal cannula for 6 weeks and the animals perfused 2 weeks after delivery had ceased. Both antibodies were stained less intensely than at the 5wk time-point. A, anti-Nogo (green) was found distributed around the edges of the lesion cavity and on the surface of the cord but little remained within the parenchyma; B, more of the anti-MAG (green) remained within the spinal cord. Blue, GFAP, Red (A), NF200, (B), endogenous MAG. Scale bar: 500µm.

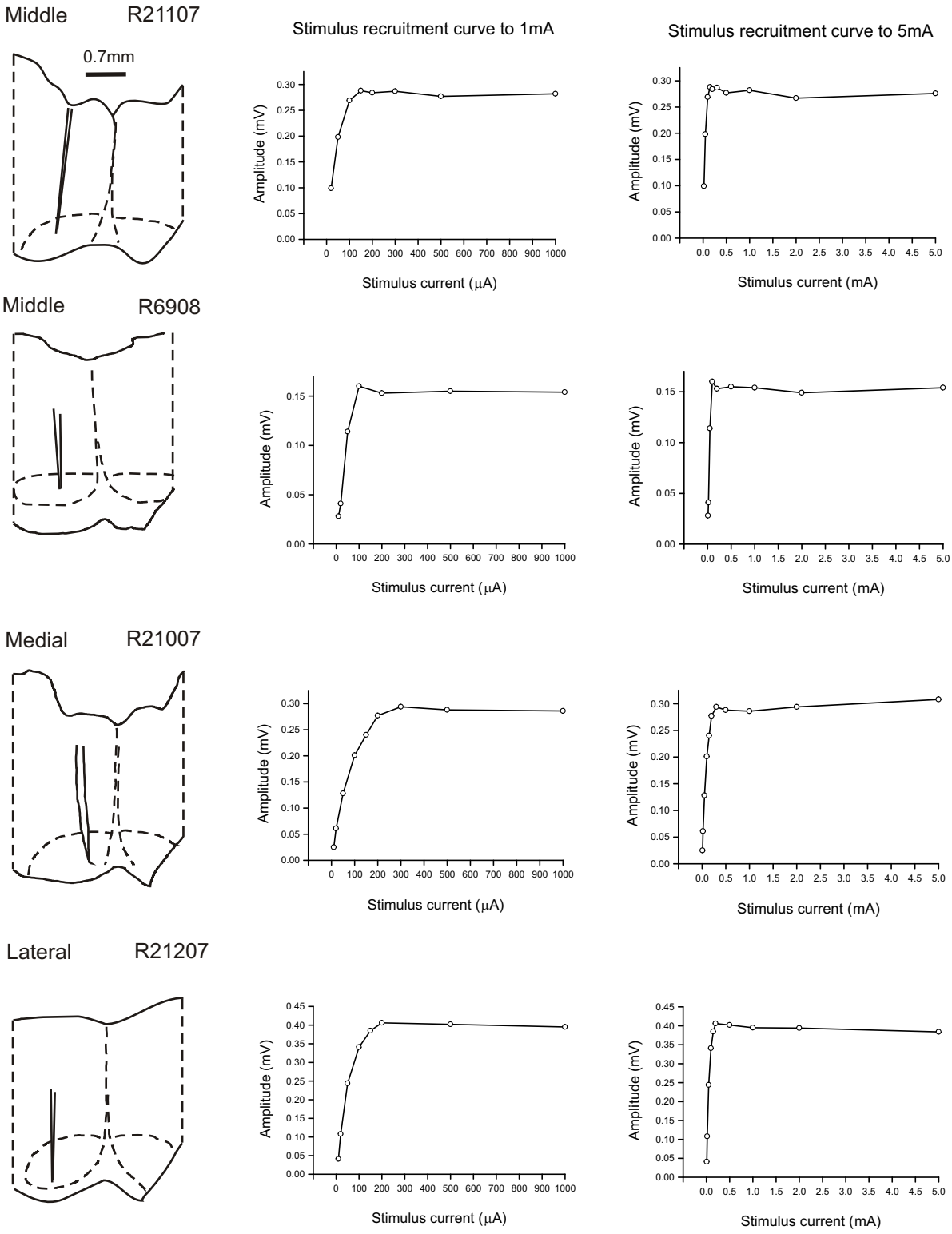


**Figure 4-6 Examples of pyramidal stimulus-recruitment curves and corresponding electrode positions for SD animals**

The diagrams to the left show reconstructions of stimulating electrode tracks. The plots to the right show corresponding stimulus-recruitment curves, one for stimulation up to 1mA and another up to 5mA.

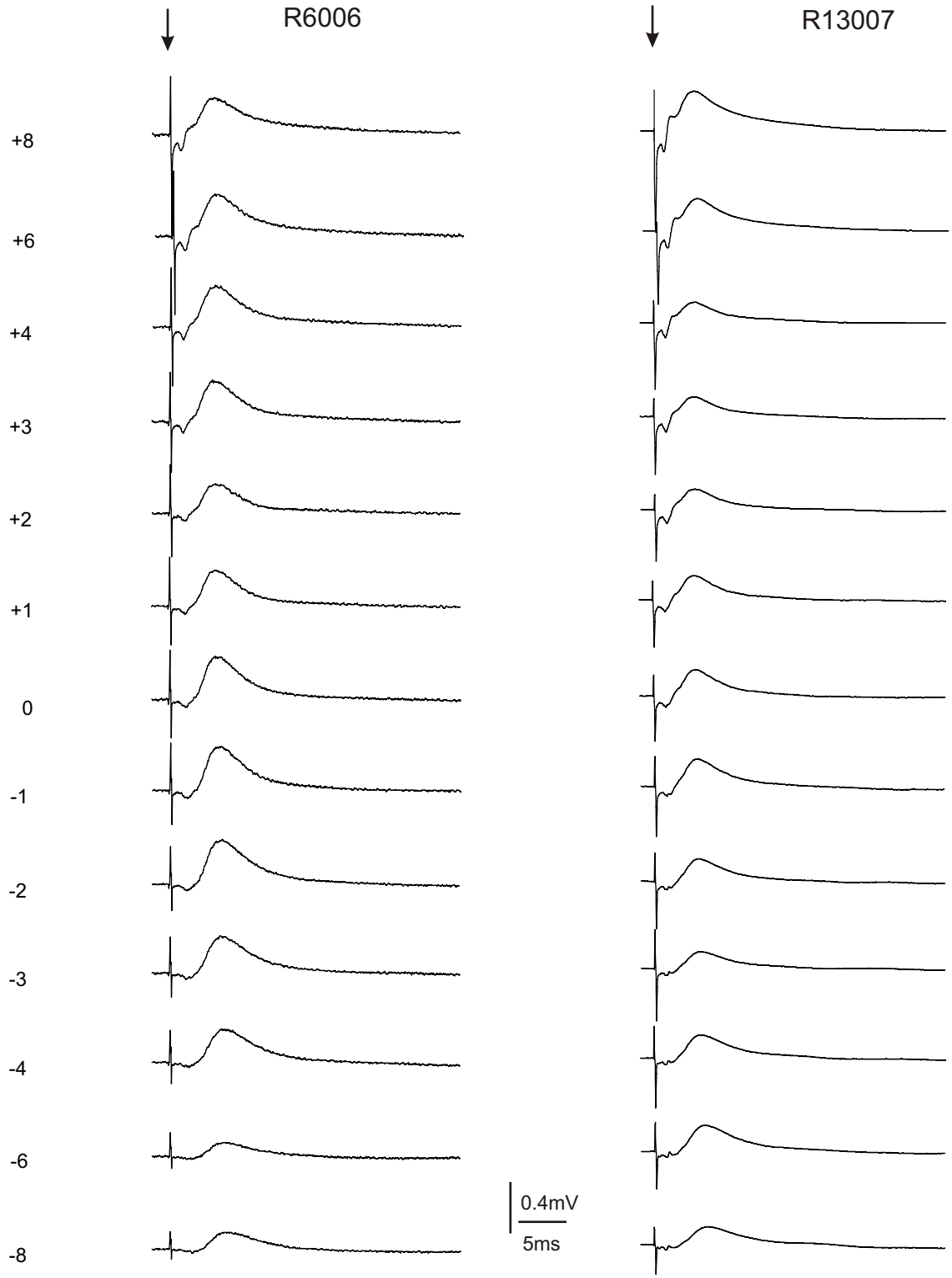


**Figure 4-7 Examples of CDPs evoked by pyramidal stimulation in normal animals**
Each column of traces shows recordings made from one animal. The recordings were made at 1mm intervals from 8mm rostral to 8mm caudal to the C4/5 segmental border as indicated. Traces recorded at +7, +5, -5, and -7mm are omitted. The traces represent averages of 50 sweeps and the calibrations apply to all traces. The arrows indicate stimulus artifacts.

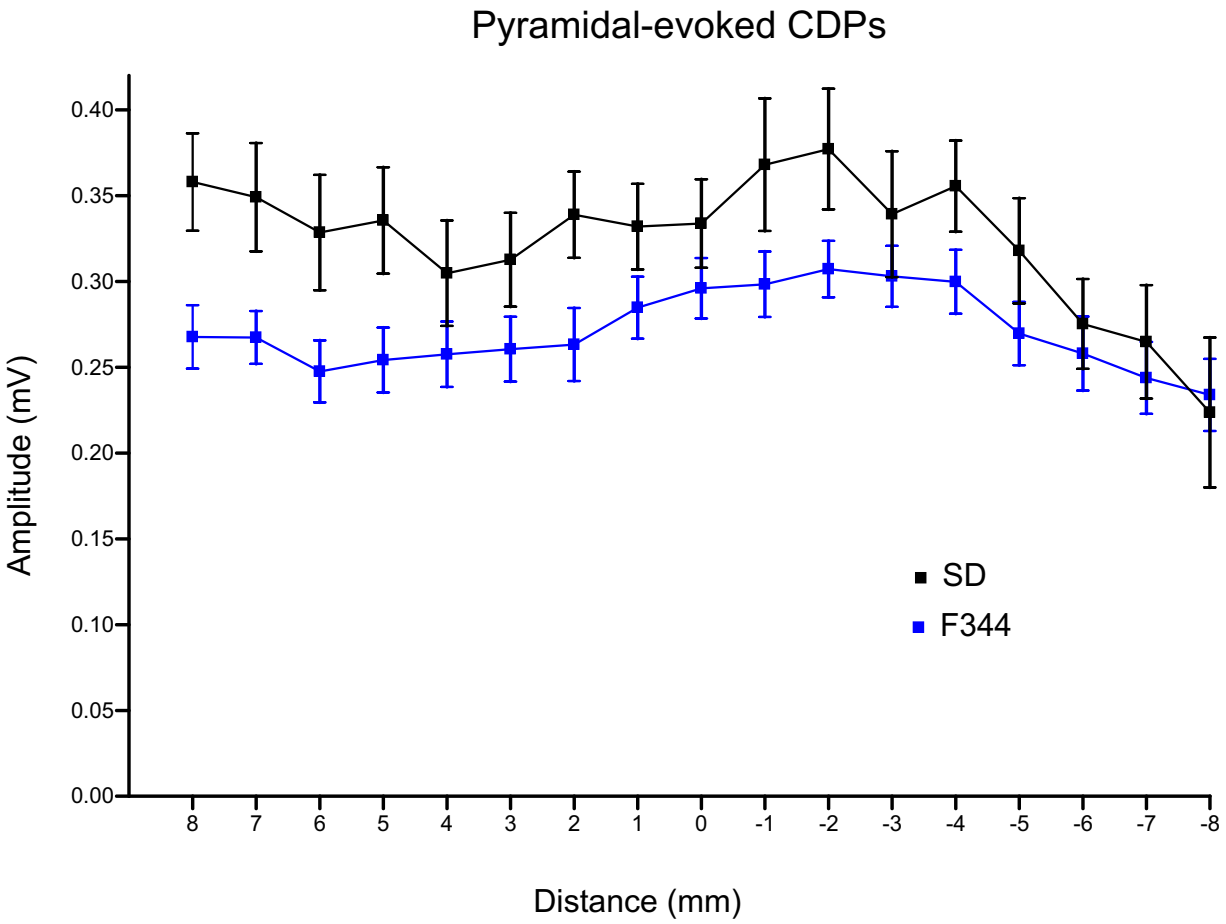


**Figure 4-8 Amplitudes of pyramidal-evoked CDPs recorded in the normal group**
The plot shows the amplitudes of CDPs recorded over the cervical spinal cord in response to pyramidal stimulation in the normal SD animals (n=11). The plot for normal F344 animals (n=18) from chapter 2 is shown for comparison. CDP amplitudes are averaged for all animals in each group, each data point showing mean +/- SEM. Recording positions are shown relative to the C4/5 border (0 mm) where dorsal column lesions were made in lesioned groups. In both SD and F344 rats, the distributions of CDP amplitudes evoked by pyramidal stimulation were fairly flat over most of the cervical cord but declines in amplitudes at further caudal locations. The amplitudes were around 0.3 mV in F344 rats and 0.35mV in SD rats. The difference are not significant.

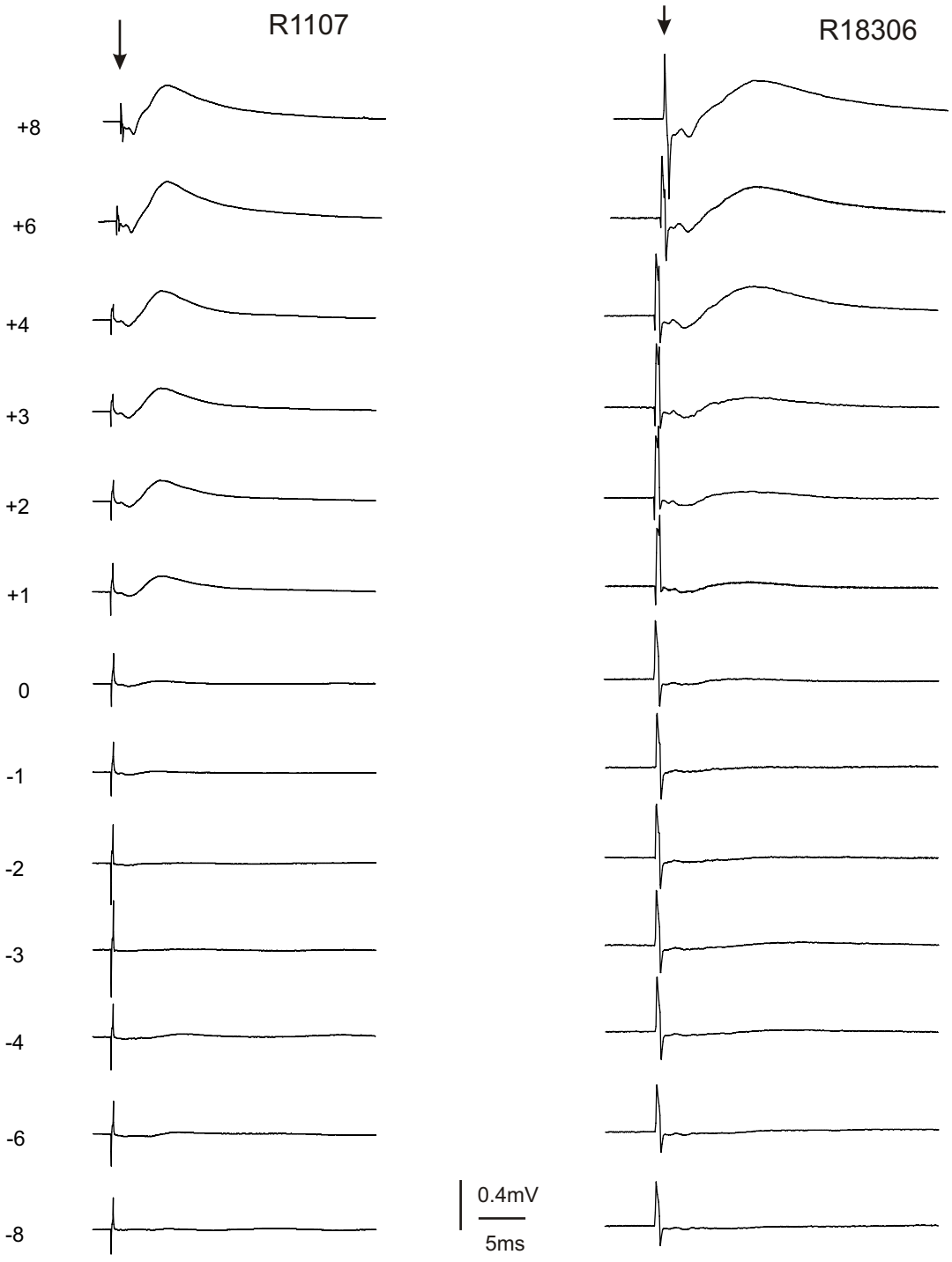


**Figure 4-9 Examples of CDPs evoked by pyramidal stimulation in the vehicle treated group**

Each column of traces shows recordings made from one animal. The recordings were recorded at 1mm intervals from 8mm rostral to 8mm caudal to the C4/5 segmental border as indicated. Traces recorded at +7, +5, -5, and -7mm are omitted. The traces represent averages of 50 sweeps and the calibrations apply to all traces. The arrows indicate stimulus artifacts.

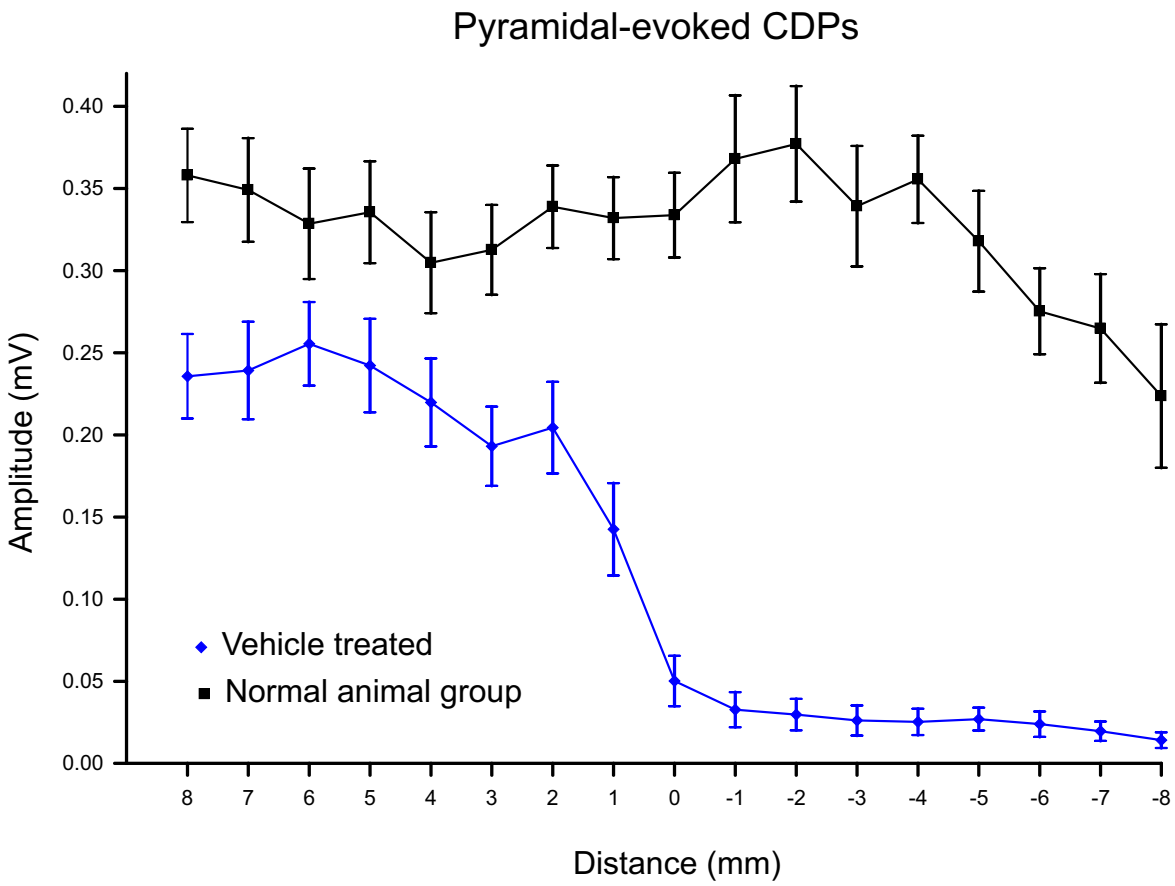


**Figure 4-10 Amplitudes of pyramidal-evoked CDPs recorded in the vehicle treated group**

The plot shows the amplitudes of CDPs recorded over the cervical spinal cord in response to pyramidal stimulation in the vehicle group (n=13). The previous plot for the normal group is also shown for comparison. CDP amplitudes are averaged for all animals in each group, each data point showing mean +/- SEM. Recording positions are shown relative to the C4/5 border (0 mm) where dorsal column lesions were made in lesioned groups. Compared to those recorded in normal animals, CDPs above the lesion were significantly smaller in the vehicle group. Small CDPs were detectable below the lesion.

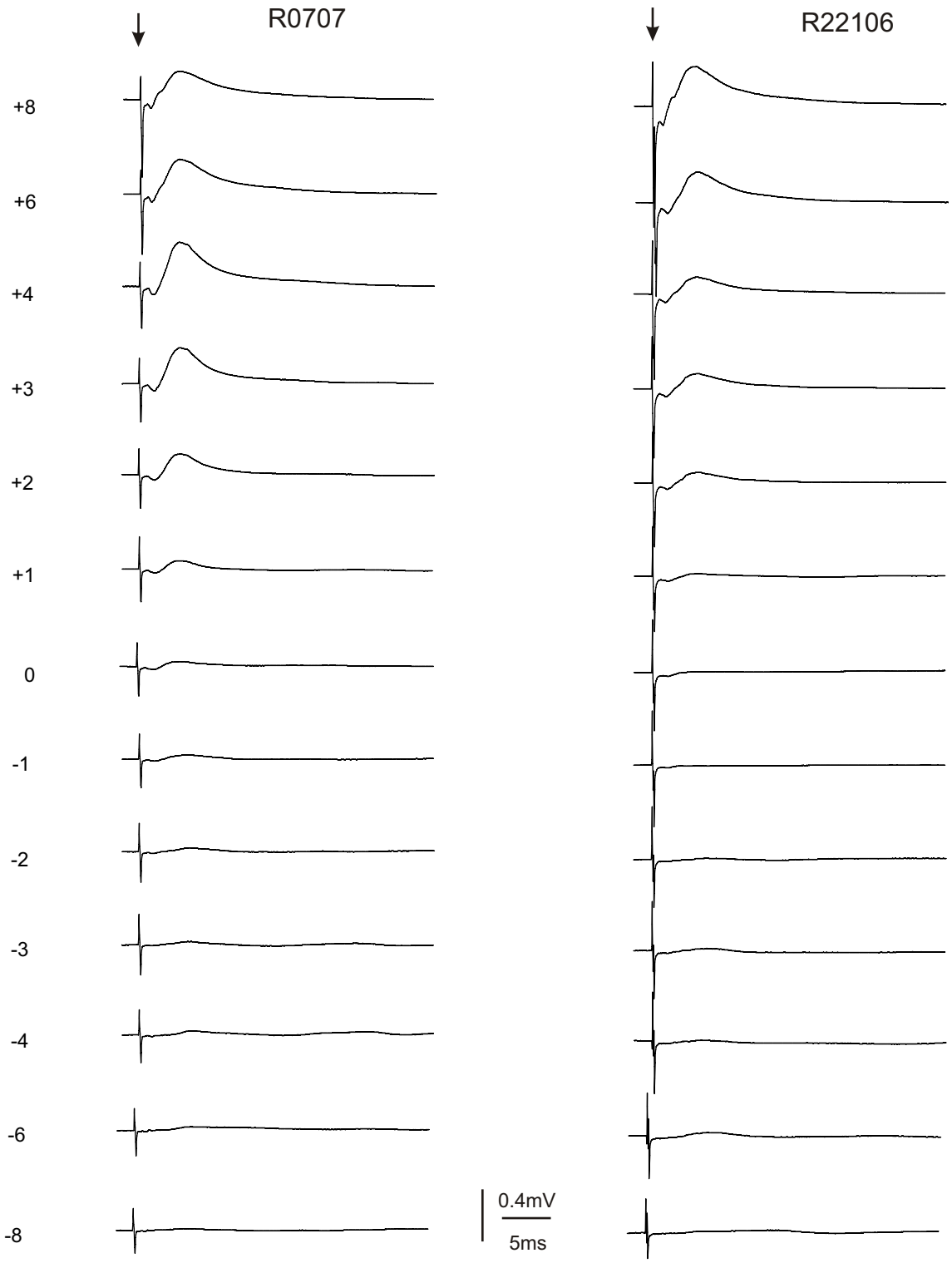


**Figure 4-11 Examples of CDPs evoked by pyramidal stimulation in the anti-Nogo treated group**

Each column of traces shows recordings made from one animal. The recordings were recorded at 1mm intervals from 8mm rostral to 8mm caudal to the C4/5 segmental border as indicated. Traces recorded at +7, +5, -5, and -7mm are omitted. The traces represent averages of 50 sweeps and the calibrations apply to all traces. The arrows indicate stimulus artifacts.

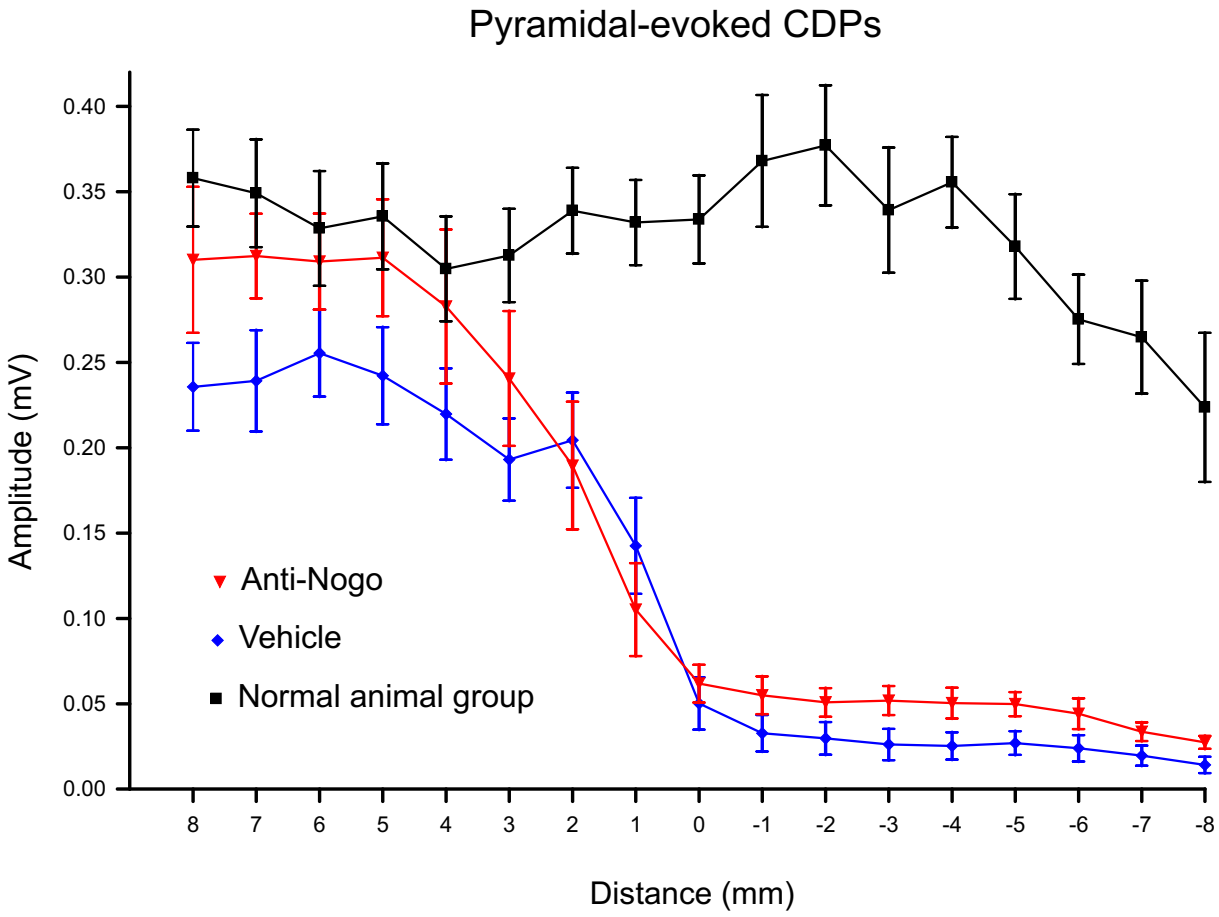


**Figure 4-12 Amplitudes of pyramidal-evoked CDPs recorded in the anti-Nogo treated group**

The plot shows the amplitudes of CDPs recorded over the cervical spinal cord in response to pyramidal stimulation in the anti-Nogo group (n=10). The previous plots for the normal group and for the vehicle group are also shown for comparison. CDP amplitudes are averaged for all animals in each group, each data point showing mean +/- SEM. Recording positions are shown relative to the C4/5 border (0 mm) where dorsal column lesions were made in lesioned groups. CDPs below the lesion tended to be larger in the anti-Nogo treated animals than vehicle treated but the difference was not significant. CDPs above the lesion were larger compared to those recorded in the vehicle group and the difference was significant at some locations.

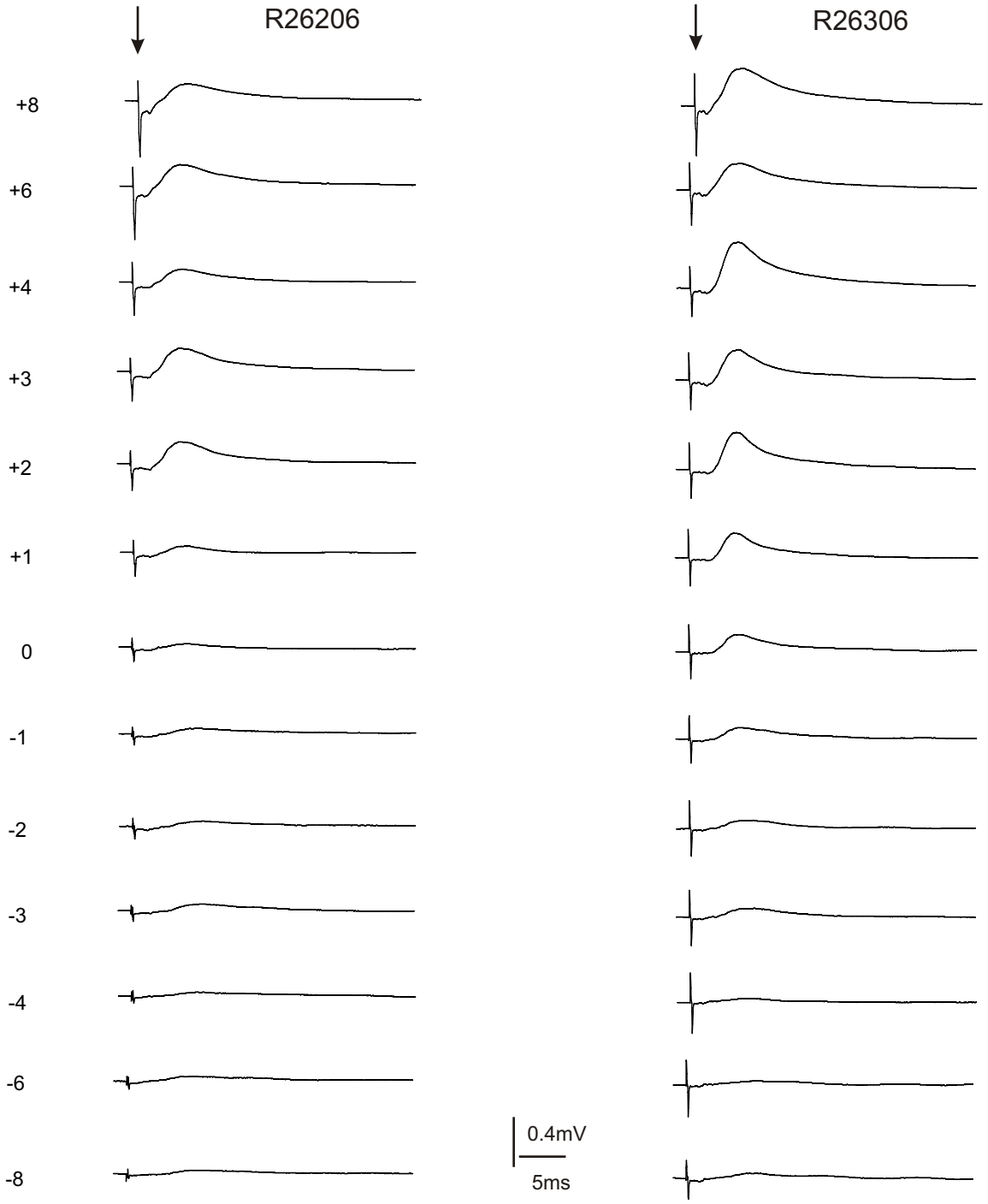


**Figure 4-13 Examples of CDPs evoked by pyramidal stimulation in the anti-MAG treated group**

Each column of traces shows recordings made from one animal. The recordings were recorded at 1mm intervals from 8mm rostral to 8mm caudal to the C4/5 segmental border as indicated. Traces recorded at +7, +5, -5, and -7mm are omitted. The traces represent averages of 50 sweeps and the calibrations apply to all traces. The arrows indicate stimulus artifacts.

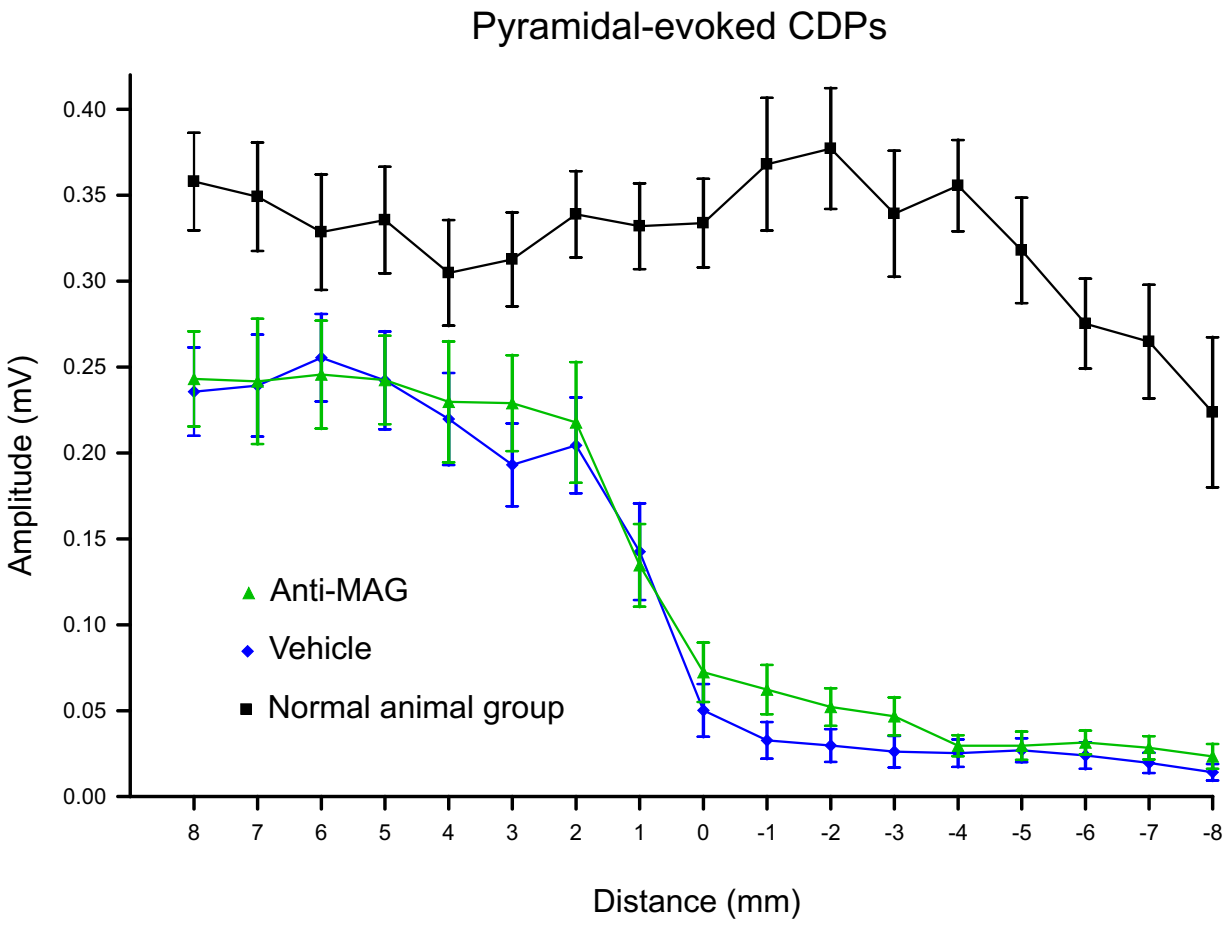


**Figure 4-14 Amplitudes of pyramidal-evoked CDPs recorded in the anti-MAG treated group**

The plot shows the amplitudes of CDPs recorded over the cervical spinal cord in response to pyramidal stimulation in the anti-MAG group (n=8). The previous plots for the normal group and for the vehicle group are also shown for comparison. CDP amplitudes are averaged for all animals in each group, each data point showing mean +/- SEM. Recording positions are shown relative to the C4/5 border (0 mm) where dorsal column lesions were made in lesioned groups. In the anti-MAG group, the distribution of CDPs was almost identical to those recorded in the vehicle group.

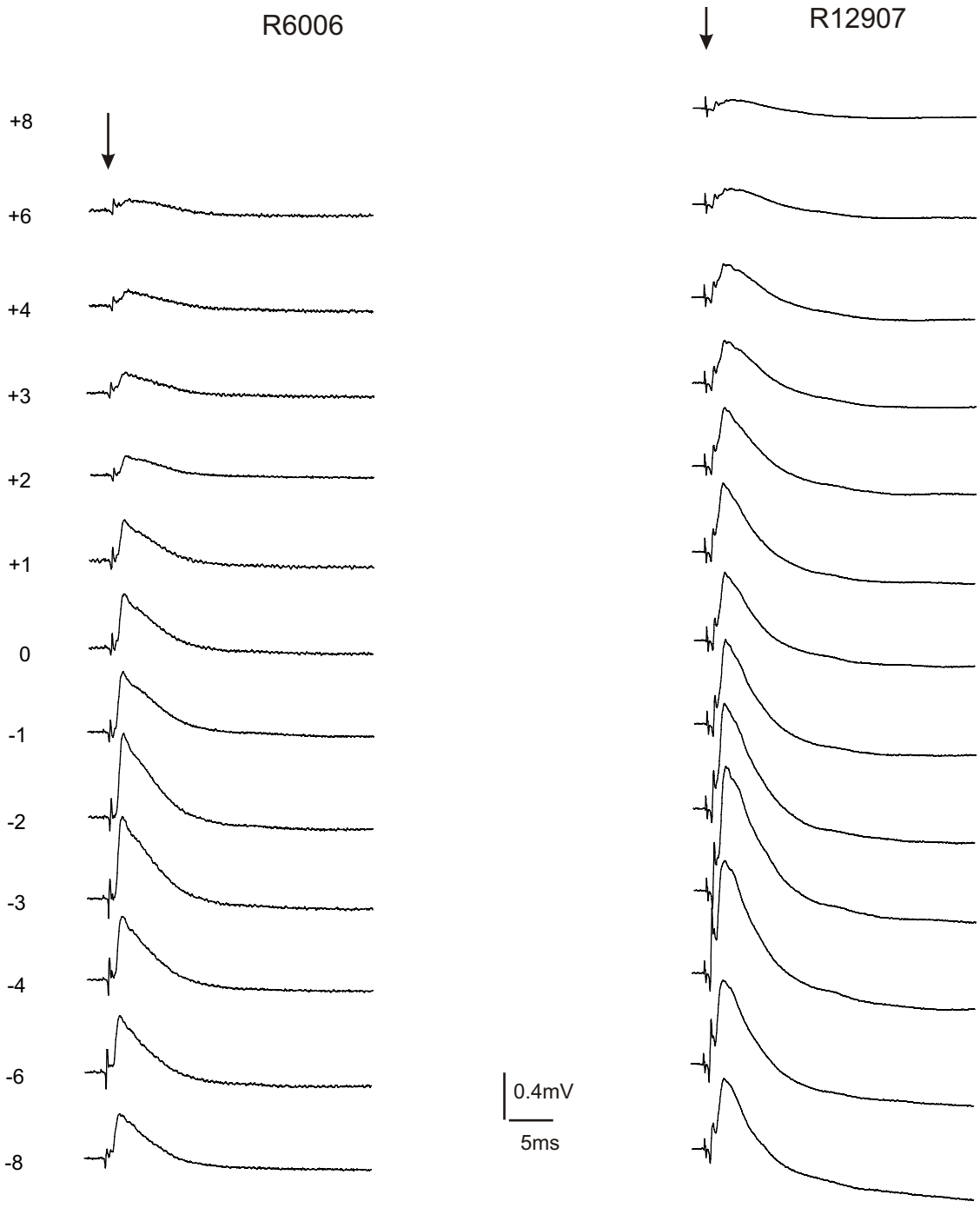


**Figure 4-15 Examples of CDPs evoked by radial nerve stimulation in the normal animal group**

Each column of traces shows recordings made from one animal. The recordings were recorded at 1mm intervals from 8mm rostral to 8mm caudal to the C4/5 segmental border as indicated. Traces recorded at +7, +5, -5, and -7mm are omitted. The traces represent averages of 25 sweeps and the calibrations apply to all traces. The arrows indicate stimulus artifacts.

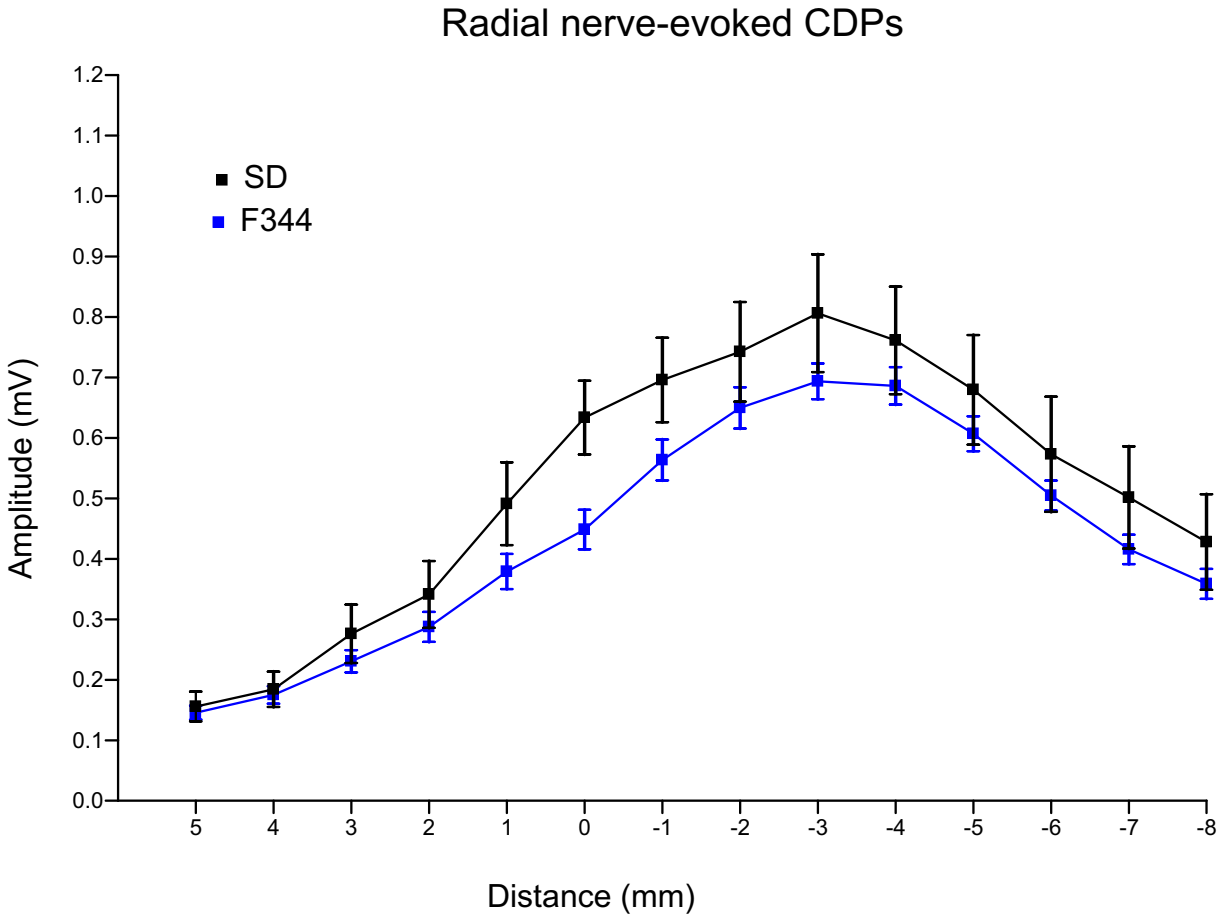


**Figure 4-16 Amplitudes of radial nerve-evoked CDPs recorded in normal SD animals compared to F344's**

The plots show the amplitudes of CDPs recorded over the cervical spinal cord in response to radial nerve stimulation in the normal animal groups. Recordings were made from normal SD (n=9) and F344 (n=22) rats. CDP amplitudes are averaged for all animals in each group, each data point showing mean +/- SEM. Recording positions are shown relative to the C4/5 border (0 mm) where dorsal column lesions were made in lesioned groups. In both SD and F344 rats, the largest potentials are produced between 0 and -5mm which corresponds to the C5 and C6 segments where radial nerve afferents enter the cord. CDPs of gradually declining amplitude are, however, evoked for several segments above and below this. The amplitudes of the biggest CDPs were 0.7mV in F344 rats and around 0.8mV in SD rats.

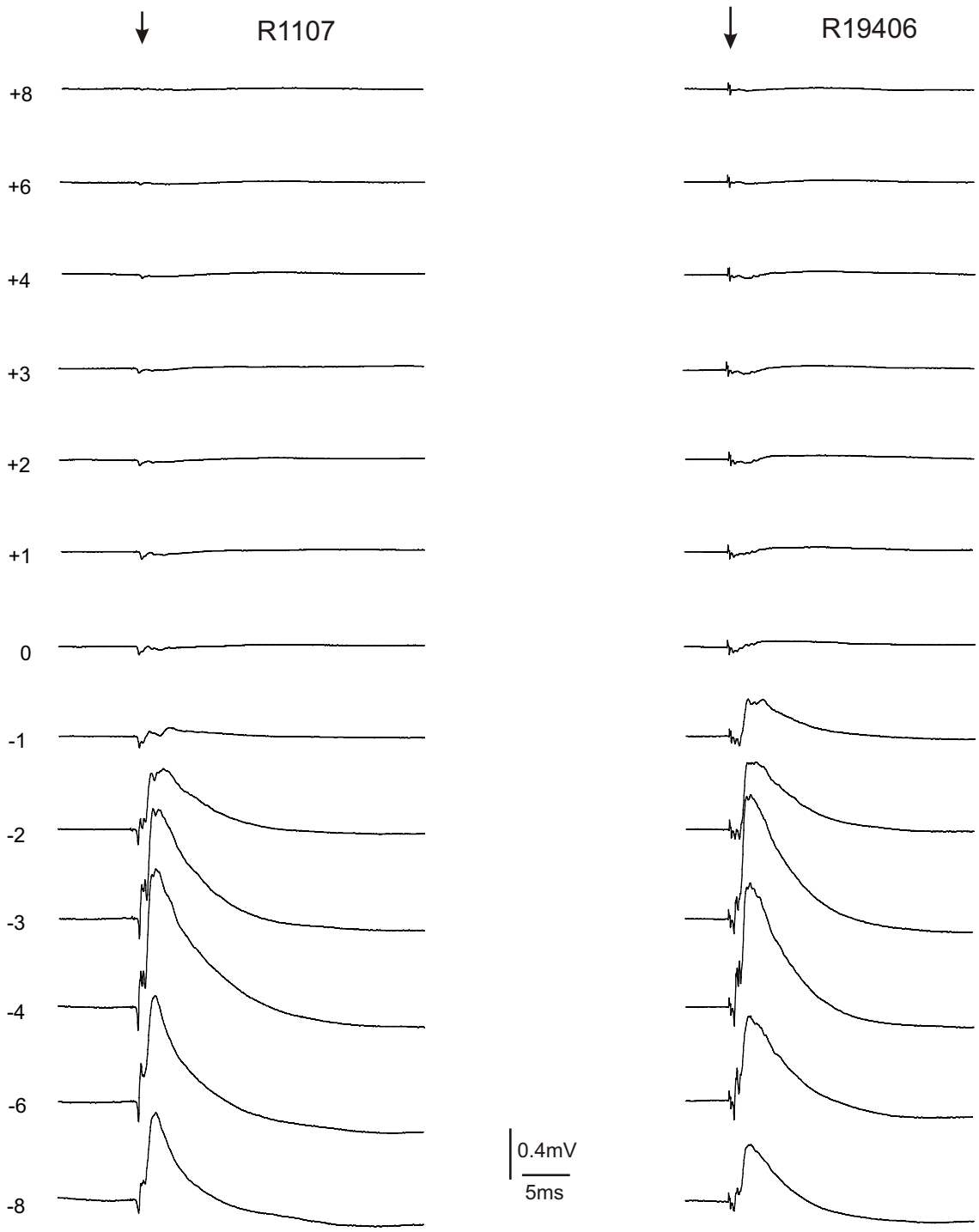


**Figure 4-17 Examples of CDPs evoked by radial nerve stimulation in the vehicle treated group**
Each column of traces shows recordings made from one animal. The recordings were recorded at 1mm intervals from 8mm rostral to 8mm caudal to the C4/5 segmental border as indicated. Traces recorded at +7, +5, -5, and -7mm are omitted. The traces represent averages of 25 sweeps and the calibrations apply to all traces. The arrows indicate stimulus artifacts.

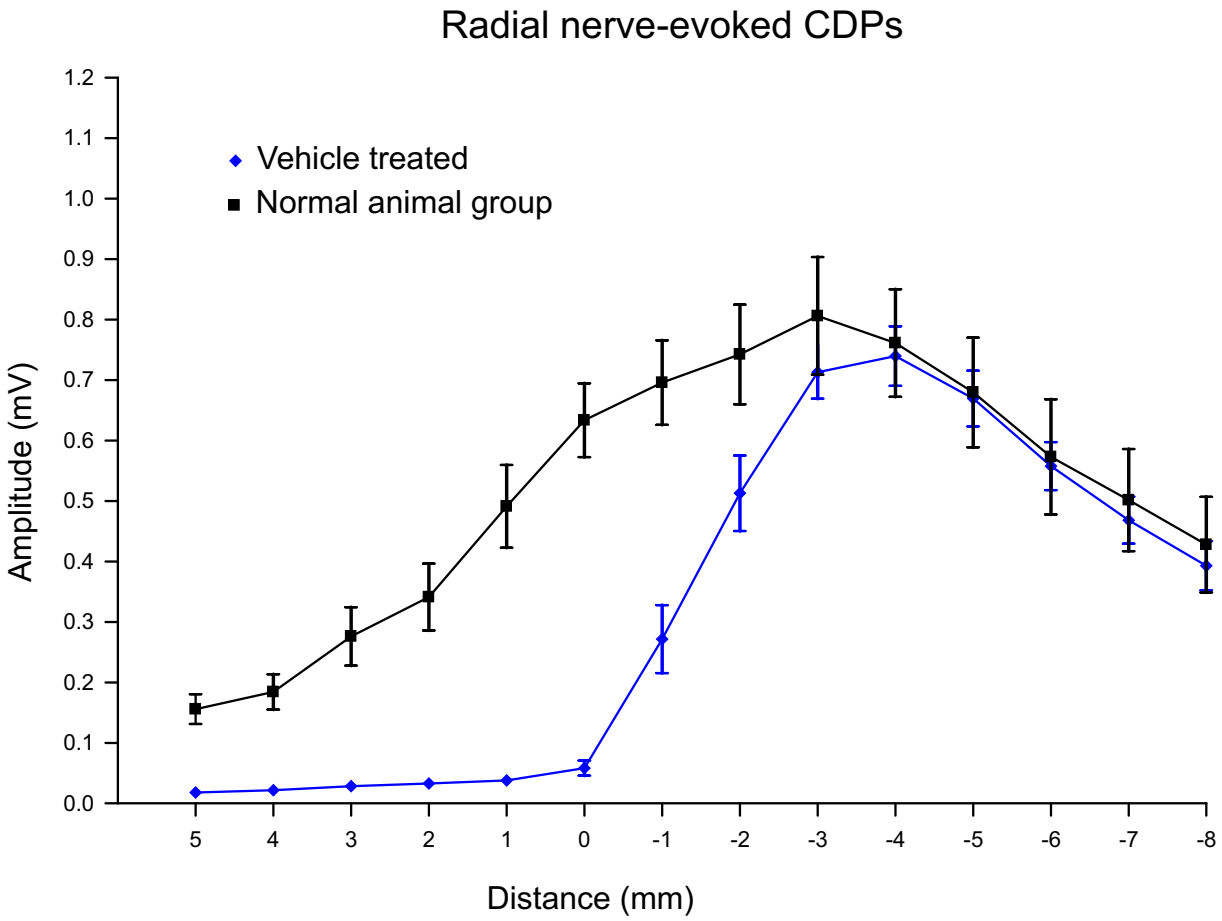


**Figure 4-18 Amplitudes of radial nerve-evoked CDPs recorded in the vehicle treated group**

The plot shows the amplitudes of CDPs recorded over the cervical spinal cord in response to radial nerve stimulation in the vehicle group (n=14). The previous plot for the normal group is also shown for comparison. CDP amplitudes are averaged for all animals in each group, each data point showing mean +/- SEM. Recording positions are shown relative to the C4/5 border (0 mm) where dorsal column lesions were made in lesioned groups. CDPs above the lesion in the vehicle group were almost abolished. CDPs below the lesion were almost same as those in normal animals.

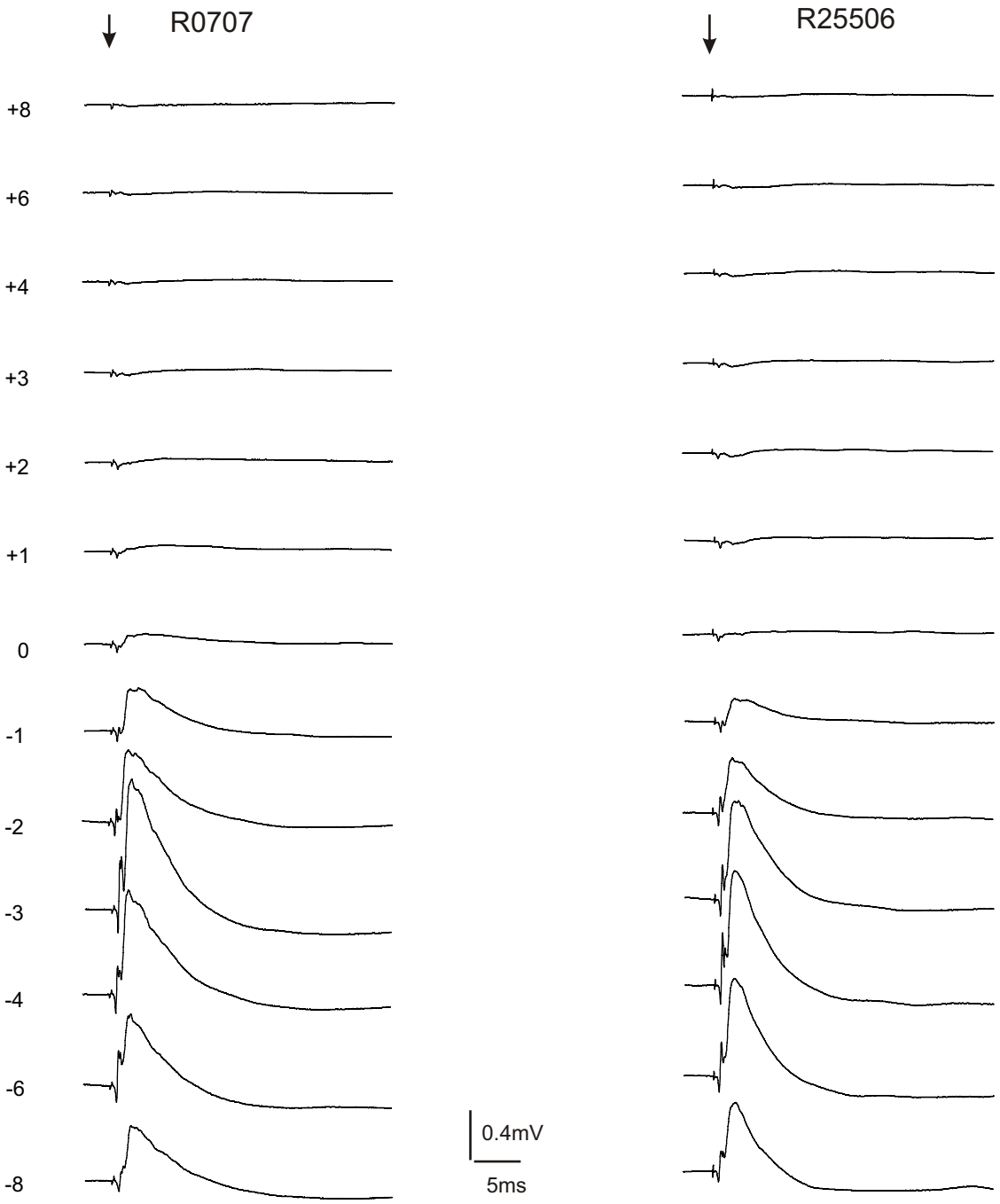


**Figure 4-19 Examples of CDPs evoked by radial nerve stimulation in the anti-Nogo treated group**
Each column of traces shows recordings made from one animal. The recordings were recorded at 1mm intervals from 8mm rostral to 8mm caudal to the C4/5 segmental border as indicated. Traces recorded at +7, +5, -5, and -7mm are omitted. The traces represent averages of 25 sweeps and the calibrations apply to all traces. The arrows indicate stimulus artifacts.

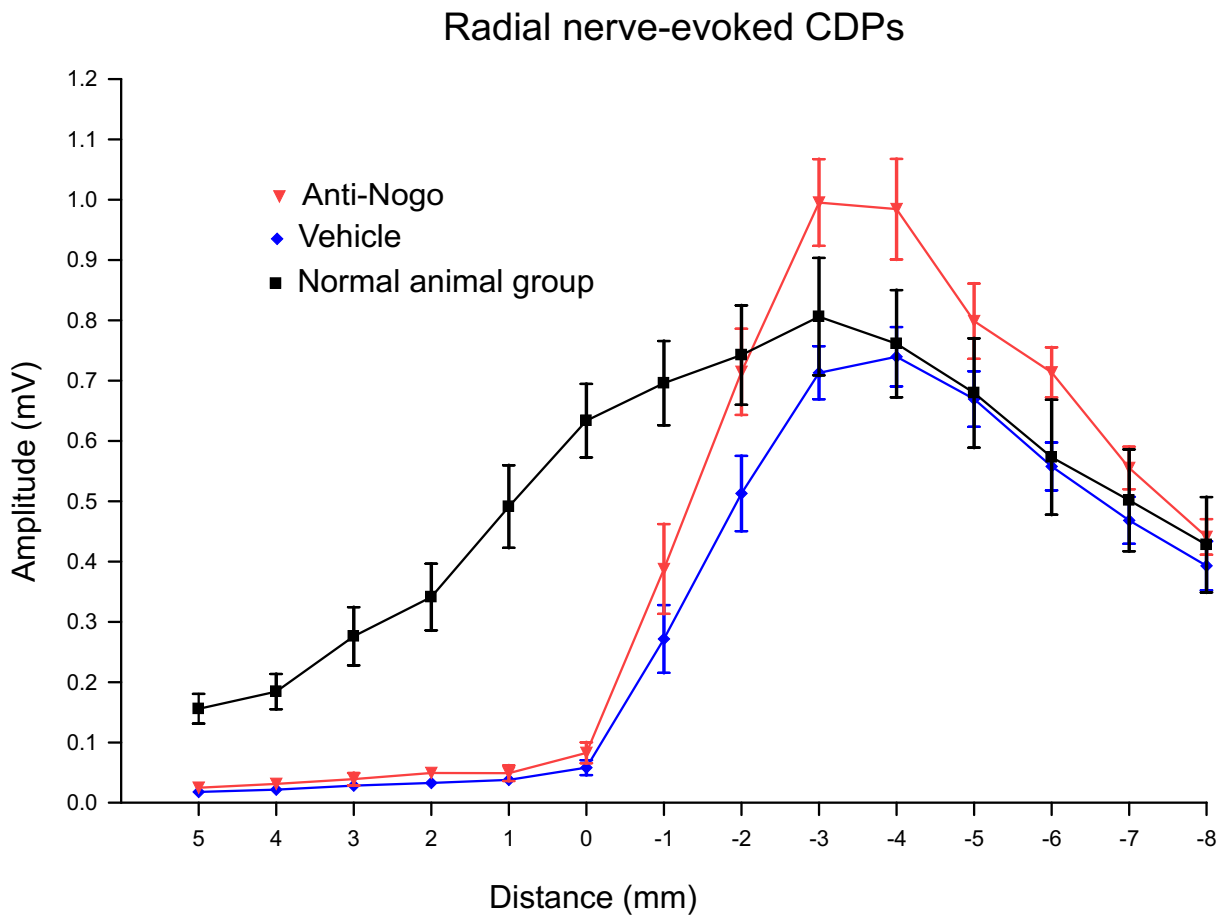


**Figure 4-20 Amplitudes of radial nerve-evoked CDPs recorded in the anti-Nogo treated group**

The plot shows the amplitudes of CDPs recorded over the cervical spinal cord in response to radial nerve stimulation in the anti-Nogo group (n=10). The previous plots for the normal group and for the vehicle group are also shown for comparison. CDP amplitudes are averaged for all animals in each group, each data point showing mean +/- SEM. Recording positions are shown relative to the C4/5 border (0 mm) where dorsal column lesions were made in lesioned groups. Below the lesion, CDPs were larger in the anti-Nogo treated group than those recorded in the vehicle group. The differences were significant at -3mm and -4mm. They were also larger than CDPs in normal animals at these caudal locations but the difference did not reach significance.

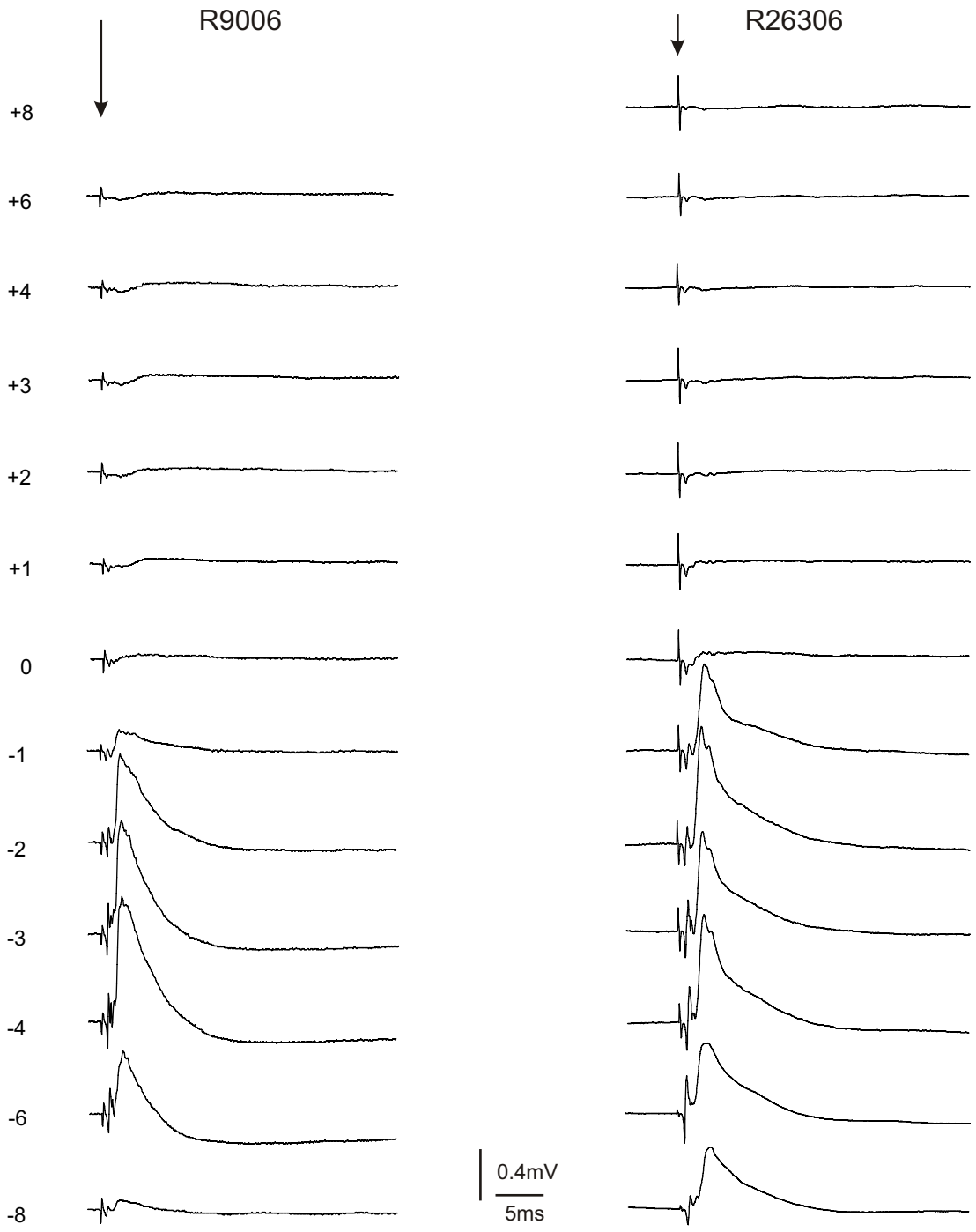


**Figure 4-21 Examples of CDPs evoked by radial nerve stimulation in the anti-MAG treated group**

Each column of traces shows recordings made from one animal. The recordings were recorded at 1mm intervals from 8mm rostral to 8mm caudal to the C4/5 segmental border as indicated. Traces recorded at +7, +5, -5, and -7mm are omitted. The traces represent averages of 25 sweeps and the calibrations apply to all traces. The arrows indicate stimulus artifacts.

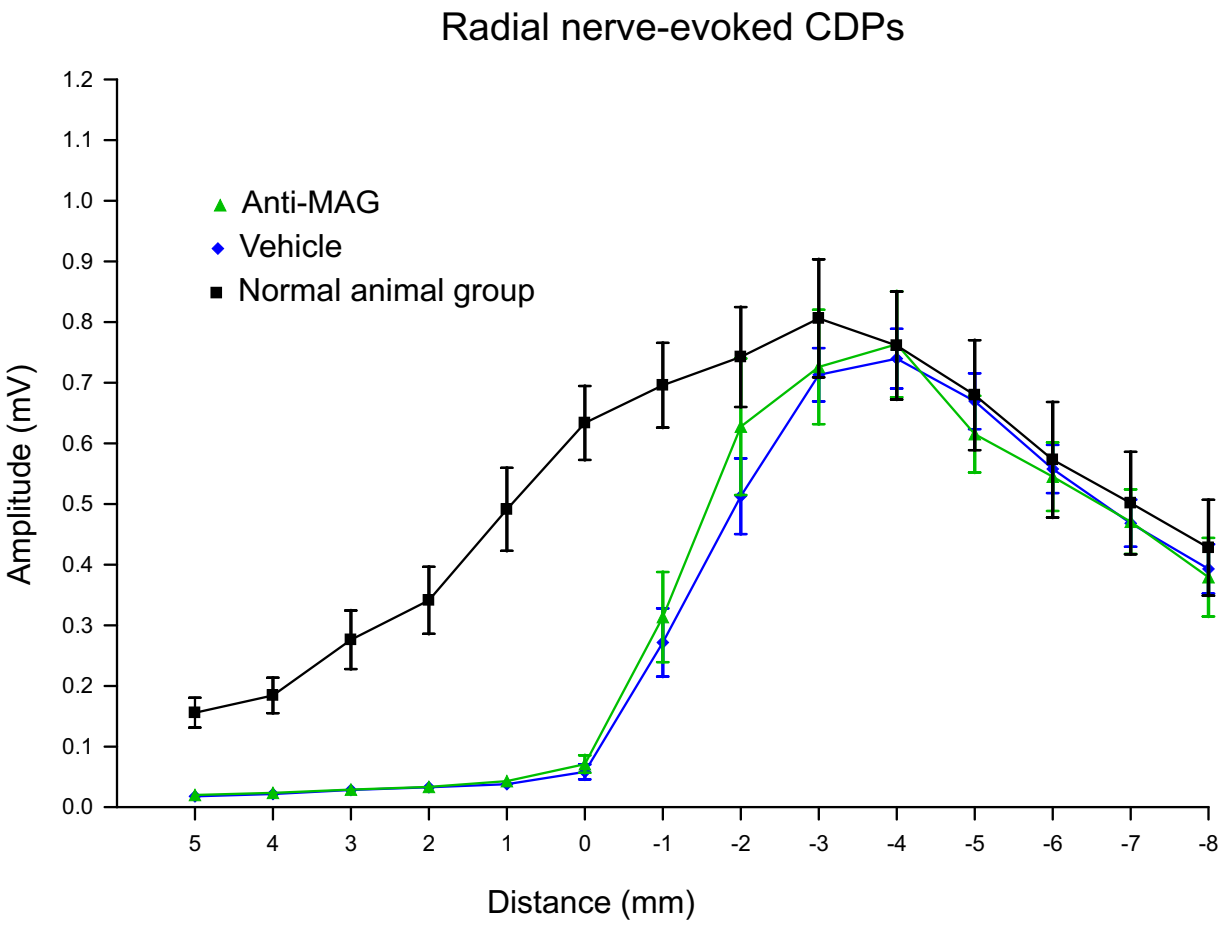


**Figure 4-22 Amplitudes of radial nerve-evoked CDPs recorded in the anti-MAG treated group**

The plot shows the amplitudes of CDPs recorded over the cervical spinal cord in response to radial nerve stimulation in the anti-MAG group (n=9). The previous plots for the normal group and for the vehicle group are also shown for comparison. CDP amplitudes are averaged for all animals in each group, each data point showing mean +/- SEM. Recording positions are shown relative to the C4/5 border (0 mm) where dorsal column lesions were made in lesioned groups. In the anti-MAG group, CDPs were almost identical to those recorded in the vehicle group.

# Final discussion and future directions

Functional recovery following SCI can be assessed by behavioural tests and electrophysiological approaches. Behavioural tests can provide evidence of improved performance in the ability of animals to fulfil sensorimotor tasks. However, the mechanisms underlying the improved function can not be elucidated and the level at which these mechanisms operate (supraspinal or spinal) are also undetermined. To investigate the mechanisms underlying recovery of function, many studies combine behavioural tests of function with anatomical assessments and draw conclusions based on correlation between the two. For example, improved functional recovery and 'sprouting' have been observed in the same animals leading to the idea that sprouting is one mechanism supporting functional recovery. However, 'sprouting' reported using tracer labelling might not always be genuine. It is possible that injury could change the properties of axons and consequently enhance their ability to transport tracers. In other words, an apparently greater density of axons may be due to enhanced labelling rather than new sprouting. Even if there is genuine sprouting following the injury, anatomical methods can not show whether functional connections have been formed. An advantage of the electrophysiological approach is that it can evaluate the function of specific spinal pathways and has the potential to provide reliable information about changes in functional connections with target pathways. A limitation of the electrophysiological approach is that some spinal pathways are difficult to study. The corticospinal and sensory pathways studied in this thesis are among the most convenient. These same pathways are also relatively accessible to study in man using non-invasive approaches. For example, intraoperative somatosensory evoked potentials and motor evoked potentials have been monitored during spine surgery and have been used for assessing changes in function in patients with SCI (Hyun et al. 2009; Sykova et al. 2006).

Electrophysiological results in this project support previous evidence that a lesion to the spinal cord alone can induce a modest degree of spontaneous plasticity in the terminations of sensorimotor pathways. As mentioned before, one of the main underlying mechanisms for plasticity is anatomical sprouting. However, synaptic plasticity is another alternative mechanism and has been shown to occur even as partial normal brain function. Long-term potentiation in the hippocampus is an example (DeFelipe 2006). Synaptic plasticity can include

changes in the quantity of neurotransmitter released at a synapse and changes in how effectively cells respond to those neurotransmitters. There are two known molecular mechanisms for synaptic plasticity. The first mechanism involves modification of existing synaptic proteins resulting in altered synaptic function (Shi et al. 1999). The other mechanism depends on second messenger neurotransmitters regulating gene transcription and changes in the levels of key proteins at synapses. This second mechanism can be triggered by protein phosphorylation but takes longer and lasts longer, providing the mechanism for long-lasting memory storage. The strength of a synapse also depends on the number of ion channels it has. Several facts suggest that neurons change the density of receptors on their postsynaptic membranes as a mechanism for changing their own excitability in response to stimuli. In a dynamic process that is maintained in equilibrium, alpha-amino-3-hydroxy-5-methyl-4-isoxazolepropionic acid receptor (AMPA receptor) is added to the membrane by exocytosis and removed by endocytosis (Pérez-Otaño et al. 2005). These processes, and by extension the number of receptors on the membrane, can be altered by synaptic activity. Since long-term potentiation relies on the influx of $Ca^{2+}$ through NMDAN-methyl D-aspartate (NMDA) channels, synaptic plasticity may be due to changes in NMDA receptors, for example changes in their subunits to allow the concentration of $Ca^{2+}$ in the cell to be lowered more quickly (Shi et al. 1999; Pérez-Otaño et al. 2005).

One strategy for treating spinal cord injury is to enhance spontaneous plasticity. Apart from the use of cell transplantation and antibodies to myelin inhibitors as investigated in this thesis, other pharmacological interventions are reported to induce plasticity. These include neurotrophins and chondroitinase. Neurotrophic factors can promote axonal plasticity in the sensorimotor cortex and spinal cord (Zhou and Shine, 2003). The inhibitory effects of CSPGs can be degraded by ChABC which removes GAG chains from the protein core. ChABC has been shown to stimulate the sprouting of injured and uninjured fibres and promote improved recovery (Bradbury et al. 2002; Barritt et al. 2006). Electrophysiological data also suggest that an improved functional performance in the ChABC treated animals is consequent to reorganization of intact primary afferent terminals after SCI (Cafferty et al. 2008). There are therefore several potential means by which plasticity following spinal cord injury might be enhanced to maximise the

function of spared pathways. Our results show that the presence of OECs within the spinal cord does not enhance spontaneous plasticity. On the other hand, transmission in both corticospinal and sensory pathways was significantly enhanced by anti-Nogo antibody treatment.

In addition to the intervention and treatments described above there is evidence that rehabilitation training can augment functional outcome in the clinic (Forrest et al. 2008; Schubert et al. 2008). The underlying mechanisms of this are under investigation in animal models. A number of studies suggest that an enriched environment that promotes locomotion after SCI is beneficial for stepping performance in rats and mice (Iankhorst et al. 2001; Van Meeteren et al. 2003; Engesser-Cesar et al. 2005). Other studies have focused on task-specific training such as reaching training and treadmill training to improve specific functions. For example, step training improves stepping and stand training improves standing (De Leon et al. 1998). Reaching training promotes plasticity and task specific recovery in rats (Girgis et al. 2007). Edgerton and colleagues have intensively investigated the effects of treadmill training on functional recovery following SCI and confirmed that improved stepping performance can be achieved following task-specific training (Ichiyama et al. 2009; Cai et al. 2006). However, the location and nature of the changes in neural substrates underlying the behavioural improvements are not well understood. Plasticity after training could be induced by an increase in the amount of trophic factors. For example, voluntary exercise can maintain the level of BDNF (Ying et al. 2005). Repetitive patterns of activation at a synapse could change the properties of that synapse (Petruska et al. 2007; Wolpaw and Tennissen, 2001) or reinforce spinal pattern generators (Bradbury and McMahon, 2006).

There is some evidence that directly relates to the corticospinal tract. Thomas and Gorassini (2005) have reported that corticospinal tract function is increased by treadmill training after incomplete injury, although their assessment of the corticospinal tract used transcranial magnetic stimulation which is probably not specific for the corticospinal tract in the rat (Nielsen et al. 2007). It has also been reported that electrical stimulation of spared corticospinal axons augments their connection below an injury (Brus-Ramer et al. 2007). Finally, Girgis et al. (2007) have reported an increased collateral sprouting of corticospinal fibres at

the spinal level and expansion of part of the forelimb cortical area in animals with cervical spinal cord injuries when they were subjected to reaching training.

However, training has not always resulted in positive improvements. There is evidence that training in one task may interfere with performance of another. Studies show that task-specific training might potentially diminish some functions while augmenting others. For example, when a spinal cat is trained to stand it learns to stand, but steps very poorly (De Leon et al. 1998). Therefore, the mechanisms of rehabilitative training have to be investigated and clearly understood in order to design the most appropriate form of training.

Spinal cord injury is a multifaceted problem and successful treatment may eventually involve strategies that combine targeting of one or more of the strategies of neuroprotection, axonal regeneration, plasticity, and rehabilitation. It might also be possible to combine several plasticity promoting treatments. For example, anti-Nogo antibody treatment could be combined with ChABC treatment if different mechanisms are involved so that a synergistic effect is obtained. Combining treatments that promote plasticity with rehabilitative training is a combination which is increasingly being investigated. In a recent study, the effect of combination of ChABC treatment and physical rehabilitation was investigated and it was found that ChABC treatment opens a window during which rehabilitation can enhance functional recovery (Garcia-Alias et al. 2009).

However, although plasticity plays a role in functional recovery following SCI, it does not always result in a beneficial outcome. For instance, sprouting following SCI is thought to contribute to autonomic dysreflexia and pain (Weaver et al. 2006; Finnerup and Jensen, 2004). Some potential treatments have the possibility to enhance the ‘bad’ plasticity. Treadmill training has been reported to exaggerate autonomic dysreflexia through a combination of enhanced vascular reactivity and central plasticity (Laird et al. 2009; Fawcett and Curt, 2009).

Combinations of individual beneficial treatments do not always provide better recovery following injury. Furthermore, adverse effects of a combinatorial treatment have been reported by a number of studies. Maier and colleagues

(2009) compared the effects of anti-Nogo antibody treatment and treadmill training in rats with incomplete SCI. Even though functional recovery was observed in both groups, axonal regeneration and sprouting of descending systems was seen only in rats with antibody treatment. Surprisingly, combinatorial treatment with both antibody and training produced a poorer locomotor performance, compared to individual treatments. It was suggested that the mechanisms underlying these changes with each treatment are not only different but possibly competitive. Therefore, a full understanding of the mechanism underlying each individual treatment as well as their potential interactions will be crucial to finding the most effective combination for future therapies.

This thesis has focused, as does much of spinal cord injury research, on the changes that occurred in the spinal cord following SCI and potential treatments. However, changes at a supraspinal level are substantial and can not be ignored (Curt et al. 2002; Corbetta et al. 2002). Changes at a supraspinal level including the cortical level may play an important role in functional recovery (Fouad et al. 2001) and modulating plasticity at a supraspinal level may prove just as important in promoting better functional recovery.

In the future, enhancing beneficial plasticity at both supraspinal and spinal cord levels should be a feasible strategy for improving sensorimotor functions based on maximising the function of spared tracts. However, this strategy is likely to be most beneficial in patients with a certain degree of spared neuronal hardware as only then can plasticity effectively translate into functional recovery. Future research in this area will need to focus on obtaining a better understanding of how different plasticity inducing treatments actually bring about improved function and perhaps better understand how treatments can be optimally combined and/or linked to rehabilitation training to maximize functional recovery while avoiding the potential adverse effect of innappropriate neural re-organization. Appropriate combinatorial treatment of pharmacological and rehabilitative training will potentially maximize the spontaneous plasticity so that better functional recovery can be attained.

# List of References

Acevedo L, Yu J, Erdjument-Bromage H, Miao RQ, Kim JE, Fulton D, Tempst P, Strittmatter SM, Sessa WC. A new role for Nogo as a regulator of vascular remodeling. Nat Med. 2004 Apr; 10(4):382-8.

Ackery A, Tator C, Krassioukov A. A global perspective on spinal cord injury epidemiology. J Neurotrauma. 2004 Oct; 21(10):1355-70.

Adamson J, Zappulla RA, Fraser A, Ryder J, Malis LI. Effects of selective spinal cord lesions on the spinal motor evoked potential (MEP) in the rat. Electroencephalogr Clin Neurophysiol. 1989 Nov-Dec;74(6):469-80.

Afifi AK and Bergman RA. Functional neuroanatomy. Lange Medical Books/McGraw-Hill, Medical Publishing Division. 2005.

Aito S, D'Andrea M, Werhagen L. Spinal cord injuries due to diving accidents. Spinal Cord. 2005 Feb; 43(2):109-16.

Akiyama Y, Honmou O, Kato T, Uede T, Hashi K, Kocsis JD. Transplantation of clonal neural precursor cells derived from adult human brain establishes functional peripheral myelin in the rat spinal cord. Exp Neurol. 2001 Jan; 167(1):27-39.

Akiyama Y, Radtke C, Kocsis JD. Remyelination of the rat spinal cord by transplantation of identified bone marrow stromal cells. J Neurosci. 2002 Aug 1; 22(15):6623-30.

Alabed YZ, Grados-Munro E, Ferraro GB, Hsieh SH, Fournier AE. Neuronal responses to myelin are mediated by rho kinase. J Neurochem. 2006 Mar; 96(6):1616-25.

Allen, A.R. Surgery of experimental lesions of spinal cord equivalent to crush injury of fracture dislocation. Preliminary report. J. Am, Med. Assoc. 1911; 57:878-880.

Alstermark B, Ogawa J, Isa T. Lack of monosynaptic corticomotoneuronal EPSPs in rats: disynaptic EPSPs mediated via reticulospinal neurons and polysynaptic EPSPs via segmental interneurons. J Neurophysiol. 2004 Apr; 91(4):1832-9.

American Spinal Injury Association. International standards for neurological classification of spinal cord injury. Chicago: ASIA; 2002. http://www.asia-spinalinjury.org

Anderson KD, Gunawan A and Steward O. Quantitative assessment of forelimb motor function after cervical spinal cord injury in rats: Relationship to the corticospinal tract. Exp Neurol. 2005 July ; 194(1):161-174.

Andrews MR, Stelzner DJ. Modification of the regenerative response of dorsal column axons by olfactory ensheathing cells or peripheral axotomy in adult rat. Exp Neurol. 2004 Dec; 190(2):311-27.

Anthes DL, Theriault E, Tator CH. Ultrastructural evidence for arteriolar vasospasm after spinal cord trauma. Neurosurgery. 1996 Oct; 39(4):804-14.

Aoki M, Fujito Y, Satomi H, Kurosawa Y, Kasaba T. The possible role of collateral sprouting in the functional restitution of corticospinal connections after spinal hemisection. Neurosci Res Sep 1986; 3 (6):617–27.

Araki T, Sasaki Y, Milbrandt J. Increased nuclear NAD biosynthesis and SIRT1 activation prevent axonal degeneration. Science. 2004 Aug 13; 305(5686):1010-3.

Arishima Y, Setoguchi T, Yamaura I, Yone K, Komiya S. Preventive effect of erythropoietin on spinal cord cell apoptosis following acute traumatic injury in rats. Spine (Phila Pa 1976). 2006 Oct 1; 31(21):2432-8.

Atwal, JK, Pinkston-Gosse J, Syken J, Stawicki S, Wu Y, Shatz C and Tessier-Lavigne M (2008) PirB is a functional receptor for myelin inhibitors of axonal regeneration. Science 322, 967-70.

Au E, Richter MW, Vincent AJ, Tetzlaff W, Aebersold R, Sage EH, Roskams AJ. SPARC from olfactory ensheathing cells stimulates Schwann cells to promote neurite outgrowth and enhances spinal cord repair. J Neurosci. 2007 Jul 4;27(27):7208-21.

Babalian A, Liang F, Rouiller EM. Cortical influences on cervical motoneurons in the rat: recordings of synaptic responses from motoneurons and compound action potential from corticospinal axons. Neurosci Res. 1993 May; 16(4):301-10.

Balentine, J.D. Hypotheses in spinal cord trauma research. In: Central Nervous System Trauma Status Report, edited by D.P. Becker and J.T. Povlishock. Bethesda, MD: NIH, 1985, p. 455-461.

Ballermann M, Fouad K. Spontaneous locomotor recovery in spinal cord injured rats is accompanied by anatomical plasticity of reticulospinal fibers. Eur J Neurosci. 2006 Apr; 23(8):1988-96.

Bambakidis NC, Miller RH. Transplantation of oligodendrocyte precursors and sonic hedgehog results in improved function and white matter sparing in the spinal cords of adult rats after contusion. Spine J. 2004 Jan-Feb; 4(1):16-26.

Banati RB, Gehrmann J, Schubert P, Kreutzberg GW. Cytotoxicity of microglia. Glia. 1993 Jan; 7(1):111-8.

Bandtlow CE, Schmidt MF, Hassinger TD, Schwab ME, Kater SB. Role of intracellular calcium in NI-35-evoked collapse of neuronal growth cones. Science. 1993 Jan 1; 259(5091):80-3.

Baptiste DC, Tighe A, Fehlings MG. Spinal cord injury and neural repair: focus on neuroregenerative approaches for spinal cord injury. Expert Opin Investig Drugs. 2009 May; 18(5):663-73.

Bareyre FM, Haudenschild B, Schwab ME. Long-lasting sprouting and gene expression changes induced by the monoclonal antibody IN-1 in the adult spinal cord. J Neurosci. 2002 Aug 15;22(16):7097-110.

Bareyre FM, and Schwab ME. Inflammation, degeneration and regeneration in the injured spinal cord: insight from DNA microarrays. Trends Neurosci. 2003; 26, 555-563.

Bareyre FM, Kerschensteiner M, Raineteau O, Mettenleiter TC, Weinmann O, Schwab ME. The injured spinal cord spontaneously forms a new intraspinal circuit in adult rats. Nat Neurosci Mar 2004; 7 (3):269–77.

Bareyre FM, Kerschensteiner M, Misgeld T, Sanes JR. Transgenic labelling of the corticospinal tract for monitoring axonal responses to spinal cord injury. Nat Med Dec 2005; 11(12): 1355-60.

Barnabé-Heider F, Frisén J. Stem cells for spinal cord repair. Cell Stem Cell. 2008 Jul 3; 3(1):16-24.

Barnett SC, Riddell JS. Olfactory ensheathing cell transplantation as a strategy for spinal cord repair--what can it achieve? Nat Clin Pract Neurol. 2007 Mar; 3(3):152-61.

Barnett SC, Alexander CL, Iwashita Y, Gilson JM, Crowther J, Clark L, Dunn LT, Papanastassiou V, Kennedy PG, Franklin RJ. Identification of a human olfactory ensheathing cell that can effect transplant-mediated remyelination of demyelinated CNS axons. Brain. 2000 Aug;123 ( Pt 8):1581-8.

Baron-Van Evercooren A, Gansmuller A, Duhamel E, Pascal F, Gumpel M. Repair of a myelin lesion by Schwann cells transplanted in the adult mouse spinal cord. J Neuroimmunol. 1992 Oct; 40(2-3): 235-42.

Barritt AW, Davies M, Marchand F, Hartley R, Grist J, Yip P, McMahon SB, Bradbury EJ. Chondroitinase ABC promotes sprouting of intact and injured spinal systems after spinal cord injury. J Neurosci. 2006 Oct 18; 26(42):10856-67.

Basso DM, Beattie MS, Bresnahan JC. A sensitive and reliable locomotor rating scale for open field testing in rats. J Neurotrauma. 1995 Feb; 12(1):1-21.

Beattie MS, Farooqui AA, Bresnahan JC. Review of current evidence for apoptosis after spinal cord injury. J Neurotrauma. 2000 Oct; 17(10):915-25.

Beattie MS, Harrington AW, Lee R, Kim JY, Boyce SL, Longo FM, Bresnahan JC, Hempstead BL, Yoon SO. ProNGF induces p75-mediated death of oligodendrocytes following spinal cord injury. Neuron. 2002 Oct 24; 36(3):375-86.

Beattie MS. Inflammation and apoptosis: linked therapeutic targets in spinal cord injury. Trends Mol Med. 2004 Dec; 10(12):580-3.

Benson MD, Romero MI, Lush ME, Lu QR, Henkemeyer M, Parada LF. Ephrin-B3 is a myelin-based inhibitor of neurite outgrowth. Proc Natl Acad Sci U S A. 2005 Jul 26; 102(30):10694-9.

Bethea JR. Spinal cord injury-induced inflammation: a dual-edged sword. Prog. Brain Res. 2000; 128, 33-42.

Bianco JI, Perry C, Harkin DG, Mackay-Sim A, Féron F. Neurotrophin 3 promotes purification and proliferation of olfactory ensheathing cells from human nose. Glia. 2004 Jan 15; 45(2):111-23.

Blesch A, Tuszynski MH. Cellular GDNF delivery promotes growth of motor and dorsal column sensory axons after partial and complete spinal cord transections and induces remyelination. J Comp Neurol. 2003 Dec 15; 467(3):403-17.

Blight AR. Morphometric analysis of a model of spinal cord injury in guinea pigs, with behavioral evidence of delayed secondary pathology. J Neurol Sci. 1991; 103:156-171.

Blight AR, Young W. Central axons in injured cat spinal cord recover electrophysiological function following remyelination by Schwann cells. J Neurol Sci. 1989 Jun; 91(1-2):15-34.

Bohlman HH, Ducker TB, Levine AM, McAfee PC. Spine trauma in adults. In Rothman RB, Simeone FA (eds). The Spine 3rd Ed. Philadelphia, WB Saunders, 1992, p. 973-1104.

Bouquet C, Nothias F. Molecular mechanisms of axonal growth. Adv Exp Med Biol. 2007;621:1-16.

Bracken MB, Holford TR. Effects of timing of methylprednisolone or naloxone administration on recovery of segmental and long-tract neurological function in NASCIS 2. J Neurosurg. 1993 Oct; 79(4):500-7.

Bracken MB, Shepard MJ, Holford TR, Leo-Summers L, Aldrich EF, Fazl M, Fehlings MG, Herr DL, Hitchon PW, Marshall LF, Nockels RP, Pascale V, Perot PL Jr, Piepmeier J, Sonntag VK, Wagner F, Wilberger JE, Winn HR, Young W. Methylprednisolone or tirilazad mesylate administration after acute spinal cord injury: 1-year follow up. Results of the third National Acute Spinal Cord Injury randomized controlled trial. J Neurosurg. 1998 Nov; 89(5):699-706.

Bradbury EJ, Khemani S, Von R, King, Priestley JV, McMahon SB. NT-3 promotes growth of lesioned adult rat sensory axons ascending in the dorsal columns of the spinal cord. Eur J Neurosci. 1999 Nov; 11(11):3873-83.

Bradbury EJ, Moon LD, Popat RJ, King VR, Bennett GS, Patel PN, Fawcett JW, McMahon SB. Chondroitinase ABC promotes functional recovery after spinal cord injury. Nature. 2002 Apr 11; 416(6881):636-40.

Bradbury EJ, McMahon SB. Spinal cord repair strategies: why do they work? Nat Rev Neurosci. 2006 Aug; 7(8):644-53.

Bray GM, Rasminsky M, Aguayo AJ. Interactions between axons and their sheath cells. Annu Rev Neurosci. 1981; 4: 127-62.

Bregman BS, Kunkel-Bagden E, Schnell L, Dai HN, Gao D, Schwab ME. Recovery from spinal cord injury mediated by antibodies to neurite growth inhibitors. Nature. 1995 Nov 30; 378(6556):498-501.

Brewer KL, Bethea JR, Yezierski RP. Neuroprotective effects of Interleukin-10 following excitotoxia spinal cord injury. Exp Neurol 1999 Oct; 159(2): 484-493.

Brines M, Cerami A. Erythropoietin-mediated tissue protection: reducing collateral damage from the primary injury response. J Intern Med. 2008 Nov; 264(5):405-32.

Brösamle C, Huber AB, Fiedler M, Skerra A, Schwab ME. Regeneration of lesioned corticospinal tract fibers in the adult rat induced by a recombinant, humanized IN-1 antibody fragment. J Neurosci. 2000 Nov 1;20(21):8061-8.

Brosamle, C., and Schwab, M.E. Cells of origin, course, and termination patterns of the ventral, uncrossed component of the mature rat corticospinal tract. J. Comp Neurol. 1997 Sep; 386(2), 293–303.

Brose K, Tessier-Lavigne M. Slit proteins: key regulators of axon guidance, axonal branching, and cell migration. Curr Opin Neurobiol. 2000 Feb; 10(1):95-102.

Brown AG, Fyffe RE, Rose PK, Snow PJ. Spinal cord collaterals from axons of type II slowly adapting units in the cat. J Physiol. 1981 Jul; 316:469-80.

Brown A, Ricci MJ, Weaver LC. NGF message and protein distribution in the injured rat spinal cord. Exp. Neurol. 2004 Jul; 188, 115–127.

Brown PJ, Marino RJ, Herbison, Ditunno Jr JF. The 72-h examination as a predictor of recovery in motor complete quadriplegia. Arch Phys Med Rehabil 1991; 72: 546-8.

Bruehlmeier M, Dietz V, Leenders KL, Roelcke U, Missimer J, Curt A. How does the human brain deal with a spinal cord injury? Eur J Neurosci Dec 1998; 10(12):3918–22.

Brus-Ramer M, Carmel JB, Chakrabarty S, Martin JH. Electrical stimulation of spared corticospinal axons augments connections with ipsilateral spinal motor circuits after injury.J Neurosci. 2007 Dec 12; 27(50):13793-801.

Bundesen LQ, Scheel TA, Bregman BS, Kromer LF. Ephrin-B2 and EphB2 regulation of astrocyte-meningeal fibroblast interactions in response to spinal cord lesions in adult rats. J Neurosci. 2003 Aug 27; 23(21):7789-800.

Burchiel KJ, Hsu FP. Pain and spasticity after spinal cord injury: mechanisms and treatment. Spine. 2001 Dec 15; 26(24 Suppl):S146-60.

Burns SP, Golding DG, Rolle Jr WA, Graziani V, Ditunno Jr JF. Recovery of ambulation in motor-incomplete tetraplegia. Arch Phys Med Rehabil Nov 1997; 78(11):1169–72.

Cadelli D, Schwab ME. Regeneration of Lesioned Septohippocampal Acetylcholinesterase-positive Axons is Improved by Antibodies Against the Myelin-associated Neurite Growth Inhibitors NI-35/250. Eur J Neurosci. 1991; 3(9):825-832.

Cadelli DS, Bandtlow CE, Schwab ME. Oligodendrocyte- and myelin-associated inhibitors of neurite outgrowth:their involvement in the lack of CNS regeneration. Exp Neurol. 1992 Jan; 115(1): 189-92.

Cafferty WB, Strittmatter SM. The Nogo-Nogo receptor pathway limits a spectrum of adult CNS axonal growth. J Neurosci. 2006 Nov 22; 26(47):12242-50.

Cafferty WB, Bradbury EJ, Lidierth M, Jones M, Duffy PJ, Pezet S, McMahon SB. Chondroitinase ABC-mediated plasticity of spinal sensory function. J Neurosci. 2008 Nov 12; 28(46):11998-2009.

Cai LL, Fong AJ, Otoshi CK, Liang Y, Burdick JW, Roy RR, Edgerton VR. Implications of assist-as-needed robotic step training after a complete spinal cord injury on intrinsic strategies of motor learning. J Neurosci. 2006 Oct 11;26(41):10564-8.

Calancie B, Needham-Shropshire B, Jacobs P, Willer K, Zych G, Green BA. Involuntary stepping after chronic spinal cord injury. Evidence for a central rhythm generator for locomotion in man. Brain. 1994 Oct; 117 ( Pt 5):1143-59.

Cameron T, Prado R, Watson BD, Gonzalez-Carvajal M, Holets VR. Photochemically induced systic lesion in the rat spinal cord. I. Behavioral and morphological analysis. Exp. Neurol. 1990 Aug; 109(2):214-223.

Cardenas DD, Ditunno J, Graziani V, Jackson AB, Lammertse D, Potter P, Sipski M, Cohen R, Blight AR. Phase 2 trial of sustained-release fampridine in chronic spinal cord injury. Spinal Cord. 2007; 45: 158-68.

Carter LM, Starkey ML, Akrimi SF, Davies M, McMahon SB, Bradbury EJ. The yellow fluorescent protein (YFP-H) mouse reveals neuroprotection as a novel mechanism underlying chondroitinase ABC-mediated repair after spinal cord injury. J Neurosci. 2008 Dec 24;28(52):14107-20.

Casale EJ, Light AR, Rustioni A. Direct projection of the corticospinal tract to the superficial laminae of the spinal cord in the rat. J Comp Neurol. 1988 Dec 8; 278(2):275-86.

Casha S, Yu WR, Fehlings MG. FAS deficiency reduces apoptosis, spares axons and improves function after spinal cord injury. Exp Neurol. 2005 Dec; 196(2):390-400.

Cayli SR, Kocak A, Yilmaz U, Tekiner A, Erbil M, Ozturk C, Batcioglu K, Yologlu S. Effect of combined treatment with melatonin and methylprednisolone on neurological recovery after experimental spinal cord injury. Eur Spine J. 2004 Dec; 13(8):724-32.

Chang HT. Subacute human spinal cord contusion: few lymfocytes and many macrophages. Spinal Cord. 2007 Feb; 45: 174-182.

Chen MS, Huber AB, van der Haar ME, Frank M, Schnell L, Spillmann AA, Christ F, Scheab ME. Nogo-A is a myelin-associated neurite outgrowth inhibitor and an antigen for monoclonal antibody IN-1. Nature. 2000 Jan 27; 403(6768):434-9.

Choi D, Li D, Law S, Powell M, Raisman G. A prospective observational study of the yield of olfactory ensheathing cells cultured from biopsies of septal nasal mucosa. Neurosurgery. 2008 May; 62(5):1140-4; discussion 1144-5.

Chuah MI, Au C. Olfactory cell cultures on ensheathing cell monolayers. Chem Senses. 1994; 19: 25-34.

Chuah MI, Choi-Lundberg D, Weston S, Vincent AJ, Chung RS, Vickers JC, West AK. Olfactory ensheathing cells promote collateral axonal branching in the injured adult rat spinal cord. Exp Neurol. 2004 Jan; 185(1):15-25.

Chung K, Langford LA, Coggeshall RE. Primary afferent and propriospinal fibers in the rat dorsal and dorsolateral funiculi. J Comp Neurol. 1987 Sep 1; 263(1):68-75.

Cliffer KD, Giesler GJ Jr. Postsynaptic dorsal column pathway of the rat. III. Distribution of ascending afferent fibers. J Neurosci. 1989 Sep; 9(9):3146-68.

Crowe MJ, Bresnahan JC, Shuman SL, Masters JN, Beattie MS. Apoptosis and delayed degeneration after spinal cord injury in rats and monkeys. Nat Med 1997; 3:73–6.

Collazos-Castro JE, López-Dolado E, Nieto-Sampedro M. Locomotor deficits and adaptive mechanisms after thoracic spinal cord contusion in the adult rat. J Neurotrauma. 2006 Jan; 23(1):1-17.

Corbetta M, Burton H, Sinclair RJ, Conturo TE, Akbudak E, McDonald JW. Functional reorganization and stability of somatosensory-motor cortical topography in a tetraplegic subject with late recovery. Proc Natl Acad Sci U S A. 2002 Dec 24;99(26):17066-71.

Coumans JV, Lin TT, Dai HN, MacArthur L, McAtee M, Nash C, Bregman BS. Axonal regeneration and functional recovery after complete spinal cord transection in rats by delayed treatment with transplants and neurotrophins. J Neurosci. 2001 Dec 1; 21(23):9334-44.

Courtine G, Roy RR, Raven J, Hodgson J, McKay H, Yang H, Zhong H, Tuszynski MH, Edgerton VR. Performance of locomotion and foot grasping following a unilateral thoracic corticospinal tract lesion in monkeys (Macaca mulatta). Brain. 2005; 128, 2338–2358.

Courtine G, Song B, Roy RR, Zhong H, Herrmann JE, Ao Y, Qi J, Edgerton VR, Sofroniew MV. Recovery of supraspinal control of stepping via indirect propriospinal relay connections after spinal cord injury. Nat Med. 2008 Jan; 14(1):69-74.

Cragg BG, Thomas PK. Changes in conduction velocity and fibre size proximal to peripheral nerve lesions. J Physiol. 1961 Jul;157:315-27.

Crang AJ, Blakemore WF. Remyelination of demyelinated rat axons by transplanted mouse oligodendrocytes. Glia. 1991; 4: 305-13.

Curt A, Alkadhi H, Crelier GR, Boendermaker SH, Hepp-Reymond MC, Kollias SS. Changes of non-affected upper limb cortical representation in paraplegic patients as assessed by fMRI. Brain. 2002 Nov;125(Pt 11):2567-78.

Das A, Sribnick EA, Wingrave JM, Del Re AM, Woodward JJ, Appel SH, Banik NL, Ray SK. Calpain activation in apoptosis of ventral spinal cord 4.1 (VSC4.1) motoneurons exposed to glutamate: calpain inhibition provides functional neuropretection. J Neurosci Res. 2005 Aug 15; 81(4):551-62.

David S, Aguayo AJ. Axonal elongation into peripheral nerves system 'bridges' after central nervous system injury in adult rats. Science. 1981; 214: 931-933.

Davies SJ, Goucher DR, Doller C, Silver J. Robust regeneration of adult sensory axons in degenerating white matter of the adult rat spinal cord. J Neurosci 1999; 5810-22.

DeFelipe J. Brain plasticity and mental processes: Cajal again. Nat Rev Neurosci. 2006 Oct; 7(10):811-7.

DeKosky ST, Styren SD, O'Malley ME, Goss JR, Kochanek P, Marion D, Evans CH, Robbins PD. Interleukin-1 receptor antagonist suppresses neurotrophin response in injured rat brain. Ann Neurol. 1996 Jan; 39(1):123-7.

Demjen D, Klussmann S, Kleber S, Zuliani C, Stieltjes B, Metzger C, Hirt UA, Walczak H, Falk W, Essig M, Edler L, Krammer PH, Martin-Villalba A. Neutralization of CD95 ligand promotes regeneration and functional recovery after spinal cord injury. Nat Med. 2004 Apr; 10(4):389-95.

Dergham P, Ellezam B, Essagian C, Avedissian H, Lubell WD, McKerracher L. Rho signaling pathway targeted to promote spinal cord repair. J Neurosci. 2002 Aug 1; 22(15):6570-7.

De Leon RD, Hodgson JA, Roy RR, Edgerton VR. Full weight-bearing hindlimb standing following stand training in the adult spinal cat. J Neurophysiol. 1998 Jul;80(1):83-91.

de Pommery J, Roudier F, Menétrey D. Postsynaptic fibers reaching the dorsal column nuclei in the rat. Neurosci Lett. 1984 Sep 7; 50(1-3):319-23.

DeVivo MJ, Krause JS, Lammertse DP. Recent trends in mortality and causes of death among persons with spinal cord injury. Arhives of Physical Medicine and Rehabilitation. 1999; 80: 1411-9.

De Winter F, Oudega M, Lankhorst AJ, Hamers FP, Blits B, Ruitenberg MJ, Pasterkamp RJ, Gispen WH, Verhaagen J. Injury-induced class 3 semaphorin expression in the rat spinal cord. Exp Neurol. 2002 May; 175(1):61-75.

Dimitrijevic MR, Gerasimenko Y, Pinter MM. Evidence for a spinal central pattern generator in humans. Ann N Y Acad Sci. 1998 Nov 16; 860:360-76.

Dimou L, Schnell L, Montani L, Duncan C, Simonen M, Schneider R, Liebscher T, Gullo M, Schwab ME. Nogo-A-deficient mice reveal strain-dependent differences in axonal regeneration. J Neurosci. 2006 May 24; 26(21):5591-603.

Ditunno JF, Cohen ME, Hauk WW, Jackson AB, Sipski ML. Recovery of upper-extremity strength in complete and incomplete tetraplegia: a ulticenter study. Arch Phys Med Rehabil 2000; 81: 389-93.

Domeniconi M, Cao Z, Spencer T, Sivasankaran R, Wang K, Nikulina E, Kimura N, Cai H, Deng K, Gao Y, He Z, Filbin M. Myelin-associated glycoprotein interacts with the Nogo66 receptor to inhibit neurite outgrowth. Neuron. 2002 Jul 18; 35(2):283-90.

Donnelly DJ, Popovich PG. Inflammation and its role in neuroprotection, axonal regeneration and functional recovery after spinal cord injury. Exp Neurol. 2008 Feb; 209(2):378-88.

Donoghue JP, Wise SP. The motor cortex of the rat: cytoarchitecture and microstimulation mapping. J Comp Neurol. 1982 Nov 20;212(1):76-88.

Doucette JR. The glial cells in the nerve fiber layer of the rat olfactory bulb. Anat Rec. 1984; 210: 385-91.

Doucette R. PNS-CNS transitional zone of the first cranial nerve. J Comp Neurol. 1991; 312: 451-66.

Dum RP, Strick PL. The origin of corticospinal projections from the premotor areas in the frontal lobe. J Neurosci. 1991 Mar; 11(3):667-89.

Dumont RJ, Okonkwo DO, Verma S, Hurlbert RJ, Boulos PT, Ellegala DB, Dumont AS. Acute spinal cord injury, part 1: Pathophysiologic mechanisms. Clin. Neuropharmacol. 2001a sep 24(5), 254-64.

Dumont RJ, Verma S, Okonkwo DO, Hurlbert RJ, Boulos PT, Ellegala DB, Dumont AS. Acute spinal cord injury, part II: contemporary pharmacotherapy. Clin Neuropharmacol. 2001b Sep-Oct; 24(5):265-79.

Duncan I.D., Aguayo A.J., Bunge R.P. and Wood P.M. Transplantation of rat Schwann cells grown in tissue culture into the mouse spinal cord. Journal of the Neurological Sciences, 1981; 49: 241-52.

Edgerton VR, Roy RR. Paralysis recovery in humans and model systems. Curr Opin Neurobiol. 2002 Dec; 12(6):658-67.

Emery E, Aldana P, Bunge MB, Puckett W, Srinivasan A, Keane RW, Bethea J, Levi AD. Apoptosis after traumatic human spinal cord injury. J Neurosurg. 1998 Dec; 89(6):911-20.

Engesser-Cesar C, Anderson AJ, Basso DM, Edgerton VR, Cotman CW. Voluntary wheel running improves recovery from a moderate spinal cord injury. J Neurotrauma. 2005 Jan;22(1):157-71.

Erbayraktar S, Grasso G, Sfacteria A, Xie QW, Coleman T, Kreilgaard M, Torup L, Sager T, Erbayraktar Z, Gokmen N, Yilmaz O, Ghezzi P, Villa P, Fratelli M, Casagrande S, Leist M, Helboe L, Gerwein J, Christensen S, Geist MA, Pedersen LØ, Cerami-Hand C, Wuerth JP, Cerami A, Brines M. Asialoerythropoietin is a nunerythropoieti cytokine with broad neuroprotective activity in vivo. Proc. Natl. Acad. Sci. U.S.A. 2003 May 27; 100(11), 6741-6746.

Farooque M, Hillered L, Holtz A, Olsson Y. Effects of methylprednisolone on extracellular lactic acidosis and amino acids after severe compression injury of rat spinal cord. J Neurochem. 1996 Mar; 66(3):1125-30.

Farooque M, Hillered L, Holtz A, Olsson Y. Effects of moderate hypothermia on extracellular lactic acid and amino acids after severe compression injury of rat spinal cord. J Neurotrauma. 1997 Jan; 14(1):63-9.

Faulkner JR, Herrmann JE, Woo MJ, Tansey KE, Doan NB, Sofroniew MV. Reactive astrocytes protect tissue and preserve function after spinal cord injury. J Neurosci. 2004 Mar 3; 24(9):2143-55.

Fawcett JW and Asher RA. The glial scar and central nervous system repair. Brain Res Bull. 1999; 49, 377-91.

Fawcett JW, Curt A, Steeves JD, Coleman WP, Tuszynski MH, Lammertse D, Bartlett PF, Blight AR, Dietz V, Ditunno J, Dobkin BH, Havton LA, Ellaway PH, Fehlings MG, Privat A, Grossman R, Guest JD, Kleitman N, Nakamura M, Gaviria M, Short D. Guidelines for the conduct of clinical trials for spinal cord injury as developed by the ICCP panel: spontaneous recovery after spinal cord injury and statistical power needed for therapeutic clinical trials. Spinal Cord. 2007; 45, 190–205.

Fawcett JW, Curt A. Damage control in the nervous system: rehabilitation in a plastic environment. Nat Med. 2009 Jul;15(7):735-6.

Féron F, Perry C, McGrath JJ, Mackay-Sim A. New techniques for biopsy and culture of human olfactory epithelial neurons. Arch Otolaryngol Head Neck Surg. 1998 Aug; 124(8):861-6.

Féron F, Perry C, Cochrane J, Licina P, Nowitzke A, Urquhart S, Geraghty T, Mackay-Sim A. Autologous olfactory ensheathing cell transplantation in human spinal cord injury. Brain. 2005 Dec; 128(Pt 12):2951-60.

Fleming JC, Norenberg MD, Ramsay DA, Dekaban GA, Marcillo AE, Saenz AD, Pasquale_Sthles M, Dietrich WD, Weaver LC. The cellular inflammatory response in human spinal cords after injury. Brain. 2006 Dec; 129: 3249-3269.

Finnerup NB, Jensen TS. Spinal cord injury pain--mechanisms and treatment. Eur J Neurol. 2004 Feb; 11(2):73-82.

Firkins SS, Bates CA, and Stelzner DJ. Corticospinal tract plasticity and astroglial reactivity after cervical spinal injury in the postnatal rats. Exp. Neurol. 1993 Mar; 120(1):1-15.

Fisher CG, Noonan VK, Smith DE, Wing PC, Dvorak MF, Kwon B. Motor recovery, functional status, and health-related quality of life in patients with complete spinal cord injuries. Spine 2005; 30: 2200-7.

Fouad K, Pedersen V, Schwab ME, Brosamle C. Cervical sprouting of corticospinal fibers after thoracic spinal cord injury accompanies shifts in evoked motor responses. Curr Biol Nov 13 2001; 11 (22):1766–70.

Forrest GF, Sisto SA, Barbeau H, Kirshblum SC, Wilen J, Bond Q, Bentson S, Asselin P, Cirnigliaro CM, Harkema S. Neuromotor and musculoskeletal responses to locomotor training for an individual with chronic motor complete AIS-B spinal cord injury. J Spinal Cord Med. 2008;31(5):509-21.

Fouad K, Klusman I, Schwab ME. Regenerating corticospinal fibers in the Marmoset (Callitrix jacchus) after spinal cord lesion and treatment with the anti-Nogo-A antibody IN-1. Eur J Neurosci. 2004 Nov; 20(9):2479-82.

Fournier AE, GrandPre T, Strittmatter SM. Identification of receptor mediating Nogo-66 inhibition of axon regeneration. Nature. 2001 Jan 18; 409:341-6.

Fournier AE, Takizawa BT, Strittmatter SM. Rho kinase inhibition enhances axonal regeneration in the injured CNS. J Neurosci 2003 Feb; 23(4):1416–23.

Franklin RJ, Gilson JM, Franceschini IA, Barnett SC. Schwann cell-like myelination following transplantation of an olfactory buld-ensheathing cell line into areas of demyelination in the adult CNS. Glia, 1996; 17: 217-24.

Franklin RJ, Gilson JM, Blakemore WF. Local recruitment of remyelinating cells in the repair of demyelination in the central nervous system. J Neurosci Res. 1997 Oct; 50(2): 337-44.

Freed CR, Breeze RE, Rosenberg NL, Schneck SA, Kriek E, Qi JX, Lone T, Zhang YB, Snyder JA, Well TH. Survival of implanted fetal dopamine cells and neurologic improvement 12 to 46 months after transplantation for Parkinson's disease. N Engl J Med. 1992 Nov; 327(22): 1549-55.

Freund P, Schmidlin E, Wannier T, Bloch J, Mir A, Schwab ME, Rouiller EM. Nogo-A-specific antibody treatment enhances sprouting and functional recovery after cervical lesion in adult primates. Nat Med. 2006 Jul; 12(7):790-2.

Freund P, Wannier T, Schmidlin E, Bloch J, Mir A, Schwab ME, Rouiller EM. Anti-Nogo-A antibody treatment enhances sprouting of corticospinal axons rostral to a unilateral cervical spinal cord lesion in adult macaque monkey. J Comp Neurol. 2007 Jun 1; 502(4):644-59.

Freund P, Schmidlin E, Wannier T, Bloch J, Mir A, Schwab ME, Rouiller EM. Anti-Nogo-A antibody treatment promotes recovery of manual dexterity after unilateral cervical lesion in adult primates--re-examination and extension of behavioral data. Eur J Neurosci. 2009 Mar;29(5):983-96.

Fu ES, Saporta S. Methylprednisolone inhibits production of interleukin-1beta and interleukin-6 in the spinal cord following compression injury in rats. J Neurosurg Anesthesiol. 2005 Apr; 17(2):82-5.

García-Alías G, Lin R, Akrimi SF, Story D, Bradbury EJ, Fawcett JW. Therapeutic time window for the application of chondroitinase ABC after spinal cord injury. Exp Neurol. 2008 Apr; 210(2):331-8.

García-Alías G, Barkhuysen S, Buckle M, Fawcett JW. Chondroitinase ABC treatment opens a window of opportunity for task-specific rehabilitation. Nat Neurosci. 2009 Sep;12(9):1145-51.

Gauthier P, Réga P, Lammari-Barreault N, Polentes J. Functional reconnections established by central respiratory neurons regenerating axons into a nerve graft bridging the respiratory centers to the cervical spinal cord. J Neurosci Res. 2002 Oct 1; 70(1):65-81.

Gensert, J.M. Goldman, J.E. Endogenous progenitors remyelinate demyelinated axons in the adult CNS. Neuron. 1997 Jul; 19(1), 197-203.

Giehl KM, Tetzlaff W. BDNF and NT-3, but not NGF, prevent axotomy-induced death of rat corticospinal neurons in vivo. Eur J Neurosci. 1996 Jun;8(6):1167-75.

Giesler GJ Jr, Nahin RL, Madsen AM. Postsynaptic dorsal column pathway of the rat. I. Anatomical studies. J Neurophysiol. 1984 Feb; 51(2):260-75.

Giovanelli Barilari M, Kuypers HG. Propriospinal fibers interconnecting the spinal enlargements in the cat. Brain Res. 1969 Jul;14(2):321-30.

Girgis J, Merrett D, Kirkland S, Metz GA, Verge V, Fouad K. Reaching training in rats with spinal cord injury promotes plasticity and task specific recovery. Brain. 2007 Nov;130(Pt 11):2993-3003.

Giuffrida R, Rustioni A. Dorsal root ganglion neurons projecting to the dorsal column nuclei of rats. J Comp Neurol. 1992 Feb 8; 316(2):206-20.

GrandPré T, Nakamura F, Vartanian T, Strittmatter SM. Identification of the Nogo inhibitor of axon regeneration as a Reticulon protein. Nature. 2000 Jan 27; 403(6768):439-44.

GrandPré T, Li S, Strittmatter SM. Nogo-66 receptor antagonist peptide promotes axonal regeneration. Nature. 2002 May 30; 417(6888):547-51.

Griffiths IR, Miller R. Vascular permeability to protein and vasogenic oedema in experimental concussive injuries to the canine spinal cord. J Neurol Sci. 1974 Jul; 22(3):291-304.

Grillner S, Zangger P. On the central generation of locomotion in the low spinal cat. Exp Brain Res. 1979 Jan 15; 34(2):241-61.

Groves AK, Barnett SC, Franklin RJ, Crang AJ, Mayer M, Blakemore WF, Noble M. Repair of demyelinated lesions by transplantation of purified O-2A progenitor cells. Nature. 1993 Apr 1; 362(6419):453-5.

Gruner JA. A monitored contusion model of spinal cord injury in the rat. J Neurotrauma 1992; 9:123-6.

Guest J, Herrera LP, Qian T. Rapid recovery of segmental neurological function in a tetraplegic patient following transplantation of fetal olfactory bulb-derived cells. Spinal Cord. 2006 Mar; 44(3):135-42.

Guízar-Sahagún G, Velasco-Hernández L, Martínez-Cruz A, Castañeda-Hernández G, Bravo G, Rojas G, Hong E. Systemic microcirculation after complete high and low thoracic spinal cord section in rats. J Neurotrauma. 2004 Nov; 21(11):1614-23.

Gulino R, Dimartino M, Casabona A, Lombardo SA, Perciavalle V. Synaptic plasticity modulates the spontaneous recovery of locomotion after spinal cord hemisection. Neurosci Res. 2007 Jan; 57(1):148-56.

Gurfinkel VS, Levik YS, Kazennikov OV, Selionov VA. Locomotor-like movements evoked by leg muscle vibration in humans. Eur J Neurosci. 1998 May; 10(5):1608-12.

Gwak YS, Hains BC, Johnson KM, Hulsebosch CE. Effect of age at time of spinal cord injury on behavioral outcomes in rat. J Neurotrauma. 2004 Aug; 21(8):983-93.

Hamers FP, Lankhorst AJ, van Laar TJ, Veldhuis WB, Gispen WH. Automated quantitative gait analysis during overground locomotion in the rat: its application to spinal cord contusion and transection injuries. J Neurotrauma. 2001 Feb; 18(2):187-201.

Hansebout RR, Blight AR, Fawcett S, Reddy K. 4-Aminopyridine in chronic spinal cord injury: a controlled, double-blind, crossover study in eight patients. J Neurotrauma. 1993 Spring; 10(1):1-18.

Harding GW, Towe AL. Fiber analysis of the pyramidal tract of the laboratory rat. Exp Neurol. 1985 Mar; 87(3):503-18.

Harvey C, Wilson SE, Greene CG, Berkowitz M, Stripling TE. New estimates of the direct costs of traumatic spinal cord injuries: results of a nationwide survey. Paraplegia. 1992; 30(12):834-50.

Hayes KC. The use of 4-aminopyridine (fampridine) in demyelinating disorders. CNS Drug Rev. 2004; 10: 295-316.

Hawryluk GW, Rowland J, Kwon BK, Fehlings MG. Protection and repair of the injured spinal cord: a review of completed, ongoing, and planned clinical trials for acute spinal cord injury. Neurosurg Focus. 2008; 25(5):E14.

Hermann GE, Holmes GM, Rogers RC, Beattie MS, Bresnahan JC. Descending spinal projections from the rostral gigantocellular reticular nuclei complex. J Comp Neurol. 2003 Jan 6;455(2):210-21.

Hicks SP, D'Amato CJ. Motor-sensory cortex-corticospinal system and developing locomotion and placing in rats. Am J Anat. 1975 May; 143(1):1-42.

Hicks SP, D'Amato CJ. Locating corticospinal neurons by retrograde axonal transport of horseradish peroxidase. Exp Neurol. 1977 Aug; 56(2):410-20.

Hill CE, Beattie MS, Bresnahan JC. Degeneration and sprouting of identified descending supraspinal axons after contusive spinal cord injury in the rat. Exp Neurol Sep 2001; 171(1):153–69.

Huang JK, Phillips GR, Roth AD, Pedraza L, Shan W, Belkaid W, Mi S, Fex-Svenningsen A, Florens L, Yates JR 3rd, Colman DR. Glial membranes at the node of Ranvier prevent neurite outgrowth. Science. 2005 Dec 16; 310(5755):1813-7.

Hummelsheim H, Wiesendanger M. Is the hindlimb representation of the rat's cortex a 'sensorimotor amalgam'? Brain Res. 1985 Oct 28;346(1):75-81.

Hyun SJ, Rhim SC, Kang JK, Hong SH, Park BR. Combined motor- and somatosensory-evoked potential monitoring for spine and spinal cord surgery: correlation of clinical and neurophysiological data in 85 consecutive procedures. Spinal Cord. 2009 Aug;47(8):616-22.

Ichiyama R, Potuzak M, Balak M, Kalderon N, Edgerton VR. Enhanced motor function by training in spinal cord contused rats following radiation therapy. PLoS One. 2009 Aug 31;4(8):e6862.

Ibrahim A, Li Y, Li D, Raisman G, El Masry WS. Olfactory ensheathing cells: ripples of an incoming tide? Lancet Neurol. 2006 May; 5(5):453-7.

Imaizumi T, Lankford KL, Kocsis JD. Transplantation of olfactory ensheathing cells or Schwann cells restores rapid and secure conduction across the transected spinal cord. Brain Res. 2000 Jan 31; 854(1-2):70-8.

Irving EA, Vinson M, Rosin C, Roberts JC, Chapman DM, Facci L, Virley DJ, Skaper SD, Burbidge SA, Walsh FS, Hunter AJ, Parsons AA. Identification of neuroprotective properties of anti-MAG antibody: a novel approach for the treatment of stroke? J Cereb Blood Flow Metab. 2005 Jan; 25(1):98-107.

Iwata A, Stys PK, Wolf JA, Chen XH, Taylor AG, Meaney DF, Smith DH. Traumatic axonal injury induces proteolytic cleavage of the voltagegated sodium channel modulated by tetrodotoxin and protease inhibitors. J Neurosci. 2004 May 12; 24(19):4605-13.

Jain N, Catania KC, Kaas JH. Deactivation and reactivation of somatosensory cortex after dorsal spinal cord injury. Nature. 1997 Apr 3; 386(6624):495-8.

Jankowska E, Lundberg A, Roberts WJ, Stuart D. A long propriospinal system with direct effect on motoneurones and on interneurones in the cat lumbosacral cord. Exp Brain Res. 1974;21(2):169-94.

Joosten EA, Schuitman RL, Vermelis ME, Dederen PJ. Postnatal development of the ipsilateral corticospinal component in rat spinal cord: a light and electron microscopic anterograde HRP study. J Comp Neurol. 1992 Dec 1; 326(1):133-46.

Jurkiewicz MT, Mikulis DJ, McIlroy WE, Fehlings MG, Verrier MC. Sensorimotor cortical plasticity during recovery following spinal cord injury: a longitudinal fMRI study. Neurorehabil Neural Repair. 2007 Nov-Dec; 21(6):527-38.

Kaas JH, Florence SL, Jain N. Subcortical contributions to massive cortical reorganizations. Neuron. 1999 Apr; 22(4):657-60.

Kennedy PR. Corticospinal, rubrospinal and rubro-olivary projections: a unifying hypothesis. Trends Neurosci. 1990 Dec; 13(12):474-9.

Kim JE, Li S, GrandPré T, Qiu D, Strittmatter SM. Axon regeneration in young adult mice lacking Nogo-A/B. Neuron. 2003 Apr 24; 38(2):187-99.

Kirkeby A, Torup L, Bochsen L, Kjalke M, Abel K, Theilgaard-Monch K, Johansson PI, Bjørn SE, Gerwien J, Leist M. High-dose erythropoietin alters platelet reactivity and bleeding time in rodents in contrast to the neuroprotective variant carbamyl-erythropoietin (CEPO). Thromb Haemost. 2008 Apr; 99(4):720-8.

Kobayashi NR, Fan DP, Giehl KM, Bedard AM, Wiegand SJ, Tetzlaff W. BDNF and NT-4/5 prevent atrophy of rat rubrospinal neurons after cervical axotomy, stimulate GAP-43 and Talpha1-tubulin mRNA expression, and promote axonal regeneration. J Neurosci. 1997 Dec 15; 17(24):9583-95.

Kohama I, Lankford KL, Preiningerova J, White FA, Vollmer TL, Kocsis JD. Transplantation of cryopreserved adult human Schwann cells enhances axonal conduction in demyelinated spinal cord. J Neurosci. 2001 Feb; 21(3): 944-50.

Krassioukov A, Claydon VE. The clinical problems in cardiovascular control following spinal cord injury: an overview. Prog Brain Res. 2006; 152:223-9.

Krenz NR, Weaver LC. Nerve growth factor in glia and inflammatory cells of the injured rat spinal cord. J.Neurochem. 2000; 74, 730-739.

Kwon BK, Liu J, Messerer C, Kobayashi NR, McGraw J, Oschipok L, Tetzlaff W. Survival and regeneration of rubrospinal neurons 1 year after spinal cord injury. Proc Natl Acad Sci U S A. 2002 Mar 5; 99(5):3246-51.

Lai C, Brow MA, Nave KA, Noronha AB, Quarles RH, Bloom FE, Milner RJ, Sutcliffe JG. Two forms of 1B236/myelin-associated glycoprotein, a cell adhesion molecule for postnatal neural development, are produced by alternative splicing. Proc Natl Acad Sci USA. 1987 Jun; 84(12):4337-41.

Laird AS, Carrive P, Waite PM. Effect of Treadmill Training on Autonomic Dysreflexia in Spinal Cord-Injured Rats. Neurorehabil Neural Repair. 2009 May 18.

Lakatos A, Franklin RJ, Barnett SC. Olfactory ensheathing cells and Schwann cells differ in their in vitro interactions with astrocytes. Glia. 2000 Dec; 32(3): 214-25.

Lankhorst AJ, ter Laak MP, van Laar TJ, van Meeteren NL, de Groot JC, Schrama LH, Hamers FP, Gispen WH. Effects of enriched housing on functional recovery after spinal cord contusive injury in the adult rat. J Neurotrauma. 2001 Feb;18(2):203-15.

Lanza DC, Deems DA, Doty RL, Moran D, Crawford D, Rowley JC 3rd, Sajjadian A, Kennedy DW. The effect of human olfactory biopsy on olfaction: a preliminary report. Laryngoscope. 1994 Jul; 104(7):837-40.

Lawrence DG, Kuypers HG. The functional organization of the motor system in the monkey. II. The effects of lesions of the descending brain-stem pathways. Brain. 1968 Mar; 91(1):15-36.

Leenen L, Meek J, Nieuwenhuys R. Unmyelinated fibers in the pyramidal tract of the rat: a new view. Brain Res. 1982 Aug 26; 246(2):297-301.

Leenen LP, Meek J, Posthuma PR, Nieuwenhuys R. A detailed morphometrical analysis of the pyramidal tract of the rat. Brain Res. 1985 Dec 16;359(1-2):65-80.

Lenehan B, Boran S, Street J, Higgins T, McCormack D, Poynton AR. Demographics of acute admissions to a National Spinal Injuries Unit. Eur Spine J. 2009 Jul; 18(7):938-42.

Li Y, Raisman G. Schwann cells induce sprouting in motor and sensory axons in the adult rat spinal cord. J Neurosci. 1994 Jul; 14(7): 4050-63.

Li Y, Field PM, Raisman G. Repair of adult rat corticospinal tract by transplants of olfactory ensheathing cells. Science, 1997; 277: 2000-2.

Li Y, Field PM, Raisman G. Regeneration of adult rat corticospinal axons induced by transplanted olfactory ensheathing cells. J Neurosci. 1998 Dec 15; 18(24):10514-24.

Li Y, Decherchi P, Raisman G. Transplantation of olfactory ensheathing cells into spinal cord lesions restores breathing and climbing. J Neurosci 2003; 23:727–31.

Li GL, Farooque M, Holtz A, Olsson Y. Apoptosis of oligodendrocytes occurs for long distances away from the primary injury after compression trauma to rat spinal cord. Acta Neuropathol. 1999 Nov; 98(5):473-80.

Li J, Baud O, Vartanian T, Volpe JJ, Rosenberg PA. Peroxynitrite generated by inducible nitric oxide synthase and NADPH oxidase mediates microglial toxicity to oligodendrocytes. Proc Natl Acad Sci U S A. 2005 Jul 12; 102(28):9936-41.

Li S, Liu BP, Budel S, Li M, Ji B, Walus L, Li W, Jirik AM, Rabacchi S, Choi E, Worley D, Sah DW, Pepinsky B, Lee D, Relton J, Strittmatter SM. Blockade of Nogo-66, myelin-associated glycoprotein, and oligodendrocyte myelin glycoprotein by soluble Nogo-66 receptor promotes axonal sprouting and recovery after spinal injury. J Neurosci 2004; 24: 10511-20.

Li S, Kim JE, Budel S, Hampton TG, Strittmatter SM. Transgenic inhibition of Nogo-66 receptor function allows axonal sprouting and improved locomotion after spinal injury. Mol Cell Neurosci. 2005 May; 29(1):26-39.

Liang FY, Moret V, Wiesendanger M, Rouiller EM. Corticomotoneuronal connections in the rat: evidence from double-labeling of motoneurons and corticospinal axon arborizations. J Comp Neurol. 1991 Sep 15; 311(3):356-66.

Liebscher T, Schnell L, Schnell D, Scholl J, Schneider R, Gullo M, Fouad K, Mir A, Rausch M, Kindler D, Hamers FP, Schwab ME. Nogo-A antibody improves regeneration and locomotion of spinal cord-injured rats. Ann Neurol. 2005 Nov; 58(5):706-719.

Lima C, Pratas-Vital J, Escada P, Hasse-Ferreira A, Capucho C, Peduzzi JD. Olfactory mucosa autografts in human spinal cord injury: a pilot clinical study. J Spinal Cord Med. 2006; 29(3):191-203; discussion 204-6.

Liu Y, Kim D, Himes BT, Chow SY, Schallert T, Murray M, Tessler A, Fischer I. Transplants of fibroblasts genetically modified to express BDNF promote regeneration of adult rat rubrospinal axons and recovery of forelimb function. J Neurosci. 1999 Jun 1; 19(11):4370-87.

Liu BP, Fournier A, GrandPré T, Strittmatter SM. Myelin-associated glycoprotein as a functional ligand for the Nogo-66 receptor. Science. 2002 Aug 16; 297(5584):1190-3.

López-Vales R, García-Alías G, Forés J, Navarro X, Verdú E. Increased expression of cyclo-oxygenase 2 and vascular endothelial growth factor in lesioned spinal cord by transplanted olfactory ensheathing cells. J Neurotrauma. 2004 Aug; 21(8):1031-43.

López-Vales R, Forés J, Verdú E, Navarro X. Acute and delayed transplantation of olfactory ensheathing cells promote partial recovery after complete transection of the spinal cord. Neurobiol Dis. 2006 Jan; 21(1):57-68.

Lu P, Yang H, Culbertson M, Graham L, Roskams AJ, Tuszynski MH. Olfactory ensheathing cells do not exhibit unique migratory or axonal growth-promoting properties after spinal cord injury. J Neurosci. 2006 Oct 25; 26(43):11120-30

Mabon PJ, Weaver LC, Dekaban GA. Inhibition of monocyte/macrophage migration to a spinal cord injury site by an antibody to the integrin alphaD: a potential new-anti-inflammatory treatment. Exp Neurol. 2000; 166: 52-64.

Mackay-Sim A, Féron F, Cochrane J, Bassingthwaighte L, Bayliss C, Davies W, Fronek P, Gray C, Kerr G, Licina P, Nowitzke A, Perry C, Silburn PA, Urquhart S, Geraghty T. Autologous olfactory ensheathing cell transplantation in human paraplegia: a 3-year clinical trial. Brain. 2008 Sep; 131(Pt 9):2376-86.

Maier IC, Ichiyama RM, Courtine G, Schnell L, Lavrov I, Edgerton VR, Schwab ME. Differential effects of anti-Nogo-A antibody treatment and treadmill training in rats with incomplete spinal cord injury. Brain. 2009 Jun; 132(Pt 6):1426-40.

Mautes AE, Weinzierl MR, Donovan F, Noble LJ. Vascular events after spinal cord injury: contribution to secondary pathogenesis. Phys. Ther. 2000 Jul; 80(7), 673-87.

McDonald JW, Liu XZ, Qu Y, et al. Transplanted embryonic stem cells survive, differentiate and promote recovery in injured rat spinal cord. Nat Med 1999 Dec; 5(12):1410 – 12.

McKenna JE and Whishaw IQ. Complete compensation in skilled reaching success with associated impairments in limb synergies, after dorsal column lesion in the rat. The Journal of Neuroscience 1999; 19: 1885-94.

McKerracher L, David S, Jackson DL, Kottis V, Dunn RJ, Braun PE. Identification of myelin-associated glycoprotein as a major myelin-derived inhibitor of neurite growth. Neuron. 1994 Oct; 13(4):805-11.

McKerracher L, Higuchi H. Targeting Rho to stimulate repair after spinal cord injury. J Neurotrauma. 2006 Mar-Apr; 23(3-4):309-17.

McNeill DL, Chung K, Carlton SM, Coggeshall RE. Calcitonin gene-related peptide immunostained axons provide evidence for fine primary afferent fibers in the dorsal and dorsolateral funiculi of the rat spinal cord. J Comp Neurol. 1988 Jun 8; 272(2):303-8.

Mi S, Lee X, Shao Z, Thill G, Ji B, Relton J, Levesque M, Allaire N, Perrin S, Sands B, Crowell T, Cate RL, McCoy JM, Pepinsky RB. LINGO-1 is a component of the Nogo-66 receptor/p75 signaling complex. Nat Neurosci. 2004 Mar; 7(3):221-8.

Miao RQ, Gao Y, Harrison KD, Prendergast J, Acevedo LM, Yu J, Hu F, Strittmatter SM, Sessa WC. Identification of a receptor necessary for Nogo-B stimulated chemotaxis and morphogenesis of endothelial cells. Proc Natl Acad Sci U S A. 2006 Jul 18; 103(29):10997-1002.

Mikol DD, Stefansson K. A phosphatidylinositol-linked peanut agglutinin-binding glycoprotein in central nervous system myelin and on oligodendrocytes. J Cell Biol. 1988 Apr; 106(4):1273-9.

Miller MW. The origin of corticospinal projection neurons in rat. Exp Brain Res. 1987; 67(2):339-51.

Mirza SK, Krengel WF 3rd, Chapman JR, Anderson PA, Bailey JC, Grady MS, Yuan HA. Early versus delayed surgery for acute cervical spinal cord injury. Clin Orthop Relat Res. 1999 Feb; (359):104-14.

Molander C, Grant G. Spinal cord cytoarchitecture. In: "The Rat Nervous System" 2nd edn; ed. Paxinos G. Academic Press, 1995 Chapter 2, pp. 39-44.

Moreau-Fauvarque C, Kumanogoh A, Camand E, Jaillard C, Barbin G, Boquet I, Love C, Jones EY, Kikutani H, Lubetzki C, Dusart I, Chédotal A. The transmembrane semaphorin Sema4D/CD100, an inhibitor of axonal growth, is expressed on oligodendrocytes and upregulated after CNS lesion. J Neurosci. 2003 Oct 8; 23(27):9229-39.

Morgenstern, D.A., Asher, R.A., Fawcett, J.W. Chondroitin sulphate proteoglycans in the CNS injury response. Prog. Brain Res. 2002;137, 313-332.

Mukhopadhyay G, Doherty P, Walsh FS, Crocker PR, Filbin MT. A novel role for myelin-associated glycoprotein as an inhibitor of axonal regeneration. Neuron. 1994 Sep; 13(3):757-67.

Nash HH, Borke RC, Anders JJ. Ensheathing cells and methylprednisolone promote axonal regeneration and functional recovery in the lesioned adult rat spinal cord. J Neurosci. 2002 Aug 15; 22(16):7111-20.

Nayak MS, Kim YS, Goldman M, Keirstead HS, Kerr DA. Cellular therapies in motor neuron diseases. Biochim Biophys Acta. 2006, 1762: 1128-38.

Neafsey EJ, Bold EL, Haas G, Hurley-Gius KM, Quirk G, Sievert CF, Terreberry RR. The organization of the rat motor cortex: a microstimulation mapping study. Brain Res. 1986 Mar;396(1):77-96.

Neumann S, Skinner K, Basbaum AI. Sustaining intrinsic growth capacity of adult neurons promotes spinal cord regeneration. Proc Natl Acad Sci U S A. 2005 Nov 15; 102(46):16848-52.

Nguyen T, Mehta NR, Conant K, Kim KJ, Jones M, Calabresi PA, Melli G, Hoke A, Schnaar RL, Ming GL, Song H, Keswani SC, Griffin JW. Axonal protective effects of the myelin-associated glycoprotein. J Neurosci. 2009 Jan 21; 29(3):630-7.

Nielsen JB, Perez MA, Oudega M, Enriquez-Denton M, Aimonetti JM. Evaluation of transcranial magnetic stimulation for investigating transmission in descending motor tracts in the rat. Eur J Neurosci. 2007 Feb;25(3):805-14.

Noble LJ and Wrathall JR. Correlative analyses of lesion development and functional status after graded spinal cord contusive injuries in the rat. Experimental Neurology. 1989;103, 34-40.

Norenberg MD, Smith J, and Marcillo A. The pathology of human spinal cord injury: defining the problems. Journal of Neurotrauma. 2004; 21: 429-40.

Novikova LN, Kellerth JO. Differential effects of eurotrophins on neuronal survival and axonal regeneration after spinal cord injury in adult rats. J Comp Neurol. 2002 Oct 21; 452(3): 255-63.

Noyes DH. Electromechanical impactor for producing experimental spinal cord injury in animals. Med Biol Eng Comput. 1987; 25:335-40.

Oertle T, van der Haar ME, Bandtlow CE, Robeva A, Burfeind P, Buss A, Huber AB, Simonen M, Schnell L, Brösamle C, Kaupmann K, Vallon R, Schwab ME. Nogo-A inhibits neurite outgrowth and cell spreading with three discrete regions. J Neurosci. 2003 Jul 2; 23(13):5393-406.

O'Leary DD, Terashima T. Cortical axons branch to multiple subcortical targets by interstitial axon budding: implications for target recognition and "waiting periods". Neuron. 1988 Dec; 1(10):901-10.

Onifer SM, Rabchevsky AG, Scheff SW. Rat models of traumatic spinal cord injury to assess motor recovery. ILAR J. 2007; 48(4):385-95.

Oyesiku NM, Wilcox JN, Wigston DJ. Changes in expression of ciliary neurotrophic factor (CNTF) and CNTF-receptor alpha after spinal cord injury. J Neurobiol. 1997 Mar; 32(3):251-61.

Papadopoulos SM, Selden NR, Quint DJ, Patel N, Gillespie B, Grube S. Immediate spinal cord decompression for cervical spinal cord injury: feasibility and outcome. J Trauma. 2002 Feb; 52(2):323-32.

Park JB, Yiu G, Kaneko S, Wang J, Chang J, He XL, Garcia KC, He Z. A TNF receptor family member, TROY, is a coreceptor with Nogo receptor in mediating the inhibitory activity of myelin inhibitors. Neuron. 2005 Feb 3; 45(3):345-51.

Parr AM, Tator CH, Keating A. Bone marrow-derived mesenchymal stromal cells for the repair of central nervous system injury. Bone Marrow Transplant. 2007 Oct; 40(7):609-19.

Patterson JT, Coggeshall RE, Lee WT, Chung K. Long ascending unmyelinated primary afferent axons in the rat dorsal column: immunohistochemical localizations. Neurosci Lett. 1990 Jan 1; 108(1-2):6-10.

Pérez-Otaño, I.; Ehlers M.D. "Homeostatic plasticity and NMDA receptor trafficking" (PDF). Trends in Neurosciences. 2005 28 (5): 229–238

Petruska JC, Ichiyama RM, Jindrich DL, Crown ED, Tansey KE, Roy RR, Edgerton VR, Mendell LM. Changes in motoneuron properties and synaptic inputs related to step training after spinal cord transection in rats. J Neurosci. 2007 Apr 18;27(16):4460-71.

Pezet S, McMahon SB. Neurotrophins: mediator and modulators of pain. Annu Rev Neurosci. 2006; 29: 507-38.

Plant GW, Christensen CL, Oudega M, Bunge MB. Delayed transplantation of olfactory ensheathing glia promotes sparing/regeneration of supraspinal axons in the contused adult rat spinal cord. J Neurotrauma. 2003 Jan; 20(1):1-16.

Polentes J, Stamegna JC, Nieto-Sampedro M, Gauthier P. Phrenic rehabilitation and diaphragm recovery after cervical injury and transplantation of olfactory ensheathing cells. Neurobiol Dis. 2004 Aug; 16(3):638-53.

Popovich PG, Guan Z, McGaughy V, et al. The neuropathological and behavioural consequences of intraspinal microglial/ macrophage activation. J Neuropathol Exp Neurol 2002; 61: 623-33.

Porter R and Lemon R. Corticospinal function and voluntary movement. Clarendon press, Oxford, 1993.

Petruska JC, Ichiyama RM, Jindrich DL, Crown ED, Tansey KE, Roy RR, Edgerton VR, Mendell LM. Changes in motoneuron properties and synaptic inputs related to step training after spinal cord transection in rats. J Neurosci. 2007 Apr 18;27(16):4460-71.

Qiu J, Cai D, Dai H, McAtee M, Hoffman PN, Bregman BS, Filbin MT. Spinal axon regeneration induced by elevation of cyclic AMP. Neuron. 2002 Jun 13; 34(6):895-903.

Quarles RH. Myelin-associated glycoprotein (MAG): past, present and beyond. J Neurochem. 2007 Mar; 100(6):1431-48.

Raineteau O, Schwab ME. Plasticity of motor systems after incomplete spinal cord injury. Nat Rev Neurosci Apr 2001; 2(4):263–73.

Raineteau O, Fouad K, Bareyre FM, Schwab ME. Reorganization of descending motor tracts in the rat spinal cord. Eur J Neurosci. 2002 Nov; 16(9):1761-71.

Ramer, M, Priestley J.V. and McMahon S.B., Functional regeneration of sensory axons into the adult spinal cord, Nature 2000 Jan 20; 403(6767):312-6.

Ramer LM, Au E, Richter MW, Liu J, Tetzlaff W, Roskams AJ. Peripheral olfactory ensheathing cells reduce scar and cavity formation and promote regeneration after spinal cord injury. J Comp Neurol. 2004a May; 17; 473(1):1-15.

Ramer LM, Richter MW, Roskams AJ, Tetzlaff W, Ramer MS. Peripherally-derived olfactory ensheathing cells do not promote primary afferent regeneration following dorsal root injury. Glia 2004b; 47:189 – 206.

Ramón-Cueto A, Nieto-Sampedro M. Regeneration into the spinal cord of transected dorsal root axons is promoted by ensheathing glia transplants. Exp Neurol. 1994 Jun;127(2):232-44.

Ramón-Cueto A A, Plant GW, Avila J, Bunge MB. Long-distance axonal regeneration in the transacted adult rat spinal cord is promoted by olfactory ensheathing glia transplants. J Neurosci 1998; 18:3803-15.

Ramón-Cueto A, Cordero MI, Santos-Benito FF, Avila J. Functional recovery of paraplegic rats and motor axon regeneration in their spinal cords by olfactory ensheathing glia. Neuron. 2000 Feb; 25(2):425-35.

Ranck JB. Extracellular stimulation In: Methods in physiological psychology-Volum 3 Electrical stimulation research techniques. Academic press, 1981; pp 2-34.

Reier PJ, Stokes BT, Thompson FJ, Anderson DK. Fetal cell grafts into resection and contusion/compression injuries of the rat and cat spinal cord. Exp Neurol. 1992 Jan; 115(1): 177-88.

Rice T, Larsen J, Rivest S, Yong VW. Characterisation of early inflammation after spinal cord injury in mice. J Neuropathol Exp Neurol. 2007; 66:184-195.

Richard M, Giannetti N, Saucier D, Sacquet J, Jourdan F, Pellier-Monnin V. Neuronal expression of Nogo-A mRNA and protein during neurite outgrowth in the developing rat olfactory system. Eur J Neurosci. 2005 Nov; 22(9):2145-58.

Richardson PM, Issa VM. Peripheral injury enhances central regeneration of primary sensory neurones. Nature. 1984 Jun 28-Jul 4; 309(5971):791-3.

Richter MW, Roskams AJ. Olfactory ensheathing cell transplantation following spinal cord injury: hype or hope? Exp Neurol. 2008 Feb; 209(2):353-67.

Riddell JS, Hadian M. Topographical organization of group II afferent input in the rat spinal cord. J Comp Neurol. 1998 May 11;394(3):357-73.

Riddell JS, Enriquez-Denton M, Toft A, Fairless R, Barnett SC. Olfactory ensheathing cell grafts have minimal influence on regeneration at the dorsal root entry zone following rhizotomy. Glia 2004; 47:150–67.

Rivlin AS, Tator CH. Effect of duration of acute spinal cord compression in a new acute cord injury model in the rat. Surg Neurol. 1978 10:38-43.

Rizek PN, Kawaja MD. Cultures of rat olfactory ensheathing cells are contaminated with Schwann cells. Neuroreport. 2006 Apr 3; 17(5):459-62.

Rolls A, Shechter R, Schwartz M. The bright side of the glial scar in CNS repair. Nat Rev Neurosci. 2009 Mar; 10(3):235-41.

Rosin C, Bates TE, Skaper SD. Excitatory amino acid induced oligodendrocyte cell death in vitro: receptor-dependent and –independent mechanisms. J Neurochem. 2004 Sep; 90(5):1173-85.

Rossignol S, Brustein E, Bouyer L, Barthélemy D, Langlet C, Leblond H. Adaptive changes of locomotion after central and peripheral lesions. Can J Physiol Pharmacol. 2004 Aug-Sep; 82(8-9):617-27.

Rouiller EM, Liang FY, Moret V, Wiesendanger M. Trajectory of redirected corticospinal axons after unilateral lesion of the sensorimotor cortex in neonatal rat; a phaseolus vulgaris-leucoagglutinin (PHA-L) tracing study. Exp Neurol. 1991 Oct; 114(1):53-65.

Ruitenberg MJ, Plant GW, Hamers FP, Wortel J, Blits B, Dijkhuizen PA, Gispen WH, Boer GJ, Verhaagen J. Ex vivo adenoviral vector-mediated neurotrophin gene transfer to olfactory ensheathing glia: effects on rubrospinal tract regeneration, lesion size, and functional recovery after implantation in the injured rat spinal cord. J Neurosci. 2003 Aug 6; 23(18):7045-58.

Ruitenberg MJ, Levison DB, Lee SV, Verhaagen J, Harvey AR, Plant GW. NT-3 expression from engineered olfactory ensheathing glia promotes spinal sparing and regeneration. Brain. 2005 Apr; 128(Pt 4):839-53.

Salgado-Ceballos H, Guizar-Sahagun G, Feria-Velasco A, Grijalva I, Espitia L, Ibarra A, Madrazo I. Spontaneous long-term remyelination after traumatic spinal cord injury in rats. Brain Res. 1998 Jan 26; 782(1-2):126-35.

Salzer JL, Holmes WP, Colman DR. The amino acid sequences of the myelin-associated glycoproteins: homology to the immunoglobulin gene superfamily. J Cell Biol. 1987 Apr; 104(4):957-65.

Santos-Silva A, Fairless R, Frame MC, Montague P, Smith GM, Toft A, Riddell JS, Barnett SC. FGF/heparin differentially regulates Schwann cell and olfactory ensheathing cell interactions with astrocytes: a role in astrocytosis. J Neurosci. 2007 Jul 4;27(27):7154-67.

Sasaki M, Lankford KL, Zemedkun M, Kocsis JD. Identified olfactory ensheathing cells transplanted into the transected dorsal funiculus bridge the lesion and form myelin. J Neurosci. 2004 Sep 29; 24(39):8485-93.

Sasaki M, Hains BC, Lankford KL, Waxman SG, Kocsis JD. Protection of corticospinal tract neurons after dorsal spinal cord transection and engraftment of olfactory ensheathing cells. Glia. 2006 Mar; 53(4):352-9.

Satake K, Matsuyama Y, Kamiya M, Kawakami H, Iwata H, Adachi K, Kiuchi K. Up-regulation of glial cell line-derived neurotrophic factor (GDNF) following traumatic spinal cord injury. Neuroreport. 2000 Nov 27; 11(17):3877-81.

Sayer FT, Kronvall E, Nilsson OG. Methylprednisolone treatment in acute spinal cord injury: the myth challenged through a structured analysis of published literature. Spine J. 2006 May-Jun; 6(3):335-43.

Schachner M, Bartsch U. Multiple functions of the myelin-associated glycoprotein MAG (siglec-4a) in formation and maintenance of myelin. Glia. 2000 Jan 15; 29(2):154-65.

Scheff SW, Rabchevsky AG, Fugaccia I, Main JA, Lumpp JE Jr. Experimental modeling of spinal cord injury: Characterization of a force-defined injury device. J Neurotrauma. 2003; 20:179-193.

Schnell L, Schwab ME. Axonal regeneration in the rat spinal cord produced by an antibody against myelin-associated neurite growth inhibitors. Nature. 1990 Jan 18; 343(6255):269-72.

Schnell L, Fearn S, Klassen H, Schwab ME, Perry VH. Acute inflammatory responses to mechanical lesions in the CNS: differences between brain and spinal cord. Eur J Neurosci. 1999 Oct; 11(10):3648-58

Schrimsher GW, Reier PJ. Forelimb motor performance following dorsal column, dorsolateral funiculi, or ventrolateral funiculi lesions of the cervical spinal cord in the rat. Exp Neurol. 1993 Apr; 120(2):264-76.

Schubert M, Beck S, Taube W, Amtage F, Faist M, Gruber M. Balance training and ballistic strength training are associated with task-specific corticospinal adaptations. Eur J Neurosci. 2008 Apr;27(8):2007-18.

Schurch B, Wichmann W, Rossier AB. Post-traumatic syringomyelia (cystic myelopathy): a prospective study of 449 patients with spinal cord injury. J Neurol Neurosurg Psychiatry. 1996 Jan; 60(1):61-7.

Schwab ME, Bartholdi D. Degeneration and regeneration of axons in the lesioned spinal cord. Physiol Rev. 1996 Apr; 76(2):319-70.

Schwab ME. Nogo and axon regeneration. Curr Opin Neurobiol. 2004 Feb; 14(1):118-24.

Schwartz M, Yoles E. Macrophages and dendritic cells treatment of spinal cord injury: from the bench to the clinic. Acta Neurochir Suppl. 2005; 93, 147-150.

Schwartz M, Yoles E. Immune-based therapy for spinal cord repair: autologous macrophages and beyond. J Neurotrauma. 2006 Mar-Apr; 23(3-4):360 –370.

Schweigreiter R, Bandtlow CE. Nogo in the injured spinal cord. J Neurotrauma. 2006 Mar-Apr; 23(3-4):384-96.

Seymour AB, Andrews EM, Tsai SY, Markus TM, Bollnow MR, Brenneman MM, O'Brien TE, Castro AJ, Schwab ME, Kartje GL. Delayed treatment with monoclonal antibody IN-1 1 week after stroke results in recovery of function and corticorubral plasticity in adult rats. J Cereb Blood Flow Metab. 2005 Oct;25(10):1366-75.

Shao Z, Browning JL, Lee X, Scott ML, Shulga-Morskaya S, Allaire N, Thill G, Levesque M, Sah D, McCoy JM, Murray B, Jung V, Pepinsky RB, Mi S. TAJ/TROY, an orphan TNF receptor family member, binds Nogo-66 receptor 1 and regulates axonal regeneration. Neuron. 2005 Feb 3; 45(3):353-9.

Shapovalov AI, Gurevitch NR. Monosynaptic and disynaptic reticulospinal actions on lumbar motoneurons of the rat. Brain Res. 1970 Jul 14;21(2):249-63.

Shi, S.H.; Hayashi Y., Petralia R.S., Zaman S.H., Wenthold R., Svoboda K., Malinow R. "Rapid spine delivery and redistribution of AMPA receptors after synaptic NMDA receptor activation". Science. 1999 284 (5421): 1811–1816.

Shields SA, Blakemore WF, Franklin RJ. Schwann cell remyelination is restricted to astrocyte-deficient areas after transplantation into demyelinated adult rat brain. J Neurosci Res. 2000 Jun; 60(5): 571-8.

Sicotte M, Tsatas O, Jeong SY, Cai CQ, He Z, David S. Immunization with myelin or recombinant Nogo-66/MAG in alum promotes axon regeneration and sprouting after corticospinal tract lesions in the spinal cord. Mol Cell Neurosci. 2003 Jun; 23(2):251-63.

Siegenthaler MM, Tu MK, Keirstead HS. The extent of myelin pathology differs following contusion and transection spinal cord injury. J Neurotrauma. 2007 Oct;24(10):1631-46.

Silver J, Miller JH. Regeneration beyond the glial scar. Nat Rev Neurosci. 2004 Feb; 5(2):146-56.

Simonen M, Pedersen V, Weinmann O, Schnell L, Buss A, Ledermann B, Christ F, Sansig G, van der Putten H, Schwab ME. Systemic deletion of the myelin-associated outgrowth inhibitor Nogo-A improves regenerative and plastic responses after spinal cord injury. Neuron. 2003 Apr 24; 38(2):201-11.

Smale KA, Douocette R, Kawaja MD. Implantation of olfactory ensheathing cells in the adult rat brain following fimbria-fornix transaction. Exp Neurol. 1996; 137: 225-33.

Smith KJ, Bennett BJ. Topographic and quantitative description of rat dorsal column fibres arising from the lumbar dorsal roots. J Anat. 1987 Aug; 153:203-15.

Soblosky JS, Song JH, Dinh DH. Graded unilateral cervical spinal cord injury in the rat: Evaluation of forelimb recovery and histological effects. Behav Brain Res. 2001; 119:1-13.

Spencer DD, Robbins RJ, Naftolin F, Marek KL, Vollmer T, Leranth C, Roth RH, Price LH, Gjedde A, Bunney BS. Unilateral transplantation of human fetal mesencephalic tissue into the caudate nucleus of patients with Parkinson's disease. N Engl J Med. 1992 nov; 327(22): 1541-8.

Spinal Injuries Association, http://www.spinal.co.uk

Spinal Cord Injury Information Network, http://www.spinalcord.uab.edu

Sternberger NH, Quarles RH, Itoyama Y, Webster HD. Myelin-associated glycoprotein demonstrated immunocytochemically in myelin and myelin-forming cells of developing rat. Proc Natl Acad Sci USA. 1979 Mar; 76(3):1510-4.

Steward O, Sharp K, Selvan G, Hadden A, Hofstadter M, Au E, Roskams J. A re-assessment of the consequences of delayed transplantation of olfactory lamina propria following complete spinal cord transection in rats. Exp Neurol. 2006 Apr; 198(2):483-99.

Steward O, Zheng B, Tessier-Lavigne M, Hofstadter M, Sharp K, Yee KM. Regenerative growth of corticospinal tract axons via the ventral column after spinal cord injury in mice. J Neurosci. 2008 Jul 2;28(27):6836-47.

Stirling DP, Khodarahmi K, Liu J, McPhail LT, McBride CB, Steeves JD, Ramer MS, Tetzlaff W. Minocycline treatment reduces delayed oligodendrocyte death, attenuates axonal dieback, and improves functional outcome after spinal cord injury. J Neurosci. 2004 Mar 3; 24(9):2182-90.

Stone TW. Cortical responses to pyramidal tract stimulation in the rat. Exp Neurol. 1972 Jun; 35(3):492-502.

Strauss DJ, DeVivo MJ, Paculdo DR, Shavelle RM. Trends in life expectancy after spinal cord injury. Archives of Physical Medicine and Rehabilitation. 2006; 87:1079-1085.

Song XY, Zhong JH, Wang X, Zhou XF. Suppression of p75NTR does not promote regeneration of injured spinal cord in mice. J Neurosci. 2004 Jan 14; 24(2):542-6.

Suberviola B, González-Castro A, Llorca J, Ortiz-Melón F, Miñambres E. Early complications of high-dose methylprednisolone in acute spinal cord injury patients. Injury. 2008 Jul; 39(7):748-52.

Swett JE and Bourassa CM. Electrical stimulation of peripheral nerve In: Methods in physiological psychology- Volum 3 Electrical stimulation research techniques. Academic press, 1981; pp 244-284.

Syková E, Jendelová P, Urdzíková L, Lesný P, Hejcl A. Bone marrow stem cells and polymer hydrogels--two strategies for spinal cord injury repair. Cell Mol Neurobiol. 2006 Oct-Nov;26(7-8):1113-29.

Takami T, Oudega M, Bates ML, Wood PM, Kleitman N, Bunge MB. Schwann cell but not olfactory ensheathing glia transplants improve hindlimb locomotor performance in the moderately contused adult rat thoracic spinal cord. J Neurosci. 2002 Aug 1; 22(15):6670-81.

Takei Y. Phosphorylation of Nogo receptors suppresses Nogo signaling, allowing neurite regeneration. Sci Signal. 2009 Mar 31; 2(64):ra14.

Tamatani M, Senba E, Tohyama M. Calcitonin gene-related peptide- and substance P-containing primary afferent fibers in the dorsal column of the rat. Brain Res. 1989 Aug 21; 495(1):122-30.

Tanaka S, Takehashi M, Iida S, Kitajima T, Kamanaka Y, Stedeford T, Banasik M, Ueda K. Mitochondrial impairment induced by poly(ADP-ribose) polymerase-1 activation in cortical neurons after oxygen and glucose deprivation. J Neurochem. 2005 Oct; 95(1):179-90.

Tang X, Davies JE, Davies SJ. Changes in distribution, cell associations, and protein expression levels of NG2, neurocan, phosphacan, brevican, versican V2, and tenascin-C during acute to chronic maturation of spinal cord scar tissue. J Neurosci Res. 2003 Feb 1; 71(3):427-44.

Tator CH, Koyanagi I. Vascular mechanisms in the pathophysiology of human spinal cord injury. J Neurosurg. 1997 Mar; 86(3):483-92.

Tewarie RS, Hurtado A, Bartels RH, Grotenhuis A, Oudega M. Stem cell-based therapies for spinal cord injury. J Spinal Cord Med. 2009; 32(2):105-14.

Thomas SL, Gorassini MA. Increases in corticospinal tract function by treadmill training after incomplete spinal cord injury. J Neurophysiol. 2005 Oct;94(4):2844-55.

Thompson HJ, Marklund N, LeBold DG, Morales DM, Keck CA, Vinson M, Royo NC, Grundy R, McIntosh TK. Tissue sparing and functional recovery following experimental traumatic brain injury is provided by treatment with an anti-myelin-associated glycoprotein antibody. Eur J Neurosci. 2006 Dec; 24(11):3063-72.

Thuret S, Moon LD, Gage FH. Therapeutic interventions after spinal cord injury. Nat Rev Neurosci. 2006 Aug; 7(8):628-43.

Toft A, Scott DT, Barnett SC, Riddell JS. Electrophysiological evidence that olfactory cell transplants improve function after spinal cord injury. Brain. 2007 Apr; 130, 4: 970-984.

Tontsch U, Archer DR, Dubois-Dalcq M, Duncan ID. Transplantation of an oligodendrocyte cell line leading to extensive myelination. Proc Natl Acad Sci USA. 1994 Nov; 91(24): 11616-20.

Tracey DJ, Waite PM. Somatosensory system. In: "The Rat Nervous System" 2nd edn; ed. Paxinos G. Academic Press, 1995 Chapter 26, pp. 689-700.

Trapp BD. Myelin-associated glycoprotein. Location and potential functions. Ann N Y Acad Sci. 1990; 05:29-43.

Tuszynski MH, Weidner N, McCormack M, Miller I, Powell H, Conner J. Grafts of genetically modified Schwann cells to the spinal cord: survival, axon growth, and myelination. Cell Transplant. 1998; 7: 187-96.

Usul H, Cakir E, Cobanoglu U, Alver A, Peksoylu B, Topbas M, Baykal S. The effects of tyrphostine Ag 556 on experimental spinal cord ischemia reperfusion injury. Surg Neurol. 2004 Jan; 61(1):45-54; discussion 54.

Vallières N, Berard JL, David S, Lacroix S. Systemic injections of lipopolysaccharide accelerates myelin phagocytosis during Wallerian degeneration in the injured mouse spinal cord. Glia. 2006 Jan 1; 53(1):103-13.

Vahlsing HL, Feringa ER. A ventral uncrossed corticospinal tract in the rat. Exp Neurol. 1980 Nov; 70(2):282-7.

Van Meeteren NL, Eggers R, Lankhorst AJ, Gispen WH, Hamers FP. Locomotor recovery after spinal cord contusion injury in rats is improved by spontaneous exercise. J Neurotrauma. 2003 Oct;20(10):1029-37.

Vogel G. Cell biology. Ready or not? Human ES cells head toward the clinic. Science. 2005 Jun 10; 308(5728):1534-8.

von Euler M, Janson AM, Larsen JO, Seiger A, Forno L, Bunge MB, Sundström E. Spontaneous axonal regeneration in rodent spinal cord after ischemic injury. J Neuropathol Exp Neurol. 2002 Jan; 61(1):64-75.

Wang KC, Koprivica V, Kim JA, Sivasankaran R, Guo Y, Neve RL, He Z. Oligodendrocyte-myelin glycoprotein is a Nogo receptor ligand that inhibits neurite outgrowth. Nature. 2002a Jun 27; 417(6892):941-4.

Wang KC, Kim JA, Sivasankaran R, Segal R, He Z. P75 interacts with the Nogo receptor as a co-receptor for Nogo, MAG and OMgp. Nature. 2002b Nov 7; 420(6911):74-8.

Wang R, Ehara K, Tamaki N. Spinal cord edema following freezing injury in the rat: Relationship between tissue water content and spinal cord blood flow. Surg Neurol. 1993; 39: 348-54.

Wang X, Baughman KW, Basso DM, Strittmatter SM. Delayed Nogo receptor therapy improves recovery from spinal cord contusion. Ann Neurol. 2006 Nov; 60(5):540-9.

Waxman, SG. Demyelination in spinal cord injury. J. Neurol. Sci. 1989 Jun; 91(1-2): 1-14.

Weidner N, Blesch A, Grill RJ, Tuszynski MH. Nerve growth factor-hypersecreting Schwann cell grafts augment and guide spinal cord axonal growth and remyelinate central nervous system axons in a phenotypically appropriate manner that correlates with expression of L1. J Comp Neurol., 1999 Nov 1; 413(4): 495-506.

Weidner N, Ner A, Salimi N, Tuszynski MH. Spontaneous corticospinal axonal plasticity and functional recovery after adult central nervous system injury. Proc. Natl.Acad. Sci. USA 2001 Mar 13; 98, 3513–8.

Weinmann O, Schnell L, Ghosh A, Montani L, Wiessner C, Wannier T, Rouiller E, Mir A, Schwab ME. Intrathecally infused antibodies against Nogo-A penetrate the CNS and downregulate the endogenous neurite growth inhibitor Nogo-A. Mol Cell Neurosci. 2006 May-Jun;32(1-2):161-73.

Weaver LC, Marsh DR, Gris D, Brown A, Dekaban GA. Autonomic dysreflexia after spinal cord injury: central mechanisms and strategies for prevention. Prog Brain Res. 2006; 152:245-63.

Willis WD Coggeshall RE Sensory mechanisms of the spinal cord: Ascending sensory tracts and their descending control. 2004, Kluwer academic/Plenum publishers, New York.

Whishaw IQ, Gorny B, Foroud A, Kleim JA. Long-Evans and Sprague-Dawley rats have similar skilled reaching success and limb representations in motor cortex but different movements: some cautionary insights into the selection of rat strains for neurobiological motor research. Behav Brain Res. 2003 Oct 17;145(1-2):221-32.

Wolpaw JR, Tennissen AM. Activity-dependent spinal cord plasticity in health and disease. Annu Rev Neurosci. 2001;24:807-43.

Wong ST, Henley JR, Kanning KC, Huang KH, Bothwell M, Poo MM. A p75(NTR) and Nogo receptor complex mediates repulsive signaling by myelin-associated glycoprotein. Nat Neurosci. 2002 Dec; 5(12):1302-8.

Wrathall JR, Pettegrew RK, Harvey F. Spinal cord contusion in the rat: Production of graded, reproducible, injury groups. Exp Neurol. 1985; 88:108-122.

Xu XM, Chen A, Guenard V, Kleitman N, Bunge MB. Bridging Schwann cell transplants promote axonal regeneration from both the rostral and caudal stumps of transacted adult rat spinal cord. J Neurocytol. 1997 Jan; 26(1): 1-16.

Xu XM, Zhang SX, Li H, Aebischer P, Bunge MB. Regrowth of axons into the distal spinal cord through a Schwann-cell-seeded mini-channel implanted into hemisected adult rat spinal cord. Eur J Neurosci 1999; 11:1723–40.

Yamashita T, Fujitani M, Yamagishi S, Hata K, Mimura F. Multiple signals regulate axon regeneration through the nogo receptor complex. Mol Neurobiol. 2005 Oct; 32: 105-11.

Yang HW, Lemon RN. An electron microscopic examination of the corticospinal projection to the cervical spinal cord in the rat: lack of evidence for cortico-motoneuronal synapses. Exp Brain Res. 2003 Apr; 149(4):458-69.

Yang H, Lu P, McKay HM, Bernot T, Keirstead H, Steward O, Gage FH, Edgerton VR, Tuszynski MH. Endogenous neurogenesis replaces oligodendrocytes and astrocytes after primate spinal cord injury. J Neurosci. 2006 Feb 22; 26(8):2157-66.

Ying Z, Roy RR, Zhong H, Zdunowski S, Edgerton VR, Gomez-Pinilla F. BDNF-exercise interactions in the recovery of symmetrical stepping after a cervical hemisection in rats. Neuroscience. 2008 Sep 9;155(4):1070-8.

Yiu G, He Z. Glial inhibition of CNS axon regeneration. Nat Rev Neurosci. 2006 Aug; 7:617- 627.

Z'Graggen WJ, Metz GA, Kartje GL, Thallmair M, Schwab ME. Functional recovery and enhanced corticofugal plasticity after unilateral pyramidal tract lesion and blockade of myelin-associated neurite growth inhibitors in adult rats. J Neurosci. 1998 Jun 15; 18(12):4744-57.

Zheng B, Ho C, Li S, Keirstead H, Steward O, Tessier-Lavigne M. Lack of enhanced spinal regeneration in Nogo-deficient mice. Neuron. 2003 Apr 24; 38(2):213-24.

Zheng B, Atwal J, Ho C, Case L, He XL, Garcia KC, Steward O, Tessier-Lavigne M. Genetic deletion of the Nogo receptor does not reduce neurite inhibition in vitro or promote corticospinal tract regeneration in vivo. Proc Natl Acad Sci U S A. 2005 Jan 25; 102(4):1205-10.

Zhou L, Shine HD. Neurotrophic factors expressed in both cortex and spinal cord induce axonal plasticity after spinal cord injury. J Neurosci Res. 2003 Oct 15; 74(2):221-6.